THE UNIVERSITY OF MANITOBA

SEDIMENTOLOGY AND DOLOMITIZATION OF THE MIDDLE DEVONIAN (GIVETIAN) SLAVE POINT FORMATION, CRANBERRY FIELD, NORTHWESTERN ALBERTA, CANADA

A THESIS

SUBMITTED TO THE FACULTY OF GRADUATE STUDIES

UNIVERSITY OF MANITOBA

IN PARTIAL FULFILLMENT OF THE REQUIREMENTS FOR THE

DEGREE OF MASTER OF SCIENCE

IN THE

DEPARTMENT OF GEOLOGICAL SCIENCES

Winnipeg, Manitoba
2000

THE UNIVERSITY OF MANITOBA

FACULTY OF GRADUATE STUDIES

*****

COPYRIGHT PERMISSION PAGE

Sedimentology and Dolomitization of the Middle Devonian (Givetian) Slave Point Formation, Cranberry Field, Northwestern Alberta, Canada

BY

Lisa A. M. Sack

A Thesis/Practicum submitted to the Faculty of Graduate Studies of The University of Manitoba in partial fulfillment of the requirements of the degree of

Master of Science

ABSTRACT

The Middle Devonian Slave Point Formation of the Western Canada Sedimentary Basin is host to several gas fields, most notably the Cranberry Gas Field, the focus of this thesis.

The Slave Point Formation can be subdivided into a Lower Slave Point (platform) that is unconformably overlain by the Upper Slave Point (reefal buildup). The Lower Slave Point is a basin-wide argillaceous limestone. Upper Slave Point reefal developments are related to slight buildups on the underlying Lower Slave Point. Colonization by *Thamnopora* created subtle platform topography within the Lower Slave Point. These subtle 'highs' acted as the loci for Upper Slave Point reefal development. Upper Slave Point sedimentation is characterized by two growth phases: 1) early progradational growth followed by: 2) backstepping to aggradational growth. The termination of Upper Slave Point reefal development occurred during the trangressive or 'drowning' phase of the Waterways Formation. This transgression is characterised by an argillaceous crinoid-brachiopod deposit, informally known as the 'Cranberry Member' of the Waterways Formation.

The Slave Point Formation has undergone at least three dolomitizing events. The major types of dolomite that occur in the Slave Point Formation in the study area are: replacive coarse crystalline dolomites (Type 2) and late-stage saddle dolomite cements (Type 3). The majority of dolomitization occurred in a burial environment. The linear orientation, restricted occurrence and stable isotopes of Type 2 dolomitized wells is suggestive of fault controlled fluid circulation during the Late Cretaceous – Early Tertiary. Dolomites formed from deep, warm, saline, basinal fluids and/or hot brines that ascended along fault conduits from deeper parts of the basin. The widespread occurrence and stable isotopes of Type 3 dolomite cements suggest the updip migration of compaction-driven dolomitizing fluids that occurred in response to basin tilting during the Late Cretaceous-Early Tertiary.

Acknowledgments

I would like to thank all the people who gave generously of their time and resources to make this thesis possible: Gulf Canada Resources Ltd. for providing the thesis topic and financial assistance, Dr. W.M. Last, Dr. N. Chow and Dr. Brian Stimpson from the University of Manitoba for their constructive criticism and valuable comments during the preparation of this manuscript; Dr. F.A. Stoakes for comments and suggestions early in the preparation of this manuscript; I. Berta (University of Manitoba) and J. Bladek (Calgary Petrographics) for the painstaking preparation of thin sections; Energy Resources Conservation Board (ERCB), Calgary, who provided fast and efficient service while core examination and sub-sampling was in progress; and the Environmental Isotope Laboratory at the University of Waterloo for performing the isotope analyses.

This thesis was funded primarily through a research grant provided by Gulf Canada Resources Ltd. and a University of Manitoba Graduate Scholarship.

Additional support came from the American Association of Petroleum Geologists (AAPG) in the form of a grant-in-aid award.

TABLE OF CONTENTS

LIST OF TABLES

LIST OF FIGURES

CHAPTER 1: INTRODUCTION

The Devonian Period of the Western Canada Sedimentary Basin is best known for the occurrence of reefs. These reefs occur in multiple phases of sedimentation and vary according to depositional setting, evolution, related facies associations, areal extent, thickness, fauna and morphology (Wendte, 1992a). Devonian reefs in the Western Canada Sedimentary Basin are a vast natural resource of major economic importance to Canada. The Devonian is the most prolific hydrocarbon-producing Period in the Western Canada Sedimentary Basin, accounting for over 60 percent of recoverable conventional crude oil in Alberta and approximately one quarter of the total in-place gas reserves (Reinson and Lee, 1993; Reinson et al., 1993a; Podruski et al., 1988). In addition, the Devonian is an important resource for scientific research because of the accessibility of its outcrops and the exceptionally fine conservation facilities that make the cores from thousands of boreholes available for public inspection (Moore, 1989).

The purpose of this thesis is to formulate a predictive model for the economic exploration of hydrocarbons within the Devonian Slave Point Formation that could be applied elsewhere in similar geological environments. The northwestern Alberta study area provides an opportunity to examine, document and interpret different carbonate depositional environments and the effects of dolomitization upon productive hydrocarbon reservoir rocks.

1.1 Objectives

The upper Middle Devonian (Givetian) Slave Point Formation of the Beaverhill

Lake Group in northwestern Alberta (Townships 95 to 97, Ranges 2 to 6 West of the Sixth Meridian) contains significant quantities of gas and gas-condensate. The objective of this thesis is to investigate the origin of various depositional and diagenetic processes in the Slave Point Formation in the study area responsible for the formation, preservation and destruction of this complex reservoir. This objective is to be achieved by investigating:

1. the various depositional facies and facies associations within the Slave Point Formation, to formulate a depositional model;
2. the stratigraphic distribution, timing and source of the major diagenetic phases in the Slave Point Formation, particularly dolomite, to formulate a model for dolomitization.

1.2 Study Area

The geological study area is located in the subsurface of northwestern Alberta approximately 500 km northwest of Edmonton. The area extends from Township 95 to 97 and Range 2 through 6 West of the Sixth Meridian, encompassing the Cranberry Slave Point Field. The Cranberry Slave Point Field has been producing gas since 1975 from the Slave Point Formation. Figure 1.1 outlines the area of detailed study for this project.

The Cranberry Field was chosen as the study area because it contains numerous petrophysical well log data and drill-cores. The study area (Fig. 1.1) contains 96 Slave Point cores and 136 geophysical well logs from wells penetrating the Slave Point Formation.

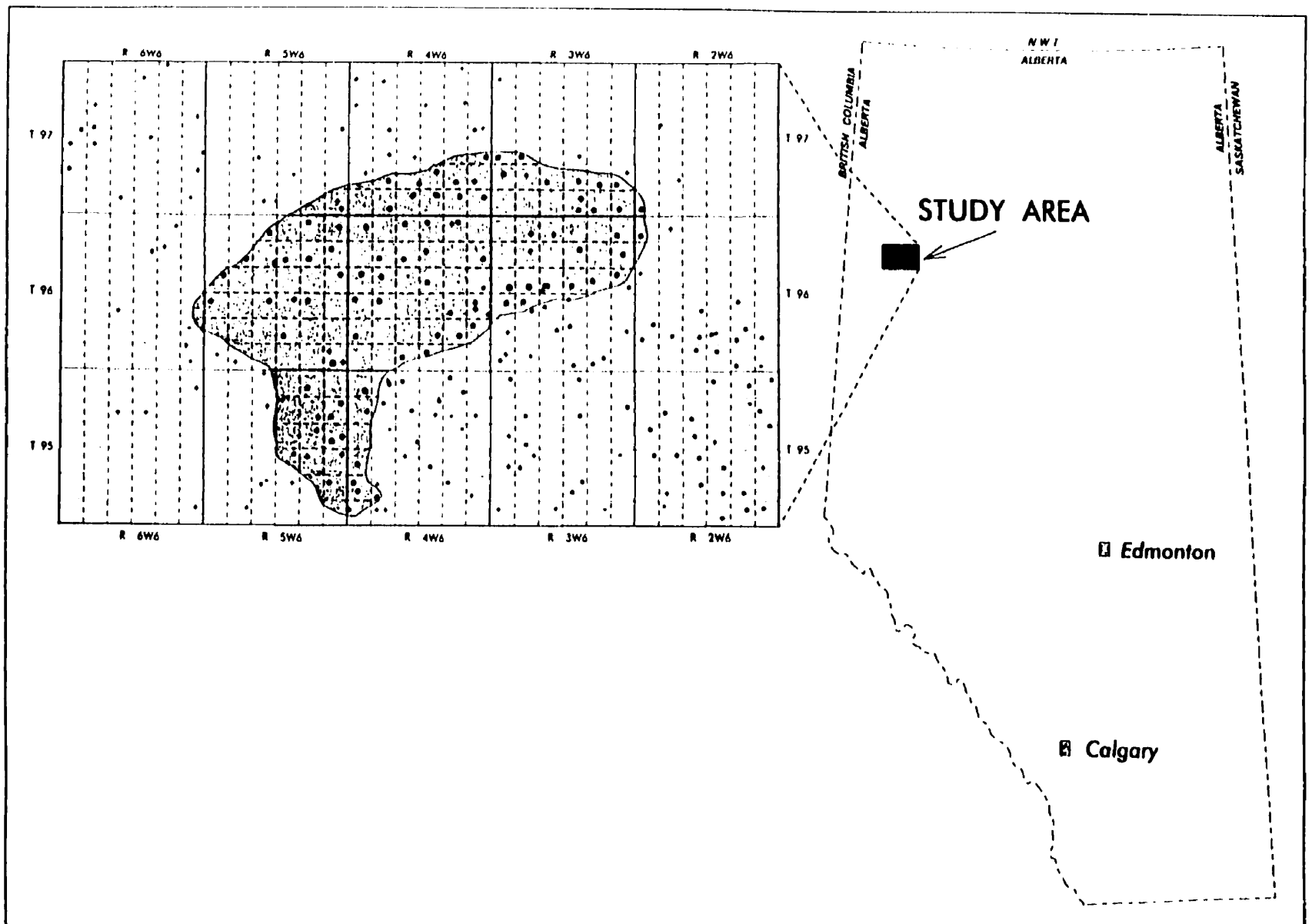

Figure 1.1. Map of Alberta and detailed map of the northern Alberta study area. Note the Slave Point Cranberry Field outline (shaded) within the study area.

1.3 Methodology

Core samples from the Slave Point Formation were examined and analysed in this study employing various analytical techniques. These techniques are outlined in the following subsections.

1.3.1 Core Examination

Slave Point drill cores from 96 wells were examined, photographed and sub-sampled at the Alberta Energy and Utilities Board (A.E.U.B.) Core Research Center in Calgary, Alberta (Fig. 1.2). Drill cores were examined in detail to determine rock type, biotic components, textural components, nature and location of porosity and formation contacts and boundaries. Core descriptions were then matched to their respective petrophysical logs to aid in stratigraphic correlations. Individual cores were depth adjusted by matching obvious changes in lithology to their corresponding petrophysical log response.

There are several classification schemes used for describing textures of carbonate rocks. The most widely accepted classification, which is used in this study, is that of Embry and Klovan (1971), which is a modification of Dunham's classification of limestones by depositional texture (Dunham, 1962); this is used in the present study because it permits the greatest detail of description of depositional textures within limestones (Table 1.1). The classification of porosity types (Table 1.2) follows the porosity classification scheme of Choquette and Pray (1970).

Emphasis in interpreting Slave Point Facies was placed on the growth forms of stromatoporoids, the dominant organism and constituent in Slave Point limestones. The growth forms of these organisms, like those of present day hermatypic corals, are a

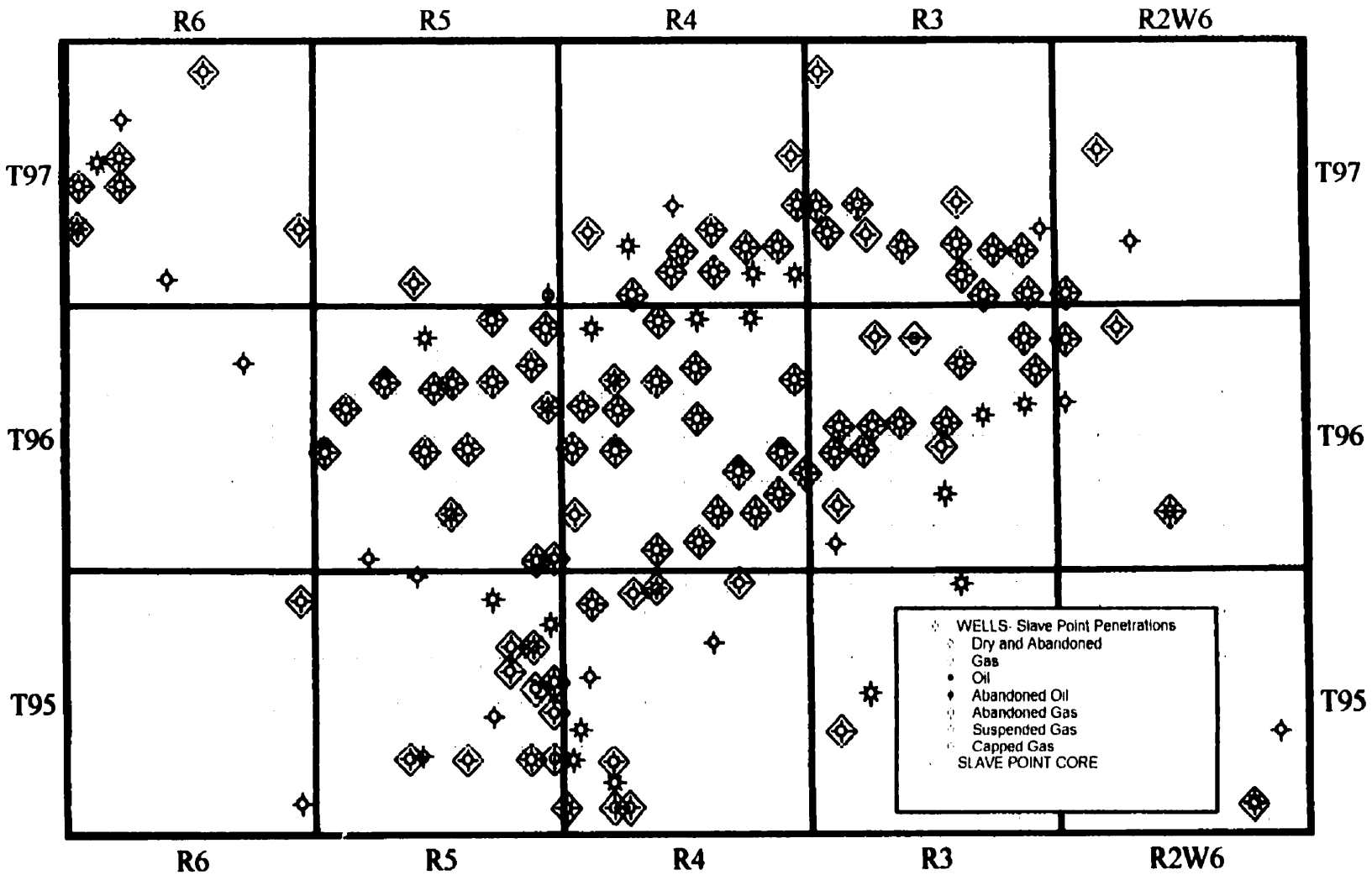

Figure 1.2. Map showing the location of Slave Point cores. Diamonds represent wells with Slave Point core(s). Scale 1:250,000.

Allochthonous Limestones Original components not organically bound during deposition						Autochthonous Limestones Original components organically bound during deposition		
Less than 10% > 2 mm components				Greater than 10% > 2 mm components		By organisms which act as baffles	By organisms which encrust and bind	By organisms which build a rigid framework
Contains lime mud (< 0.03 mm)		No lime mud		Matrix supported	> 2mm component supported			
Mud supported		Grain Supported						
Less than 10% grains (> 0.03 mm < 2mm)	Greater than 10% grains							
Mudstone	**Wacke-stone**	**Pack-stone**	**Grain-stone**	**Floatstone**	**Rudstone**	**Boundstone**		
						Baffle-stone	**Bind-stone**	**Frame-stone**

Table 1.1. Dunham's Classification of Limestones (modified after Embry and Klovan, 1971; and James, 1984).

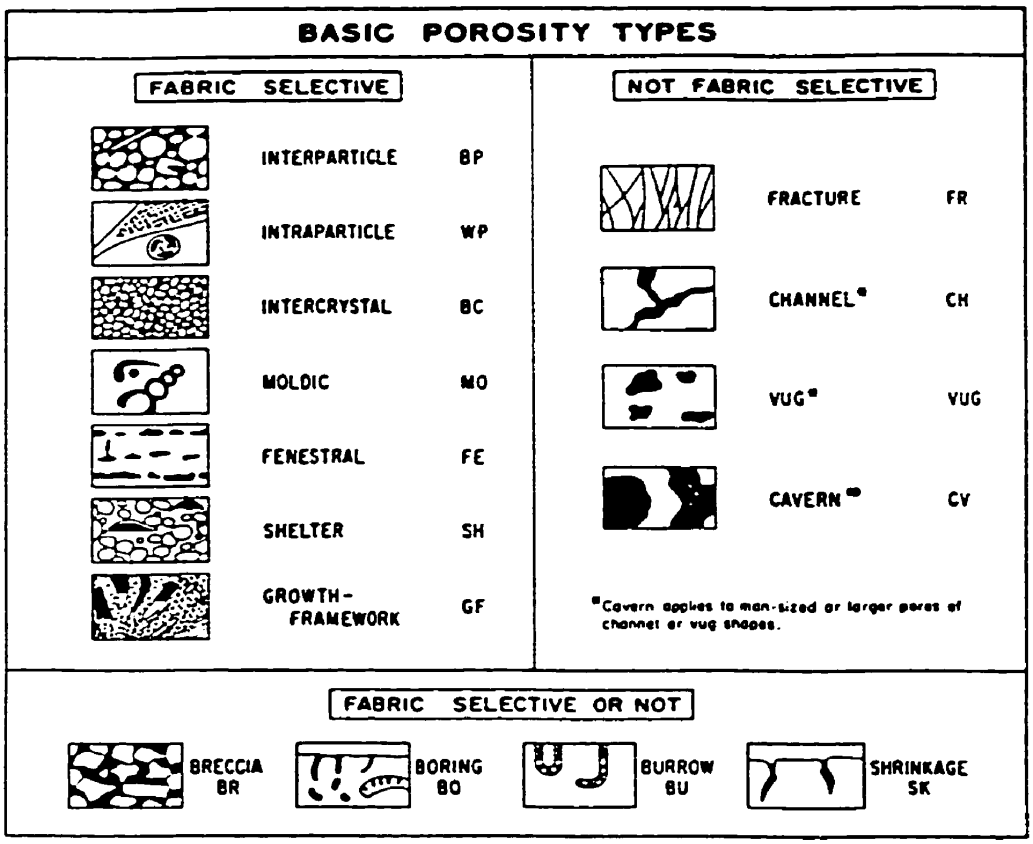

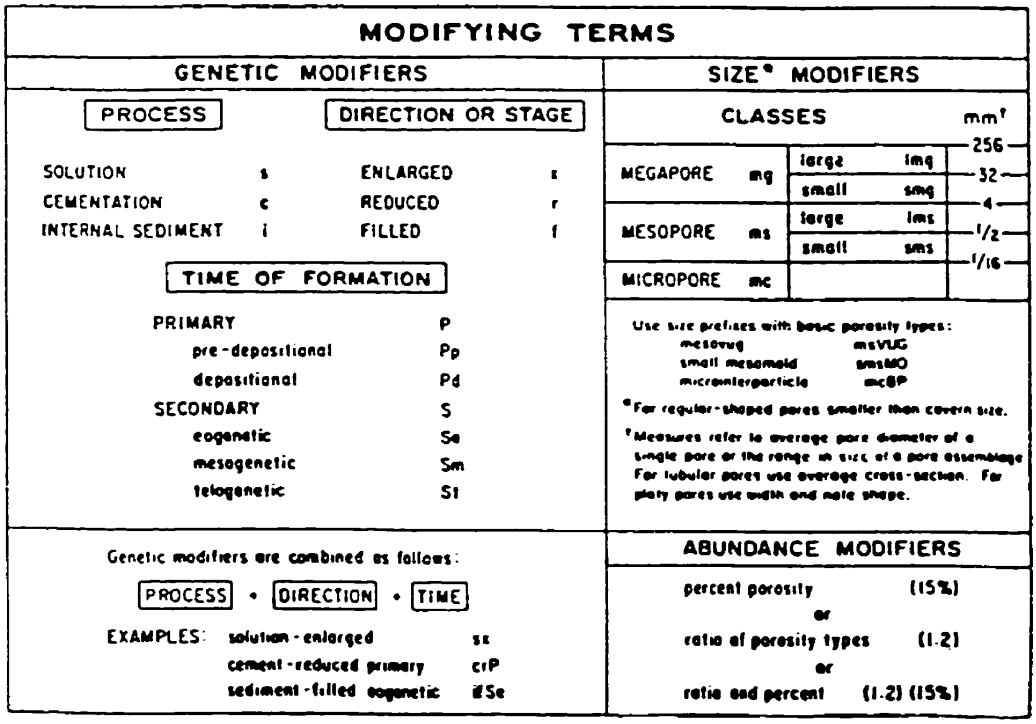

Table 1.2. Geologic classification of pores and pore systems in carbonate rocks (Choquette and Pray, 1970).

response to such controls as nutrient supply, water energy, water turbidity, sediment supply and water depth, and hence reflect the environment of deposition. As the growth forms of stromatoporoids are of such importance as environmental indicators, the terminology used in this study is reviewed here (from Wendte, 1992b):

Tabular - flat, plate-like forms varying from a few mm (wafer) to several cm thick.

Cylindrical - branching, dendroid forms excluding *Amphipora*; most commonly *Stachyodes*.

Amphipora - a distinctive finger-shaped stromatoporoid, usually 2 to 4 mm in diameter and with a central canal and a peripheral ring of vesicles in well-preserved forms.

Bulbous - small head-shaped forms with diameters less than 8 cm.

Hemispherical - large head-shaped forms with diameters greater than 8 cm.

Irregular - irregular forms not assigned to other growth habits, commonly adapted to an encrusting habit.

A comprehensive legend of the symbols denoting fossils, sedimentary strucutres, diagenetic features and porosity types can be found in Appendix C.

1.3.2 Stratigraphic Picks

Petrophysical logs from 136 conventional subsurface wells were examined to determine stratigraphic relationships in the study area. Following the completion of the core descriptions stratigraphic subdivisions were established and correlated. A total of 9 stratigraphic picks were made (Appendix A). Formation level picks include, in ascending order: Muskeg, Watt Mountain, Slave Point, Beaverhill Lake and Muskwa Formations.

A schematic of the stratigraphic nomenclature used in this study is illustrated in Figure 1.3. The Slave Point was subdivided into a Lower Slave Point Formation and an Upper Slave Point Formation. The Waterways Formation was also subdivided into a Lower Waterways Formation (includes the Cranberry Member) and an Upper Waterways Formation.

The computer mapping program Geographix was used to construct structure and isopach maps from the stratigraphic picks.

1.3.3 Cross Sections

Many petrophysical logs (50) were incorporated into cross sections (Fig. 1.4). Cross sections (Appendix B) are used to illustrate two-dimensional geometry and lateral extent of individual Slave Point facies and associated cycles. Correlation of stratigraphic intervals between wells was based on the interpretation of depositional and diagenetic patterns identified through detailed core (Appendix C) examination. All cross sections were datumed stratigraphically on the top of a shale marker within the Lower Slave Point, interpreted as a relatively flat conformable depositional surface (Wendte, 1992c).

1.3.4 Thin-Section Petrography

The main goal of the thin-section examination was to characterize and decipher the main diagenetic phases, particularly dolomite, of the Slave Point Formation. Samples for thin section petrography (150) were specifically chosen to be representative of all facies within the Slave Point Formation, but particular attention was given to the productive reservoir facies in the study area. The 150 standard-thickness thin sections were prepared, examined and photographed utilizing a conventional Nikon™ binocular petrographic microscope, a Nikon™ fluorescence microscope with blue light excitation

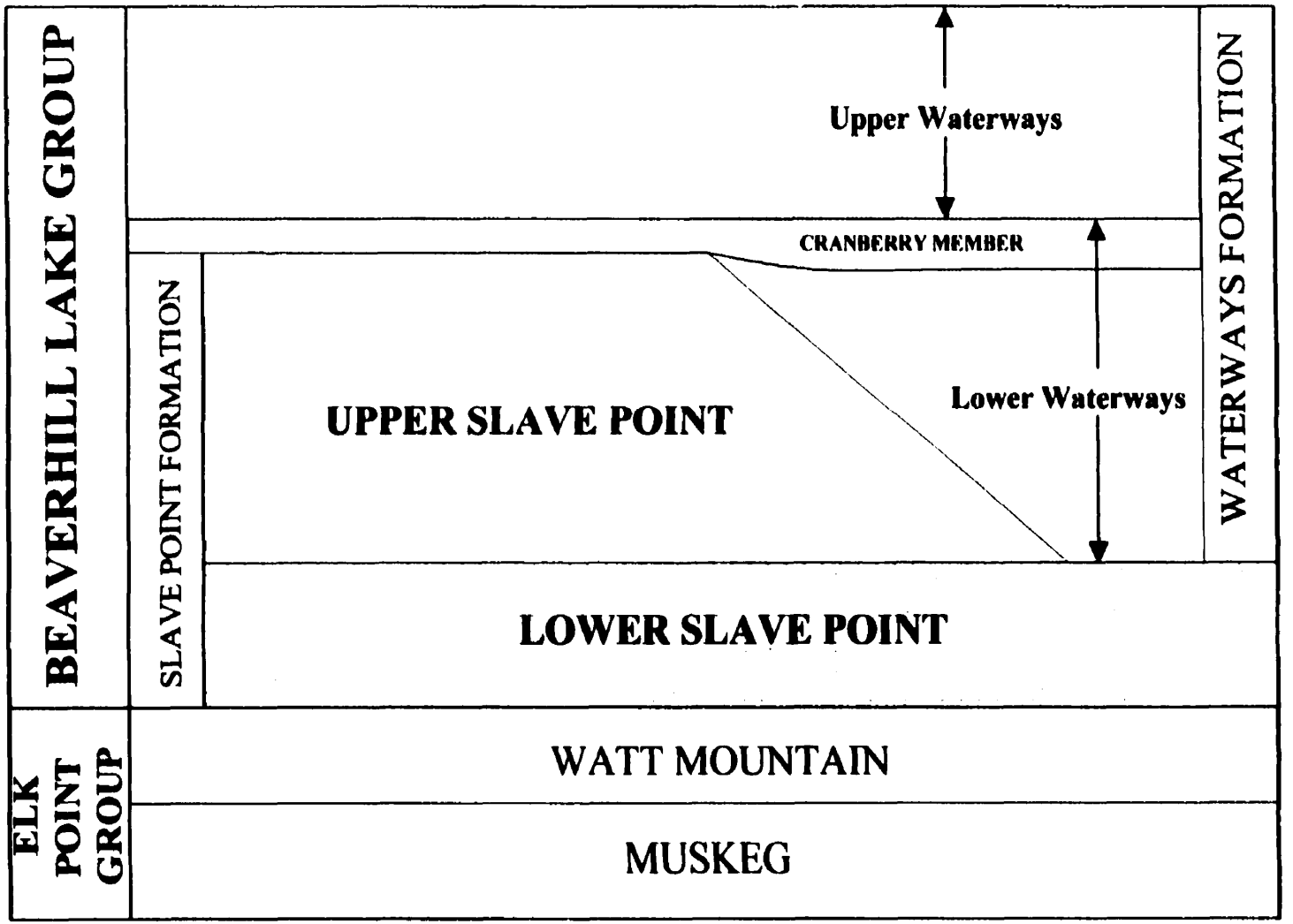

Figure 1.3. Schematic stratigraphic column illustrating stratigraphic relationships from south (left) to north (right) across the study area. The Upper Slave Point reefal buildup developed over platform carbonates of the Lower Slave Point. Waterways Formation argillaceous carbonates and shales are laterally equivalent to and overlie the Upper Slave Point. No scale is implied.

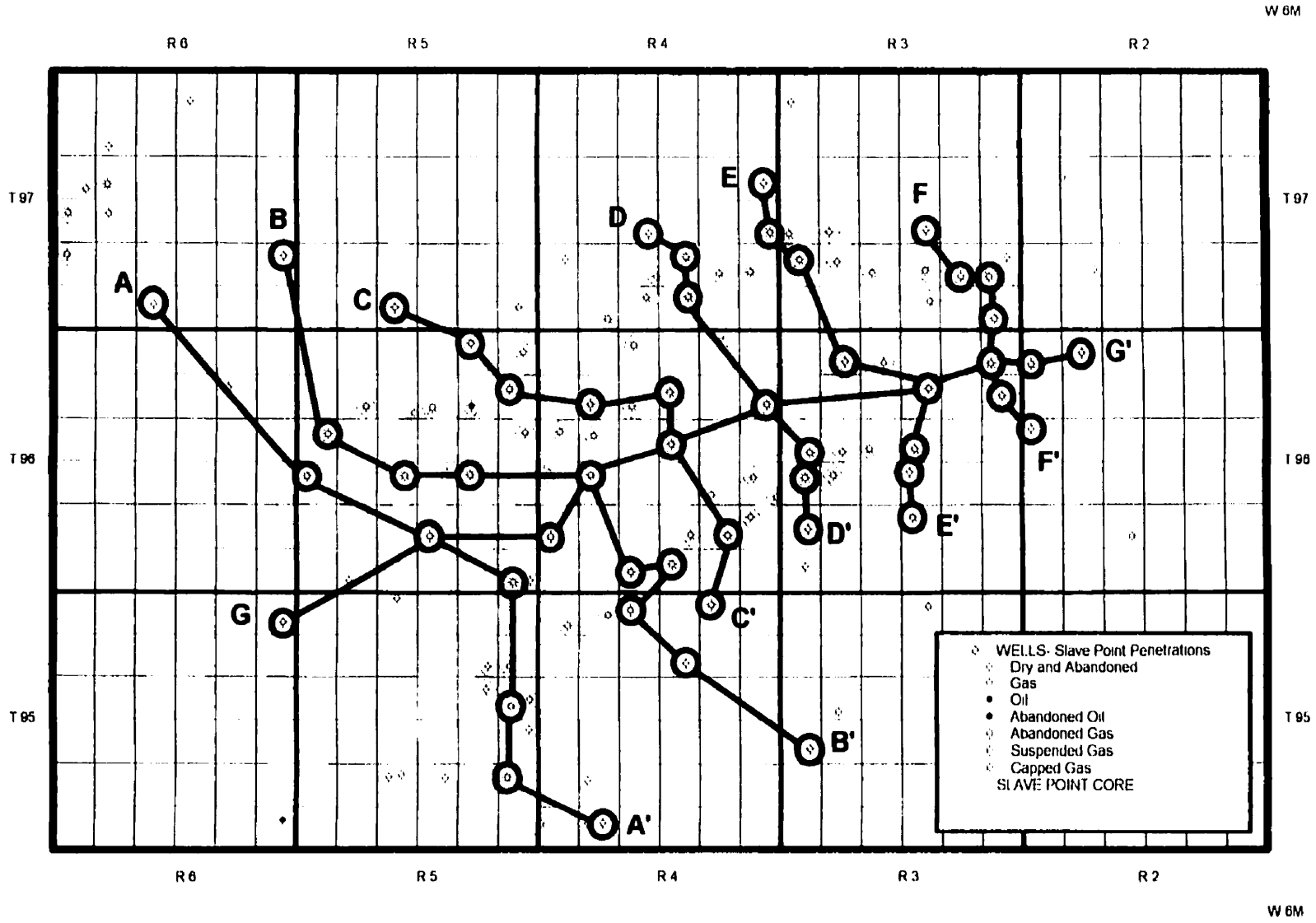

Figure 1.4. Map showing the location of cross-sections A-A' through G-G'constructed in the study area (Appendix B). Diamonds represent Slave Point cored wells. Note the Slave Point Cranberry Field outline (shaded). Scale 1:250,000.

and a Technosyn™ cold cathodoluminescence microscope (model 8200 Mk II) mounted on a Nikon™ Optiphot microscope. The fluorescence and cathodoluminescence microscopes were used to differentiate between diagenetic mineral phases. Operating conditions for cathodoluminescence petrography were 20 KV voltage, 300-400 uA gun current and a 0.05-0.10 torr operating vacuum.. Unpolished thin sections were stained with Alizarin Red S to help differentiate between dolomite and calcite (Evamy, 1963) and potassium ferricyanide to distinguish between non-ferroan and ferroan carbonates (Dickson, 1965).

The petrographic descriptions (Table 1.3) and crystal size divisions (Table 1.4) follow Folk (1972) and dolomite crystal textures and fabrics (Table 1.5) are classified after Sibley and Gregg (1987).

1.3.5 X-ray Diffraction

A few milligrams of each isotope analysis sample were crushed with an agate mortar and pestle and mounted on a glass slide using acetone. Slides were irradiated to determine mineralogy using a Philips PW1710 X-ray powder diffractometer with Cu Kα radiation (40 mA and 40 kV) and 1° slits. A scan speed of 6° 2-theta/minute (fast scan) was used with a scan range of 3° to 65° 2-theta. The $CaCO_3$ content (in mole%) of all isotope samples were derived from x-ray diffractometer data according to the method of Goldsmith and Graf (1958a,b).

1.3.6 Carbonate Cement Stable Isotopes

Calcite cement (n=7) and dolomite cement (n=13) samples were analyzed for carbon ($^{13}C/^{12}C$) and oxygen ($^{18}O/^{16}O$) isotope ratios at the Environmental Isotope Laboratory, University of Waterloo. Powdered carbonate samples ranging from 40 to 120

					Limestones, partly dolomitized limestones, and primary dolomites					Replacement dolomites (V)		
					>10% Allochems Allochemical rocks (I and II)		<10% Allochems Microcrystalline rocks (III)					
					Sparry calcite cement > microcrystalline ooze matrix	Microcrystalline ooze matrix > sparry calcite cement	1–10% Allochems	<1% Allochems	Undisturbed bioherm rocks (IV)	Allochem ghosts		No allochem ghosts
					Sparry allochemical rocks (I)	Microcrystalline allochemical rocks (II)						
Volumetric allochem composition	<25% Intraclasts			>25% Intraclasts (I)	Intrasparrudite (II:Lr) Intrasparite (II:La)	Intramicrudite* (III:Lr) Intramicrite* (III:La)	Most abundant allochem	Intraclasts: intraclast-bearing micrite* (IIIi:Lr or La)	Micrite (IIIm:L); if disturbed, dismicrite (IIImX:L); if primary dolomite, dolomicrite (IIIm:D)	Biolithite (IV:L)	Evident allochem	Finely crystalline intraclastic dolomite (VI:D3) etc.	Medium crystalline dolomite (V:D4)
		<25% Oolites		>25% Oolites (O)	Oösparrudite (Io:Lr) Oösparite (Io:La)	Oömicrudite* (IIo:Lr) Oömicrite* (IIo:La)		Oolites: oolite-bearing micrite* (IIIo:Lr or La)				Coarsely crystalline oolitic dolomite (Vo:D5) etc.	Finely crystalline dolomite (V:D3)
			Volume ratio of fossils to pellets	>3:1 (b)	Biosparrudite (Ib:Lr) Biosparite (Ib:La)	Biomicrudite (IIb:Lr) Biomicrite (IIb:La)		Fossils: fossiliferous micrite (IIIb; Lr, La, or L1)				Aphenocrystalline biogenic dolomite (VB:D1) etc.	
				3:1–1:3 (bp)	Biopelsparite (Ibp:La)	Biopelmicrite (IIbp:La)		Pellets: pelletiferous micrite (IIIp:La)				Very finely crystalline pellet dolomite (Vp:D2) etc	etc.
				<1:3 (p)	Pelsparite (Ip:La)	Pelmicrite (IIp:La)							

Table 1.3. Folk's Classification of carbonate rocks (Folk, 1972).

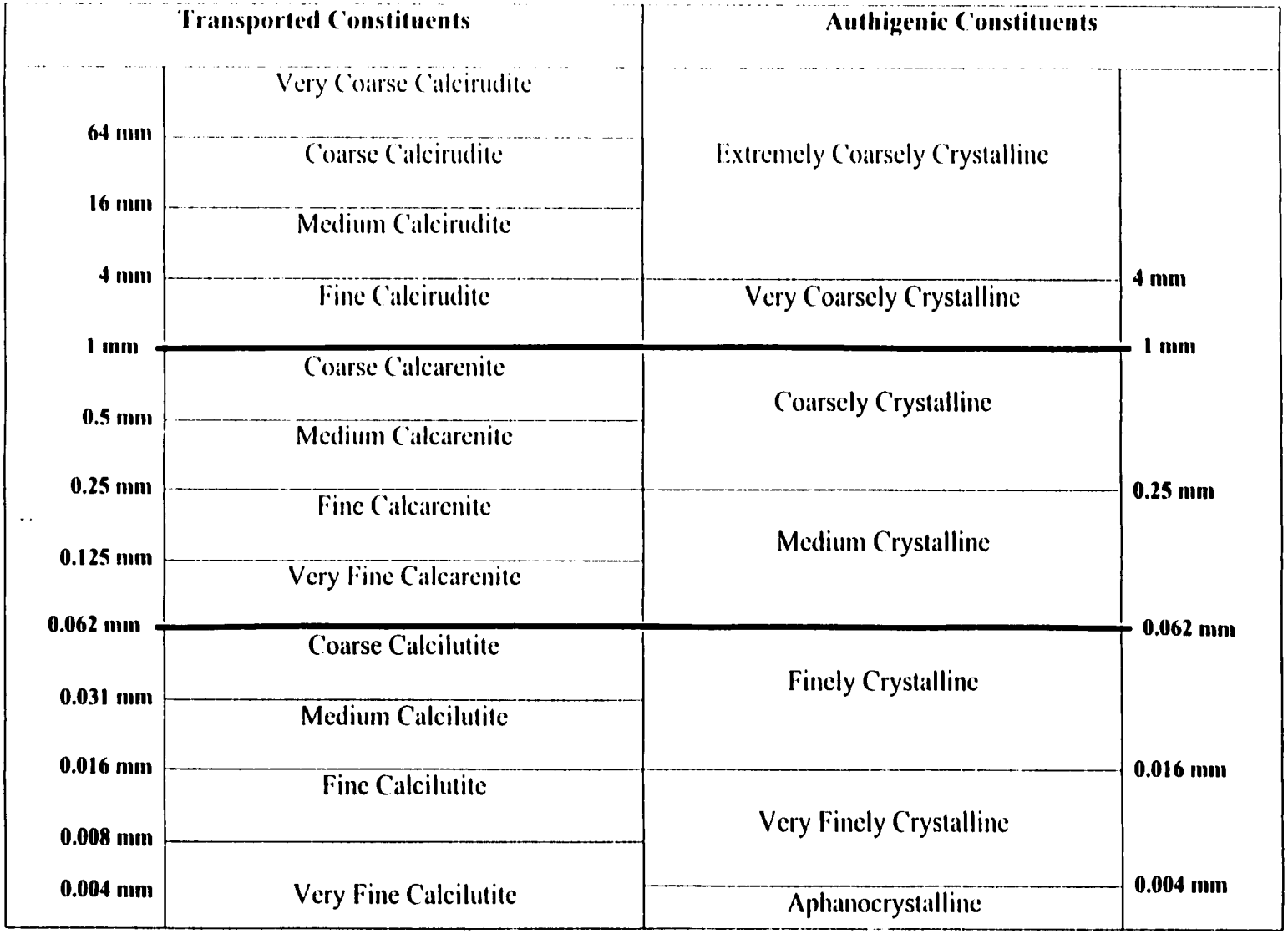

Table 1.4. Folk's grain-size scale for carbonate rocks (Folk, 1972).

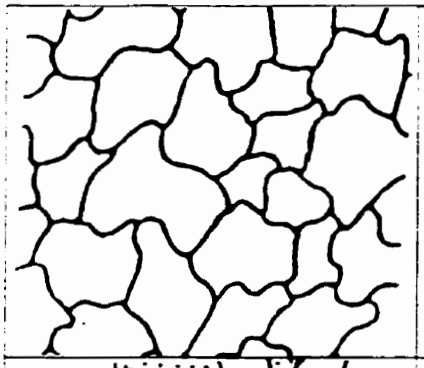	**NONPLANAR:** Closely packed anhedral crystals with mostly curved, lobate, serrated, or otherwise irregular intercrystalline boundaries. Preserved crystal-face junctions are rare and crystals often have undulatory extinction in crossed polarized light.
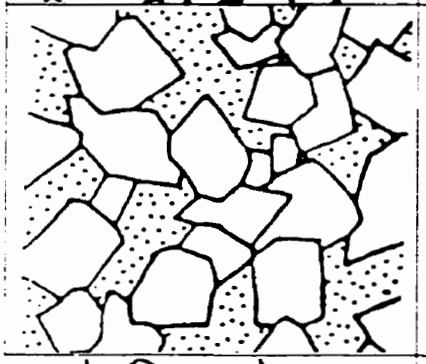	**PLANAR-E (EUHEDRAL):** Most dolomite crystals are euhedral rhombs; crystal-supported with intercrystalline area filled by another mineral or porous (as in sucrose texture).
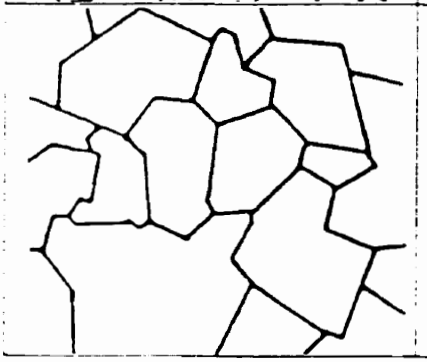	**PLANAR-S (SUBHEDRAL):** Most dolomite crystals are subhedral to anhedral with straight, compromise boundaries and many crystal-face junctions. Low porosity and/or low intercrystalline matrix.

Table 1.5. Classification of dolomite textures; no scale is implied (Sibley and Gregg, 1987).

mg were collected by using a dental drill on slabs or where possible removal of crystals from incompletely filled pores followed by grinding with a pestle and mortar. Powdered samples were analyzed by x-ray diffraction to verify mineralogy. The samples were prepared for isotopic analysis by reacting powdered samples in anhydrous H_3PO_4, following procedures described by Walters et al. (1972), modified after McCrea (1950) and Epstein et al. (1964). For pure dolomite samples, evolved CO_2 was collected after a reaction time of 24 hours at 50°C. For mixtures of calcite and dolomite, CO_2 evolved from calcite was extracted after 1 hour of reaction at 25°C. In addition, the reaction to evolve CO_2 from dolomite was initiated after reaction with anhydrous H_3PO_4 at 25°C for 4 hours to remove calcite. Gas evolved during this first period was discarded and then the remaining sample reacted for 18 hours at 50°C. Results, shown in Appendix D, are reported in conventional per mil (‰) notation relative to the PeeDee Belemnite (PDB) standard using standard correction procedures (Craig, 1957). No corrections for acid fractionation were made for dolomite. The reproducibility for both oxygen and carbon isotopes is ± 0.2‰.

1.4 Stratigraphy

Stratigraphic nomenclature of the Devonian Beaverhill Lake Group has been studied extensively, with numerous revisions of the stratigraphic nomenclature and boundaries. Although the purpose of this thesis is not to redefine the stratigraphic nomenclature of the middle Devonian, some correlation with previous research is necessary. This discussion of the stratigraphy focuses on the variability within and relationships between Devonian members, formations and groups in the northwestern

Alberta study area. Figure 1.5 illustrates middle Devonian stratigraphic nomenclature and relationships in Alberta.

1.4.1 Watt Mountain Formation

The Watt Mountain Formation was proposed by Law (1955) and later re-defined by Belyea and Norris (1971). The type section is located in northern Alberta in the Steen River 2-22-117-5w6 well (standard reference section). The formation is the uppermost unit of the Elk Point Group (Fig. 1.5) and includes green, silty and pyritic shales, arkosic or quartzose sandstones, nodular and argillaceous limestones or dolostones and minor amounts of anhydrite. The Watt Mountain Formation is fossiliferous. Kramers and Lerbekmo (1967) discovered the remains of fresh- and brackish-water algae (*Cyzica* sp.), primitive fish (*Antiarchs*) and primitive plants (*Psilophytes*) in the area east of Lesser Slave Lake, central Alberta. Skall (1975) identified late Givetian ostracods in an area south of Great Slave Lake.

In the study area Watt Mountain Formation sandstones and shales overlie Muskeg Formation anhydrites and dolomites, and are unconformably overlain by the Lower Slave Point (Fig 1.5). The Lower Slave Point is partially equivalent to the Fort Vermilion Formation in the study area.

1.4.2 Fort Vermilion Formation (Lower Slave Point)

The Fort Vermilion Formation consists of a series of interbedded anhydrites, dolostones, limestones and shales that were originally considered to be the basal member of the Slave Point Formation (Law, 1955). The type section is located in northern Alberta in the California Standard Steen River 2-22-117-5w6 well.

Norris (1963) raised the Fort Vermilion to formational status because of the

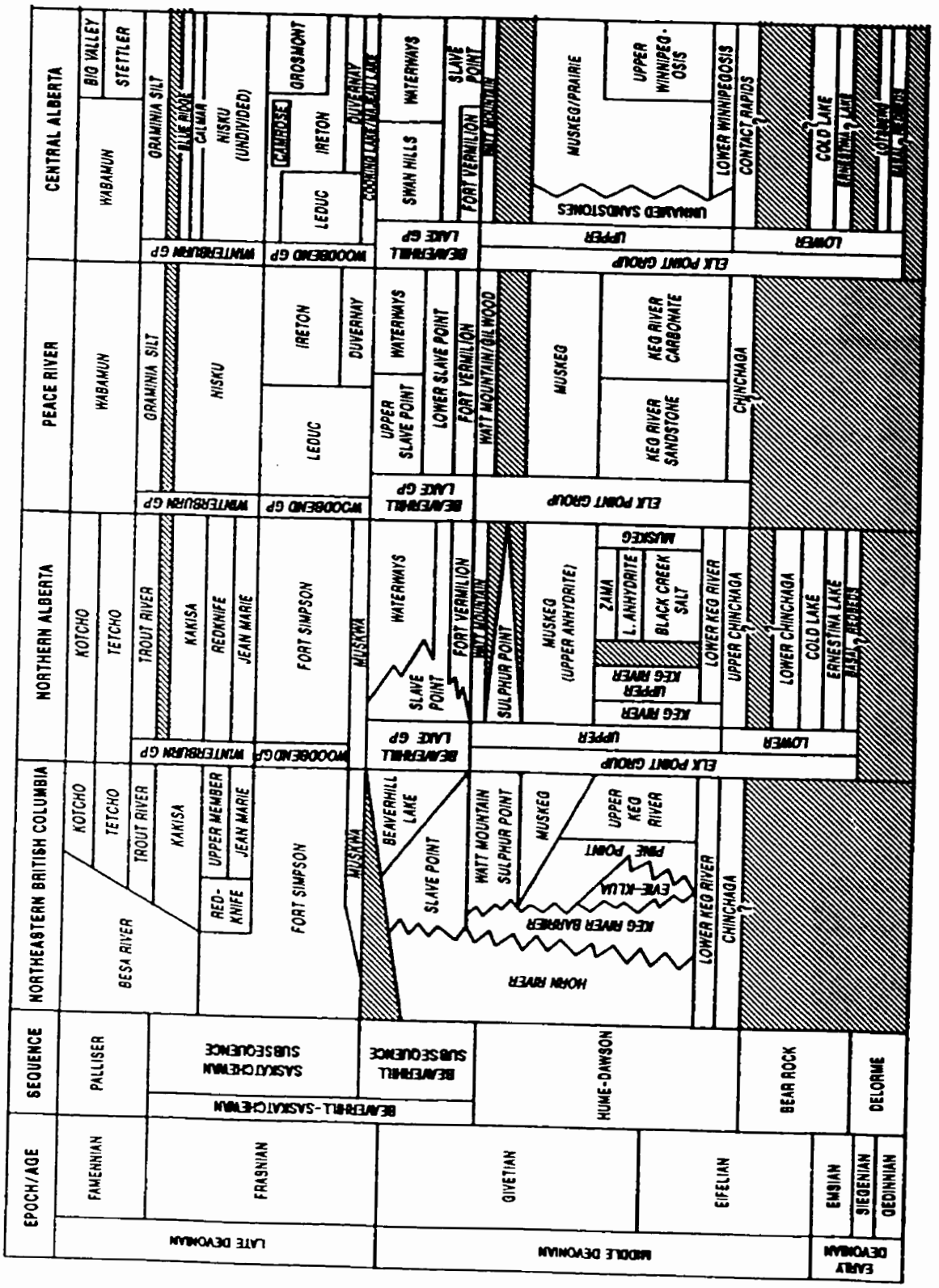

Figure 1.5. The regional stratigraphy and stratigraphic relationships in Alberta and B.C. (Reinson et al., 1993b). The Peace River nomenclature is used in this study.

ability to recognize this group of sediments over a wide area. Leavitt and Fischbuch (1968) re-defined the formation in the Steen River well and thus revised the Slave Point Formation. The Fort Vermilion is described in later reports either as a member (McCamis and Griffith, 1967; Belyea and Norris, 1971; Meijer Dress, 1986) or as a formation (Norris and Uyeno, 1983; Park and Jones, 1985).

There are many conflicting views on the exact position of the boundary between the Fort Vermilion Formation and the underlying coarse clastics and shales of the Watt Mountain Formation (upper Elk Point Group). Fong (1959, 1960), Thomas and Rhodes (1961) and Murray (1965, 1966) placed the base of the Fort Vermilion at the top of a thin sandstone unit (Gilwood Sandstone) within the Watt Mountain Formation. Leavitt and Fischbuch (1968) placed the contact between the Fort Vermilion and the Watt Mountain at the change in lithology from predominantly anhydrite (Fort Vermilion) to predominantly shale (Watt Mountain).

North of the Peace River Arch and east of the Sixth Meridian, the Fort Vermilion is characterized by anhydrites and halite indicative of peritidal and shallow, restricted shelf environments (Burrowes and Krause, 1987). West of the Sixth Meridian, these deposits are transitional to more open-marine carbonates that are not readily distinguished from carbonates of the overlying Slave Point Formation and are therefore included in the Slave Point Formation (Craig, 1987). This is particularly evident immediately north of the Peace River Arch in the Cranberry study area, where the Fort Vermilion is represented by an open marine carbonate facies (Campbell, 1992; Craig, 1987) indistinguishable from and therefore included in the Slave Point Formation (as part of the Lower Slave Point). The Lower Slave Point, is therefore, at least partially the

lateral equivalent of the Fort Vermilion Formation in the study area, varying in thickness between 16 and 73 m.

The end of Fort Vermilion (Lower Slave Point) sedimentation was caused by a transgression that lowered marine water salinity. As a result, shallow shelf carbonates were deposited, representing the first stage of the Slave Point (Upper Slave Point) deposition (Craig, 1987).

The contact between the Fort Vermillion Formation and the Slave Point has been described as: 1) unconformable (Law, 1955; Norris, 1963; Murray, 1966), and 2) conformable (Crawford, 1972; Craig, 1987). In the study area the contact between the Lower Slave Point (Fort Vermilion Formation) and the Upper Slave Point is conformable.

1.4.3 Slave Point Formation (Upper Slave Point)

The Slave Point is a widespread shallow-marine carbonate formation that extends from the central Alberta Basin southeast of the Peace River Arch northward to its type section near Great Slave Lake in the N.W.T. The Slave Point is thickest in northeast B.C. and northwest Alberta, and thins progressively to a zero edge where it onlaps the Peace River Arch (Reinson et al., 1993b). Slave Point deposition was primarily aggradational to backstepping in style and resulted in the development of a wide carbonate platform or bank, termed the Hay River Bank, that extended north of the Peace River Arch Fringing Reef Complex to a barrier reef complex in northeast British Columbia and southern Northwest Territories (Oldale and Munday, 1994). The Peace River Arch remained emergent throughout the Slave Point interval.

An open marine channel or embayment occurs to the west and northwest of the Slave Point Formation in northeast B.C. and the southern N.W.T. An extension of this embayment, the Hotchkiss Channel, extended into Alberta along the north flank of the Peace River Arch, separating the Peace River Arch Fringing Reef Complex from the Hay River Bank. Significant gas and gas-condensate (i.e., Cranberry) discoveries have been made in platform complexes fringing this embayment (Fig 1.6). The Middle Devonian reef complexes of the Slave Point Formation occur along two separate trends: 1) those fringing the exposed granitic landmass of the Peace River Arch (i.e., Cranberry) and; 2) those forming isolated reef banks seaward of the fringing complexes (i.e., North Chinchaga).

Cameron (1918) first described the Slave Point Formation on the west shore of Great Slave Lake as a series of gray, thin-bedded, flat-lying, fine to medium-grained limestones. The name Slave Point Formation was formally proposed by Cameron (1922). In addition, Cameron (1922) and Norris (1965) indicated that limestones of the Slave Point Formation were present further north of the type area in low scarps and hills along the western shore of Great Slave Lake. Campbell (1950) defined the Slave Point in the subsurface as bounded by Upper Devonian shales above and by the Amco Shale (Watt Mountain Formation) below. Law (1955) described the Slave Point of northwestern Alberta as a brown to light gray, cryptocrystalline, microfragmental or chalky and slightly dolomitic limestone in the California Standard Steen River 2-22-117-5W6M well (standard reference section). Fossils included brachiopods, ostracods and poorly preserved colonial organisms such as stromatoporoids, corals and algae. A basal evaporite unit was also present (Fort Vermilion Member). Subsequently, Law (1955)

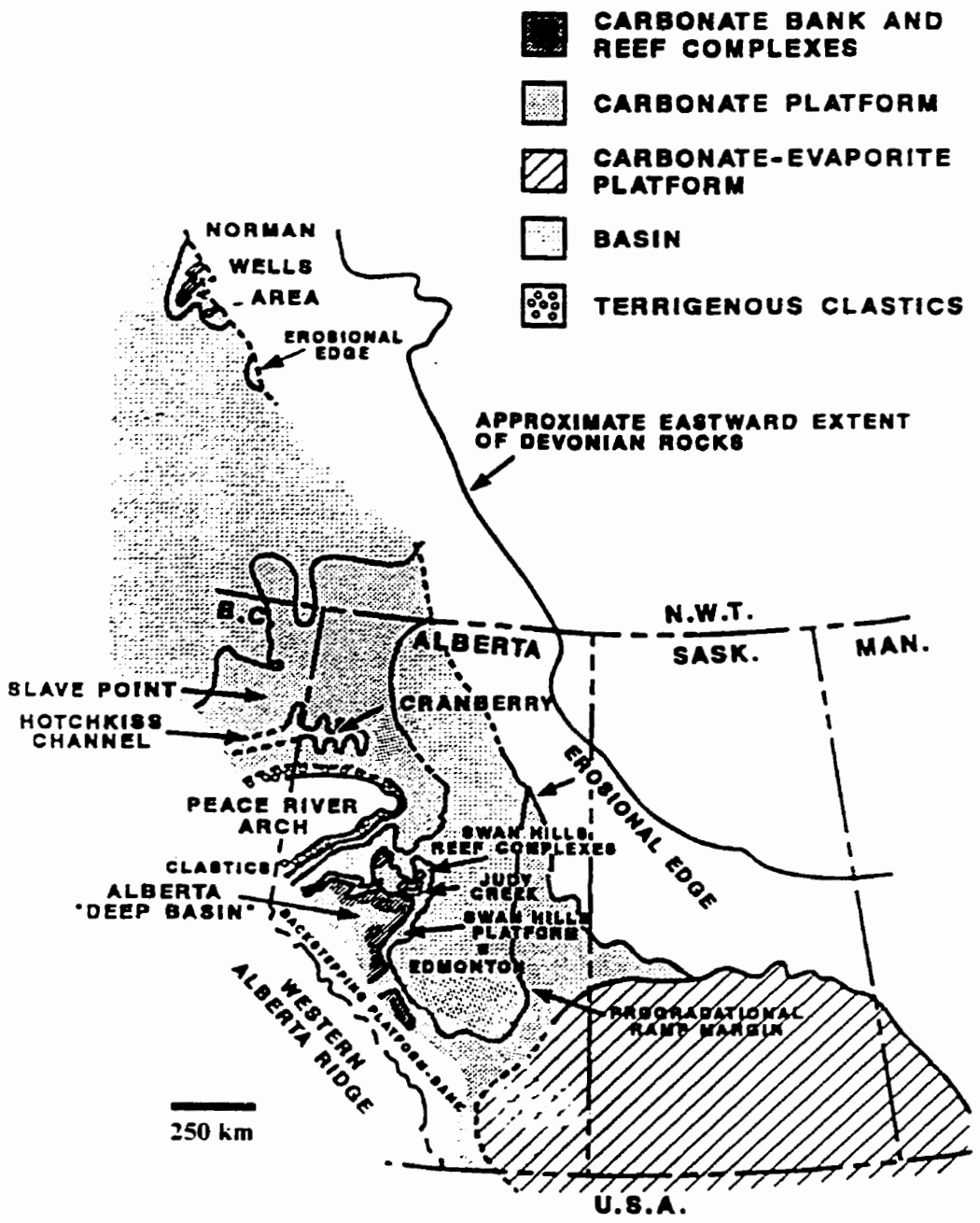

Figure 1.6. Paleogeography of the Slave Point Formation in Alberta and northeast B.C. (modified after Campbell, 1992).

redefined the Slave Point to exclude the Amco Shale and recognized the Fort Vermilion Member as a basal sequence of interbedded anhydrites and carbonates. The stratigraphic nomenclature presented by Law (1955) is generally accepted and followed in scientific literature.

Several biostratigraphic and paleoecologic studies of the Slave Point Formation have determined an upper Middle Devonian (Givetian) age for the Slave Point Formation (Braun et al., 1988; Braun 1967; Featherstone 1982; Norris and Uyeno, 1983, 1981; Uyeno 1979, 1974; McGill, 1966, 1963).

Additional studies of the Slave Point Formation include regional sedimentological and paleogeographic studies in northeastern British Columbia (Budrevics, 1974; Torrie, 1973; Griffin, 1965; Gray and Kassube, 1963;) and northern Alberta (Dunham et al., 1983; Hiscock, 1984; Kwiatkowski, 1985; Tooth and Davies, 1987, 1988; Gosselin et al., 1988; Gosselin, 1990); geochemical studies (Cameron, 1966; Sikabonyi, 1958); Slave Point dolomite studies (Hutton, 1994, Qing and Mountjoy, 1989a,b, 1991); and a study on the association of stylolitic carbonates and organic matter within the Slave Point Formation (Dunham and Larter, 1981).

There are suprisingly few publications that have directly addressed the Slave Point Formation in the study area. Crawford (1972) presented a facies analysis of the Slave Point in northern Alberta. Craig (1987) described the depositional environments of the Slave Point Formation in the Peace River Arch area. Tooth and Davies (1989) and Davies and Tooth (1987) divided the Slave Point Formation in the Gift Lake Field into four major lithofacies units: 1) the Basal Platform, 2) the Basal Bank, 3) the Stromatoporoid Reef and 4) the Forereef Sand Apron. Campbell (1992) examined the

Slave Point Formation in the Cranberry Field and divided the Slave Point into two megasequences: 1) a lower, progradadtional limestone succession and associated interior lagoon, and 2) an upper, aggradational to backstepping reefal buildup. He suggested that the reefal buildups were eventually drowned and abandoned and that the remnant deeper water lagoon at Cranberry was later filled by open marine crinoidal lime mudstones and wackestones. Bloy and McKellar (1992) suggested that the Slave Point was deposited around a downwarp or trough that extended from just east of Cranberry west to British Columbia. They described the Slave Point reservoir facies at Cranberry as mudbanks, composed primarily of peloids with scattered stromatoporoids and corals, deposited in a low energy, stressed environment. Bloy and McKellar proposed the term "otter unit" for the post-Slave Point basin fill. They noted that the 'otter unit" was deposited after the mudbanks and prior to the overlying Waterways Formation, and acts as a lateral seal at Cranberry.

The end of Slave Point deposition occurred gradually in the Peace River Arch area (Burrowes and Krause, 1987; Craig, 1987). When sea level rose sufficiently to inhibit platform growth around the Peace River Arch, the shallow water faunal elements higher on the Arch maintained their growth, resulting in the development of the reef complexes of the Swan Hills Formation. These conditions existed until a later sea level rise stopped their growth and the area was covered by deposits of the Waterways Formation (Craig, 1987).

The contact between the Slave Point Formation and the overlying Waterways Formation has been proposed as: 1) unconformable (Park and Jones, 1985; Norris and Uyeno, 1983; Featherstone, 1982; Belyea and Norris, 1971; Norris, 1965, 1963; Douglas,

1959; Law, 1955; Warren and Stelck, 1950); 2) disconformable (Crawford, 1972; Braun, 1967); 3) paraconformable (Carrigy, 1959); 4) gradational (Williams, 1977); and 5) conformable (Meijer Drees, 1986). North of the Peace River Arch, in the Cranberry study area, the upper surface of the Slave Point Formation is commonly a submarine hardground, a disconformable boundary, that is erosional, pyritized, with fossils typically truncated (Gosselin et al., 1988). Hadley and Jones (1990) suggested this surface may represent a hiatus, subsequent erosion, submarine cementation and/or omission before deposition of the overlying Waterways Formation.

1.4.4 Waterways Formation

Warren (1933) proposed the name Waterways Formation for the sequence of rocks in the McMurray area that lie unconformably below the Lower Cretaceous and above the Devonian evaporites. The Waterways Formation was later subdivided by Crickmay (1957) into five members, in ascending order: Firebag, Calmut, Christina, Moberly and Mildred. Norris (1963) recognized these same five members in the Bear Biltmore No.1 7-11-87-17w4 well, which is now used as a standard reference section. The Waterways Formation consists of a sequence of clinoforming interbedded argillaceous, fossiliferous limestones and gray-green calcareous shales that form a basin-fill facies younger than the Slave Point Formation (Hadley and Jones, 1990). A northern and/or northeastern source is proposed for the origin of the Waterways siliciclastic sediments (Braun et al., 1988). Only a thin basal portion is chronostratigraphically equivalent to the sediments of the Slave Point (Upper Slave Point) in the study area.

An important aspect of the Waterways Formation is that it differs from most other basin-fill successions, such as those of the later Woodbend and Winterburn Groups.

Although, in overall geometry and depositional patterns it is similar, compositionally it is different. The Waterways is dominantly composed of fine-grained carbonate lacking any significant clay-shale content. The reason for this compositional difference is thought to be the result of the shallow bathymetry of this initial basin-filling unit combined with the large areas of the basin that existed as shallow water carbonate platforms that shed material into the adjacent coeval basinal settings (Stoakes, 1992).

The Waterways Formation in the study area consists of interbedded calcareous shales, lime mudstones and wackestones. The Waterways Formation onlaps and overlies the Slave Point Formation in the study area, creating an effective stratigraphic trap in the study area (Crawford, 1972; Craig, 1987).

1.5 Structural Influences

The Peace River Arch (PRA) is interpreted as a structure that originated in the early Paleozoic an as an uplift over an incipient rift that extended from the western passive continental margin (Cant, 1988). By the Middle Devonian another phase of uplift had occurred, resulting in crustal tension, which was relieved by normal faulting. The faults formed horsts and grabens oriented approximately parallel and perpendicular to the axis of the PRA (Fig. 1.7) (Cant, 1988). The crests of these fault blocks were the centers for the development of numerous reef carbonates in a wide belt around the PRA (O'Connell et al., 1990).

The Peace River Arch had a profound influence on Slave Point sedimentation. During deposition of the Slave Point Formation the entire region was relatively stable with slow, even subsidence so that Slave Point carbonates onlap a stable PRA (Cant,

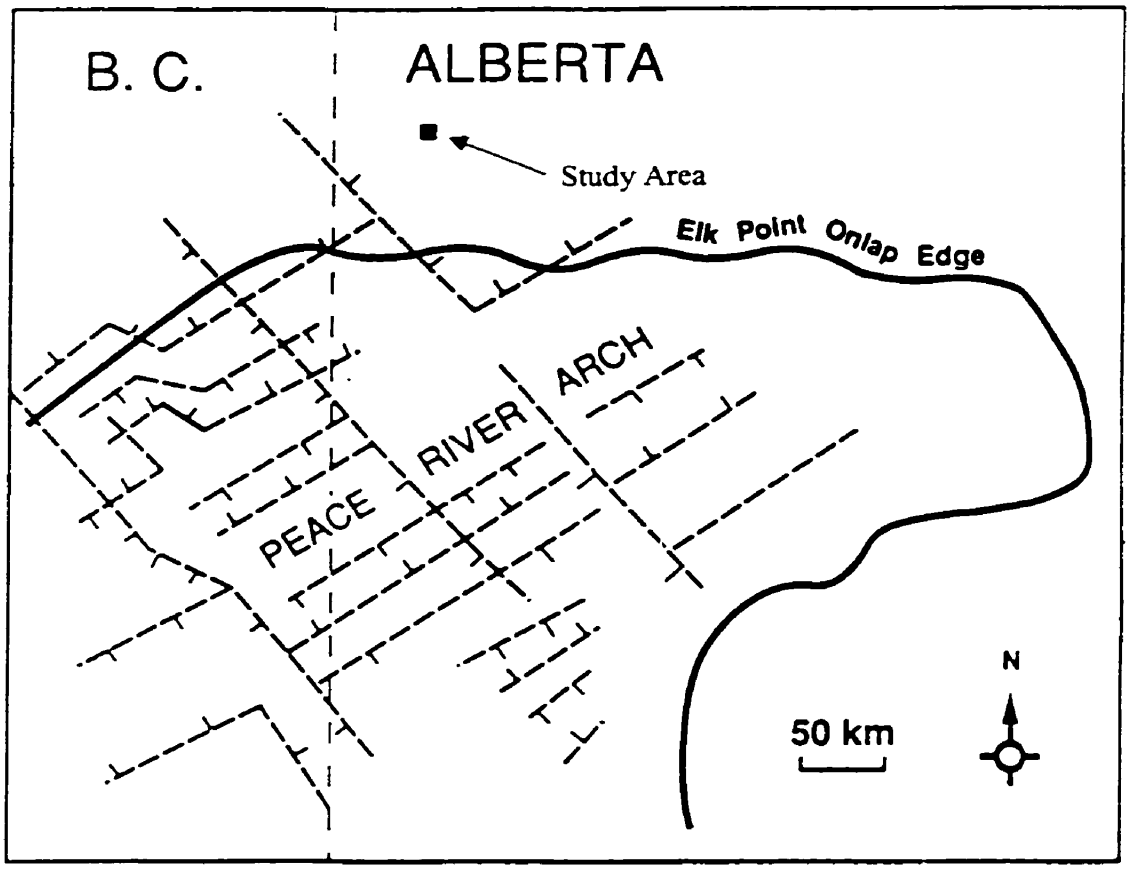

Figure 1.7. Interpreted faults that offset Paleozoic rocks and have more than 40 m of throw in the Peace River Arch area (Bell and McCallum, 1990)

1988). Keith (1990) indicates that the PRA was a high, stable feature at the beginning of Slave Point time. The basin surrounding the PRA in the study area remained relatively stable, subsiding slowly and evenly throughout Slave Point deposition (Keith, 1990). At the end of Slave Point time a period of instability commenced with an increasing rate of differential subsidence away from the PRA.

The Slave Point Formation in other areas of the Western Canada Sedimentary Basin (WCSB) appears to be strongly influenced by antecedent topography of the underlying Precambrian (Podruski et al., 1988). Tooth and Davies (1989) suggest that irregular topography on the Precambrian unconformity surface strongly influenced depositional facies and thickness and had a major control on the localization of the Slave Point reef complex at Gift Lake. Gosselin et. al. (1989) points to the Peace River Arch as a basement controlled, periodically active rift shoulder which influenced reef distribution during the deposition of the Slave Point Formation in the Golden and Evi Fields.

A third order residual structure map on the surface of the Watt Mountain Formation in the study area (Fig. 1.8) clearly illustrates a northeast-southwest trending antecedent topographic high that has influenced Slave Point deposition. Whether this high is related to the Precambrian is uncertain, as only three wells penetrate the Precambrian, in the study area. However, Craig (1987) proposes that Slave Point reefal developments in the Peace River Arch area may be in part related to a slight buildup on the underlying subtidal shelf or Precambrian highs.

In the WCSB, tectonic loading took place during two widely spaced periods: 1) the Antler orogeny from Late Devonian to Early Carboniferous, and 2) the Columbian and the Laramide orogenies from Late Jurassic to early Tertiary (Qing and Mountjoy,

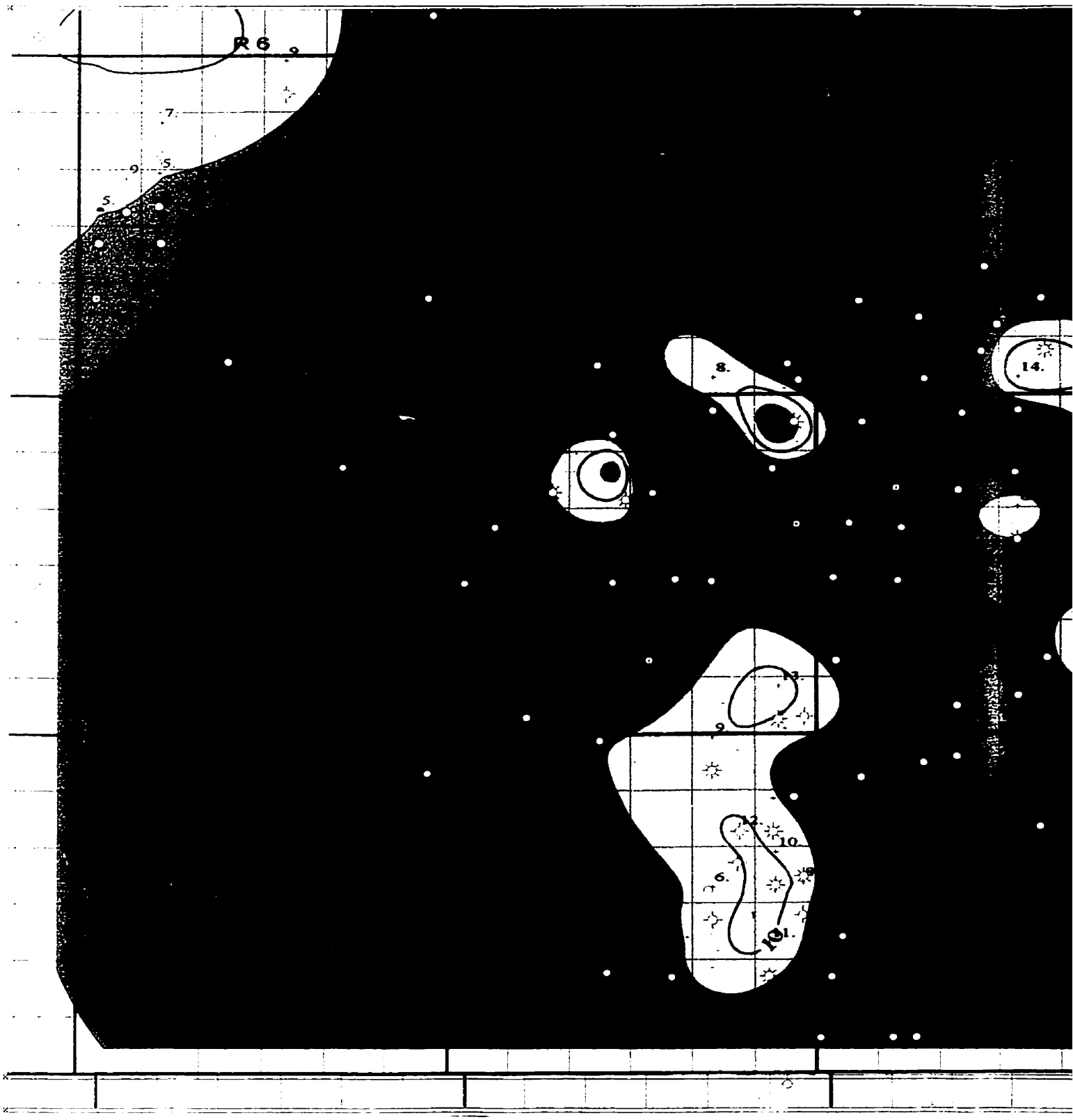

Figure 1.8. Watt Mountain third order residual stru
the northeast-southwest trending residual hig
is 5 m.

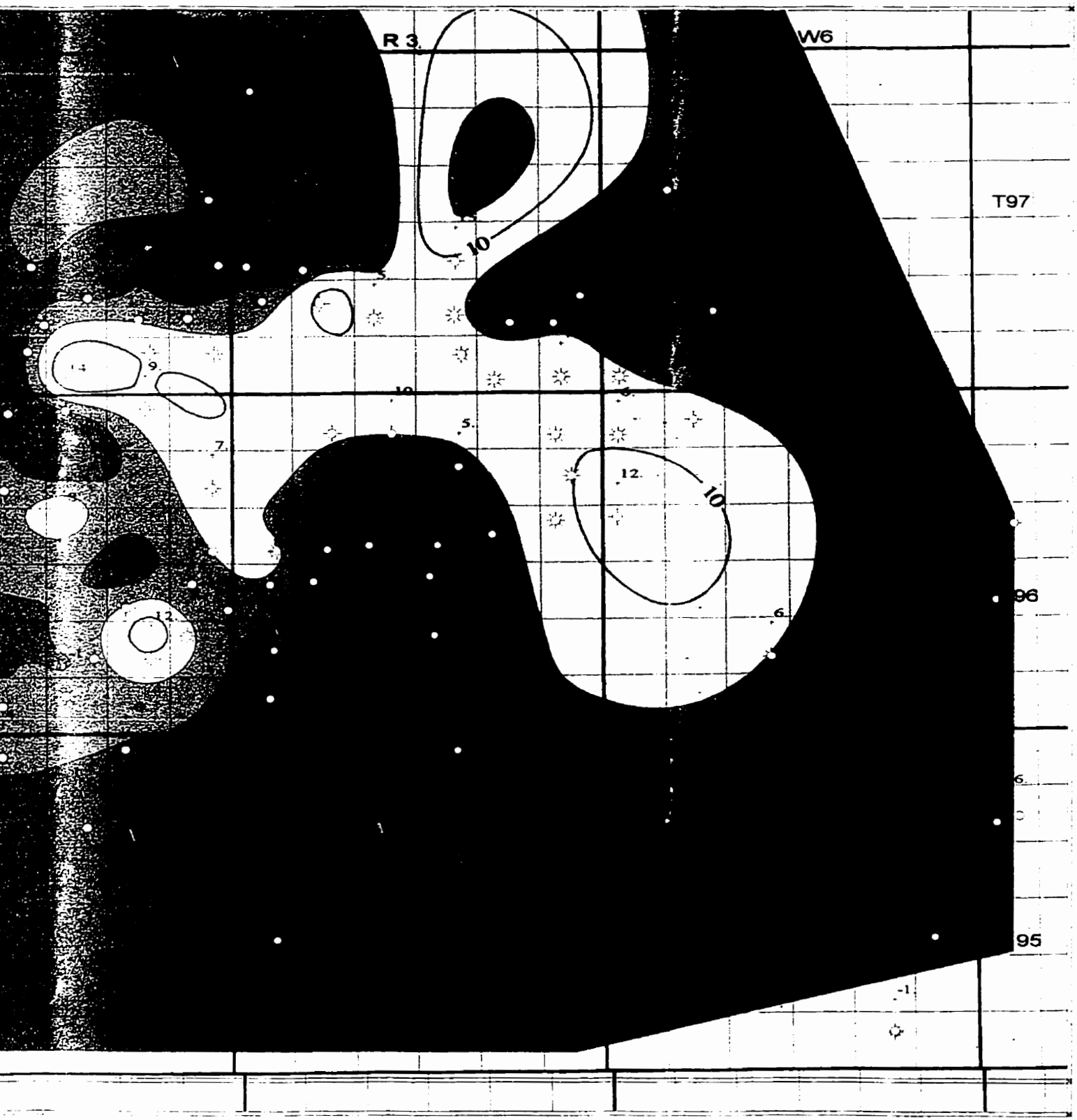

residual structure map. Scale 1:150,000. Note
g residual high in the study area. Contour Interval

1994). Figure 1.9 illustrates a structure map of the top of the Slave Point Formation across the study area. Regional southwest dip is broken by numerous northeast-southwest trending, normal and reverse faults with throws on the order of tens of meters. Fault interpretation is based entirely on geologic control. Faulting in the study area appears to be post-Beaverhill Lake Group in age. The majority of faulting appears to be early Mississippian in age or younger (White, 1995) and probably originated during the Antler orogeny from Late Devonian to Early Carboniferous.

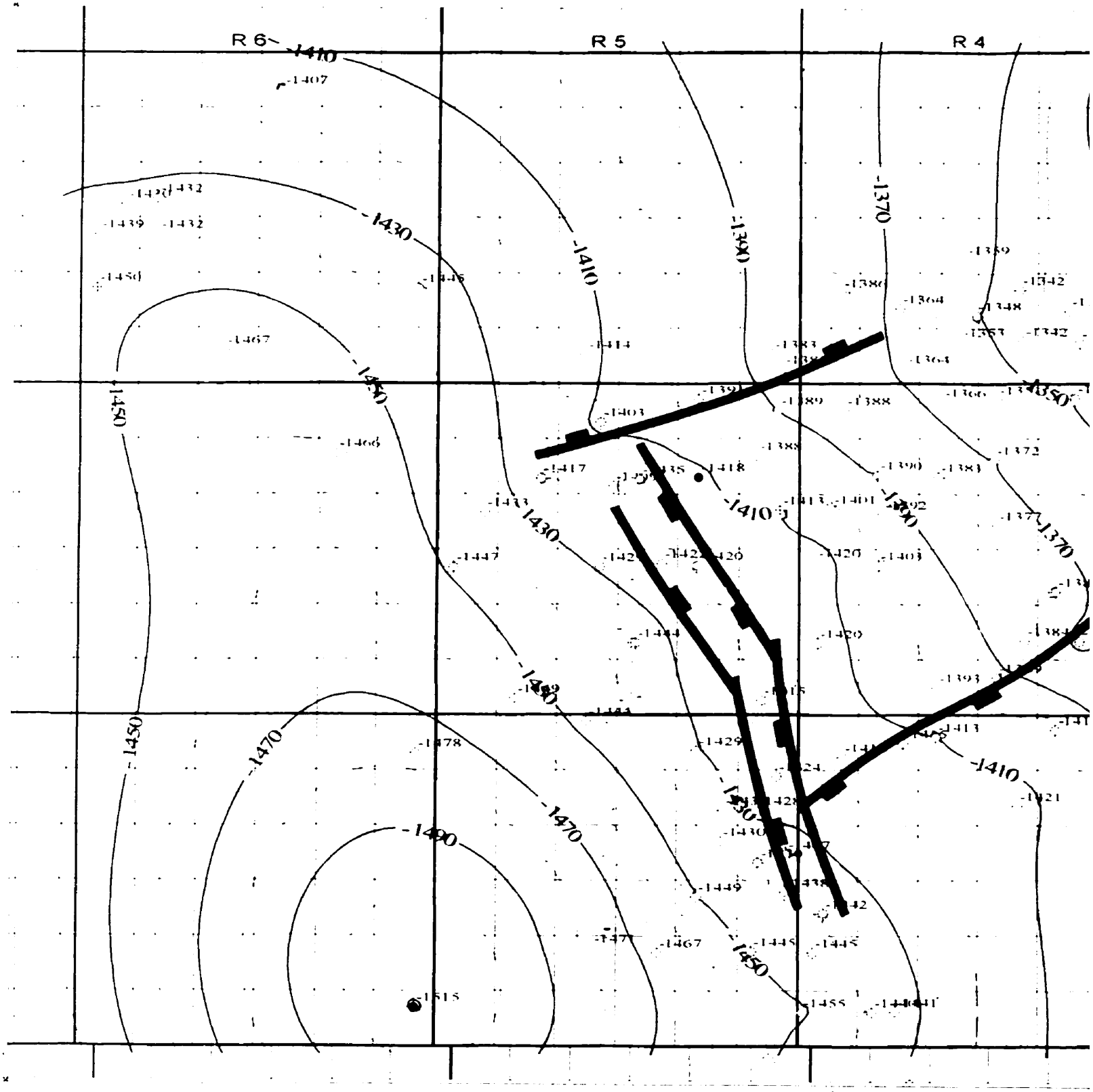

Figure 1.9. Slave Point structure map. Scale 1:150,000. Note t
fault system. Fault interpretation is based on geologic c
10 m.

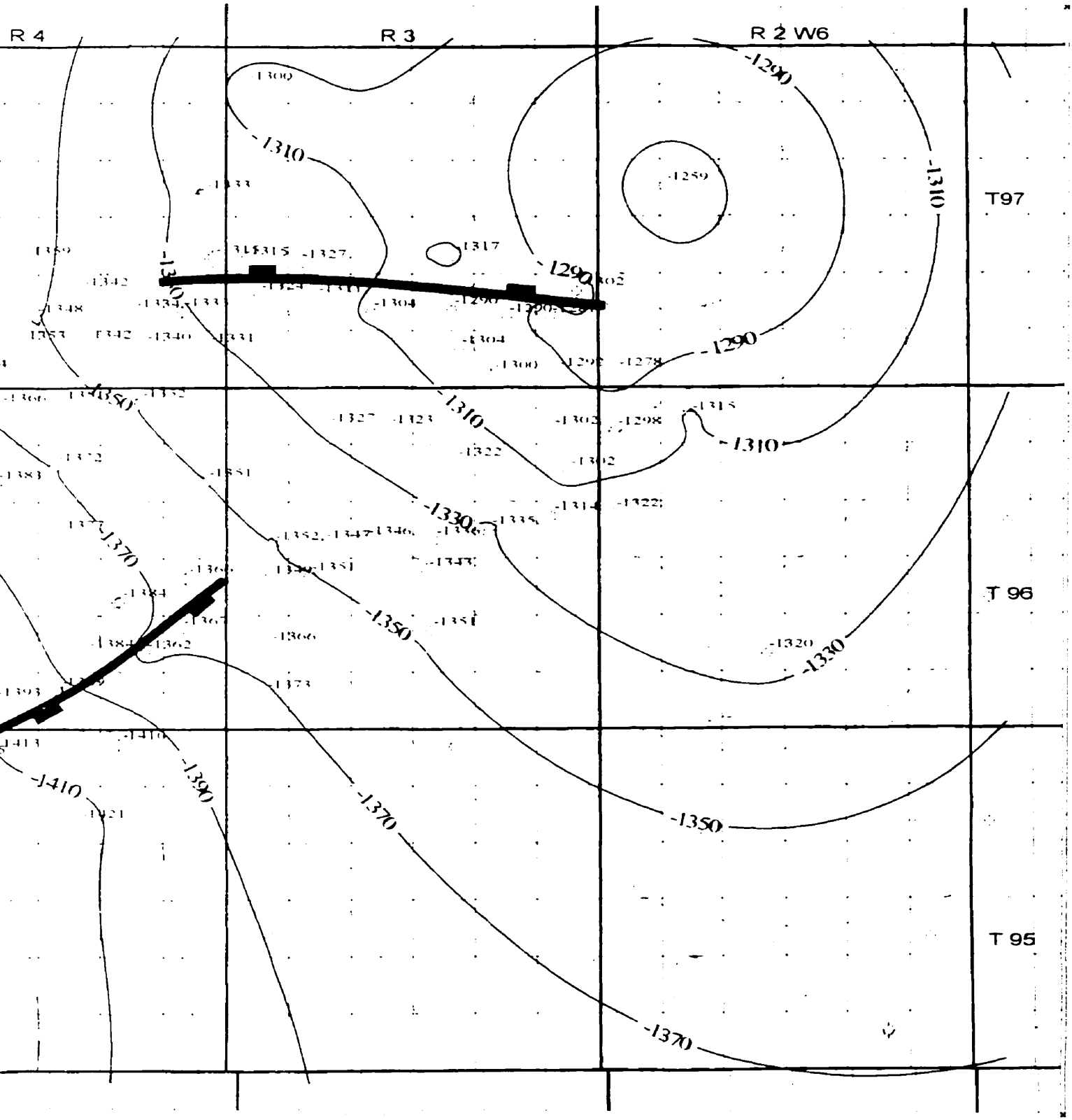

:150,000. Note the major north-south
ed on geologic control. Contour Interval is

CHAPTER 2: SEDIMENTOLOGY

2.1 Introduction

The purpose of this chapter is to formulate a depositional model, which examines the various carbonate facies, associated depositional cycles and environments. Geological subdivisions within the study area were defined through gamma, sonic, and neutron-density logs and interpretation from core descriptions (Appendix C). The Slave Point Formation unconformably overlies the Watt Mountain Formation and is characterized by a clean gamma curve (Fig. 2.1). The Slave Point Formation has been informally subdivided on the basis of extensive core study into a Lower Slave Point and an Upper Slave Point (Fig. 2.1). Similarly, the Waterways Formation has been subdivided into a Lower Waterways and Upper Waterways (Fig. 2.1).

The Lower Slave Point – Upper Slave Point contact is based on numerous core descriptions, in turn correlated to a petrophysical log response. The contact begins stratigraphically above a regionally correlatable argillaceous limestone to calcareous shale unit (Fig 2.1). Similarly the Upper Slave Point – Lower waterways contact, occurs 20 to 45 m above the conformable Lower Slave Point – Upper Slave Point contact, at the first pronounced rightward shift of the gamma ray and spontaneous potential curves (Fig. 2.1).

2.2 Slave Point Facies

The Slave Point Formation exhibits a wide variety of organic and inorganic constituents, depositional textures, primary sedimentary structures and color.

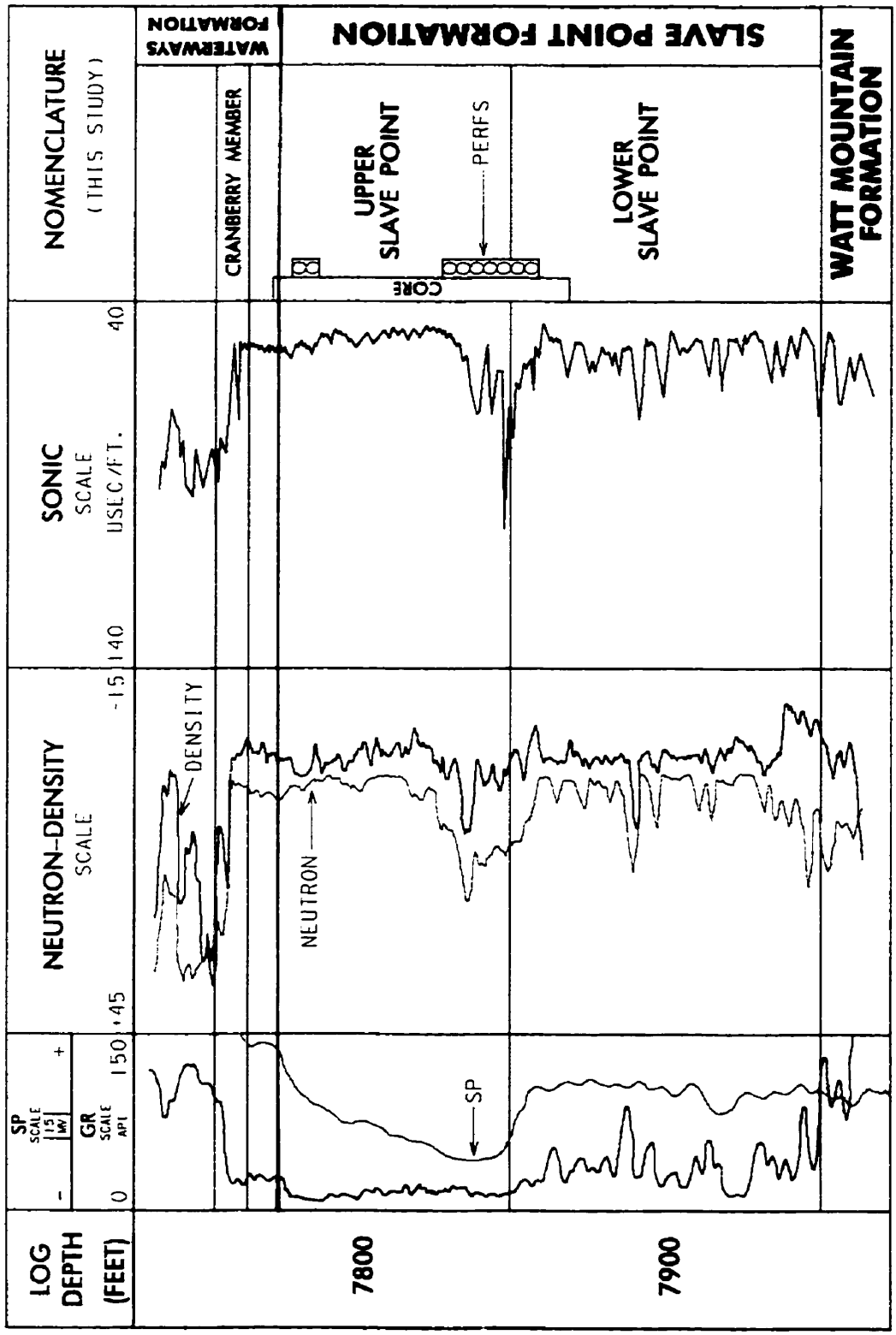

Figure 2.1. Type log showing typical log responses, units picked for this study, cored interval and producing intervals (perfs) for the Slave Point Formation in the Cranberry study area.

Sedimentary packages defined on the basis of fossil assemblages, depositional texture, relative position and relative thickness, are grouped into broader depositional facies. Environmental interpretations of these facies are based on the depositional attributes, mentioned previously, comparison with modern analogues, and on vertical and lateral facies associations. Most of the Slave Point facies can be grouped into 5 typical carbonate depositional environments (Fig. 2.2): foreslope, reef flat, lagoon, fore reef and basin.

Paleo-water depths of the facies were estimated according to their relative position on a cross-section datumed on a marker that approximates a time-synchronous, depositional flat surface. The vertical relief measured along a cycle boundary between a given facies and reference limestone deposited at or very near sea level, such as a tidal flat laminite, will approximate the paleobathymetry of the given facies (Wendte, 1992c,d).

Examination of cores in this study reveals 14 major depositional facies: 3 of which are part of the basal laterally widespread Lower Slave Point, which is overlain by 7 depositional facies of the more localized reefal buildup of the Upper Slave Point. The Upper Slave Point facies are overlain or laterally adjacent to 4 facies of the Waterways Formation. These depositional facies are named according to Embry and Klovan's (1971) modification of Dunham's (1962) carbonate rock classification (Chapter 1). Emphasis in interpreting these depositional facies was also placed on the growth forms of stromatoporoids, the dominant organism and frame-builder in the Slave Point Formation, as described previously (Chapter 1). The 96 core descriptions are in Appendix C.

The depositional facies of the Slave Point and Waterways Formations are

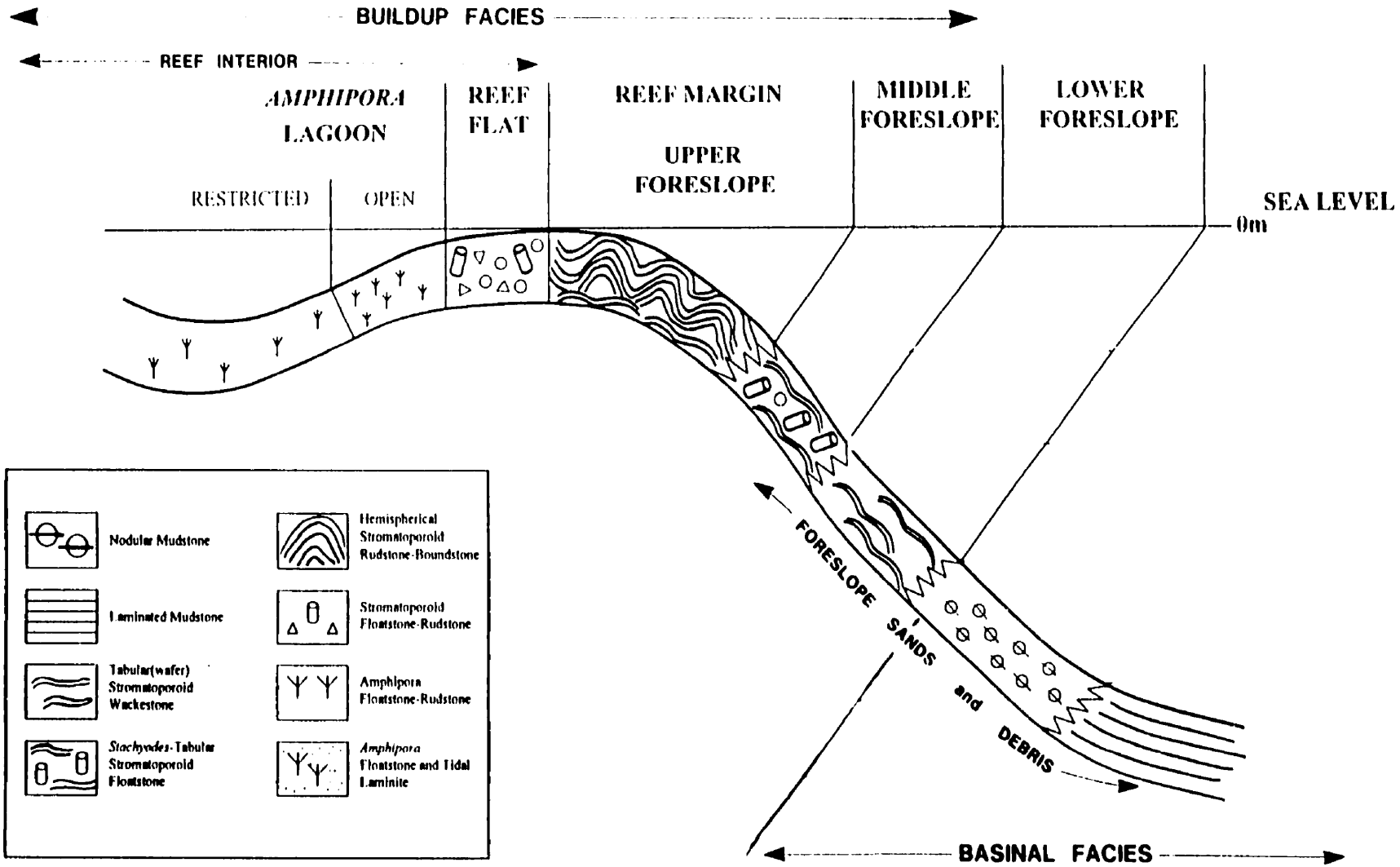

Figure 2.2. Typical cross-section of a Devonian (Swan Hills) reef margin illustrating the different reef zones and environments of different reef-building forms (after Wendte, 1992d).

summarized in Figure 2.3 and are discussed below.

2.2.1 Facies 1: Mudstone

This facies consists of grey to dark grey lime to very argillaceous mudstone with a laminated to slightly nodular fabric (Fig. 2.4). Although fauna is sparse, disarticulated atrypid brachiopods (Craig, 1987) and crinoids, when present, generally represent less than 10% of the total rock volume.

The matrix consists dominantly of lime mud (micrite) (≥ 50%), peloidal grains and ostracods. The matrix often shows a bimodal grain size with grainier (peloids?) areas (burrows?) within a more micritic matrix. Porosity is not developed in this facies.

The lower contact of this facies is a fairly widespread log marker in the northern Alberta study area. It corresponds to a change from the regressive sandstones and shales of the underlying Watt Mountain Formation to the nodular mudstones of the Lower Slave Point above (Fig. 2.1). Although rarely observed in cores in the study area, this change is reflected as a sharp contact characterized by pyrite mineralization and sub-rounded to rounded shale clasts originating from the underlying Watt Mountain Formation (Fig. 2.5). The upper contact of Facies 1 is commonly sharp (can also be gradational) into the overlying nodular brachiopod-crinoidal wackestones of Facies 2 (Fig. 2.6).

This facies indicates a low-energy, relatively deep (i.e. below storm wave base) subtidal environment of deposition. The sparse fauna and low diversity of organisms suggests a restrictive, perhaps slightly above normal marine salinity conditions, environment of deposition.

It is difficult to estimate paleo-water depths for this cycle, as no depth diagnostic criteria are present. However, deposition possibly occurred in relatively deep water

		FACIES	ROCK TYPES	IMPORTANT CONSTITUENTS	SEDIMENTARY STRUCTURES
Lower Waterways	14	**Nodular Brachiopod Wackestone**	Dark-colored brachiopod lime wackestone	Abundant brachiopods; common crinoids	Extensive burrowing, carbonaceous shale partings
	13	**Nodular Mudstone**	Medium-colored lime mudstone; minor wackestone	Crinoids, ostracods, gastropods	Extensive burrowing
	12	**Laminated Mudstone**	Dark-colored lime mudstone		
	11	**Stromatoporoid Wackestone and Floatstone**	Medium-colored lime wackestone and floatstone	Fragments of tabular, hemispherical stromatoporoids, *Stachyodes*, *Amphipora*, *Thamnopora*, brachiopods, crinoids	Some burrowing
Upper Shave Point	10	**Bulbous Stromatoporoid Grainstone**	Light-colored bulbous stromatoporoid lime grainstone and packestone	Common bulbous stromatoporoids; some irregular stromatoporoids	
	9	**Lime Packestone**	Light- to Medium-colored lime packestone, minor grainstone	Common micritic lumps and/or peloids; calcispheres	Some burrowing
	8	**Hemispherical Stromatoporoid Rudstone and Boundstone**	Light- to Medium-colored hemispherical and bulbous stromatoporoid lime boundstone; minor rudstone	Abundant *in situ* hemispherical and tabular stromatoporoids, common bulbous, irregular stromatoporoids	
	7	**Tidal Laminite**	Medium-colored laminated lime packestone; minor lime mudstone	Cryptomicrobial laminations, peloids, *Amphipora*	Planar-fenestrae
	6	***Amphipora* Rudstone and Floatstone**	Medium- to dark-colored Amphipora lime rudstone and floatstone; minor wackestone	Abundant *Amphipora*; common calcispheres; some bulbous stromatoporoids, *Stachyodes*.	
	5	**Tabular Stromatoporoid Floatstone and Rudstone**	Light- to dark-colored tabular stromatoporoid lime rudstone and boundstone	Abundant tabular stromatoporoids; common hemispherical; some *Stachyodes*, *Thamnopora*	Abundant binding
	4	***Stachyodes* – *Thamnopora* Floatstone**	Light- to dark-colored *Stachyodes* and *Thamnopora* lime floatstone	Abundant *Stachyodes*; some *Thamnopora*, bulbous stromatoporoids	
Lower Shave Point	3	***Thamnopora* Wackestone**	Dark- to medium-colored *Thamnopora* lime wackestone	common *Thamnopora*, some tabular (wafer) stromatoporoids, *Stachyodes*, brachiopods, crinoids	
	2	**Nodular Brachiopod – Crinoidal Wackestone**	Dark-colored brachiopod-crinoidal lime wackestone	Common brachiopods and crinoids	Extensive burrowing, carbonaceous shale partings
	1	**Mudstone**	Dark-colored lime mudstone	Brachiopods, crinoids	burrowing, carbonaceous shale partings

Figure 2.3. Summary of depositional facies within the study area. Note: facies are not necessarily represented in a vertical facies succession order.

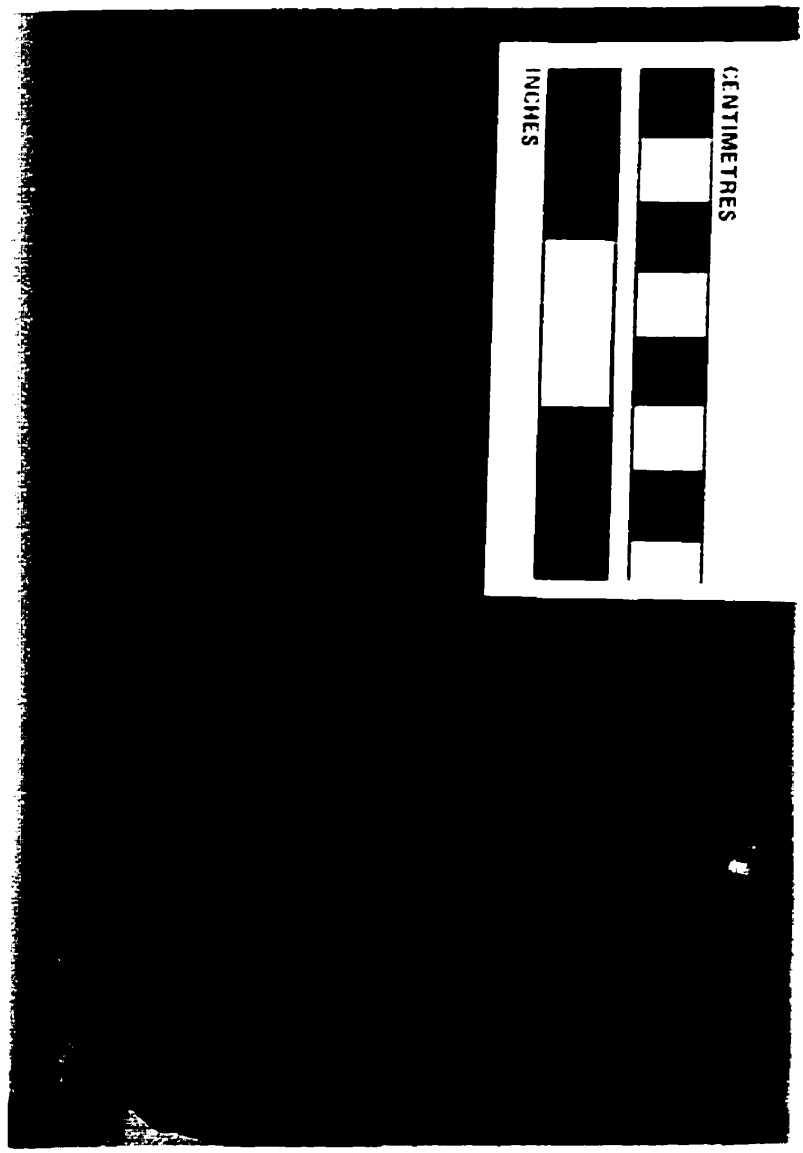

Figure 2.4. Core Photo of Facies 1. Note the dark grey mudstone with a nodular texture; 10-10-97-4w6, 2261 m (7414 ft).

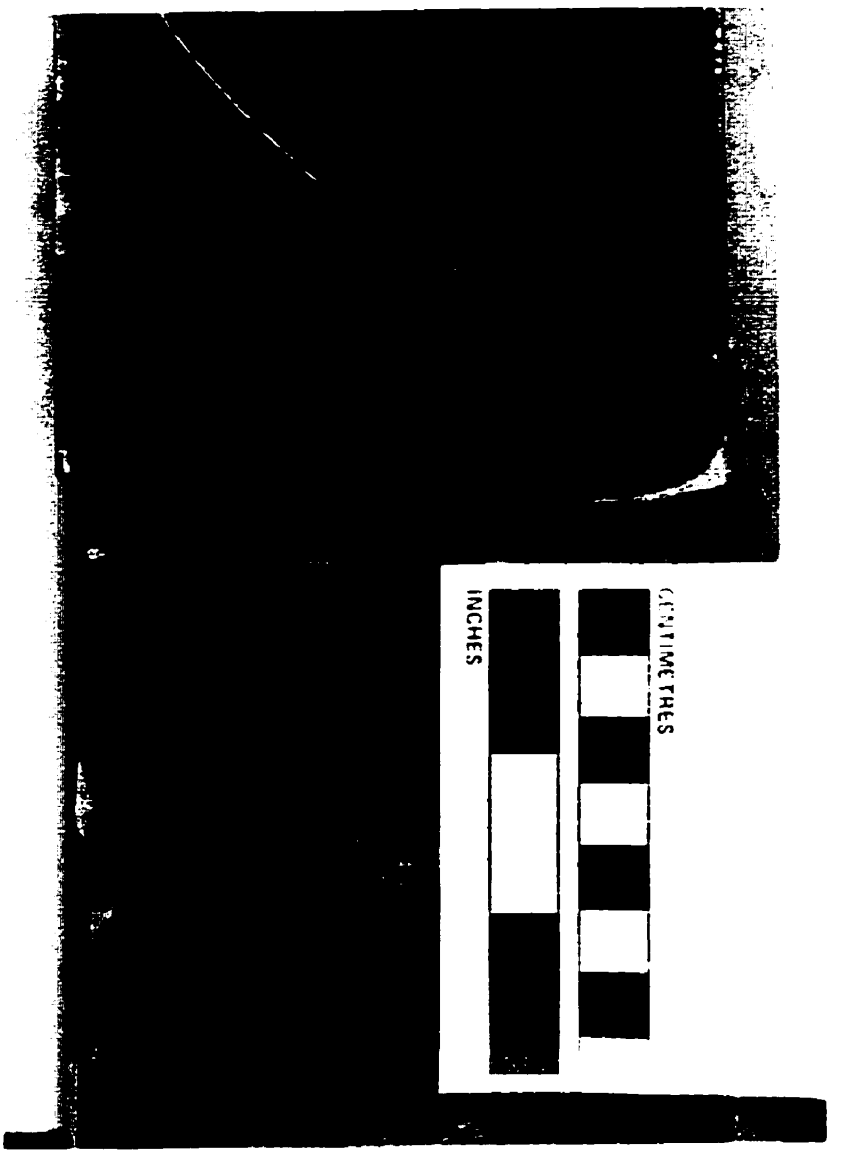

Figure 2.5. Core Photo of Facies 1. Watt Mountain – Slave Point contact. Note the sharp nature of the contact between the Watt Mountain green shale (bottom) and the dark mudstone (top) of the Lower Slave Point; 10-10-97-4w6, 2273 m (7456 ft).

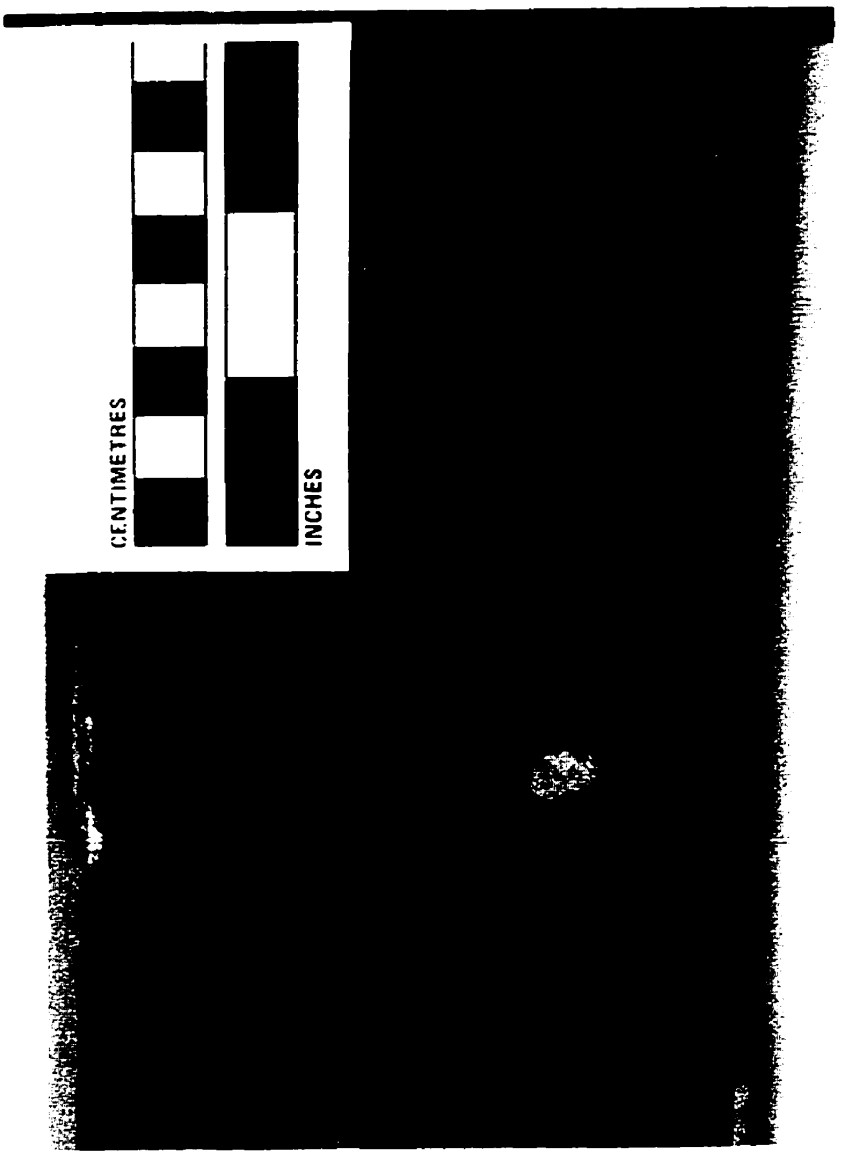

Figure 2.6. Core Photo of the Facies 1. Facies 1 – Facies 2 contact. Note Facies 1 mudstone (bottom) is sharply overlain by the nodular wackestone with scattered brachiopods and crinoids (top) of Facies 2; 10-10-97-4w6, 2239 m (7345 ft).

depths of some 10's of meters.

2.2.2 Facies 2: Nodular Brachiopod-Crinoidal Wackestone

This facies consists of dark grey to dark brown lime wackestone with a skeletal wackestone to packstone matrix and an extensively mottled, nodular fabric (Fig. 2.7), very similar to that previously described for Facies 1. Disarticulated atrypid brachiopods (Craig, 1987) and crinoids are commonly present but generally represent less than 10% of the total rock volume. Pisoids may also occur (rare?) in beds up to 5 cm thick within Facies 2.

The matrix consists dominantly of lime mud (micrite), peloidal grains, ostracods and gastropods. The matrix often shows a bimodal grain size with grainier (peloids?) areas (burrows?) within a more micritic matrix. Porosity is not developed in this facies.

The lower contact of this facies is commonly gradational with underlying Facies 1 (Fig. 2.6). The upper contact of Facies 2 can also be gradational into overlying Facies 1 or 3 (Fig. 2.8) or a very sharp, erosional contact characterized by stylolites where underlying Facies 4 or 11 (Fig. 2.9). This sharp, erosional upper contact is recognized on both the spontaneous-potential and gamma-ray logs and informally subdivides the Slave Point Formation into a Lower Slave Point and an Upper Slave Point (Fig. 2.1).

This facies indicates a low energy, relatively deep, subtidal environment of deposition. A low energy, subtidal depositional regime is also supported by the predominance of biogenic structures over wave or current structures within this facies (Rosenthal, 1988). The distinctive mottled texture is interpreted to be the result of bioturbation and suggests well-circulated, oxygenated waters below storm wave base.

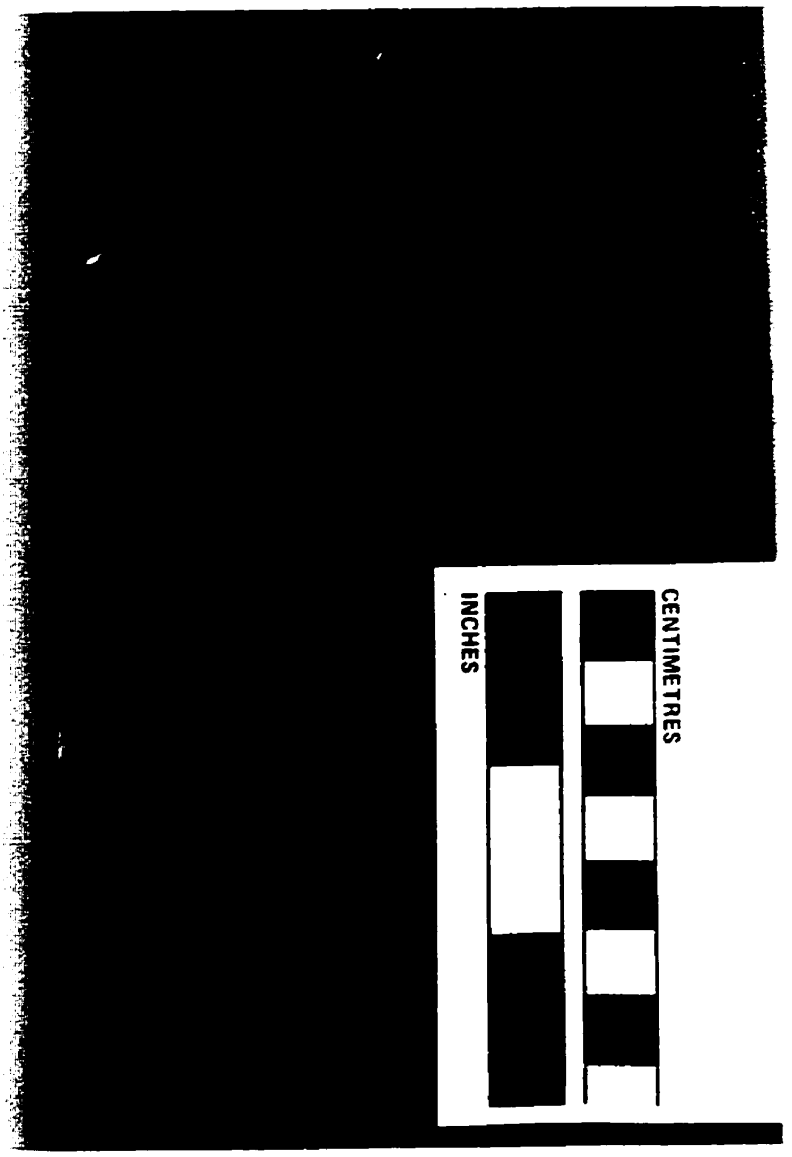

Figure 2.7. Core Photo of Facies 2. Note the dark grey wackestone with scattered atrypid brachiopods and crinoids and the characteristic nodular texture; 10-10-97-4w6, 2240 m (7349 ft).

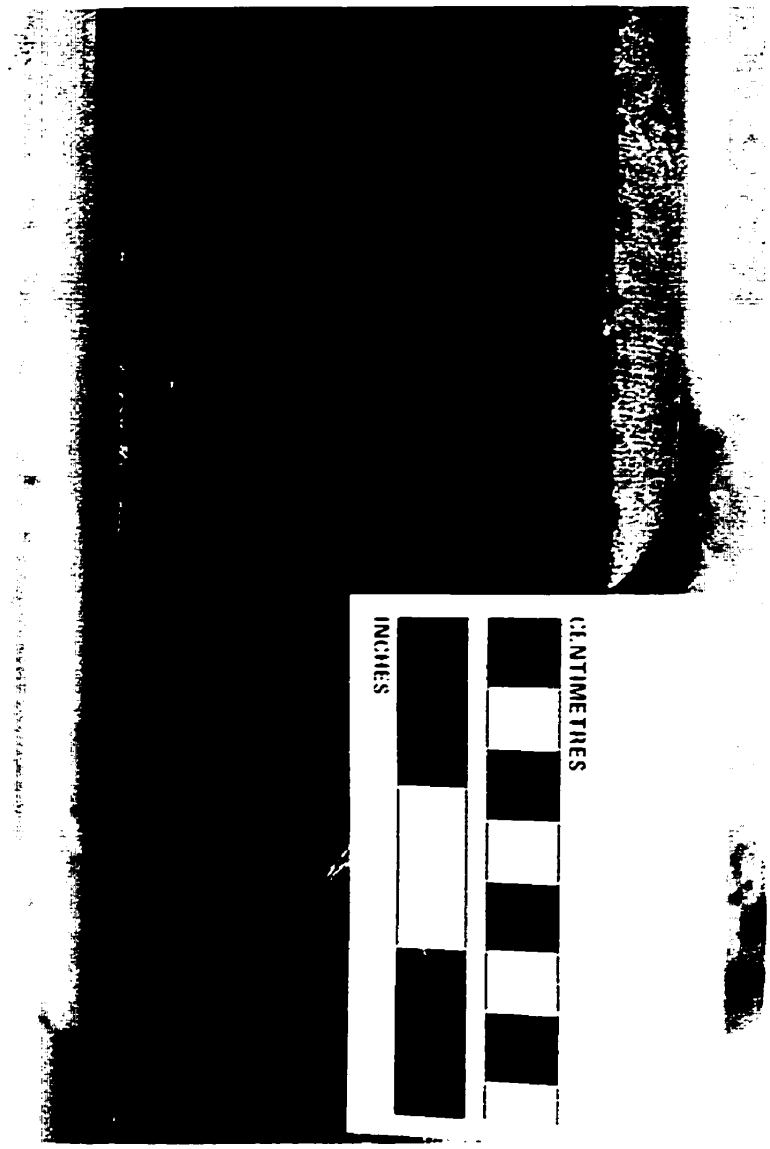

Figure 2.8. Core Photo of Facies 2. Facies 2 – Facies 3 contact. Note the gradational contact between Facies 2 (bottom) and Facies 3 (top); 10-23-95-5w6, 2338 m (7670 ft).

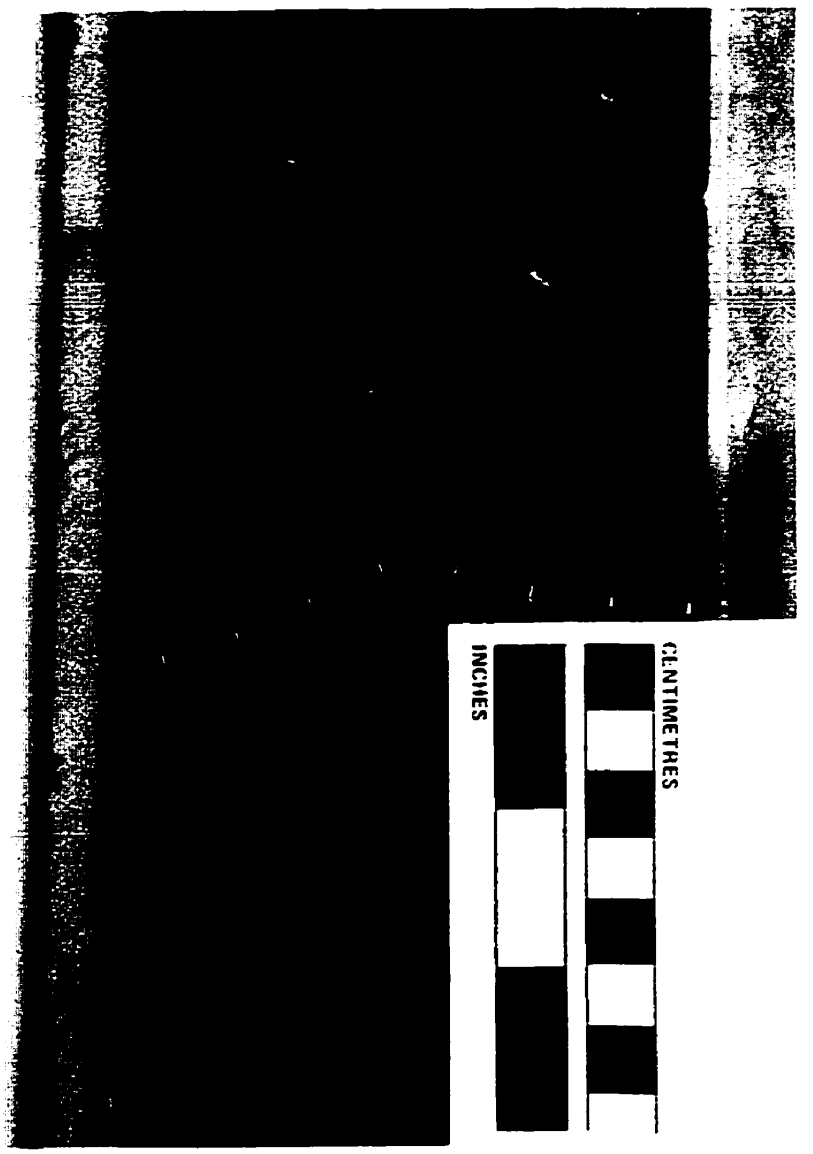

Figure 2.9. Core Photo of Facies 2. Facies 2 – Facies 4 contact. Note Facies 2 (bottom) is sharply overlain by Facies 4 (top); 10-27-96-3w6, 2167 m (7110 ft).

The presence of open-marine organisms such as brachiopods and crinoids suggests waters of normal marine salinities (Jamieson, 1971; Wilson, 1975; Rosenthal, 1988).

It is difficult to estimate absolute water depths for this cycle. Modern brachiopod-crinoid banks have been found at depths of up to 700 meters (Neumann, 1977) and no depth-diagnostic criteria are present within this facies. Wendte (1992c) established paleowater depths between 22 to 30m for similar nodular mudstone deposits of the Swan Hills Formation in the Judy Creek area. Deposition of this facies possibly occurred in relatively deep water depths of some 10's of meters, under conditions somewhat shallower and more open marine relative to Facies 1 .

2.2.3 Facies 3: Thamnopora Wackestone

This facies consists of dark brown lime wackestone with a skeletal wackestone to packstone matrix and an irregular nodular fabric (Fig. 2.10). The dendroid coral, *Thamnopora*, is the dominant organism. Tabular (wafer) stromatoporoids, cylindrical stromatoporoids (*Stachyodes*), brachiopod and crinoid fragments are common secondary constituents. Wafer stromatoporoids are commonly *in situ*, but may also be broken, suggesting some degree of transportation. *Stachyodes* are often encrusted by corals. It should be noted that Facies 3 is not present in all wells with core (Fig. 2.11). The more basinal nodular wackestone of Facies 2 can grade vertically and laterally into Facies 3.

The matrix consists of lime mud (micrite), peloidal grains, ostracods and gastropods. Porosity is non-existent in this facies. Minor (<10% of rock volume) dolomitization of the micritic matrix is apparent in some wells, but does not contribute any significant porosity.

The lower contact of this facies is gradational, where underlain by Facies 1 or 2,

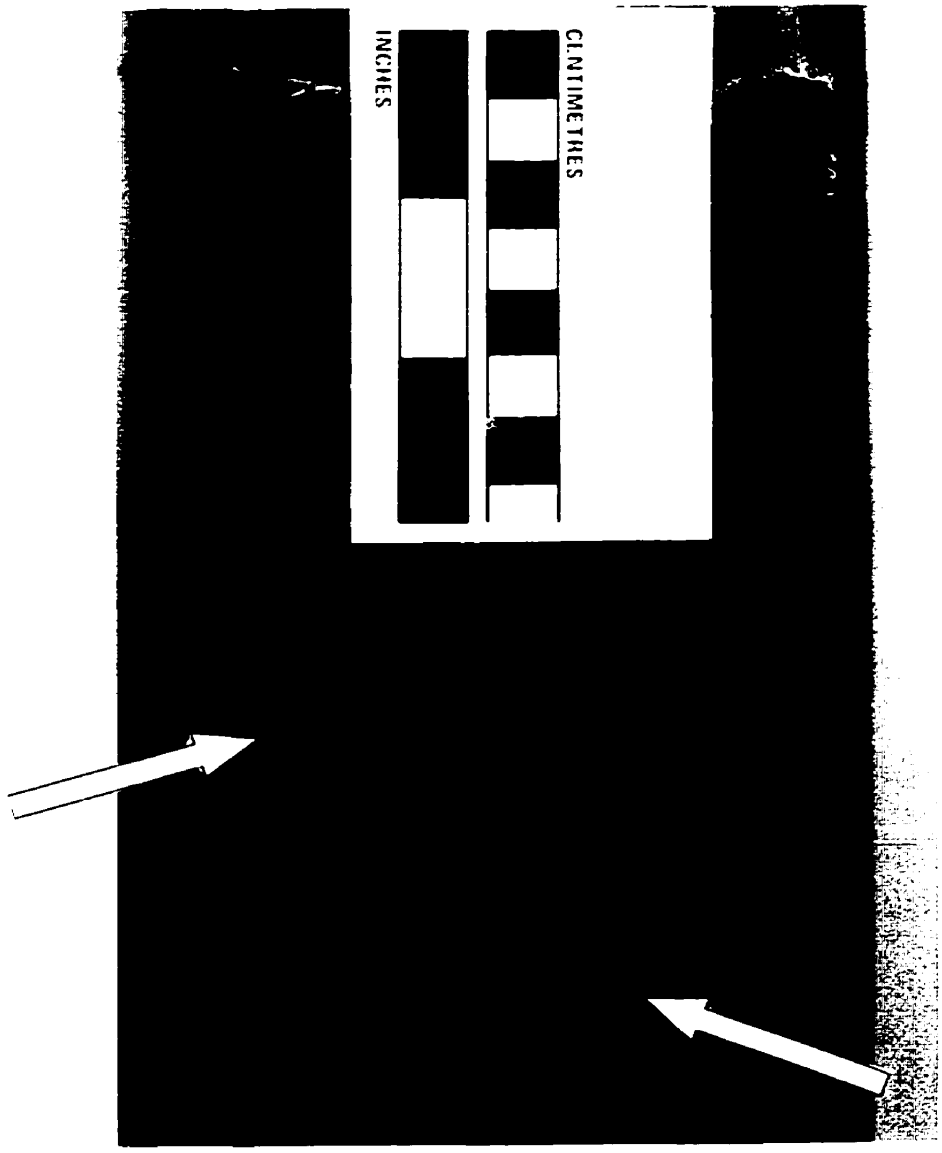

Figure 2.10. Core Photo of Facies 3. Note the dark brown wackestone with scattered *Thamnopora* (arrows); 7-10-97-3w6, 2172 m (7126 ft).

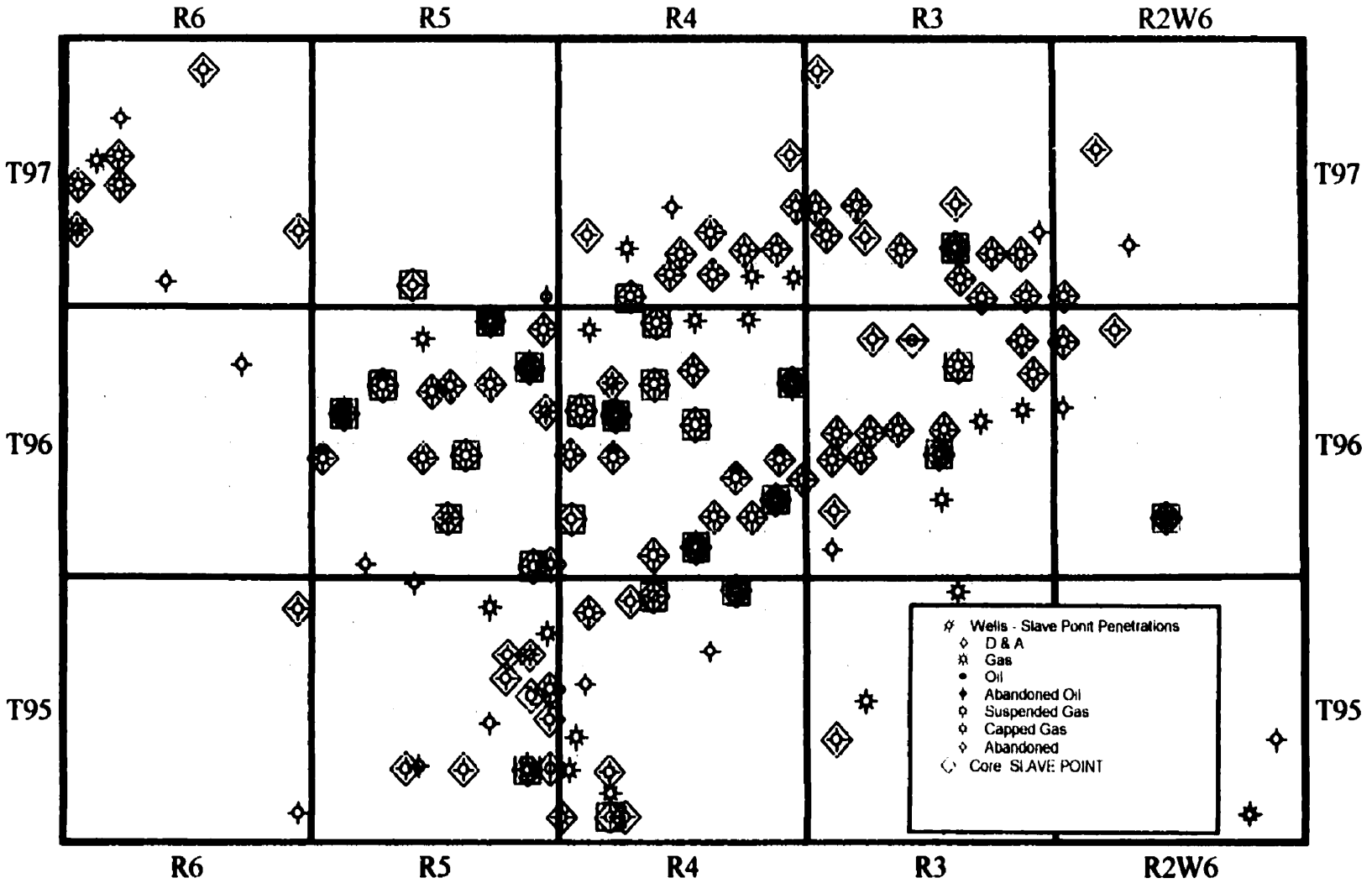

Figure 2.11. Facies 3 Map. Scale 1:250,000. Diamonds represent Slave Point wells with core. Open squares represent Slave Point cores, which were deep enough to encounter Facies 3. Filled Squares represent the occurrence of Facies 3.

(Fig. 2.8). The upper contact of Facies 3 is very similar to that described previously for Facies 2. The upper contact is commonly sharp and erosional, characterized by stylolites (Fig. 2.12) or gradational, where overlain by Facies 4 or 12. Where Facies 3 is present the upper contact (recognizable on both the spontaneous-potential and gamma-ray logs) informally subdivides the Slave Point Formation into a Lower Slave Point and an Upper Slave Point (Fig. 2.1), similar to that described previously for Facies 2.

This facies indicates a low to moderate energy, relatively shallow, subtidal environment of deposition. Where present the *Thamnopora* wackestone of Facies 3 is transitional between the more basinal Facies 2 and the shallower, higher energy *Stachyodes* and *Thamnopora* floatstone of Facies 4. This relationship and the presence of open-marine fauna in this facies supports a relatively deep (at or just below storm wave base), well-circulated, oxygenated platform setting under conditions somewhat shallower and more open marine relative to Facies 2 .

Deposition of this facies probably occurred in water depths less than 22 m (Wendte, 1992c).

2.2.4 Facies 4: Stachyodes - Thamnopora Floatstone

This facies consists of brown to dark brown lime floatstone and rudstone with a wackestone to packstone to grainstone (minor) matrix. Fauna consists of dominantly of *Stachyodes* and *Thamnopora*. Broken tabular and bulbous stromatoporoids, brachiopods and crinoids are common secondary constituents (Fig. 2.13).

The matrix consists of lime mud (micrite), peloidal grains and ostracods. The matrix can show a bimodal grain size with grainy (peloids?) areas (burrows?) within a more micritic matrix. Porosity within this facies is dominantly primary interparticle.

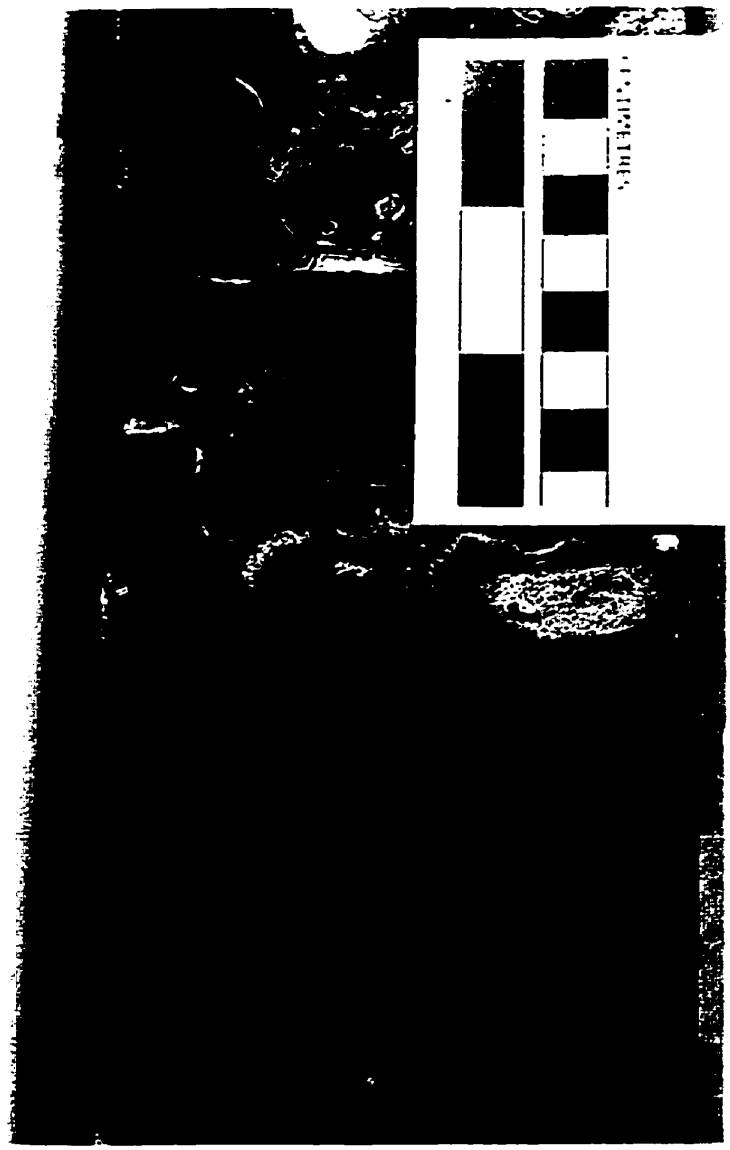

Figure 2.12. Core Photo of Facies 3. Facies 3 – Facies 4 contact. Note the sharp nature of the contact between the *Thamnopora* wackestone (bottom) of Facies 3 and the *Stachyodes* and *Thamnopora* floatstone (top) of Facies 4;7-10-97-3w6, 2172 m (7126 ft).

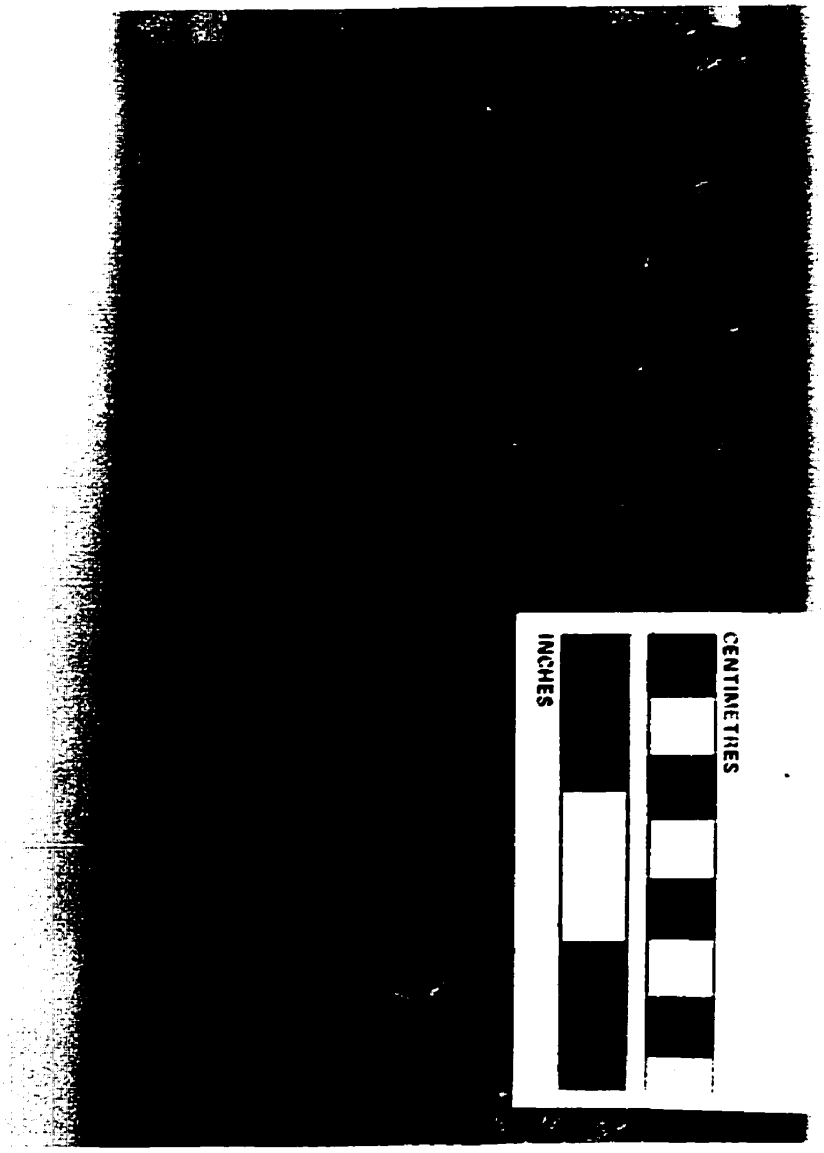

Figure 2.13. Core Photo of Facies 4. Note the dark brown floatstone containing scattered *Stachyodes* and *Thamnopora* (t); 7-10-97-3w6, 2170 m (7119 ft).

Porosity can be bimodal (rare) with moldic porosity occurring in a fine-grained dolomitic matrix with intercrystalline porosity. Facies 4 is a minor reservoir facies in the study area, with an average porosity of 7%.

The lower contact of this facies is commonly a sharp, erosional, stylolitized contact (Fig. 2.12) where overlying Facies 2 or 3, as described previously. The upper contact of Facies 4 may be either gradational where overlain by Facies 5 or a sharp stylolitized contact where overlain by either Facies 5 or 6 (Fig. 2.14).

The abundance and form of the skeletal components of this facies indicates higher oxygen levels and energy conditions relative to Facies 3. The *Stachyodes* and *Thamnopora* floatstones of Facies 4 are overlain by tabular stromatoporoid rudstones and boundstones of Facies 5 (where present). This relationship and the diverse open-marine fauna of this facies supports a relatively shallow (above storm wave base), well-circulated and oxygenated lower to middle foreslope setting. This facies is similar to the foreslope Subfacies B described by Gosselin et. al. (1989) for the Slave Point Formation in the Golden and Evi Fields of northwestern Alberta.

Deposition of this facies probably occurred in water depths between 10 to 20 m. Wendte (1992c) established paleowater depths between 10 to 20 m for similar lower and middle foreslope limestone deposits of the Swan Hill Formation in the Judy Creek area.

2.2.5 Facies 5: Tabular Stromatoporoid Floatstone and Rudstone

This facies is characterized by light to dark brown lime floatstone and rudstone (boundstone rare) with a skeletal lime grainstone matrix. Fauna consists dominantly of whole/broken *in situ* tabular (0.5 to 5 cm thick) (Fig. 2.15) and hemispherical stromatoporoids with irregular (encrusting) stromatoporoids, *Stachyodes*, *Thamnopora*,

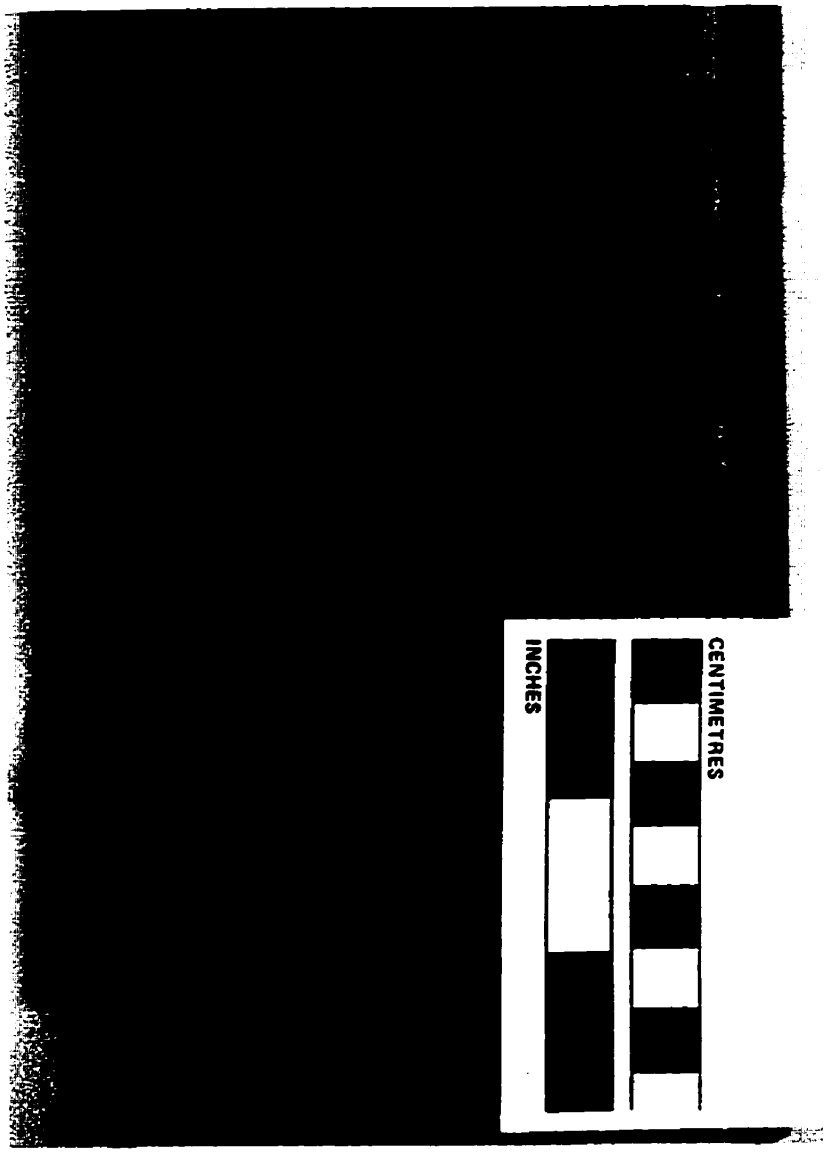

Figure 2.14. Core Photo of Facies 4. Facies 4 – Facies 5 contact. Note the gradational contact between the *Stachyodes* floatstone (bottom) of Facies 4 and the tabular stromatoporoid floatstone (top) of Facies 5; 10-27-96-3w6, 2162m (7094 ft).

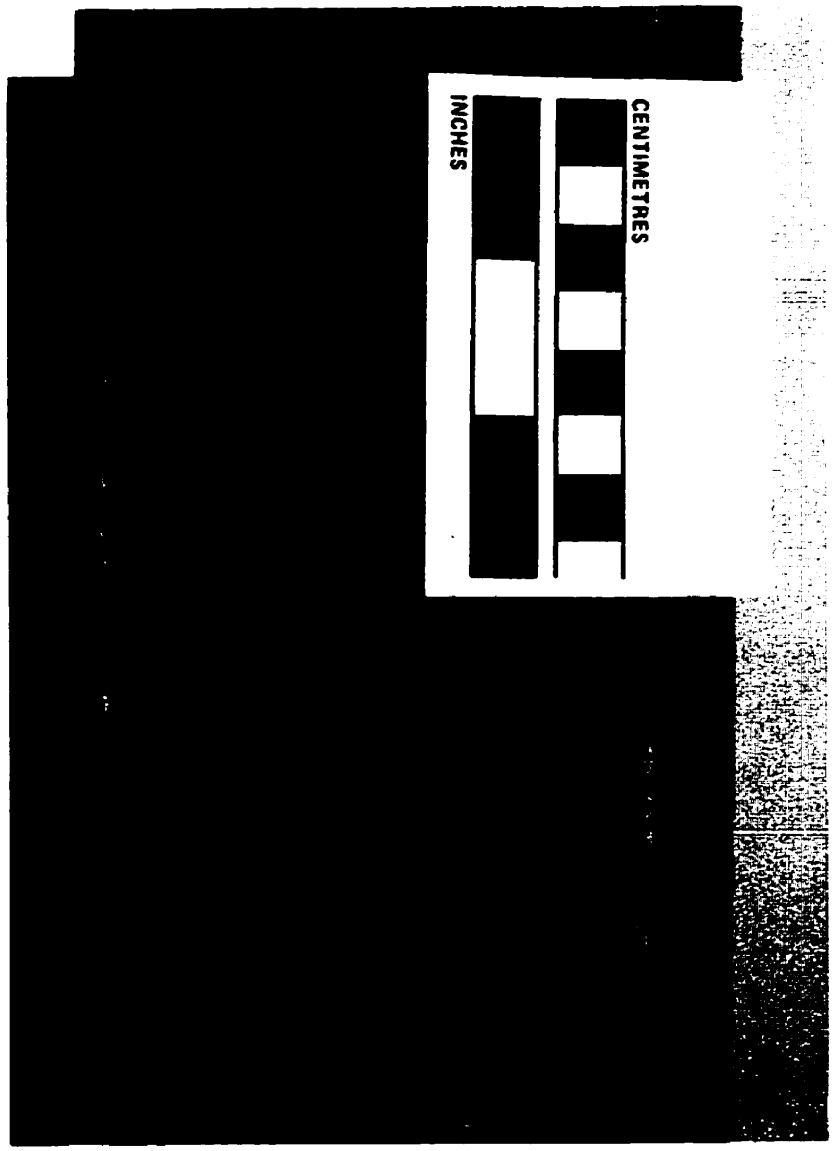

Figure 2.15. Core Photo of Facies 5. Cm-thick stromatoporoid with intraparticle and growth-framework porosity encrusted by a massive stromatoporoid (top); 5-17-97-3w6, 2286 m (7500ft).

crinoids and brachiopods as common secondary constituents (Fig. 2.16). Facies 5 forms a narrow band along the margins of the Upper Slave Point 'reef' (Fig. 2.17) and as such has rarely been observed in core.

The matrix consists of dominantly peloidal grains. Skeletal components consist of fragments of the larger stromatoporoids, ostracod, gastropod, brachiopod and crinoid fragments, and indistinguishable bioclastic debris. Where this facies has been encountered in core it displays dominantly primary interparticle to minor intraparticle and growth-framework porosity. Facies 5 is a reservoir facies in the study area, with an average porosity of 11%.

The lower contact of Facies 5 may be either gradational or a sharp stylolitized boundary where overlying Facies 4 (Fig. 2.14) as described previously. The upper contact of Facies 5 may be a sharp stylolitized contact (Fig. 2.18) where overlain by Facies 6 or 7 or gradational where overlain by Facies 8.

This facies indicates a high energy, wave-swept, relatively shallow environment of deposition. The diversity and robust nature of the open-marine fauna also supports a relatively shallow, well-circulated and oxygenated upper foreslope - reef margin setting. This facies is similar to Subfacies C and D of Gosselin et. al. (1989) and Facies 1 in the Stromatoporoid Reef of Davies and Tooth (1987), described as upper foreslope - reef margin deposits for the Slave Point Formation in the Golden, Evi and Gift Lake Fields of northern Alberta.

Deposition of this facies probably occurred in water depths between 0.5 to 10 m. Wendte (1992c) established paleowater depths between 0 (sea level) to 10 m for similar upper foreslope –reef margin limestone deposits of the Swan Hill Formation in the Judy

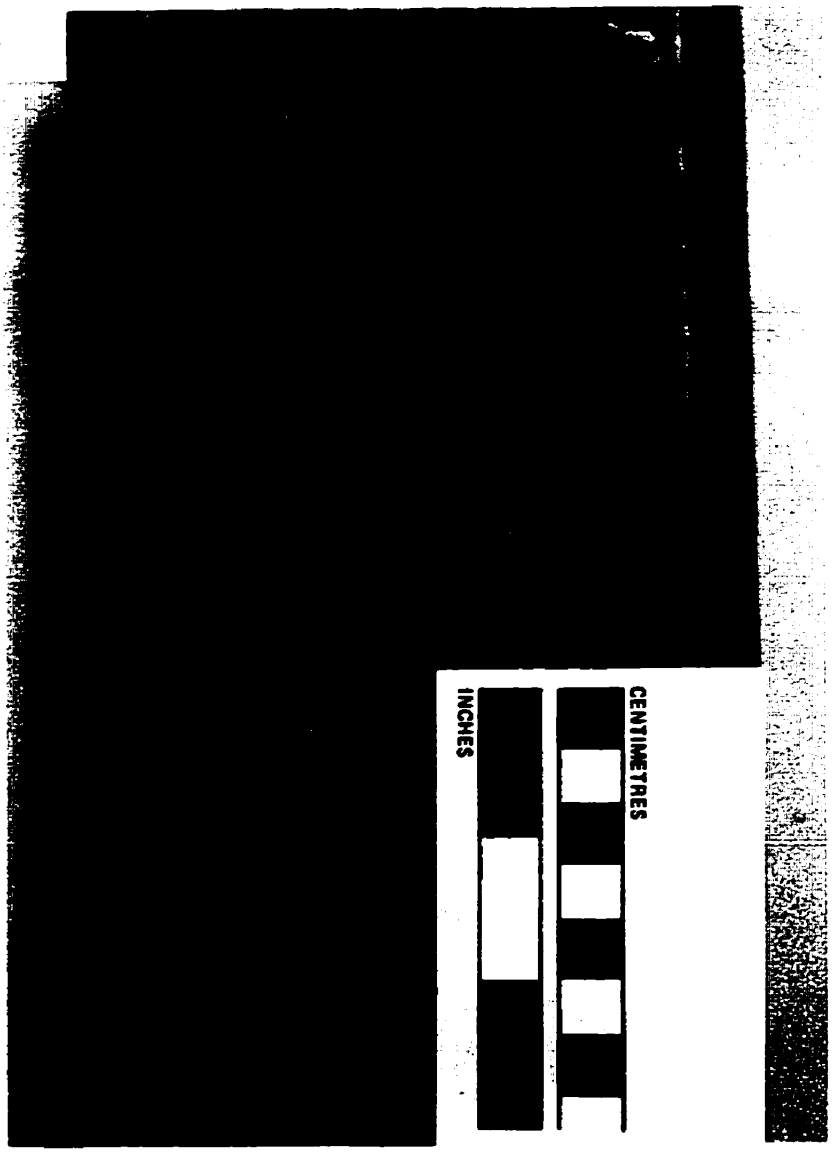

Figure 2.16. Core Photo of Facies 5. Brown to light brown rudstone with whole/broken tabular stromatoporoids in a grainstone matrix; 5-17-97-3w6, 2287 m (7503 ft)

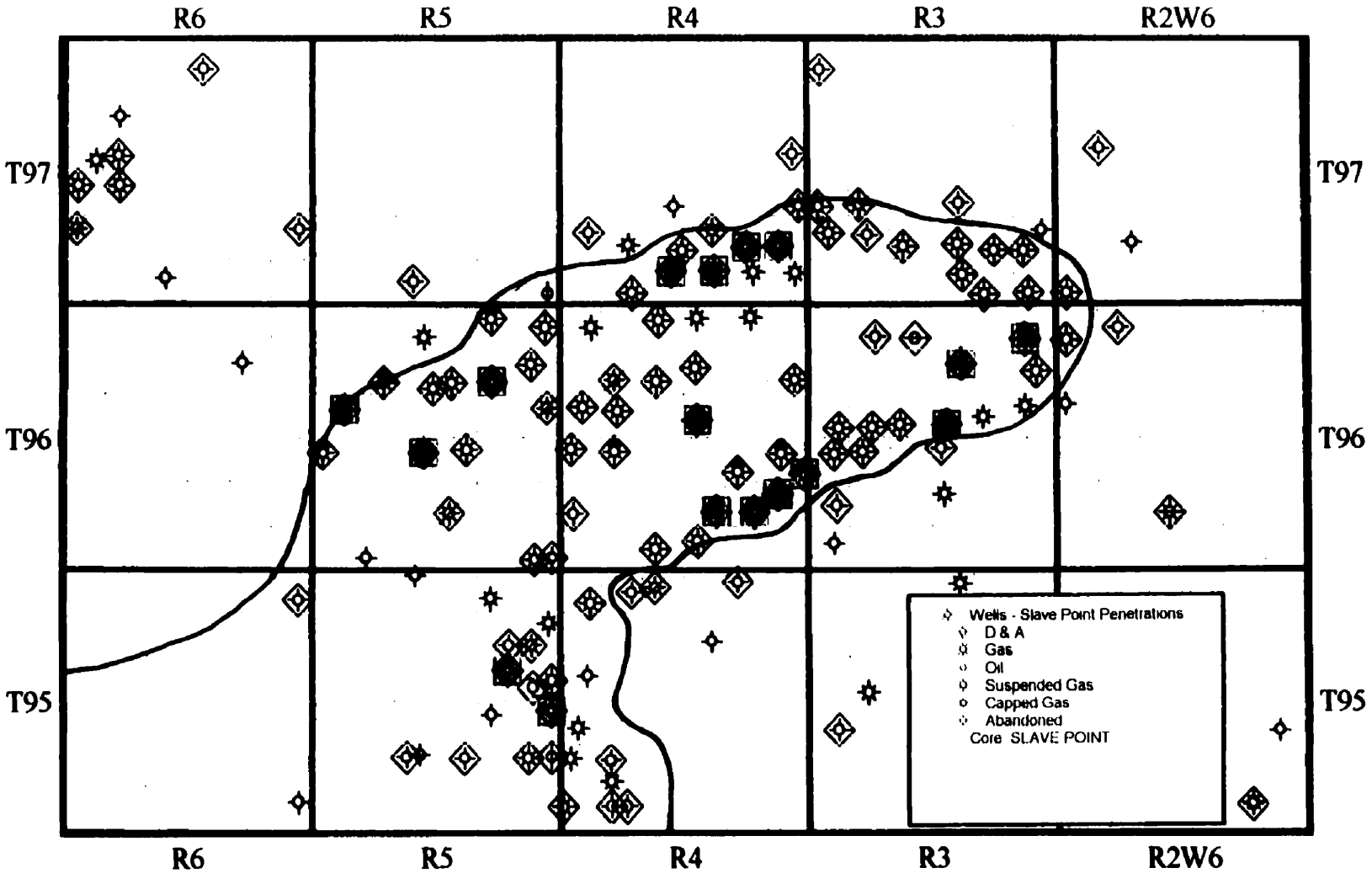

Figure 2.17. Facies 5 Map. Scale 1:250,000. The Upper Slave Point 'reefal'margin is shown as a black line. Diamonds represent wells with Slave Point core. Filled squares represent the occurrence of Facies 5 in the study area.

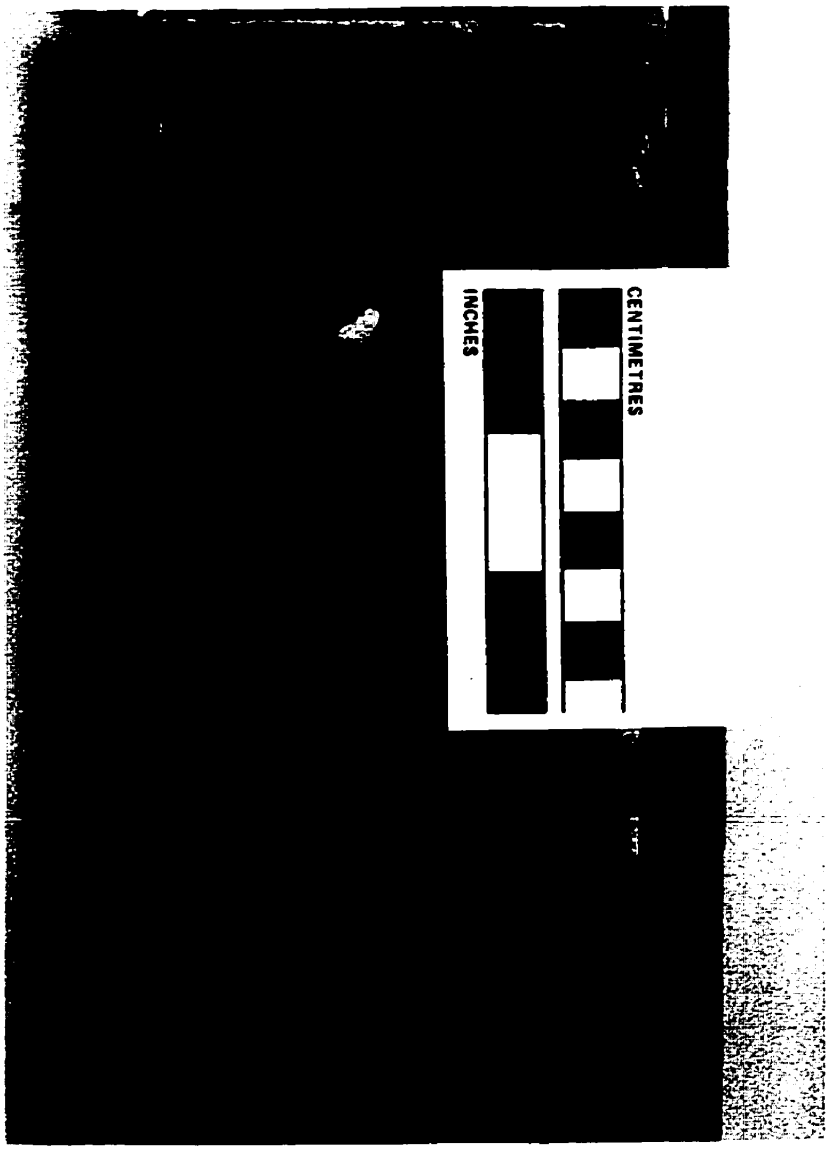

Figure 2.18. Core photo of Facies 5. Facies 5 – Facies 6 contact. Although most of the contact has been removed by a saw cut the transition from the dark brown tabular stromatoporoid rudstone (bottom) of Facies 5 and the grey *Amphipora* wackestone (top) of Facies 6 is typically sharp; 10-27-96-3w6, 2160 m (7086 ft).

Creek area.

2.2.6 Facies 6: Amphipora Rudstone and Floatstone

This facies consists of brown to dark brown lime rudstone, floatstone and wackestone with a lime mudstone to packestone matrix (Subfacies 6a) and/or a packestone to grainstone matrix (Subfacies 6b). *Amphipora* coenostea is the dominant organism (Fig. 2.19). *Stachyodes*, bulbous stromatoporoids, *Thamnopora*, brachiopods and crinoids may also be present. Low faunal diversity but large numbers of individual forms characterize this facies. Subfacies 6a (and to a lesser extent Subfacies 6b) is commonly interbedded with laminites of Facies 7 in meters-thick, shallowing-upward cyclic successions.

The matrix consists of micrite (≥ 50%) and peloidal grains in the lime mudstone to packstone matrix, to dominantly peloidal grains in the lime grainstone matrix. Calcispheres, ostracods and gastropods commonly occur in the matrix. Porosity within Subfacies 6a is generally non-existent in a dominantly limestone lithology, except where dolomitization has occurred leaving vuggy and moldic porosity (Fig. 2.20). Subfacies 6b commonly displays interparticle porosity with an average porosity between 2 to 5 %.

The lower contact of this facies is a very sharp stylolitized contact where overlying Facies 4 or 5 (Fig. 2.18). The upper contact of this facies may be either gradational where overlain by Facies 7 or a sharp boundary where overlain by Facies 7, 9 or 10 (Fig. 2.21).

The low diversity fauna and the lime mudstone to packstone matrix in Subfacies 6a is diagnostic of low energy, lagoonal deposition characterized by restricted circulation (Gosselin et. al., 1989; Tooth and Davies, 1989). Subfacies 6b probably represent

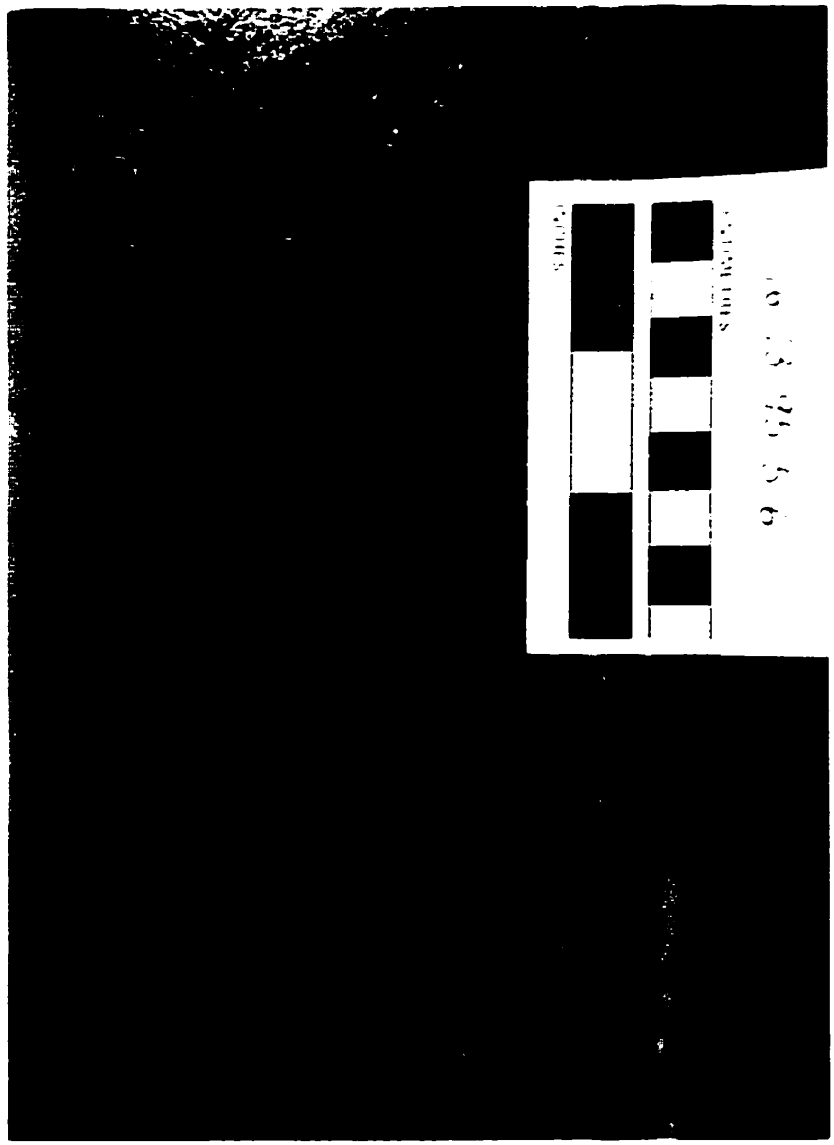

Figure 2.19. Core photo of Facies 6. A dark brown *Amphipora* rudstone (Subfacies 6a). Note the central canals of numerous bisected *Amphipora* coenostea; 16-13-95-5w6, 2345 m (7694 ft).

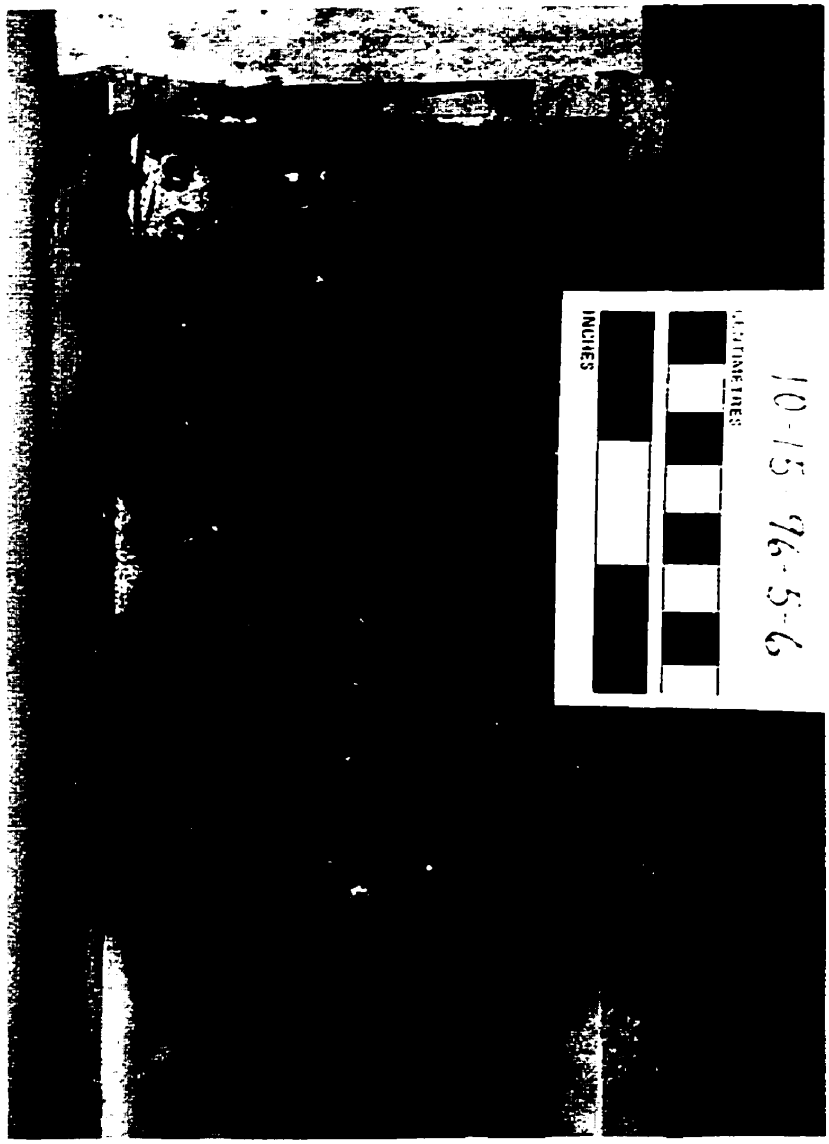

Figure 2.20. Core Photo of Facies 6. Note the open *Amphipora* molds after dolomitization. A clear to brown calcite cement partially fills some of the molds; 10-15-96-5w6, 2377 m (7799 ft).

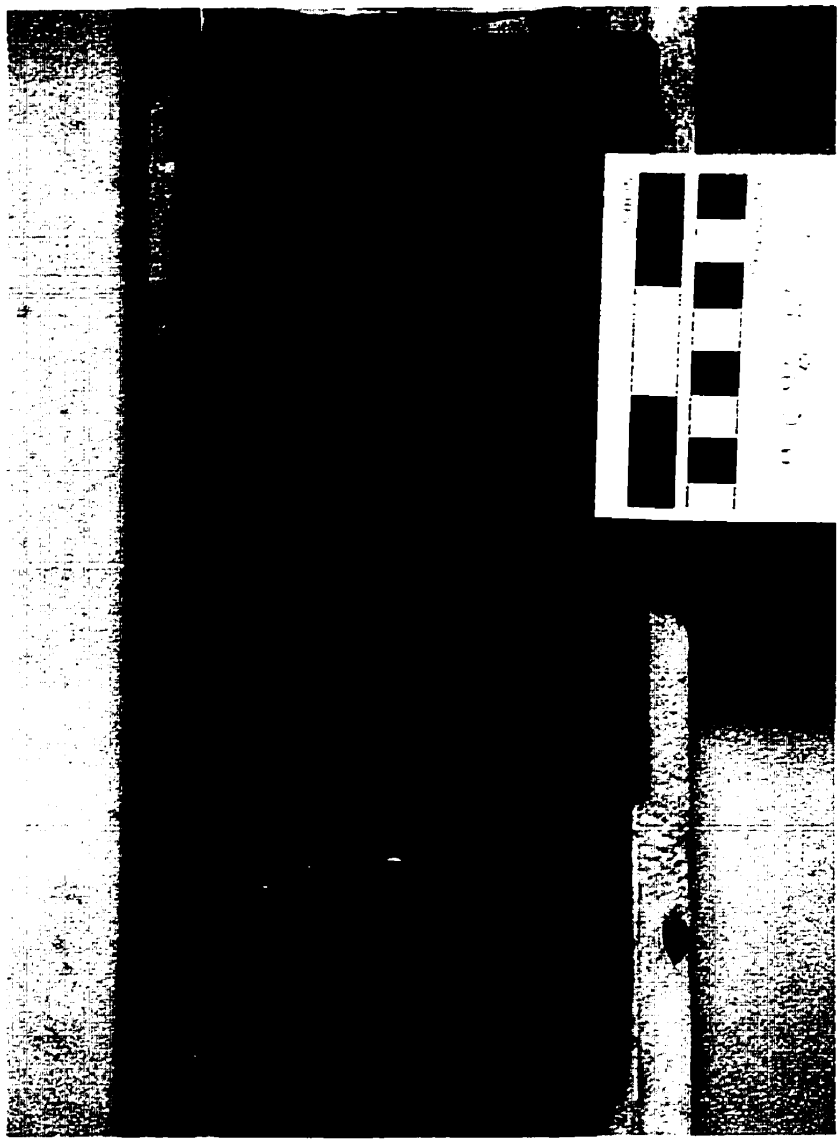

Figure 2.21. Core photo of Facies 6. Facies 6 – Facies 7 contact. Note the sharp contact between the *Amphipora* floatstone (bottom) of Facies 6 and the laminite (top) of Facies 7; 11-14-96-5w6, 2383.5 m (7820 ft).

backreef or open lagoon depositional settings developed just inward of the respective margin (Tooth and Davies, 1989).

Deposition of this facies probably occurred in water depths less than 5 m. Wendte (1992c) established paleowater depths between 0 (sea level) to 5 m for similar *Amphipora* lagoonal deposits of the Swan Hill Formation in the Judy Creek area.

*2.2.7 Facies 7: **Tidal Laminite***

This facies consists of grey to brown lime packstone to mudstone (grainstone matrix minor). *Amphipora* coenostea may be present (<10% total rock volume). This facies commonly displays cryptomicrobial laminations and planar-fenestral fabrics. The laminations consist of alternating thin cryptomicrobial and/or bituminous laminae (≤ 0.2 mm) and thick, lighter colored carbonate laminae (0.5 to 5mm thick) and vary from flat to slightly irregular (Fig. 2.22). A planar-fenestral fabric characterizes this facies and consists of elongate open voids or cement-filled voids (Fig. 2.23) too large to be depositional (cf. Tebbutt et al., 1965).

The matrix consists of micrite (≥ 50%) and peloidal material. Calcispheres and gastropods commonly occur in the matrix. Porosity within this facies is generally non-existent in a dominantly limestone lithology, except where dolomitization (minor) has occurred leaving vuggy porosity.

The lower contact of this facies is sharp when overlying Facies 6 (Fig. 2.21). The upper contact is commonly a sharp boundary where overlain by Facies 6, 9 or 10 (Fig. 2.24).

The nature of the bituminous laminae suggest that many may be the remains of microbial algal films with carbonate deposited on a sediment trapping surface. In the

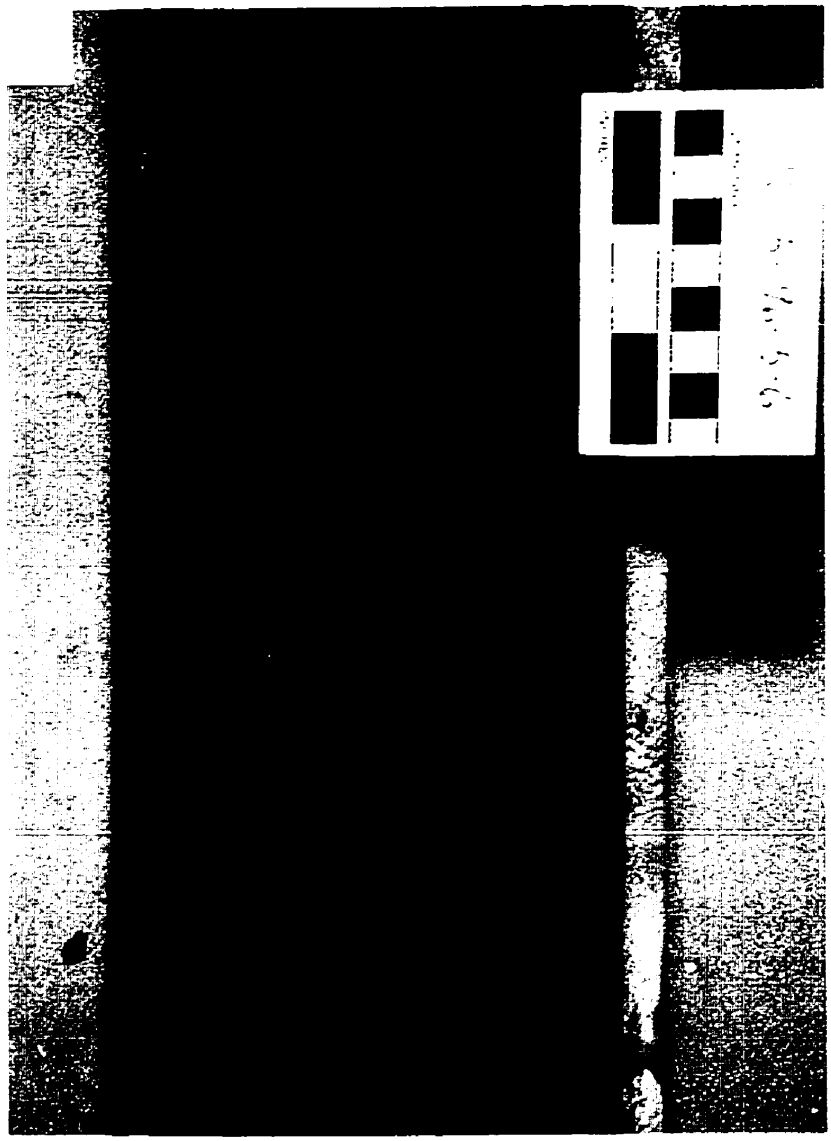

Figure 2.22. Core Photo of Facies 7. Characteristic laminated fabric of this facies; 10-15-96-5w6, 2379 m (7805 ft).

Figure 2.23. Core Photo of Facies 7. Planar-fenestral porosity filled by a white dolomite cement; 10-15-96-5w6, 2377 m (7799 ft).

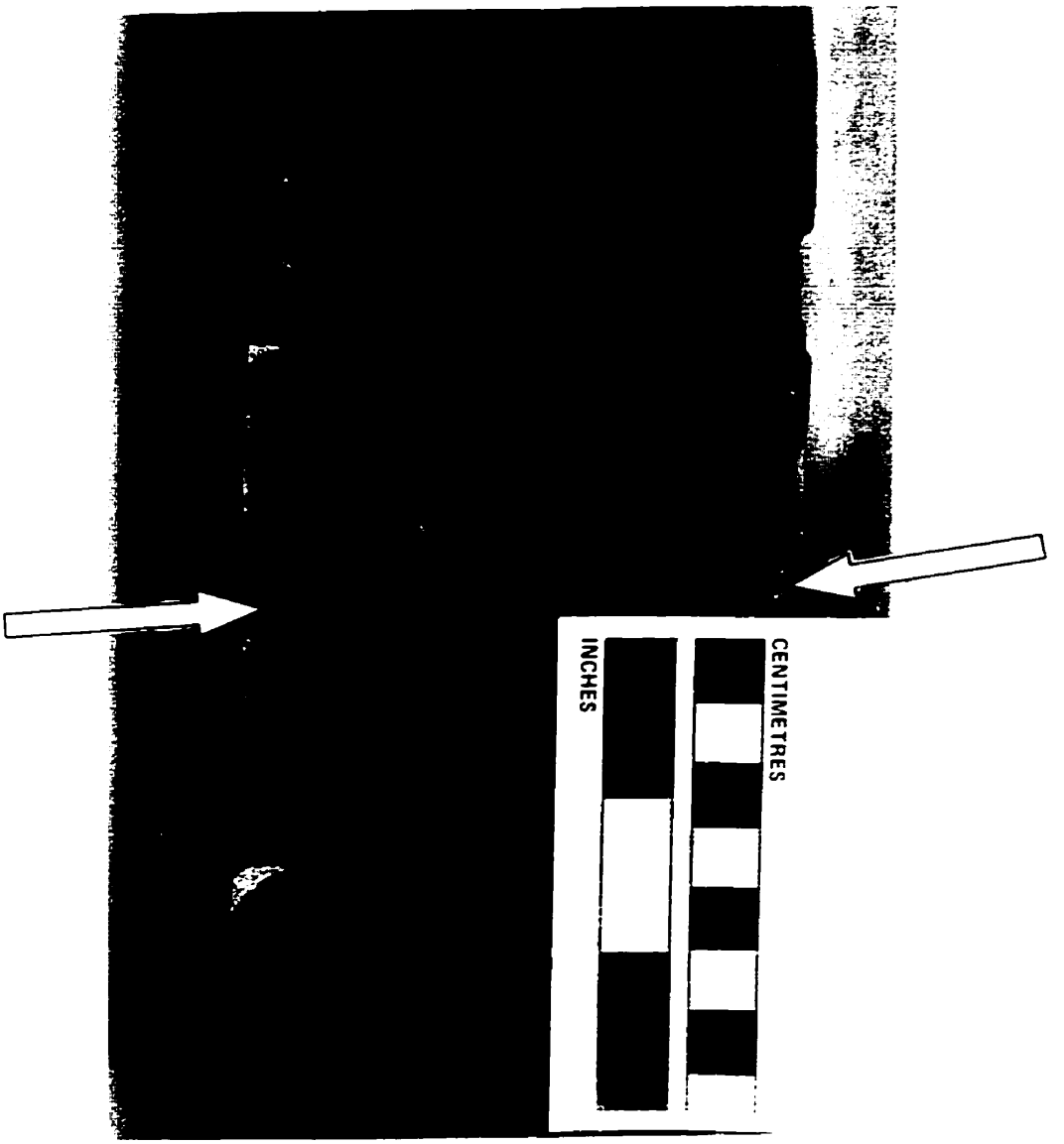

Figure 2.24. Core Photo of Facies 7. Facies 7 – Facies 10 contact. Note the sharp contact (arrows) between the laminite (bottom) of Facies 7 and the bulbous stromatoporoid floatstone (top) of Facies 10; 6-4-96-4w6, 2271 m (7450 ft).

modern, similar deposits are found in upper intertidal and lower supratidal environments (Wendte, 1992c). The characteristic planar-fenestral fabric of this facies is thought to form either by the decay of algal films or by shrinkage of sediments due to alternating periods of wetting and drying (Shinn, 1968). In modern normal salinity environments of deposition this fabric occurs most commonly in the upper parts of tidal flats, the upper intertidal and lower supratidal environments (Shinn, 1968).

The sparsity of open-marine fauna and the presence of cryptomicrobial laminations and fenestral fabrics in this facies supports a shallow subtidal to supratidal restricted lagoonal setting. This facies is similar to Subfacies G of Gosselin et. al. (1989) described as shallow lagoonal deposits in the Slave Point Golden and Evi Fields of northwestern Alberta. Tooth and Davies (1989) and Davies and Tooth (1987) described a similar facies in the Slave Point Gift Field and interpreted these deposits to be representative of the lagoonal environment.

Deposition of this facies probably occurred in water depths of less than 0.5 m. Wendte (1992c) established paleowater depths between 0 (sea level) to 0.5 m for similar tidal flat deposits of the Swan Hill Formation in the Judy Creek area.

2.2.8 Facies 8: Hemispherical Stromatoporoid Rudstone and Boundstone

This facies consists of light brown to brown lime rudstone and boundstone with a skeletal lime grainstone matrix. Fauna are abundant and diverse, most of which show considerable abrasion and fragmentation. *In situ* and broken hemispherical stromatoporoids are the most abundant constituents (Fig. 2.25). *Stachyodes*, tabular (0.5 to 5 cm thick), irregular (encrusting) and bulbous stromatoporoids, brachiopods and crinoids are common secondary constituents. Facies 8 forms a narrow band along the

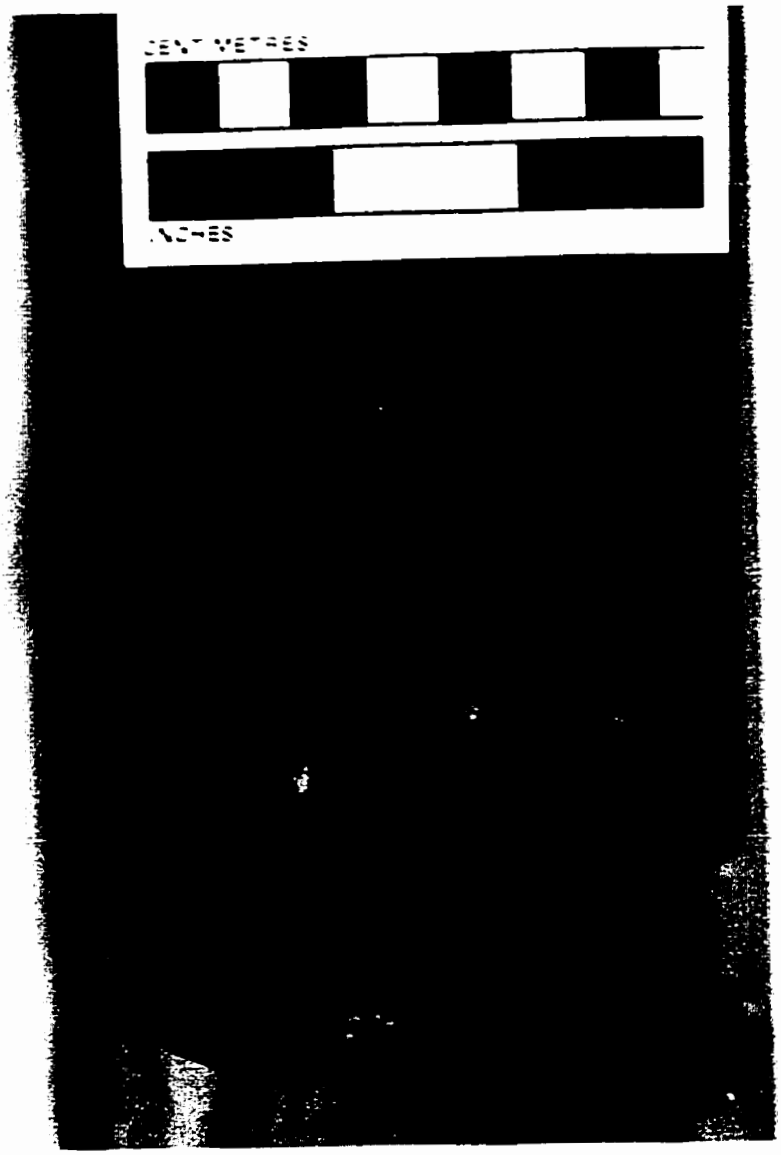

Figure 2.25. Core Photo of Facies 8. Large hemispherical stromatoporoid characteristic of this facies; 9-19-96-5w6, 2373 m (7785 ft).

margins of the Upper Slave Point reefal buildup and as such has rarely been observed in core. Facies 8 grades laterally (i.e. toward the interior of the Upper Slave Point 'reefal' buildup) into Facies 6 and 7.

The matrix consists dominantly of peloidal grains. Skeletal components consist of fragments of the larger stromatoporoids, ostracod, gastropods, calcispheres, brachiopod and crinoid fragments, and indistinguishable bioclastic debris. Where this facies has been encountered in core it displays dominantly primary interparticle to minor intraparticle and growth-framework porosity. Facies 8 is a reservoir facies in the study area, with an average porosity of 8%.

The lower contact of this facies is commonly gradational when overlying Facies 5. The upper contact of Facies 8 is typically a sharp contact where overlain by Facies 9 (Fig. 2.26).

This facies indicates a high energy, wave-swept, relatively shallow environment of deposition. The diversity and robust nature of the open-marine fauna that characterize this facies also supports a relatively shallow, well-circulated and oxygenated reef margin setting. Limestones deposited along the margin are predominantly abraded, hemispherical, bulbous and irregular stromatoporoid lime rudstones to boundstones with a skeletal grainstone to packstone matrix (Wendte, 1992b). This facies is similar to Subfacies D of Gosselin et. al. (1989) for Slave Point Formation in the Golden and Evi Fields; and is similar to the massive and hemispherical stromatoporoid floatstone and rudstone facies described by Tooth and Davies (1989) and Davies and Tooth (1987), as reef margin deposits for the Slave Point Gift Lake Field.

Deposition of this facies probably occurred in water depths less 5 m. Wendte

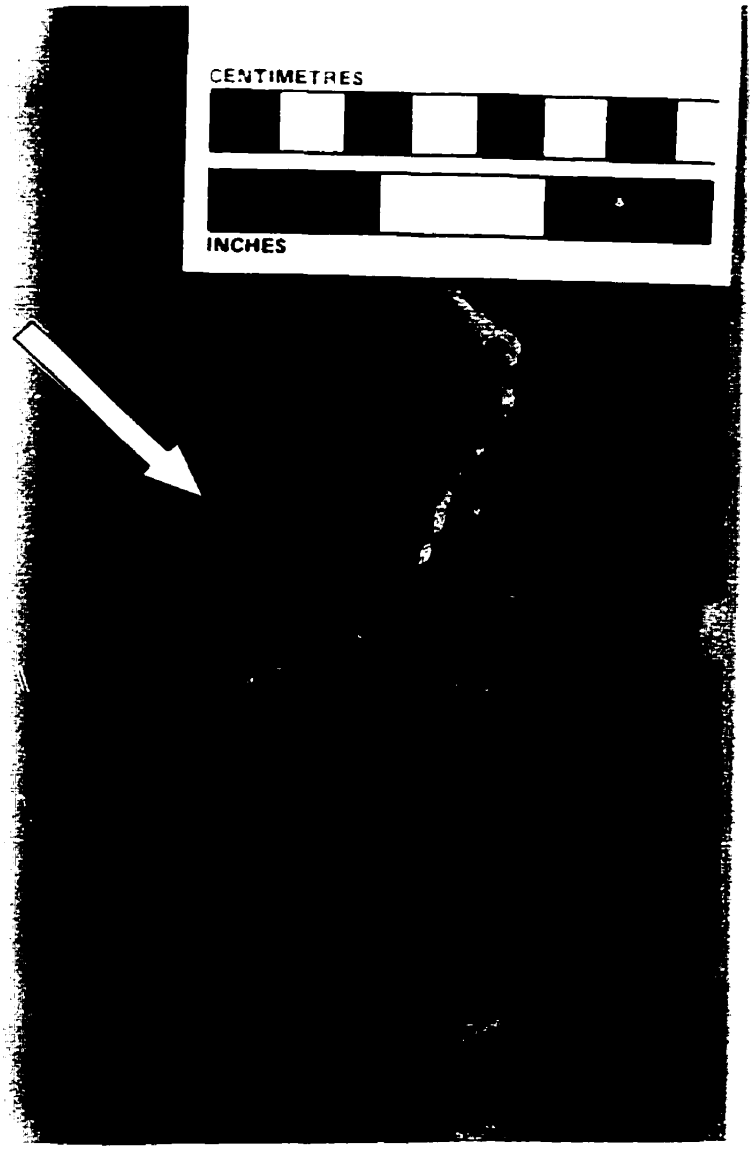

Figure 2.26. Core Photo of Facies 8. Facies 8 – Facies 9 contact. Note the sharp, stylolitized contact (arrows) between the hemispherical boundstone (bottom) of Facies 8 and the bulbous stromatoporoid grainstone (top) of Facies 10; 9-19-96-5w6,2368.5 m (7771 ft).

(1992c) established paleowater depths between 0 (sea level) to 10 m for similar upper foreslope –reef margin limestone deposits of the Swan Hills Formation in the Judy Creek area.

2.2.9 Facies 9: Lime Packestone

This facies is characterized by brown to dark brown wackestone to packstone with a mottled or nodular texture. Carbonaceous partings are common. Whole/fragments of *Thamnopora*, *Amphipora*, *Stachyodes*, bulbous and tabular stromatoporoids, brachiopods and crinoids (Fig. 2.27) may be present as minor constituents (<10% total rock volume). Facies 9 grades laterally into Facies 10.

The matrix consists of micrite (≥ 50%) and peloidal grains. Fragments of the larger bioclasts, ostracods, gastropods and indistinguishable bioclastic debris commonly occur within the matrix. Facies 9 is not a reservoir facies in the study area.

The lower contact of Facies 9 is a very sharp contact where underlain by Facies 6 or Facies 7 (Fig. 2.24). The upper contact is commonly sharp where overlain by Facies 10 (Fig. 2.28) or a sharp burrowed erosional contact where overlain by Facies 13. This burrowed surface commonly shows evidence of cylindrical excavations, 1 to 2 cm in diameter and up to 5 cm long, (burrows of ichnogenus *Gloss.fungites*?). This contact is recognizable on both the spontaneous-potential and gamma-ray logs and separates the Upper Slave Point from the overlying Waterways Formation (Fig. 2.1).

This facies is characterized by sparse fauna. The presence of carbonaceous partings and the lateral gradational relationship of this facies with Facies 10 suggest a lower energy, slightly more protected environment of deposition relative to Facies 10 (see section 2.2.10). Indicators of extremely shallow conditions, such as oolites,

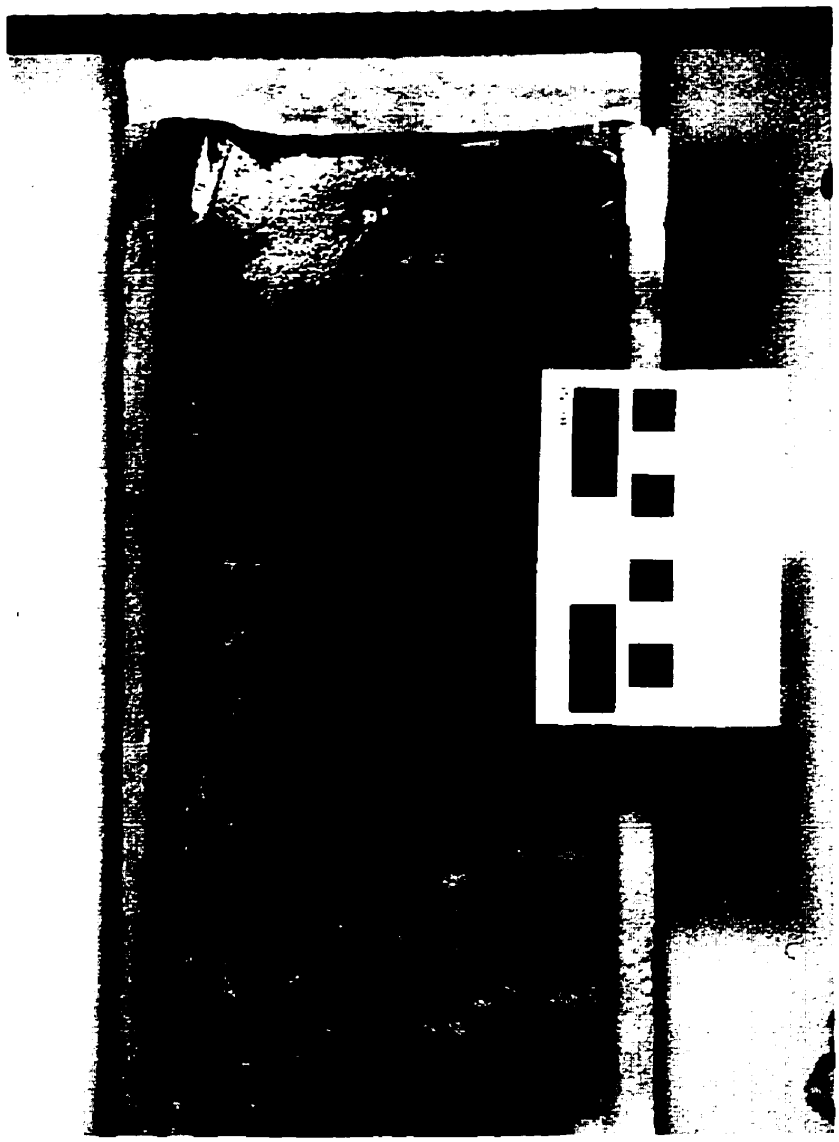

Figure 2.27. Core Photo of Facies 9. Note the lack of fauna in a nodular lime packstone; 4-36-96-3w6, 2107 m (6913 ft).

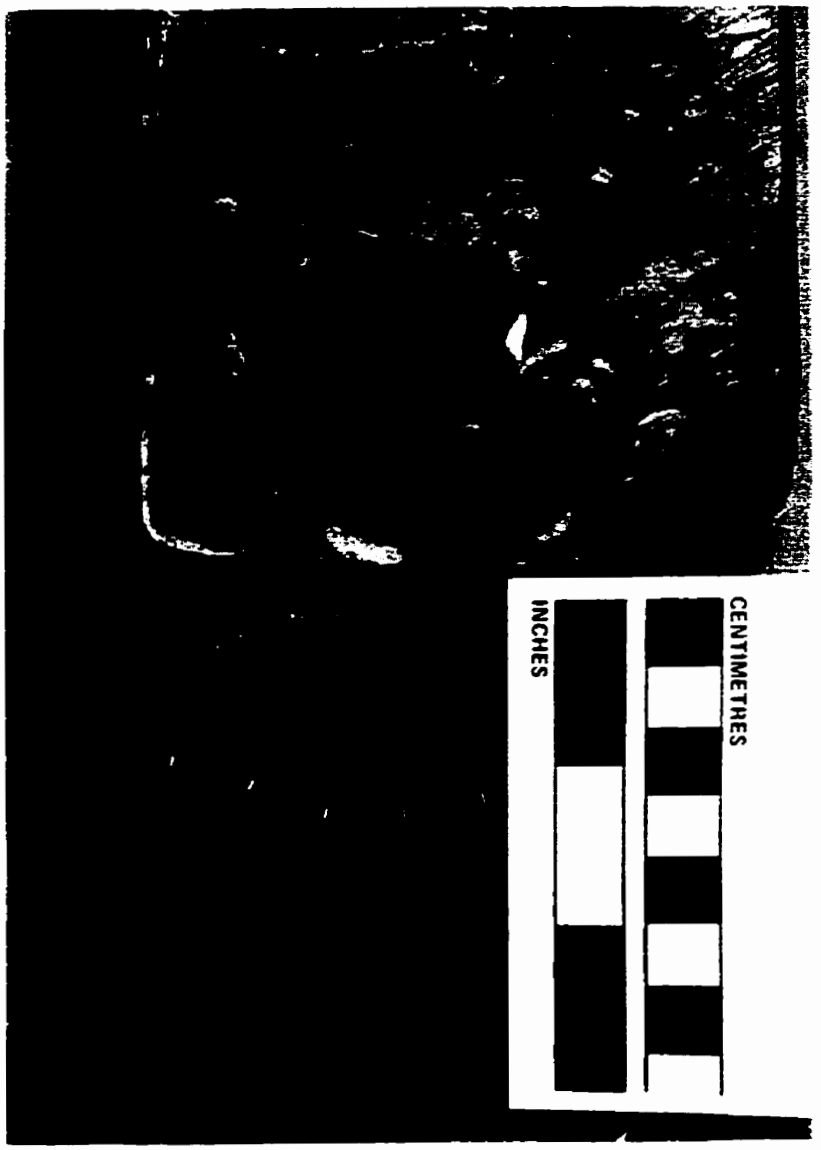

Figure 2.28. Core Photo of Facies 9. Facies 9 – Facies 10 contact. Note the sharp contact (arrows) between the grey lime packstone (bottom) of Facies 9 and the bulbous stromatoporoid grainstone of Facies 10; 16-13-95-5w6, 2341 m (7681 ft).

cemented-grain clasts and lumps are absent (Wendte, 1992b). Low angle laminations and ovoid fenestrae, indicative of shallow (above wave base) and emergent conditions do not occur. The relationship between Facies 9 and the underlying deposits of Facies 6 (shallow lagoon) and 7 (shallow subtidal to supratidal) suggest a deeper water environment of deposition relative to Facies 6 and 7.

Deposition of this facies probably occurred in water depths between 5 to 15 m. Wendte (1992c) established paleowater depths between 5 to 15 m for similar deep shoal lime grainstone and packstone deposits of the Leduc Formation in the Redwater area.

2.2.10 Facies 10: Bulbous Stromatoporoid Grainstone

This facies consists of light brown to brown lime floatstone to wackestone with a skeletal lime grainstone matrix. Fauna consists dominantly of bulbous stromatoporoids (Fig. 2.29), most of which are commonly fragmented and encrusted. Whole/fragments of *Stachyodes*, hemispherical, irregular (encrusting), and tabular stromatoporoids, are common secondary constituents. *Amphipora*, brachiopods and crinoids occur rarely. This facies grades laterally into Facies 9 toward the interior of the Upper Slave Point reefal buildup.

The matrix consists dominantly of peloidal grains. Skeletal components consist of fragments of the larger stromatoporoids, ostracods, calcispheres and indistinguishable bioclastic debris. Porosity within this facies is dominantly primary interparticle that in many cases appears to be enhanced by secondary limestone leaching of the grainstone matrix. Facies 10 is the main reservoir facies in the study area, with an average porosity of 9%.

The lower contact of this facies is commonly very sharp where underlain by

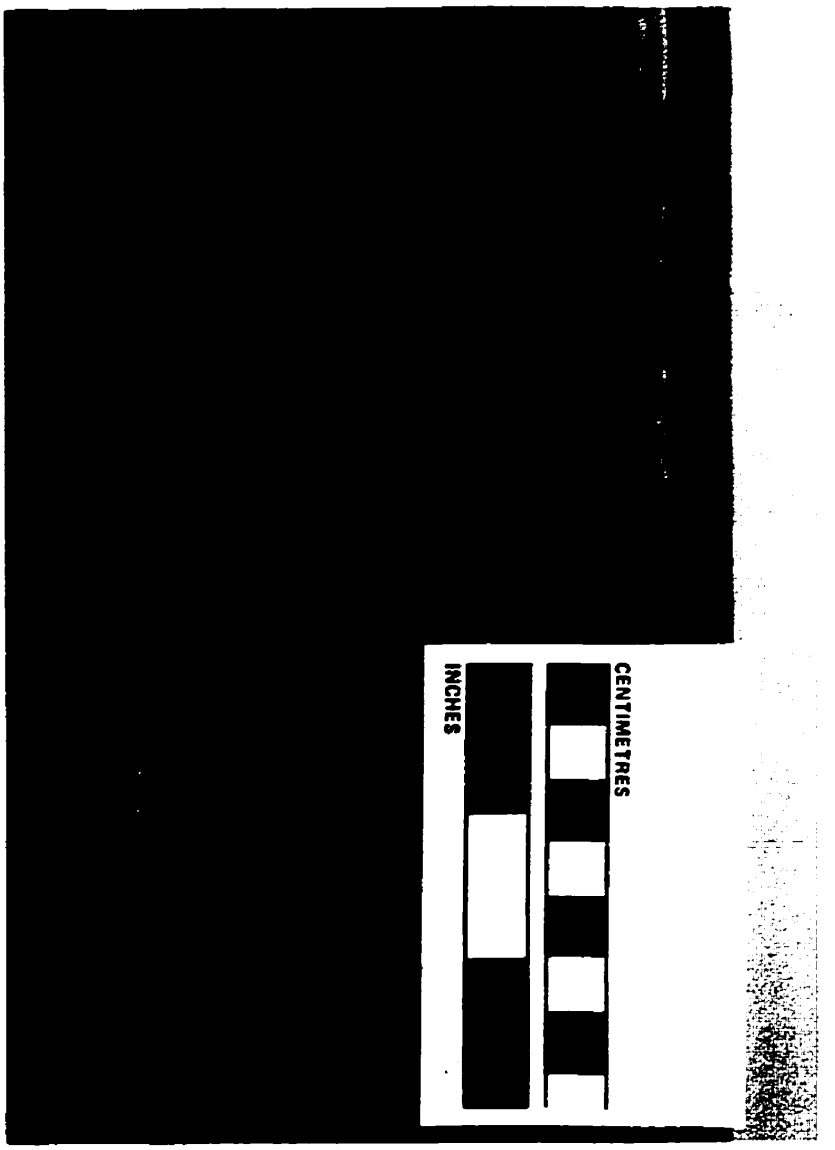

Figure 2.29. Core Photo of Facies 10. Bulbous stromatoporoids in a light brown grainstone matrix with interparticle porosity; 5-17-97-3w6, 2271.5 m (7452 ft).

Facies 6, 7 or 8. The upper contact is typically a sharp burrowed erosional contact or hardground surface where overlain by Facies 14 (Fig. 2.30). This burrowed surface commonly shows evidence of cylindrical excavations, 1 to 2 cm in diameter and up to 5 cm long, (burrows of ichnogenus *Gloss.fungites* ?). This surface also may exhibit surficial pyrite mineralization rimming the burrows, which becomes more diffuse inward (Fig. 2.30), further enhancing the visibility of this contact. This contact is recognizable on both the spontaneous-potential and gamma-ray logs and separates the Upper Slave Point from the overlying Waterways Formation (Fig. 2.1).

This facies is characterized by fragmented and low diversity fauna. The lateral relationship of this facies with Facies 9 suggest a higher energy, open marine environment of deposition relative to Facies 10 (see section 2.2.9). Indicators of extremely shallow conditions are absent (see section 2.2.9). The relationship between Facies 10 and the underlying deposits of Facies 8 (shallow reef margin) suggest a deeper water environment of deposition relative to Facies 8. Encrusted fauna suggest that energy levels fluctuated and/or were intermittently 'stressed' (Wendte, 1992b).

Deposition of this facies probably occurred in water depths between 5 to 15 m. Wendte (1992c) established paleowater depths between 5 to 15 m for similar deep shoal lime grainstone and packstone deposits of the Leduc Formation in the Redwater area.

2.2.11 Facies 11: Stromatoporoid Wackestone and Floatstone

This facies is characterized by brown to dark brown wackestone and floatstone with a packstone matrix and an irregular mottled, nodular texture (Fig. 2.31). The stromatoporoid wackestone commonly grade upwards into floatstone. Fauna consist of abraded whole/fragments of *Stachyodes*, tabular and bulbous stromatoporoids,

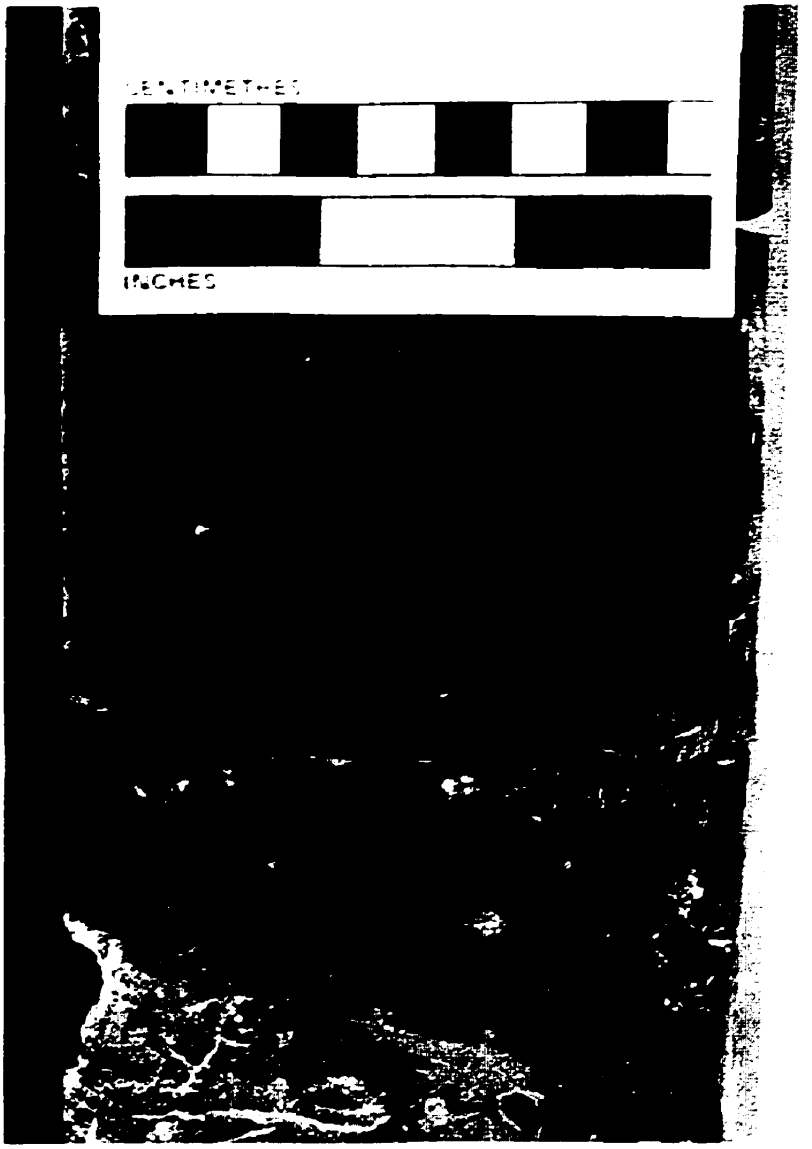

Figure 2.30. Core Photo of Facies 10. Facies 10 - Facies 14 contact. The hardground/pyritized surface of the bulbous stromatoporoid grainstone (bottom) of Facies 10 and the overlying nodular brachiopod wackestone (top) of Facies 14; 3-25-95-5w6, 2267 m (7438 ft).

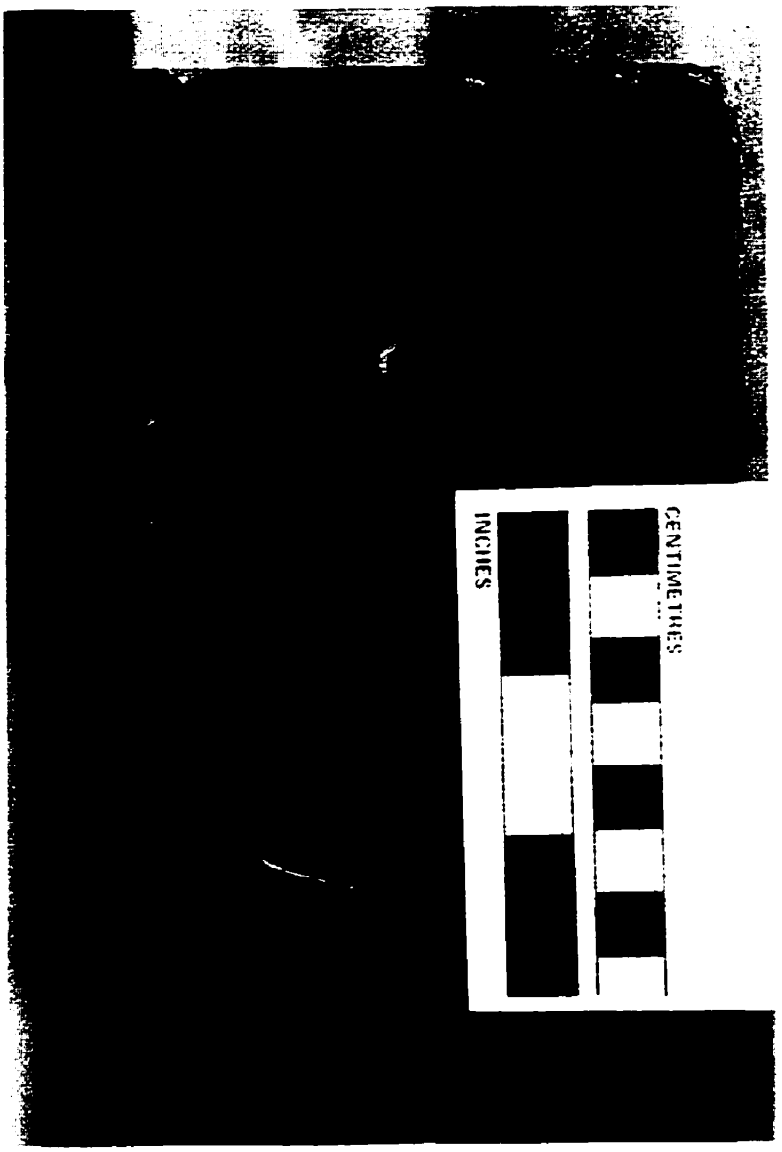

Figure 2.31. Core Photo of Facies 11. Dark brown stromatoporoid wackestone containing *Stachyodes* and *Thamnopora*; 13-15-96-3w6, 2123m (6965 ft).

disarticulated crinoids and brachiopods. Facies 11 grades laterally into Facies 5 and 8. The matrix consists dominantly of micrite (≥ 50%), and peloidal grains. Fragments of the larger bioclasts, ostracods and indistinguishable bioclastic debris commonly occur within the matrix. Porosity is non-existent in a dominantly limestone lithology.

The lower contact of Facies 11 is commonly sharp where underlain by Facies 1 or 2. The upper contact is commonly sharp where overlain by Facies 13 (Fig. 2.32).

The lateral gradational relationship between this facies and Facies 5 and 8, along with the micritic nature and the faunal assemblage indicate a relatively deep, open marine environment. The relationship between Facies 11 and the overlying deposits of Facies 13 (deep water basinal deposits) also suggests a relatively deep water environment of deposition. This facies is similar to the forereef wackestones described by Tooth and Davies (1989) and Davies and Tooth (1987) for the Slave Point Formation at Gift Lake.

Deposition of this facies probably occurred in water depths greater than 10 meters, under conditions somewhat shallower than Facies 13. Wendte (1992c) established paleowater depths between 22 to 30 m for similar skeletal wackestone deposits of the Swan Hills Formation in the Judy Creek area

2.2.12 Facies 12: Laminated Mudstone

This facies is part of the Lower Waterways Formation and is restricted to basinal areas (Fig. 2.2). Facies 12 is characterized by unfossiliferous calcareous mudstone with a laminated appearance (Fig. 2.33). Fauna are generally absent except for rare small brachiopods and crinoids.

The matrix consists of micrite and fine-grained terrigenous material (generally ≤ 25% total rock volume). Porosity is non-existent in a dominantly limestone lithology.

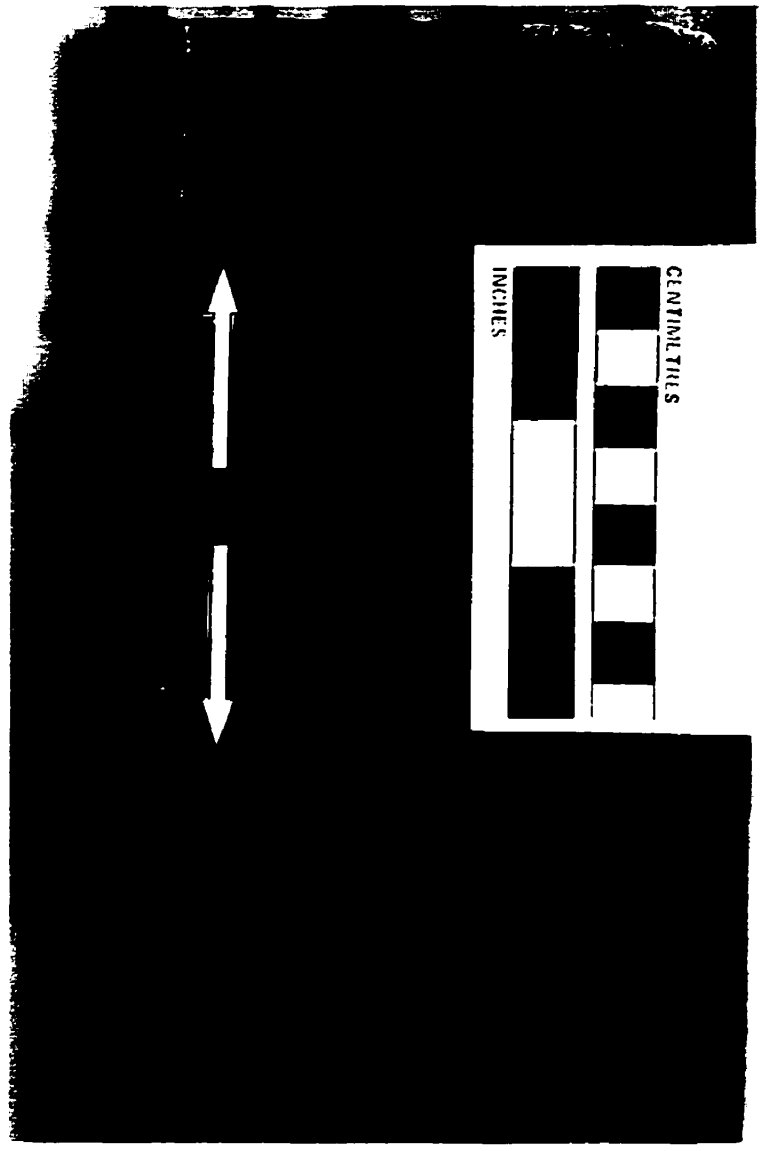

Figure 2.32. Core Photo of Facies 11. Facies 11 - Facies 13 contact. Note the gradational nature of the contact between the stromatoporoid floatstone of Facies 11 (bottom) and the nodular lime mudstone (top) of Facies 13; 13-15-96-3w6; 2096 m (6877 ft).

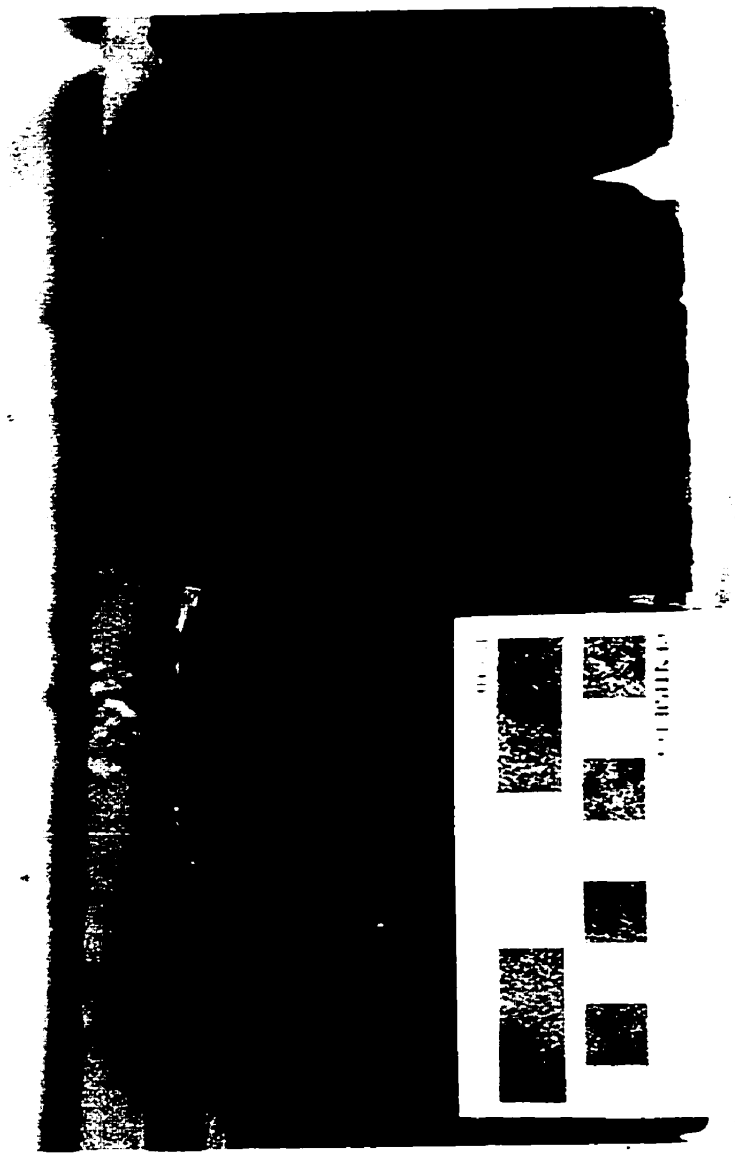

Figure 2.33. Core Photo of Facies 12. Note the dark brown laminated mudstone characteristic of this facies; 7-15-97-3w6, 2133.6 m (7000 ft).

The lower contact of Facies 12 is a very sharp contact when overlying Facies 1 or 2. The upper contact is commonly sharp where overlain by Facies 13.

Facies 12 is characterized by a lack of fauna and a laminated texture. This facies indicates deposition in relatively deep water (below storm wave base), low energy environment. Additionally, the general absence of open marine organisms such as crinoids and burrowing infauna suggests an anoxic environment of deposition. The relationship between Facies 12 and the overlying deposits of Facies 13 (deep water basinal deposits) also suggests a relatively deeper water environment of deposition relative to Facies 13.

Deposition of this facies probably occurred in water depths greater than 30 m, under conditions somewhat deeper than Facies 13. Wendte (1992c) established paleowater depths greater than 30 m for similar basinal laminite deposits of the Swan Hills Formation in the Judy Creek area

2.2.13 Facies 13: Nodular Mudstone

This facies is also part of the Lower Waterways Formation. Facies 13 is characterized by dark brown to brown unfossiliferous mudstone to sparsely fossiliferous mudstone to wackestone matrix with a mottled, nodular texture (Fig. 2.34).

The matrix consists of micrite and fine-grained terrigenous material (generally ≤ 25% total rock volume). Porosity is non-existent in a dominantly limestone lithology.

The lower contact of Facies 13 when overlying Facies 12 is commonly sharp. When Facies 13 overlies Facies 9 or 10 the contact is sharp and erosional, as described previously for Facies 9 and 10. The upper contact of Facies 13 is gradational where overlain by Facies 14 (Fig. 2.35).

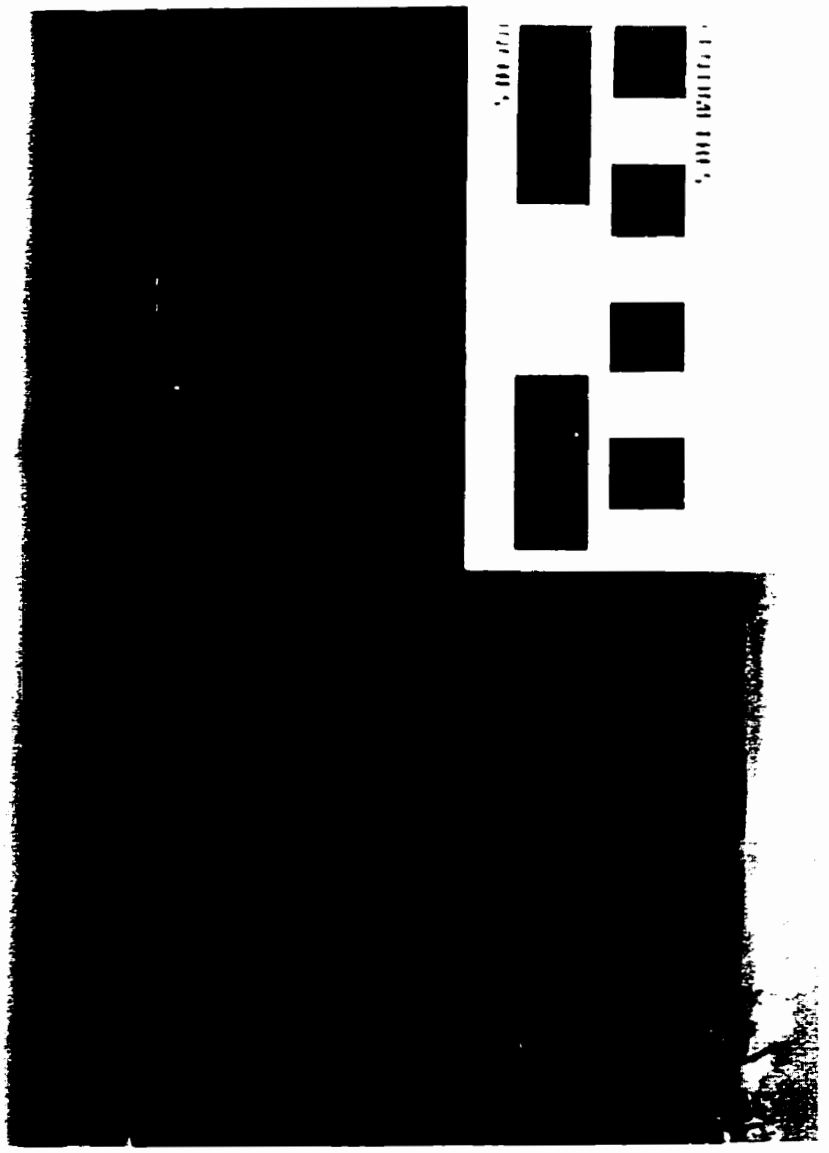

Figure 2.34. Core Photo of Facies 13. Note the brown mudstone with the distinctive nodular texture; 5-21-96-3w6, 2127.5 m (6980 ft).

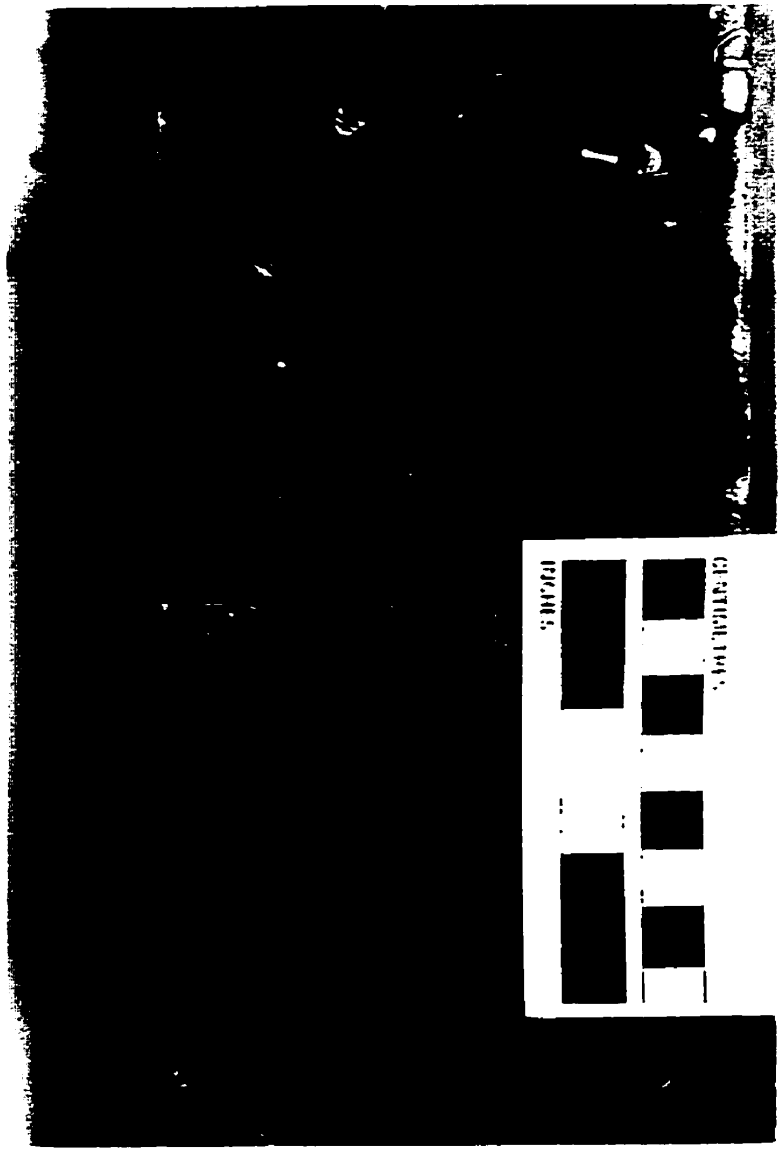

Figure 2.35. Core Photo of Facies 13. Facies 13 – Facies 14 contact. Note the gradational contact between the nodular mudstone (bottom) of Facies 13 and the and nodular brachiopod wackestone (top) of Facies 14; 7-33-96-3w6, 2244 m (7362 ft).

The lateral relationship of this facies with the underlying Facies 12 (laminated mudstone) suggests a relatively shallower water, subtidal (below storm wave base) environment of deposition relative to Facies 12. The sparse fauna and low diversity of organisms suggests a restrictive, perhaps slightly above normal marine salinity conditions, environment of deposition.

It is difficult to estimate paleo-water depths for this cycle, as no depth diagnostic criteria is present. However, deposition of this facies probably occurred in water depths less than 30 m, under conditions somewhat shallower than Facies 12. Wendte (1992c) established paleowater depths between 22 to 30 m for similar nodular mudstone deposits of the Swan Hills Formation in the Judy Creek area

2.2.14 Facies 14: Nodular Brachiopod Wackestone

This facies is also part of the Lower Waterways Formation and forms a laterally extensive deposit which 'caps' Facies 9 of the Upper Slave Point and Facies 13 of the Lower Waterways in the study area. Facies 14 is characterized by dark brown fossiliferous lime wackestones with a mudstone to packstone matrix and a characteristic mottled, nodular texture. Its nodular appearance is derived from the combination of burrowing, compaction and formation of wispy 'horsetail' stylolites. Skeletal components are dominated by brachiopods (Fig. 2.36). Crinoid fragments are common secondary constituents. Facies 14 is informally acknowledged as the 'Cranberry Member' of the Waterways Formation in the study area.

The matrix consists of micrite. Porosity is non-existent in a dominantly limestone lithology.

The lower contact of Facies 14 with the underlying Facies 13 is commonly

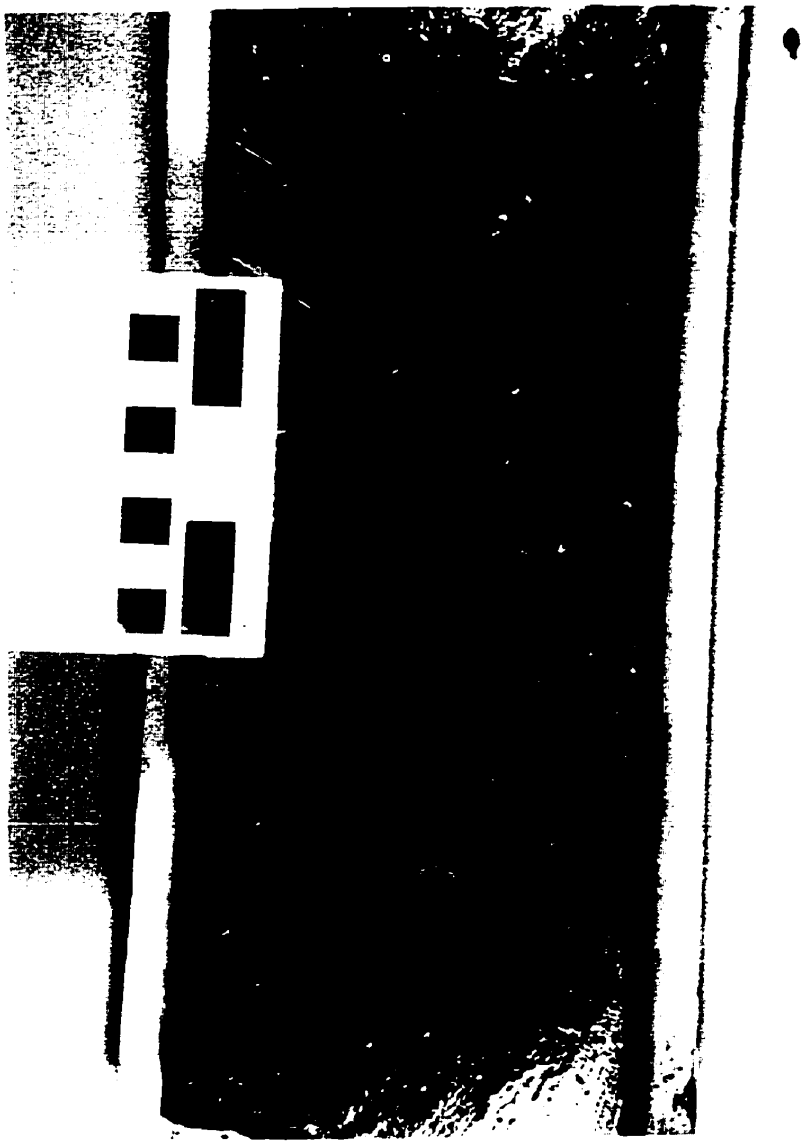

Figure 2.36. Core Photo Facies 14. Dark brown nodular wackestone with scattered atrypid brachiopod and crinoid fragments; 4-36-96-3w6, 2091 m (6860 ft).

gradational (Fig. 2.35), where Facies 14 'caps' Upper Slave Point Facies 9 and 10 the contact is a sharp burrowed, pyritized, erosional contact or hardground surface as described previously for Facies 9 and 10 (Fig. 2.30). The upper contact of Facies 14 is another sharp, pyritized hardground surface (Fig. 2.37) overlain by calcareous shales of the Upper Waterways. This surface may also show evidence of small borings (*Trypanites?*).

This facies indicates a low energy, relatively deep, subtidal (below storm wave base) environment of deposition, similar to that previously described for Facies 2. The presence of open-marine organisms such as brachiopods and crinoids suggests waters of normal marine salinities (Jamieson, 1971; Wilson, 1975; Rosenthal, 1988). The lateral relationship of this facies with the underlying Facies 13 (nodular mudstone) suggests a relatively shallower water, subtidal (below storm wave base), more open marine environment of deposition relative to Facies 13.

It is difficult to estimate absolute water depths for this cycle. Modern brachiopod-crinoid banks have been found at depths of up to 700 meters (Neumann, 1977) and no depth-diagnostic criteria are present within this facies. Wendte (1992c) established paleowater depths between 22 to 30m for similar nodular mudstone deposits of the Swan Hills Formation in the Judy Creek area. Deposition of this facies possibly occurred in water depths greater than 20 m, under conditions somewhat shallower and more open marine relative to Facies 13 .

2.4 Discussion

The Slave Point Formation comprises a complex array of depositional facies that

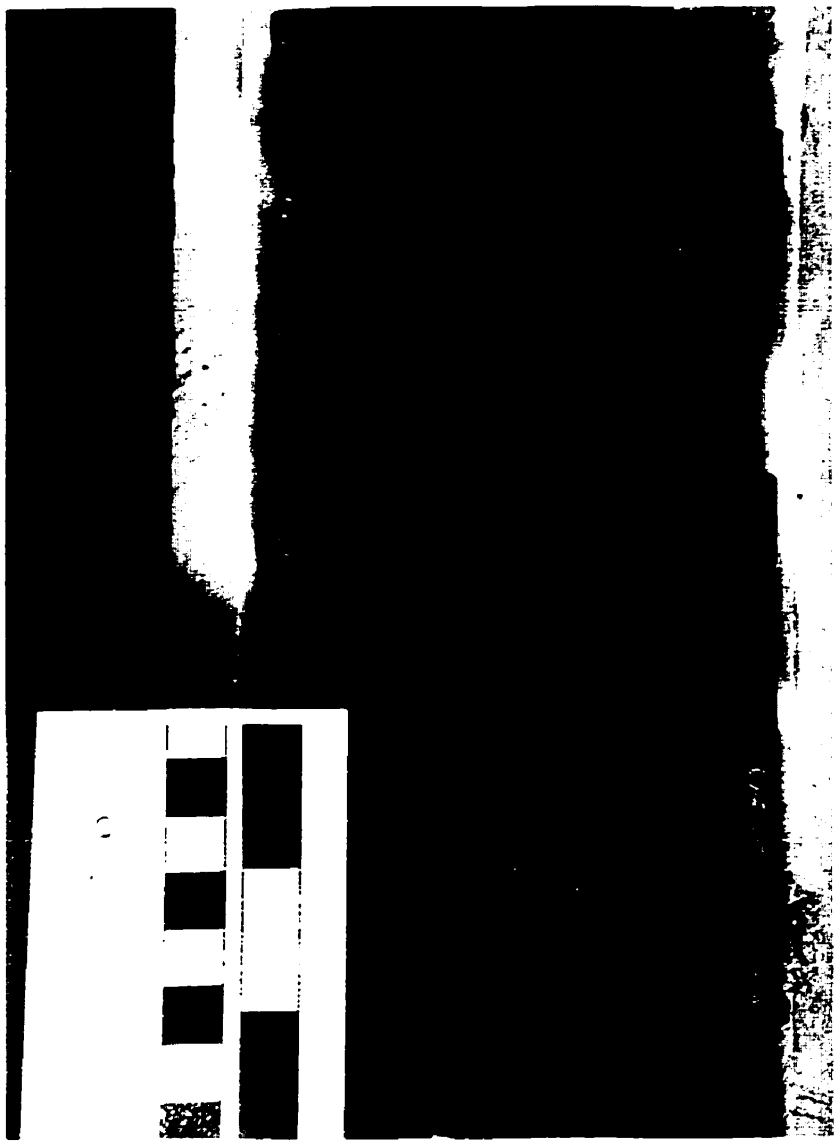

Figure 2.37. Core Photo Facies 14. Facies 14 (Lower Waterways) – Upper Waterways contact. Note the sharp, bored, pyritized hardground surface between Facies 14 (bottom) and the calcareous shales (top) of the Upper Waterways; 5-21-96-3w6, 2126 m (6975 ft).

reflect both lateral and evolutionary changes in depositional environment. The occurrence of reservoir quality porosity in the limestone-dominated succession is directly tied to specific facies. Therefore, an understanding of Slave Point depositional patterns and facies distribution is fundamental to successfully exploring for hydrocarbons.

Figure 2.38 shows the distribution and profile of Slave Point and Waterways Formation depositional facies along cross section B-B' from northwest to southeast across the Cranberry Field. This cross section shows that the lateral and vertical distribution of facies does not remain uniform.

It is evident from Figure 2.38 that the Lower Slave Point is dominantly composed of Facies 1 and 2. Facies 1 and 2 are regionally extensive across the study area. Facies 3 laterally grades into Facies 1 and/or 2.

Figure 2.38 also shows that the Upper Slave Point is composed of Facies 4 through 10. Upper Slave Point Facies 4 overlies Facies 1, 2 and 3. Facies 4, in turn, is overlain by Upper Slave Point Facies 5 and/or 6. Facies 4 can also grade laterally into Facies 5. Facies 5 is more areally restricted than Facies 4 and forms a 'reefal' margin. Facies 5 is overlain by Facies 8 and/or Facies 6. Facies 6 and 7 are restricted to the interior lagoon of the Upper Slave Point 'reefal' buildup. These two facies form numerous shallowing – upward cycles within the lagoon. There are many lateral facies changes within the lagoon environment. Facies 6 and/or 7 are overlain by Facies 9 and/or 10. The lateral 'reefal' margin equivalent of Facies 6 and 7 is Facies 8. Facies 8 is areally restricted and forms the Upper Slave Point 'reefal' margin. Facies 8 is overlain by Facies 10. Facies 10 grades laterally and vertically into the interior of the 'reefal' buildup into Facies 9.

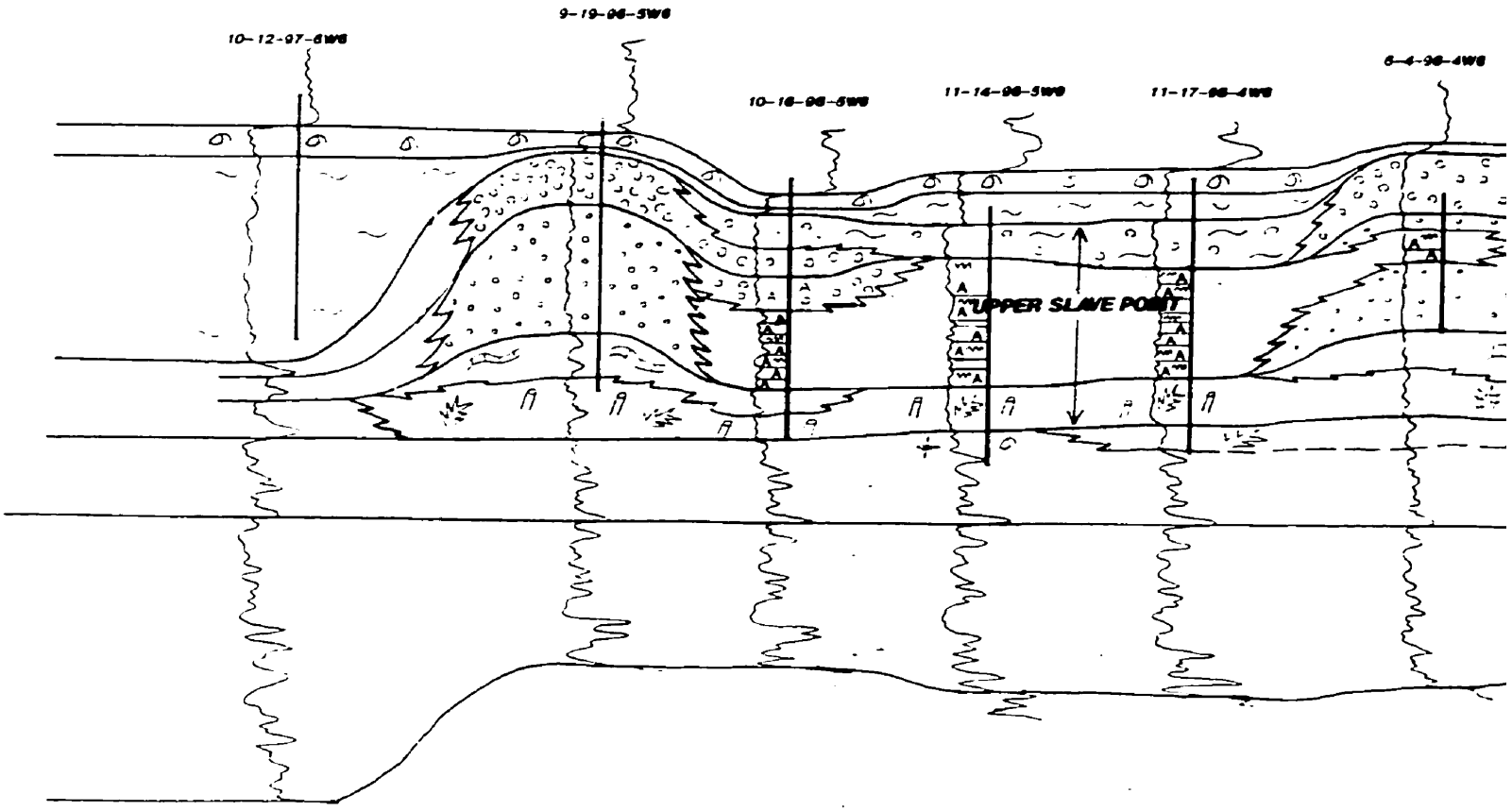

Figure 2.38. Stratigraphic cross-section B-B' showing the d
paleobathymetric profile of Slave Point and Waterwa
facies from northwest to southeast across the Cranbe
Appendix B for facies legend.

B'

TIGRAPHIC CROSS-SECTION

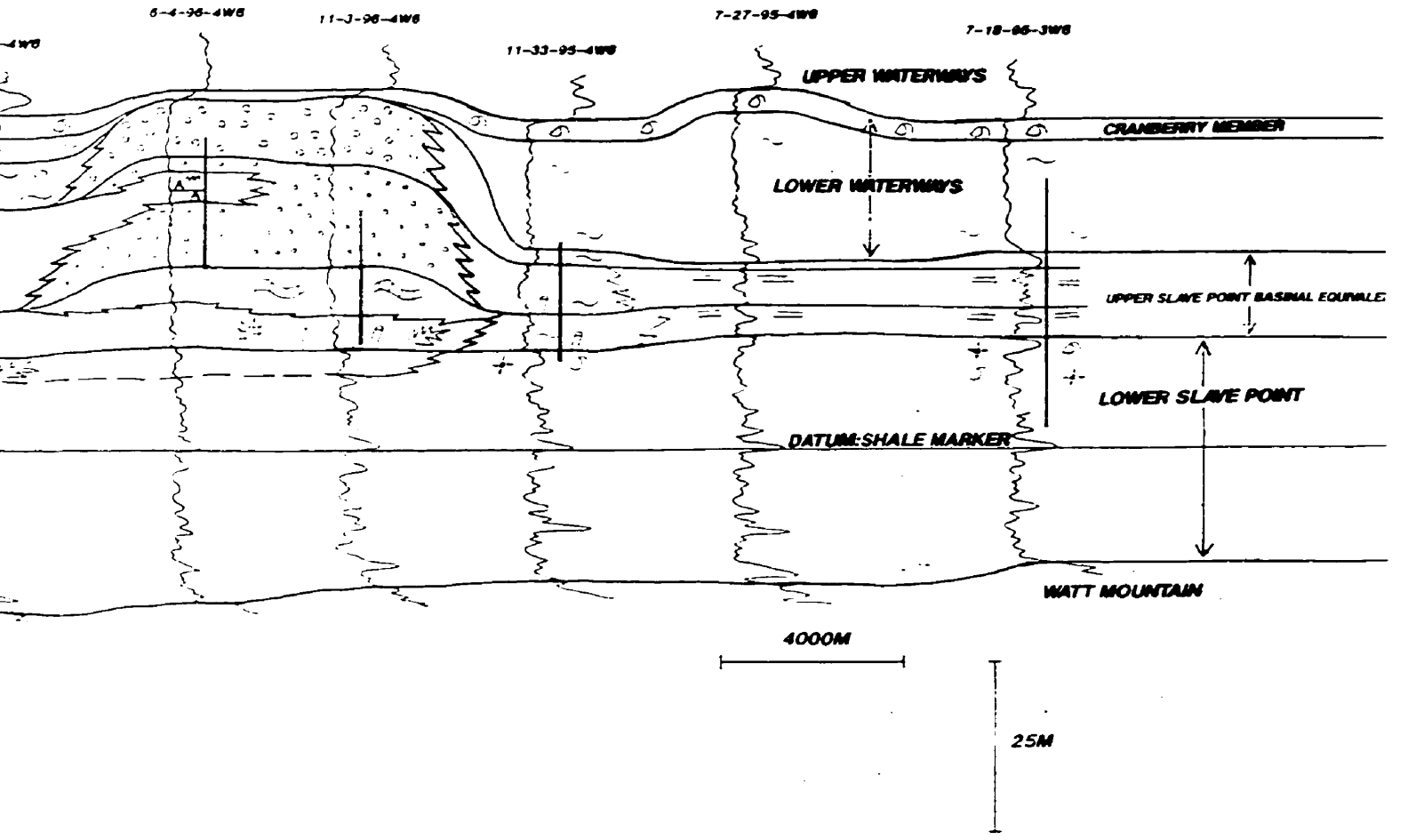

on B-B' showing the distribution and
ave Point and Waterways Formation depositional
east across the Cranberry Field study area. See

Figure 2.38 also shows that Facies 11 forms the correlative forereef deposits to Facies 5 and 8.

The Lower Waterways, from Figure 2.38, is composed of Facies 12, 13 and 14. Facies overlies Facies 1 and/or 2 of the Lower Slave Point in basinal areas. Facies 12 grades laterally into Facies 11 (toward the Upper Slave Point 'reefal' buildup) and vertically into Facies 13. Facies 13 grades vertically into Facies 14, the Cranberry Member. Both Facies 13 and 14 onlap and overlie the Upper Slave Point 'reefal buildup'.

2.5 Summary

The Slave Point Formation in the Cranberry study area has been informally subdivided, on the basis of an extensive core study, into a Lower Slave Point and an Upper Slave Point (Fig. 2.1). Similarly, the Waterways Formation has been informally subdivided, into a Lower Waterways and an Upper Waterways. These major subdivisions of the Slave Point and Waterways Formation in the study area are associated with specific facies, which are in turn related to specific depositional environments (Fig. 2.39).

The Lower Slave Point laterally widespread across the study area and is composed of Facies 1, 2 and 3. The Upper Slave Point is composed of Facies 4 through 10. Facies 4, 5 and 10 comprise the primary reservoir development in the study area. The Lower Waterways is comprised of Facies 12 through 14. These facies are related to the regressive basin-filling style of sedimentation embodied in the Waterways Formation. Although the Lower Waterways does not contain any reservoir quality porosity, it plays a significant role in providing the lateral and top seal to porous Upper Slave Point

	FACIES		ROCK TYPES	IMPORTANT CONSTITUENTS	DEPOSITIONAL ENVIRONMENT
Lower Waterways	14	Nodular Brachiopod Wackestone	Dark-colored brachiopod lime wackestone	Abundant brachiopods; common crinoids	Basin
	13	Nodular Mudstone	Medium-colored lime mudstone; minor wackestone	Crinoids, ostracods, gastropods	Basin
	12	Laminated Mudstone	Dark-colored lime mudstone		Basin
	11	Stromatoporoid Wackestone and Floatstone	Medium-colored lime wackestone and floatstone	Fragments of tabular, hemispherical stromatoporoids, *Stachyodes*, *Amphipora*, *Thamnopora*, brachiopods, crinoids	Forereef
Upper Slave Point	10	Bulbous Stromatoporoid Grainstone	Light-colored bulbous stromatoporoid lime grainstone and packestone	Common bulbous stromatoporoids; some irregular stromatoporoids	Open Shoal
	9	Lime Packestone	Light- to Medium-colored lime packestone; minor grainstone	Common micritic lumps and/or peloids; calcispheres	Restricted Shoal
	8	Hemispherical Stromatoporoid Rudstone and Boundstone	Light- to Medium-colored hemispherical and bulbous stromatoporoid lime boundstone; minor rudstone	Abundant *in situ* hemispherical and tabular stromatoporoids; common bulbous, irregular stromatoporoids	Upper Foreslope (Reef Margin)
	7	Tidal Laminite	Medium-colored laminated lime packestone; minor lime mudstone	Cryptomicrobial laminations, peloids, *Amphipora*	Restricted Lagoon
	6	*Amphipora* Rudstone and Floatstone	Medium- to dark-colored Amphipora lime rudstone and floatstone; minor wackestone	Abundant *Amphipora*; common calcispheres; some bulbous stromatoporoids, *Stachyodes*.	Open Lagoon
	5	Tabular Stromatoporoid Floatstone and Rudstone	Light- to dark-colored tabular stomatoporoid lime rudstone and boundstone	Abundant tabular stromatoporoids; common hemispherical; some *Stachyodes*, *Thamnopora*	Upper Foreslope (Reef Margin)
	4	*Stachyodes* – *Thamnopora* Floatstone	Light- to dark-colored *Stachyodes* and *Thamnopora* lime floatstone	Abundant *Stachyodes*; some *Thamnopora*, bulbous stromatoporoids	Middle Foreslope
Lower Slave Point	3	*Thamnopora* Wackestone	Dark- to medium-colored *Thamnopora* lime wackestone	common *Thamnopora*, some tabular (wafer) stromatoporoids, *Stachyodes*, brachiopods, crinoids	Lower Foreslope
	2	Nodular Brachiopod – Crinoidal Wackestone	Dark-colored brachiopod-crinoidal lime wackestone	Common brachiopods and crinoids	Platform
	1	Mudstone	Dark-colored lime mudstone	Brachiopods, crinoids	Platform

Figure 2.39. Summary of depositional facies and their interpreted environment of deposition in the Cranberry study area. Note: facies are not necessarily represented in a vertical facies succession order.

sediments. The Upper Waterways, although not evaluated extensively in this study, is laterally widespread across the study area and is comprised of alternating calcareous shales and argillaceous limestones (post-Slave Point).

CHAPTER 3: SLAVE POINT DEPOSITIONAL HISTORY

3.1 Introduction

A depositional model comprising 14 facies has been constructed to explain the shallow-water facies development in the Slave Point Formation on the basis of 96 cores.

The Slave Point Formation shows both lateral and vertical facies variations (Appendix B). Shifts in facies correspond to cycles of sedimentation (Wendte, 1992c). These cycles, described in the following sections, are generally less than 10 m thick and correspond to the relative third-order Devonian cycles.

3.2 Depositional Cycles

For many years investigators have recognized that carbonate facies tended to occur in distinct vertical associations termed upward shoaling cycles or sequences. The terms cycle and sequence are used interchangably (Wendte, 1992c). These cycles typically have sharp to thinly transitional upper and lower contacts. Almost all cycle boundaries are characterized by the occurrence of either deep water over shallow water facies or more basinward over bankward facies. An understanding of the context of cyclicity provides a general model that can be used to highgrade and evaluate potential reservoir, source and seal facies.

The Devonian cycles in the Western Canada Sedimentary Basin (WCSB) can be considered in terms of three relative levels that are easily definable (Wendte, 1992c). First order cycles encompass genetically related packages of sediments that may be traced across basins of deposition and record a complete movement of sea level from one

fall to the next. These cycles contain a number of rock units of formational level and generally equate to group status (i.e. Beaverhill Lake Group).

Second order cycles consist of packages of upwarding-shoaling cycles that generally equate individually or collectively to formation level status (i.e. Slave Point Formation). These cycles reflect small-scale movements of sea level superimposed on the first order cycles (Fig. 3.1).

Third order cycles also consist of an upward shoaling succession of facies but generally only thinly developed (on the order of a few meters) and characterize platform interior and lagoonal settings (Fig. 3.2). The identifiable extent of these cycles, however, is not uniform across environments of carbonate deposition (i.e., a reef). Third order cycles are best expressed in "incompetent" environments especially sensitive to sea level rises (i.e., lagoonal environments). These third order cycles represent stages of sedimentation that include 'reef' growth (i.e., Upper Slave Point) and concomitant and reciprocal basinal deposition.

The second and third order cycles are the basic building blocks for discerning the evolution of Devonian strata in the WCSB. Understanding the nature of both second and third order cycles is key to understanding the distribution and quality of reservoir units in hydrocarbon pools.

Core and log observations in this study indicate that the Slave Point and Waterways Formations can be subdivided into 5 distinct second order cycles: 1) Cycle 1 - Lower Slave Point Basal Platform; 2) Cycle 2 - Upper Slave Point Basal Bank; 3) Cycle 3 - Upper Slave Point 'Reef'; 4) Cycle 4 - Upper Slave Point Shoal; and 5) Cycle 5 - Lower Waterways Basin-Fill,

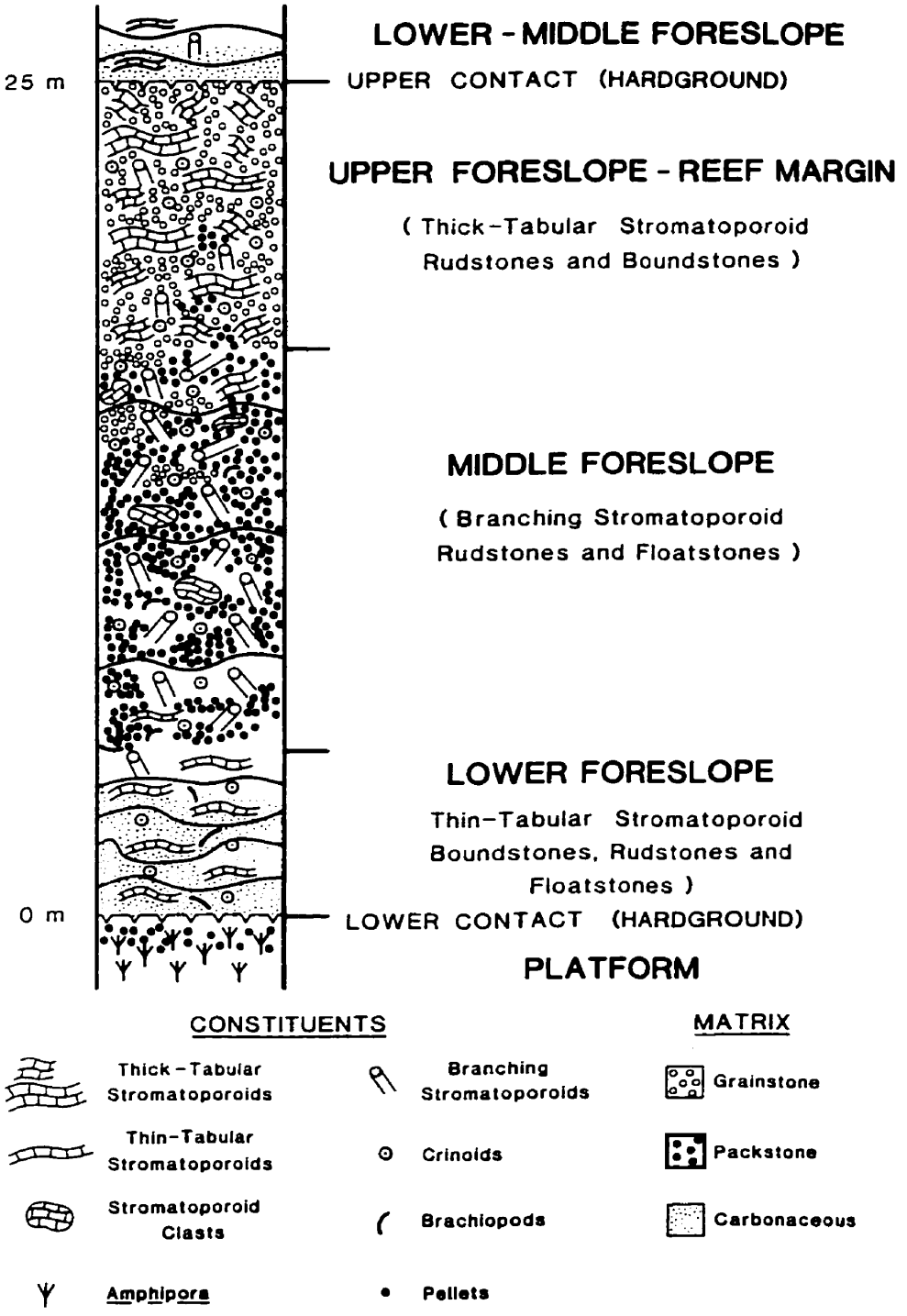

Figure 3.1. Typical succession of facies in a Devonian second order cycle along a reef margin (Wendte, 1992c).

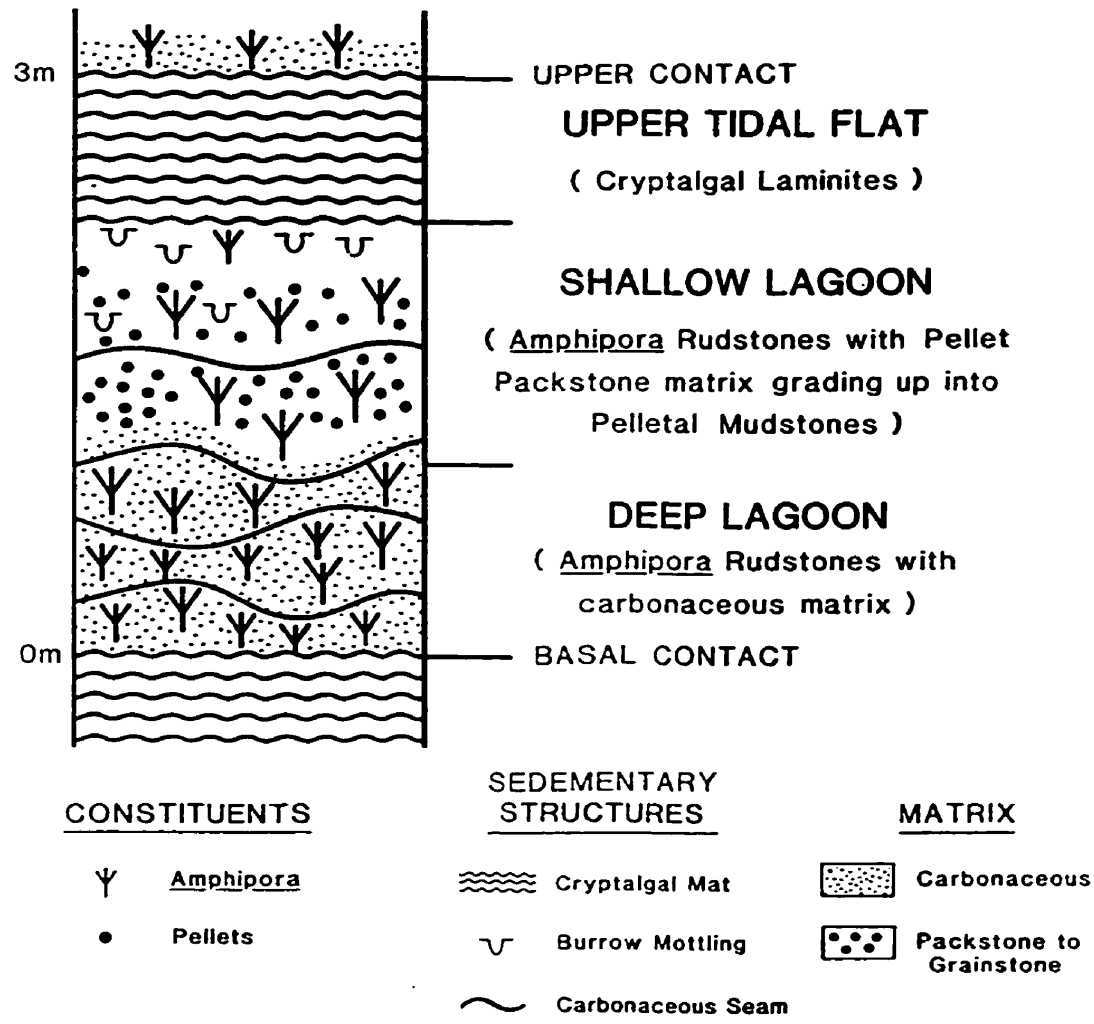

Figure 3.2. Typical succession of facies in a 'complete' Devonian third order cycle within the lagoon of the Slave Point Formation.

Figure 3.3 illustrates the characteristic log response and correlation of Slave Point and Waterways cycles and associated facies in the 'reefal' buildup and basinal settings.

3.2.1 Cycle 1: Lower Slave Point Basal Platform

In the study area, the Lower Slave Point Basal Platform consists of a shoaling upward succession of facies unconformable with the underlying shales and sandstones of the Watt Mountain Formation.

Cycle is characterized by three facies: Facies 1, Facies 2 and Facies 3. The mudstone of Facies 1 grades upward into the nodular brachiopod-crinoidal wackestone of Facies 2. Facies 2, in turn, may grade upward into the *Thamnopora* wackestone of Facies 3, where Facies 3 is present (Fig 2.12). The relationship between Facies 1, 2 and 3 suggests a shoaling or shallowing upward succession. These facies comprise the basal, laterally extensive Lower Slave Point Basal Platform, which displays a relatively uniform log character (Fig. 2.38) and varies in total thickness from 16 to 73 m toward the north (Fig. 3.4), forming an asymmetric wedge in the study area. This asymmetric pattern generally reflects the onlap of the Lower Slave Point onto the Peace River Arch in a southerly direction as well as increased subsidence rates away from the Arch in an east-west trend through the northern part of the study area (Craig, 1987). Figure 3.4 suggests that differentiation of Slave Point paleogeography into basin and reefal buildups, observed as thins and thicks respectively, had begun towards the end of Lower Slave Point Basal Platform time. The distribution of Lower Slave Point thicks and thins is opposite to that of the Upper Slave Point (Fig 3.5), that is Upper Slave Point thicks are developed on Lower Slave Point thins and vice-versa. This represents the infilling aspect

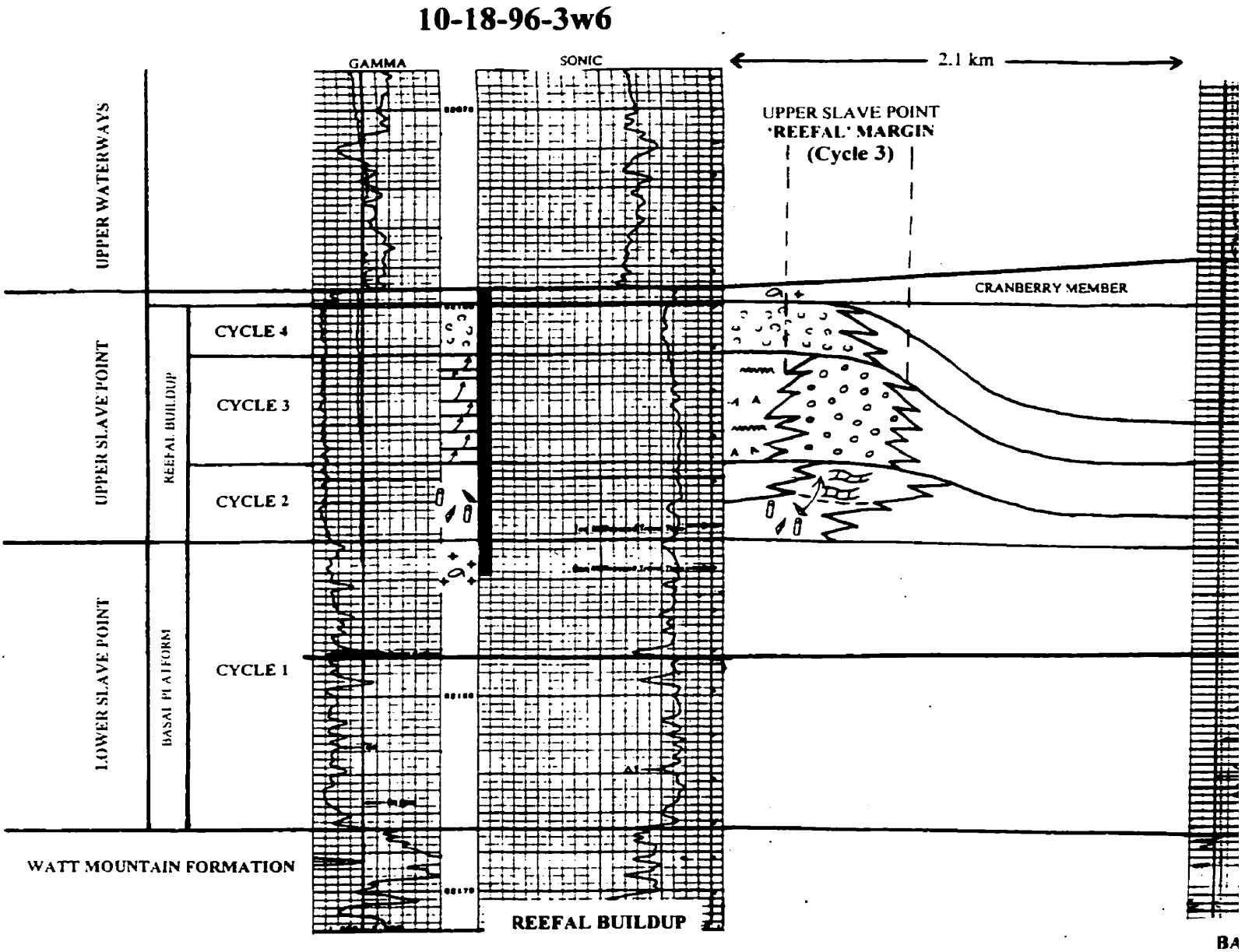

Figure 3.3. Characteristic log response and stratigraphic rela
buildup well and a basinal well.

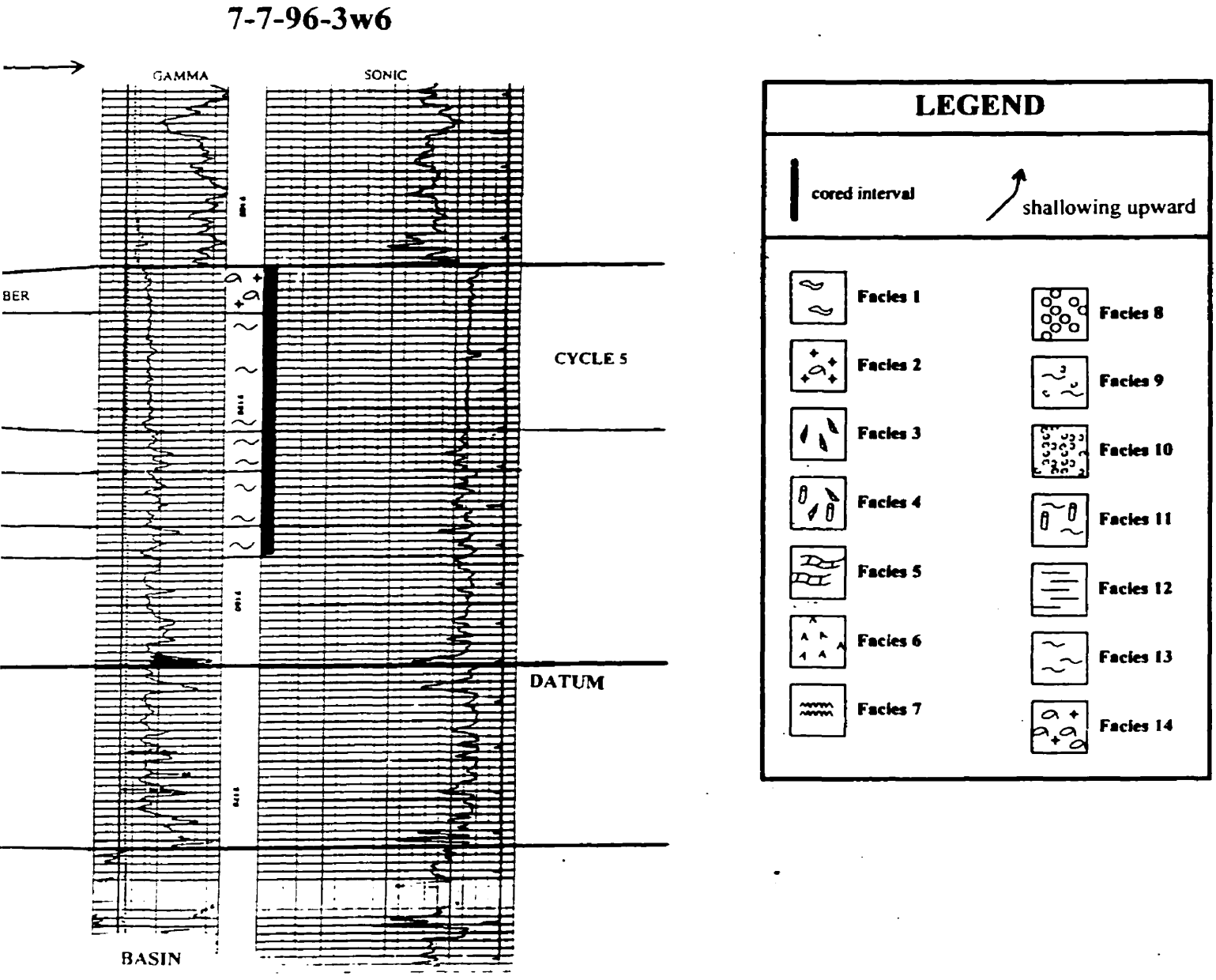

tigraphic relationships between a 'reefal'

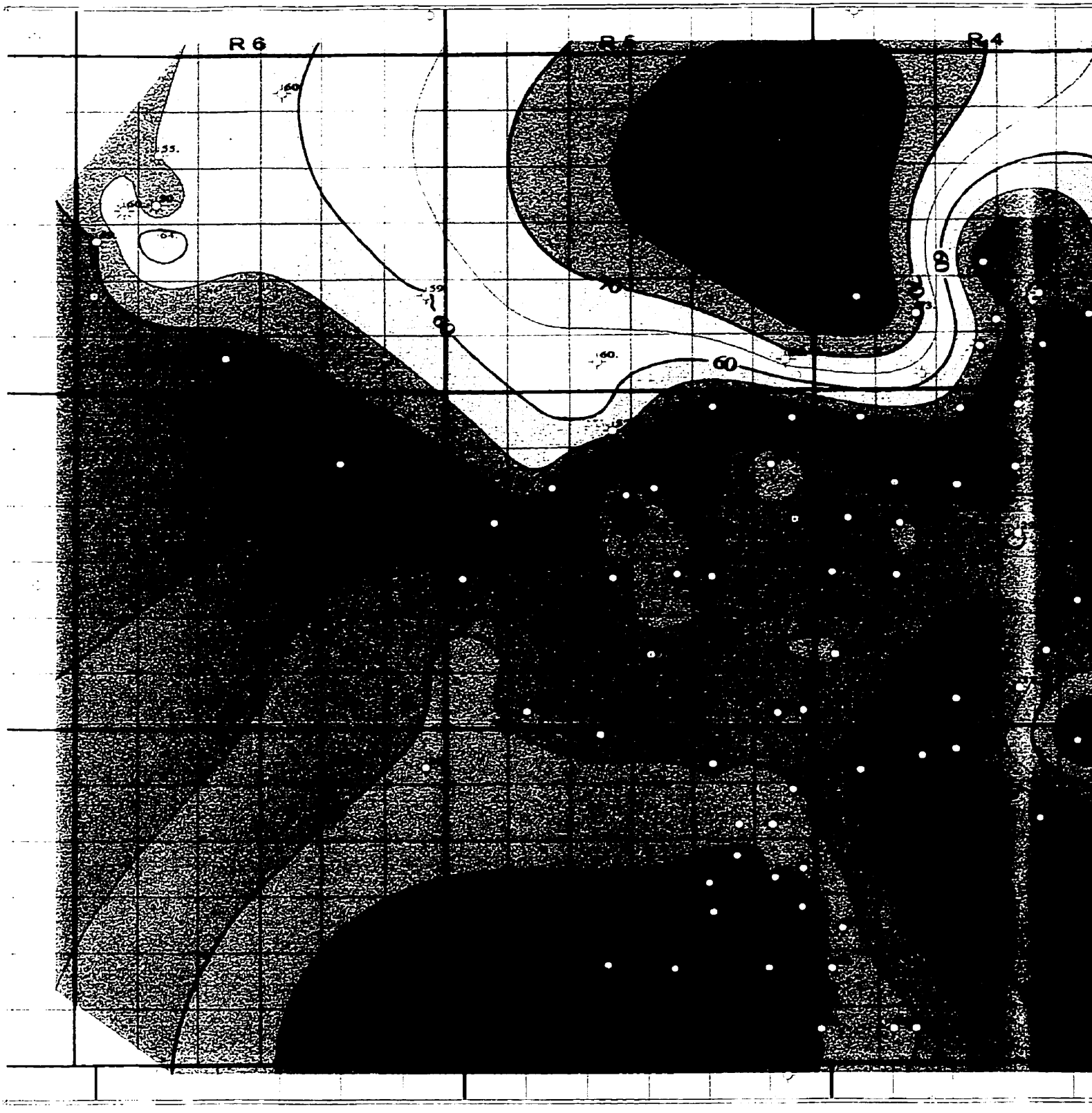

Figure 3.4. Lower Slave Point isopach map. Scale 1:150,0
Lower Slave Point towards the north in the study a

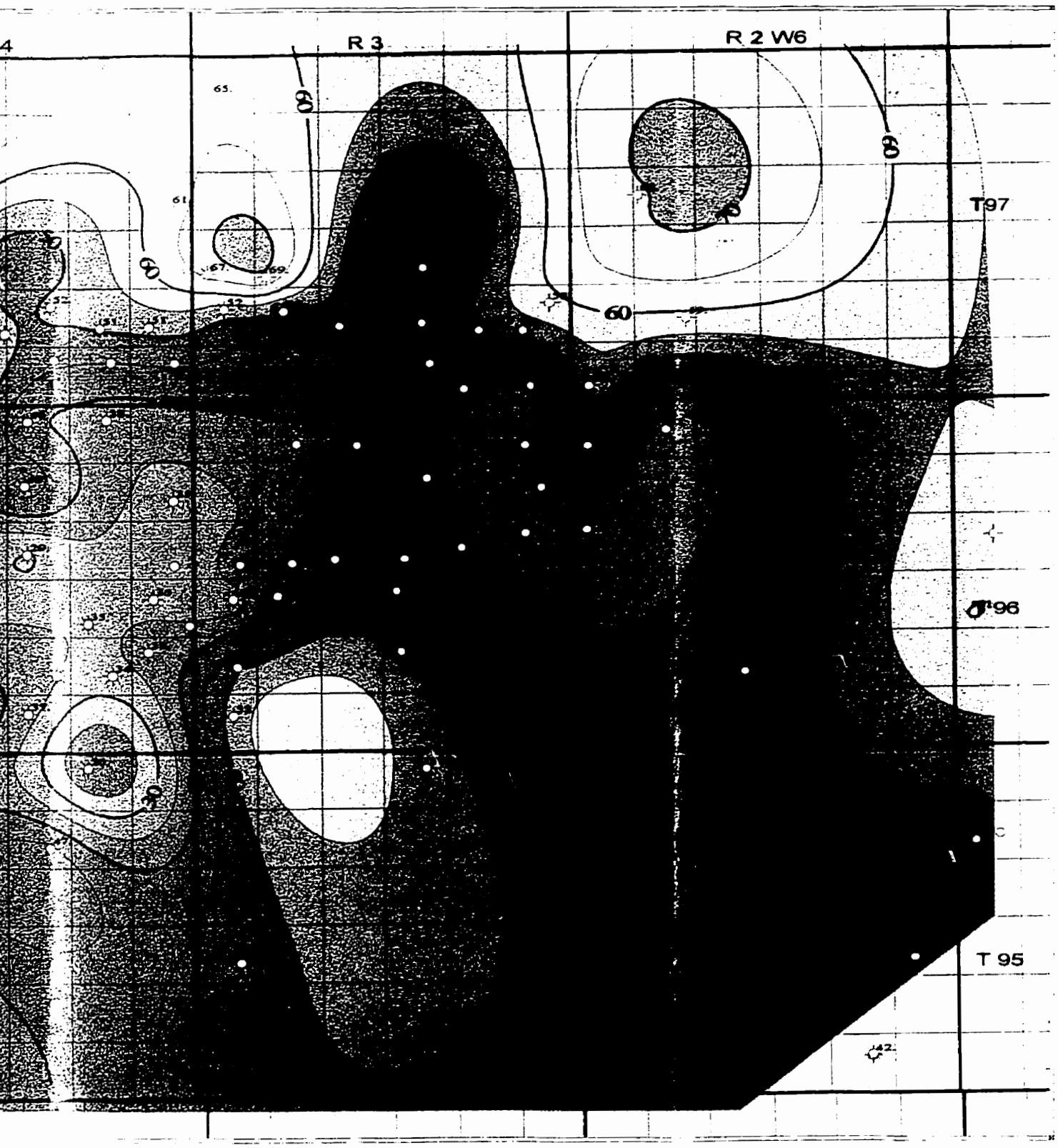

ale 1:150,000. Note the thickening of the
the study area. Contour Interval is 5 m.

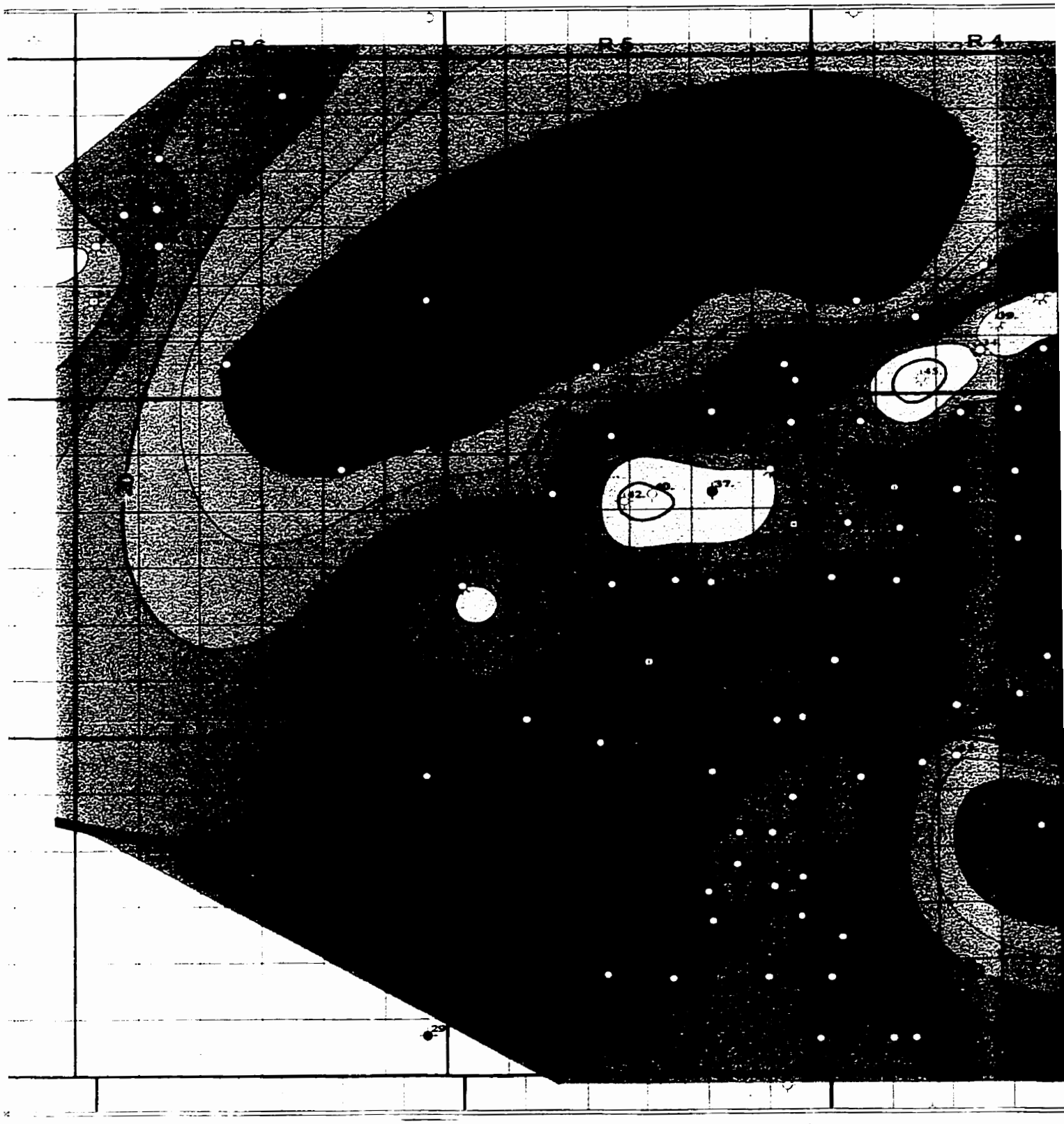

Figure 3.5. Upper Slave Point isopach map. Scale
Upper Slave Point along the northern marg
buildup (solid black line). Contour Interva

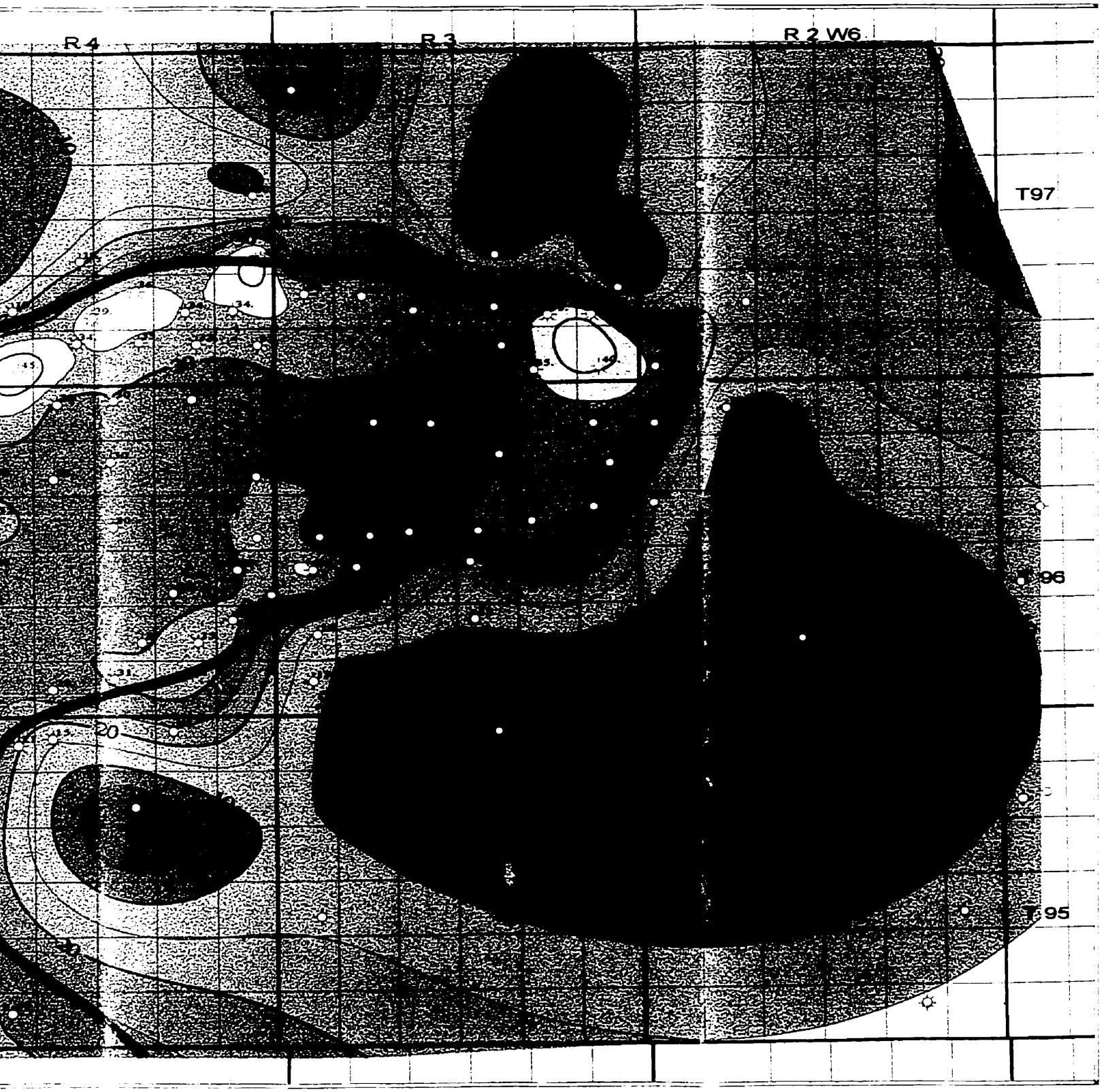

opach map Scale 1:150,000. Note the thickening of the
the northern margin of the Upper Slave Point 'reefal'
. Contour Interval is 5 m.

of Lower Slave Point deposition versus the transgressive aggradational aspect of Upper Slave Point deposition (Campbell, 1992).

The Lower Slave Point Basal Platform represents platform to shallow bank development (Craig, 1987). This laterally extensive cycle acted as the platform upon which the Upper Slave Point Basal Bank developed. Subtle paleotopographic highs were colonized by Facies 3 *Thamnopora* during the Lower Slave Point Basal Platform cycle and were the preferred sites for later Upper Slave Point Basal Bank deposition.

The contact between the Lower Slave Point Basal Platform and the Upper Slave Point Basal Bank is typically a sharp, erosional surface (Fig. 2.13; Fig. 2.16).

3.2.2 Cycle 2 : Upper Slave Point Basal Bank

In the study area, the Upper Slave Point Basal Bank consists of a shoaling upward succession of facies conformable with the underlying Lower Slave Point Basal Platform.

Cycle 2 is characterized by two facies: Facies 4 and Facies 5. The *Stachyodes* - *Thamnopora* wackestone of Facies 4 commonly grade upward into the tabular stromatoporoid floatstone and rudstone of Facies 5, where Facies 5 is present (Fig 2.17). This second order cycle comprises the lower third of the Upper Slave Point 'reefal' buildup and varies in thickness between 3 to 13 m in the study area (Fig. 3.6).

Upper Slave Point Basal Bank deposition appears to have been controlled by subtle paleotopographic highs colonized by *Thamnopora* during Lower Slave Point Basal Platform deposition (Facies 3). The Upper Slave Point Basal Bank has no equivalent interior lagoonal sediments which suggests a progradational style of growth (Campbell, 1992); reflecting open marine conditions, shallow bathymetry and moderate to high carbonate production. During Cycle 2 deposition the antecedent topography of Cycle 1

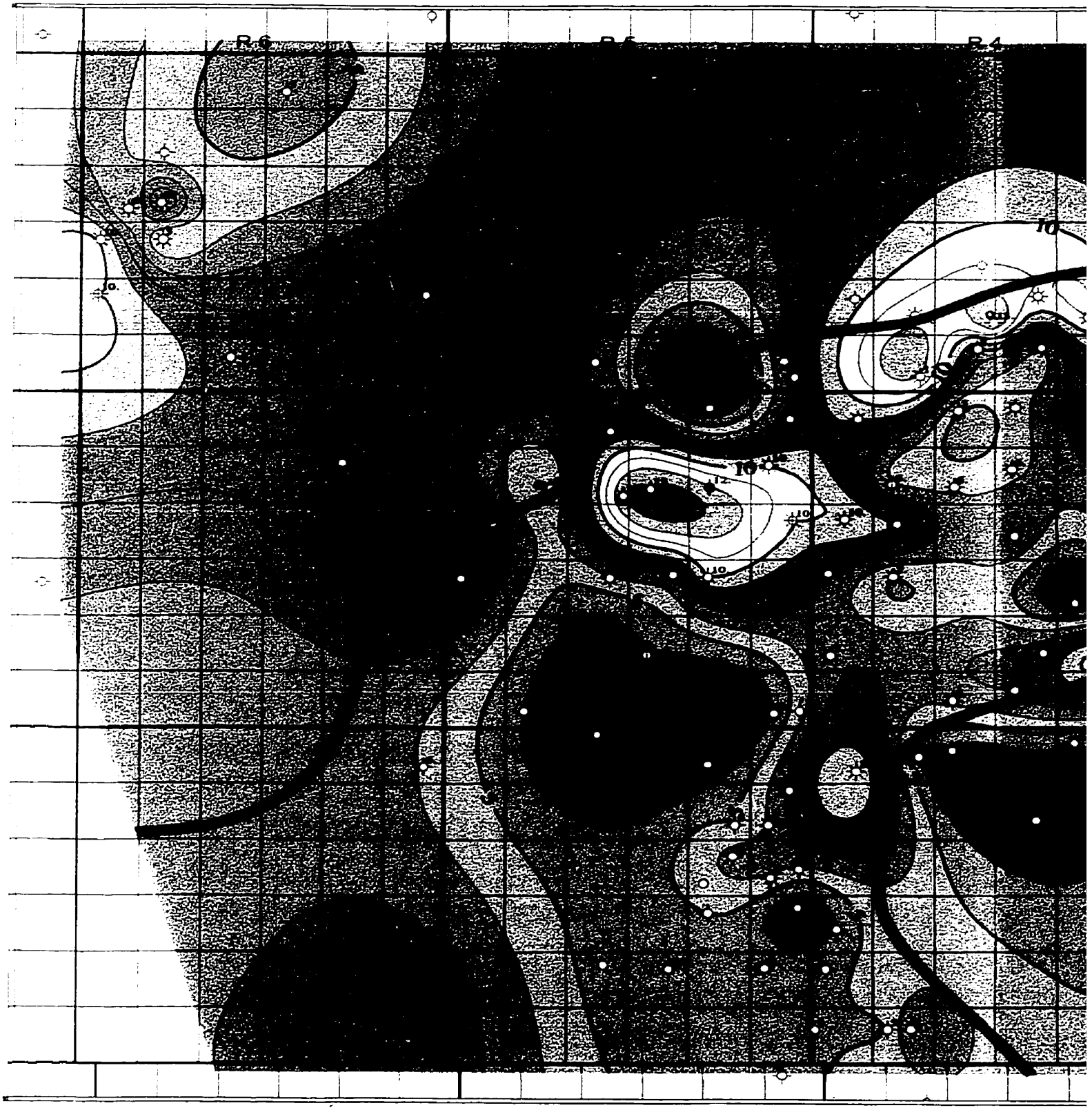

Figure 3.6. Cycle 2 - Upper Slave Point Basal Bank isopa
Note the outline of the Upper Slave Point 'reefal'
Contour Interval is 1 m.

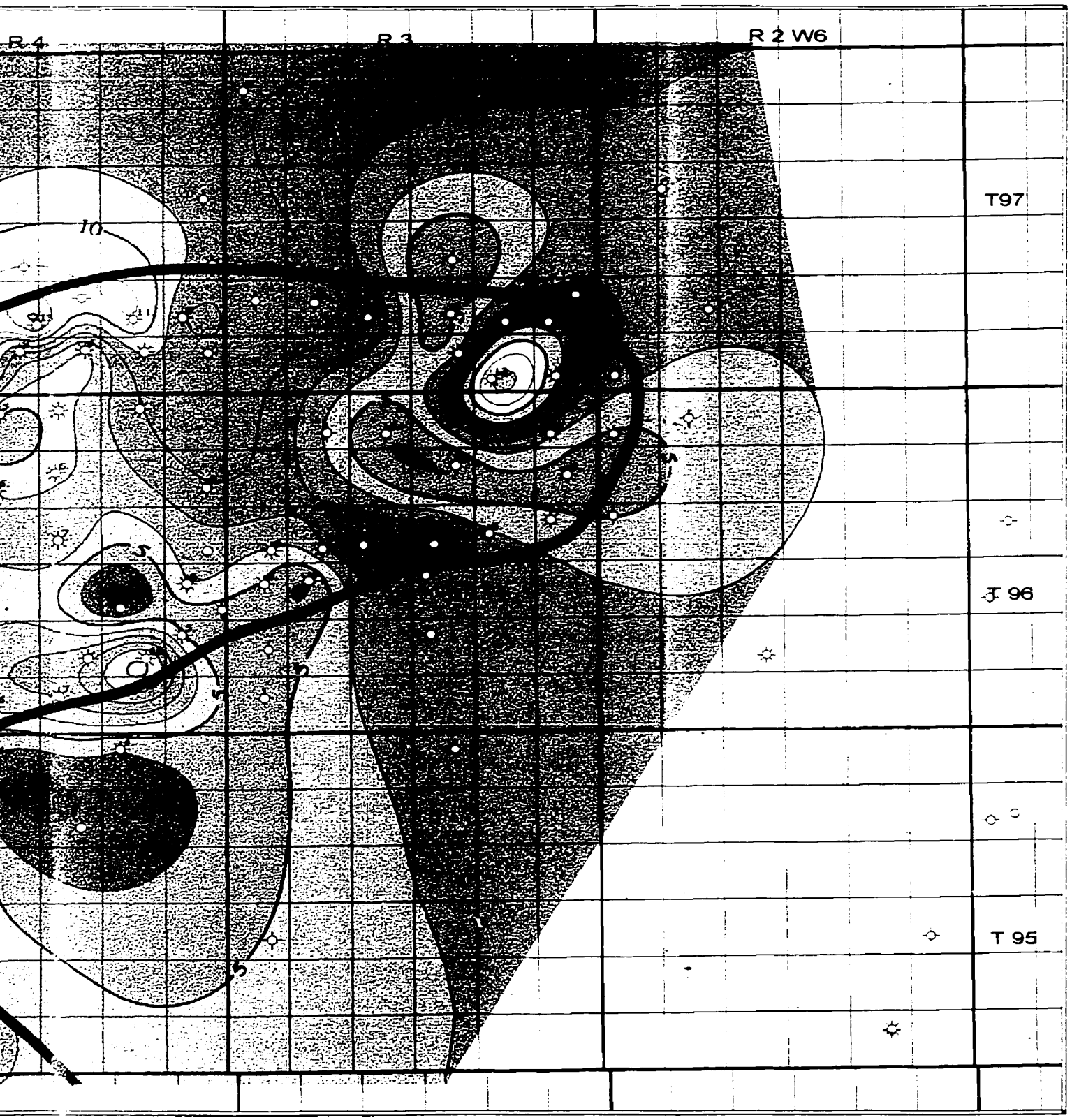

sal Bank isopach map. Scale 1:150,000.
Point 'reefal' margin (solid black line).

became further emphasized and a distinct 'reef' and basin configuration became established (Fig. 3.6). This second-order cycle represents the initial 'reefing' or growth cycle of the Upper Slave Point 'reefal' buildup.

Correlative foreslope deposits are the deeper water deposits of Facies 11. These deposits consist of the slightly bioturbated stromatoporoid wackestone deposited in the forereef or foreslope environment.

The upper contact of the Upper Slave Point Basal Bank and the overlying Upper Slave Point 'Reef' is typically sharp (Fig. 2.18).

3.2.3 Cycle 3: Upper Slave Point 'Reef'

In the study area, the Upper Slave Point 'Reef' is composed of numerous shoaling upward sequences (third order cycles) conformable with the underlying Upper Slave Point Basal Bank.

Cycle 3 is characterized by three facies: Facies 6, Facies 7 and Facies 8. The *Amphipora* rudstone and floatstone of Facies 6 grade upward into the cyptomicrobial laminite of Facies 7. Facies 6 and 7 form numerous shoaling or shallowing upward (third order) cycles within the interior or lagoon of the Upper Slave Point 'Reef'.

The hemispherical stromatoporoid rudstone and boundstone of Facies 8 is the lateral 'reefal' margin equivalent to the lagoonal deposits of Facies 6 and 7. However, few wells have encountered the Cycle 3 margin, indicating that this margin forms a relatively narrow band along the 'reefal' buildup edge (Fig. 3.7). The cyclicity observed in the lagoonal facies is not generally expressed in the 'reefal' margin environment (Wendte, 1992c). Cycle 3 varies in total thickness between 11 and 25 m (Fig. 3.8) in the study area. Figure 3.8 shows that depositional patterns established at the end of Cycle 2

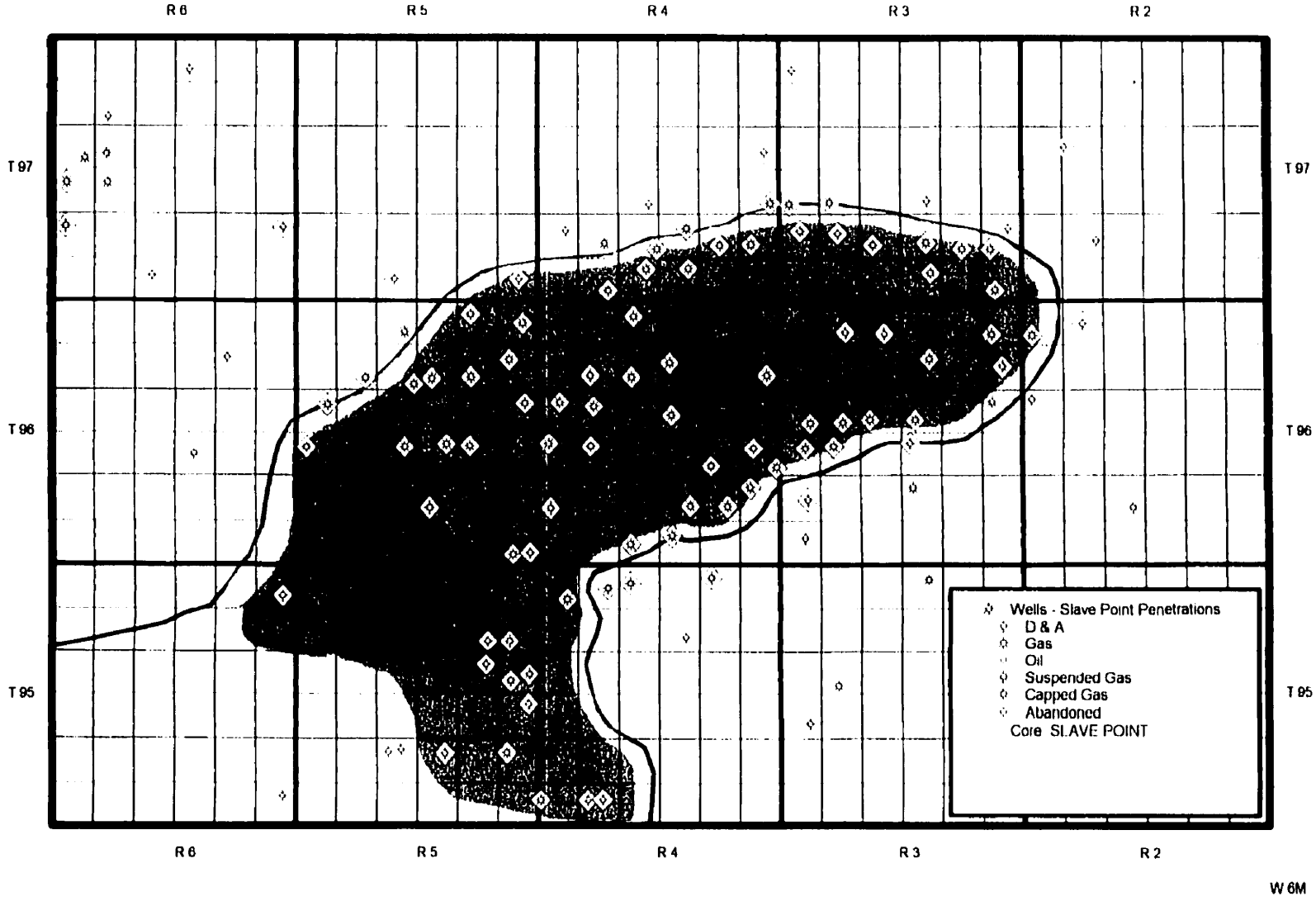

Figure 3.7. Cycle 3 - Upper Slave Point 'Reef' depositional facies map. Note the relationship between the 'reefal' margin, Facies 8 (yellow) and its lateral equivalent lagoonal facies, Facies 6 and 7 (green).

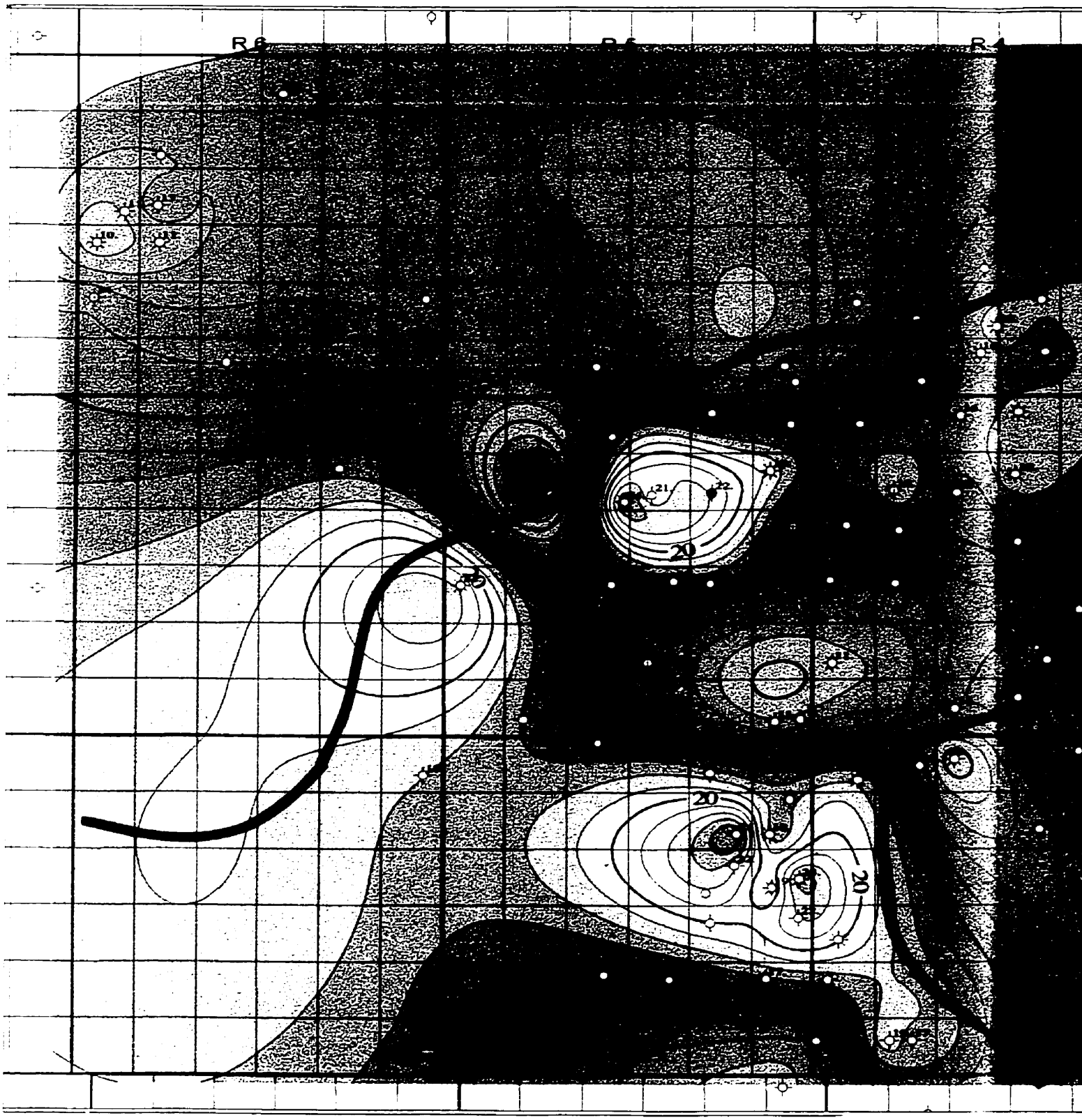

Figure 3.8. Cycle 3 - Upper Slave Point 'Reef' isopac
outline of the Upper Slave Point 'reefal' margi
Interval is 1 m.

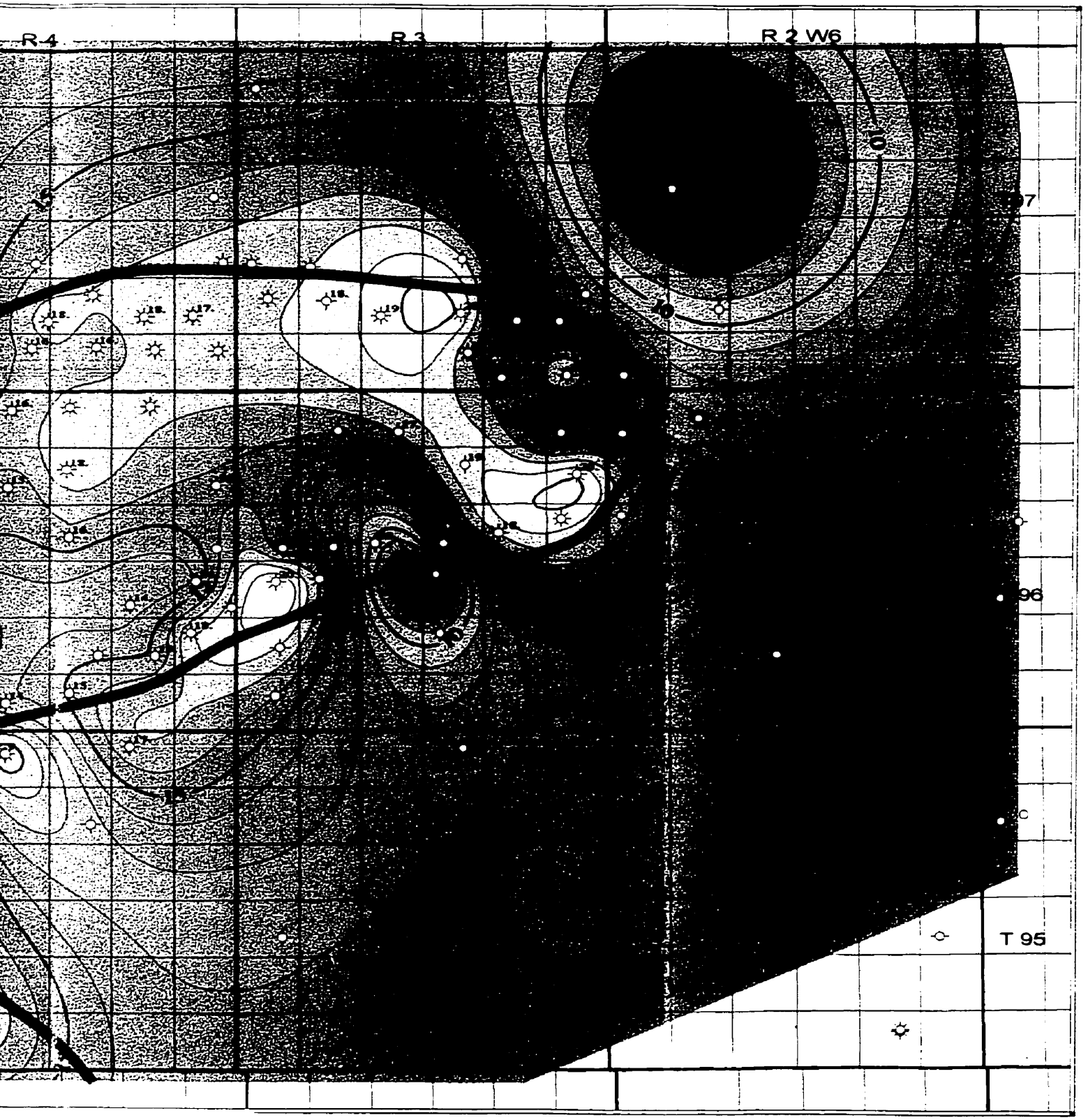

'Reef' isopach map. Scale 1:150,000. Note the 'reefal' margin (solid black line). Contour

are generally maintained through to the end of Cycle 3 sedimentation with an overall increase in bathymetric relief.

Correlative foreslope deposits are the deeper water deposits of Facies 11. These deposits consist of the slightly bioturbated stromatoporoid wackestone deposited in the forereef or foreslope environment.

The upper contact between the Upper Slave Point 'Reef' and the Upper Slave Point Shoal is typically sharp (Fig. 2.24; Fig. 2.26), reflecting an abrupt change in depositional style.

3.2.4 Cycle 4 : Upper Slave Point Shoal

In the study area, the Upper Slave Point Shoal is characterized by two facies: Facies 9 and Facies 10. Lime packstone of Facies 9 which grade laterally and vertically into the bulbous stromatoporoid grainstone of Facies 10 (Fig. 3.9). These sediments represent a high energy shoal (Facies 10) and a interior low energy muddy shoal (Facies 9. This cycle 'caps' the Upper Slave Point 'Reef' cycle and represents the final phase of the 'reefal' buildup. Figure 3.3 shows that Facies 10 formed an elevated rim, up to 8 meters higher than the center of the lagoon (White, 1995; Campbell, 1992). The Lower Waterways (post-Slave Point) thins (1 to 2 m) over this Cycle 4 rim and thickens over the lagoonal and basinal areas.

Cycle 4 varies in total thickness between 5 to 13 m in the study area. The depositional pattern established during Cycle 2 and maintained during Cycle 3 is preserved to the end of Cycle 4 (Fig. 3.10).

The contact between the Upper Slave Point Shoal and the Lower Waterways Basin-Fill cycle is typically an abrupt, burrowed, pyritized, marine-cemented hardground

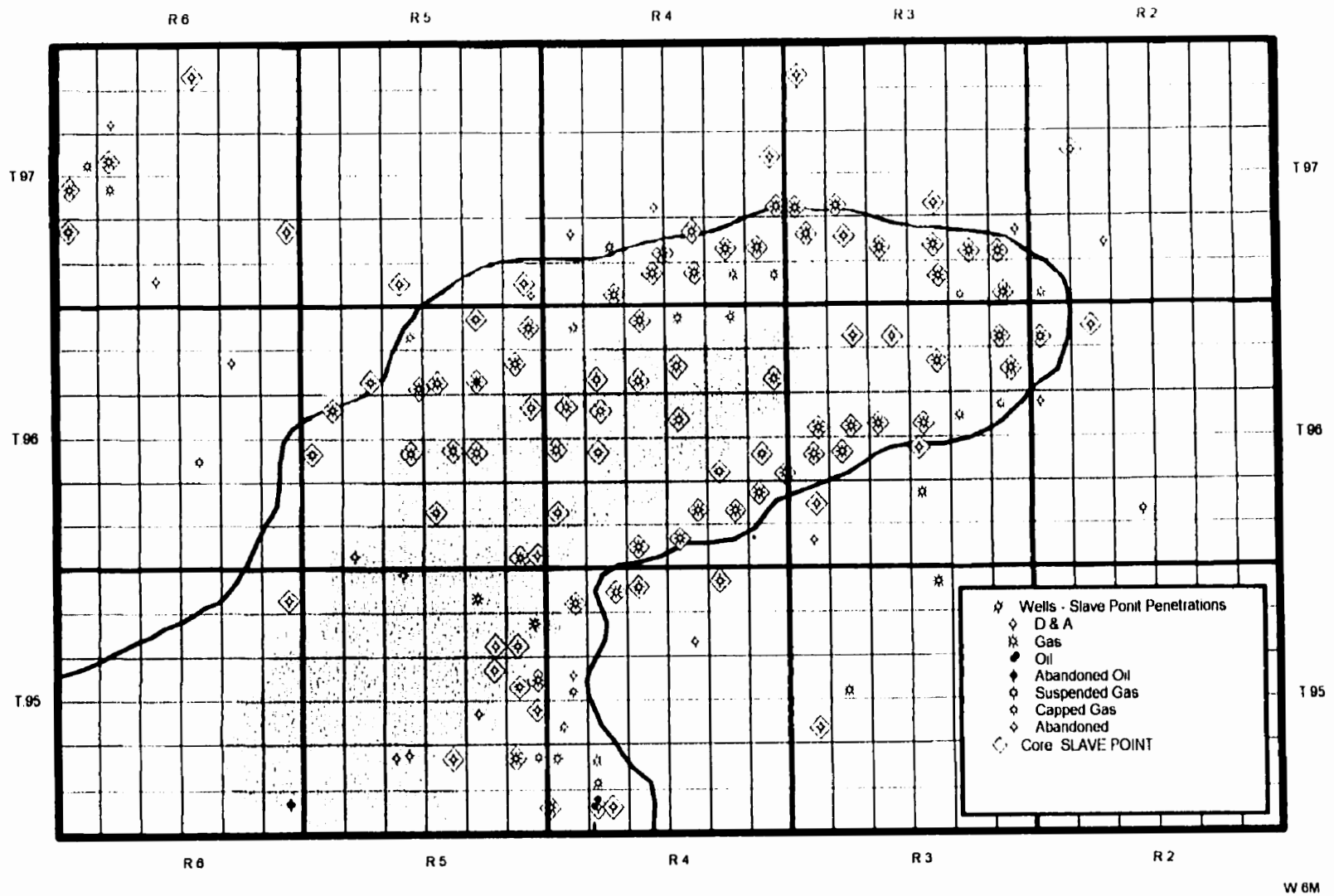

Figure 3.9. Cycle 4 – Upper Slave Point Shoal. Scale 1:150,000. Note the relationship between the interior lime packstone, Facies 9 (brown) and its lateral equivalent facies, the marginal bulbous stromatoporoid grainstone of Facies 10 (yellow).

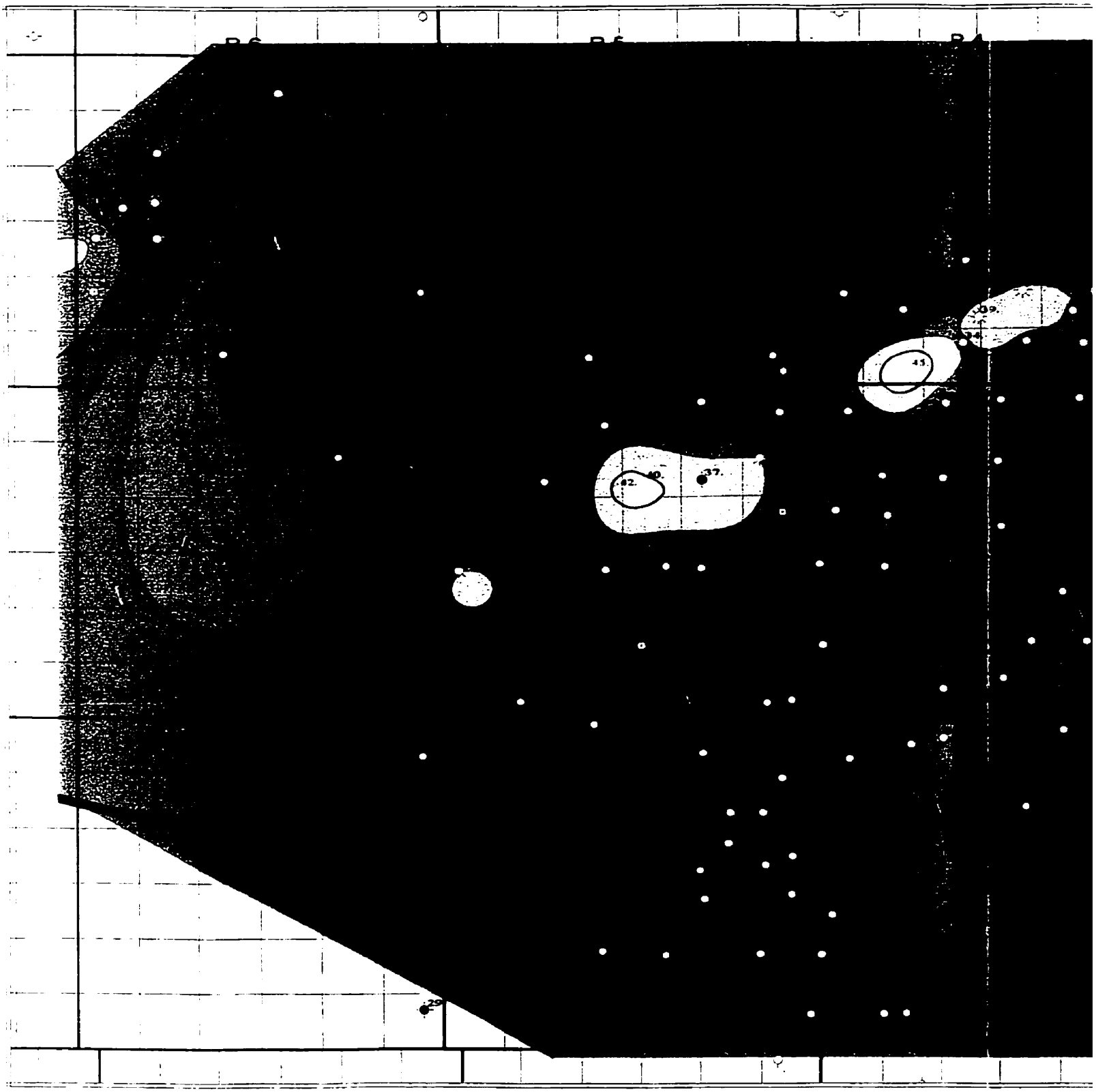

Figure 3.10. Upper Slave Point isopach map. Scale 1:150
Upper Slave Point 'reefal' margin (solid black line

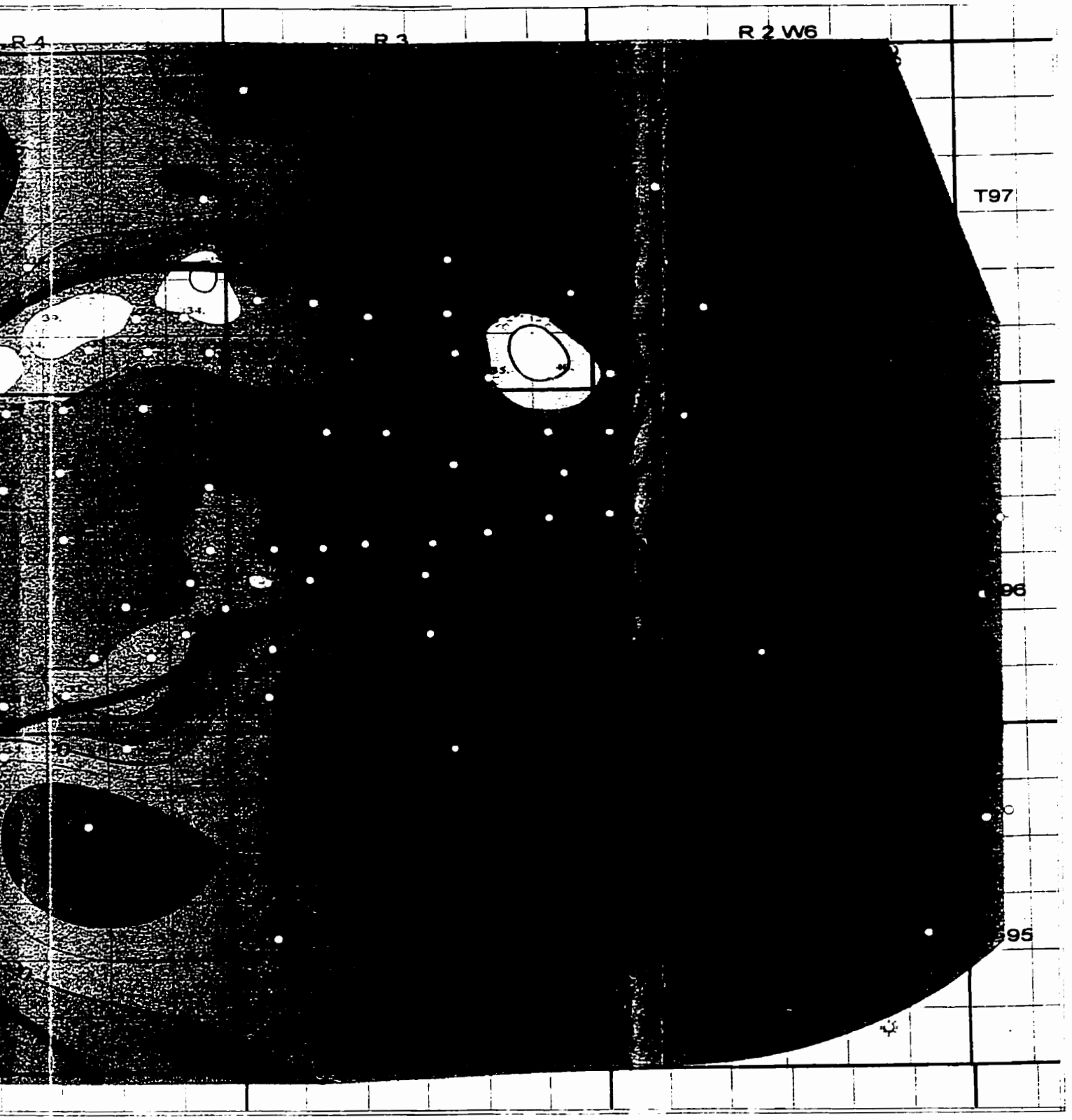

nap. Scale 1:150,000. Note the outline of the
(solid black line). Contour Interval is 1 m.

surface (Fig. 2.30), reflecting an abrupt change in depositional style.

3.2.5 Cycle 5: Lower Waterways Basin Fill

In the study area, the Lower Waterways Basin-Fill consists of a shoaling upward succession of facies disconformable with the underlying Upper Slave Point Shoal.

Cycle 5 is characterized by three facies: Facies 12, Facies 13 and Facies 14. The laminated mudstone of Facies 12 grade upwards into the nodular mudstone of Facies 13, which commonly grades upwards into the nodular brachiopod wackestone of Facies 14 ('Cranberry Member'). The laminated mudstone is restricted to relatively deep water anoxic, basinal environments. This cycle was deposited after the termination Upper Slave Point Shoal deposition and filled in the basinal areas, eventually onlapping and encasing the Upper Slave Point 'reefal' buildup. This cycle varies in thickness between 1 m along the Upper Slave Point 'reefal' margin to 8 m in the center of the lagoon and up to 34 m in basinal areas (Fig. 3.11). Figure 3.11 shows the paleobathymetric contrast at the end of Cycle 4 sedimentation between the top of the 'reefal' buildups and the basin floor is a maximum of 34 meters in the study area.

3.3 Slave Point Depositional Model

The depositional history of the Slave Point Formation is based on the distribution and relationship of facies and cycles and interpretations of depositional environments, which have been described previously. The interpretation has relied heavily on previous well-established Devonian paleoecology studies (Lecompte, 1958; Klovan, 1964, Embry and Klovan, 1972; 1971).

The division of the Slave Point into second order cycles of sedimentation permits

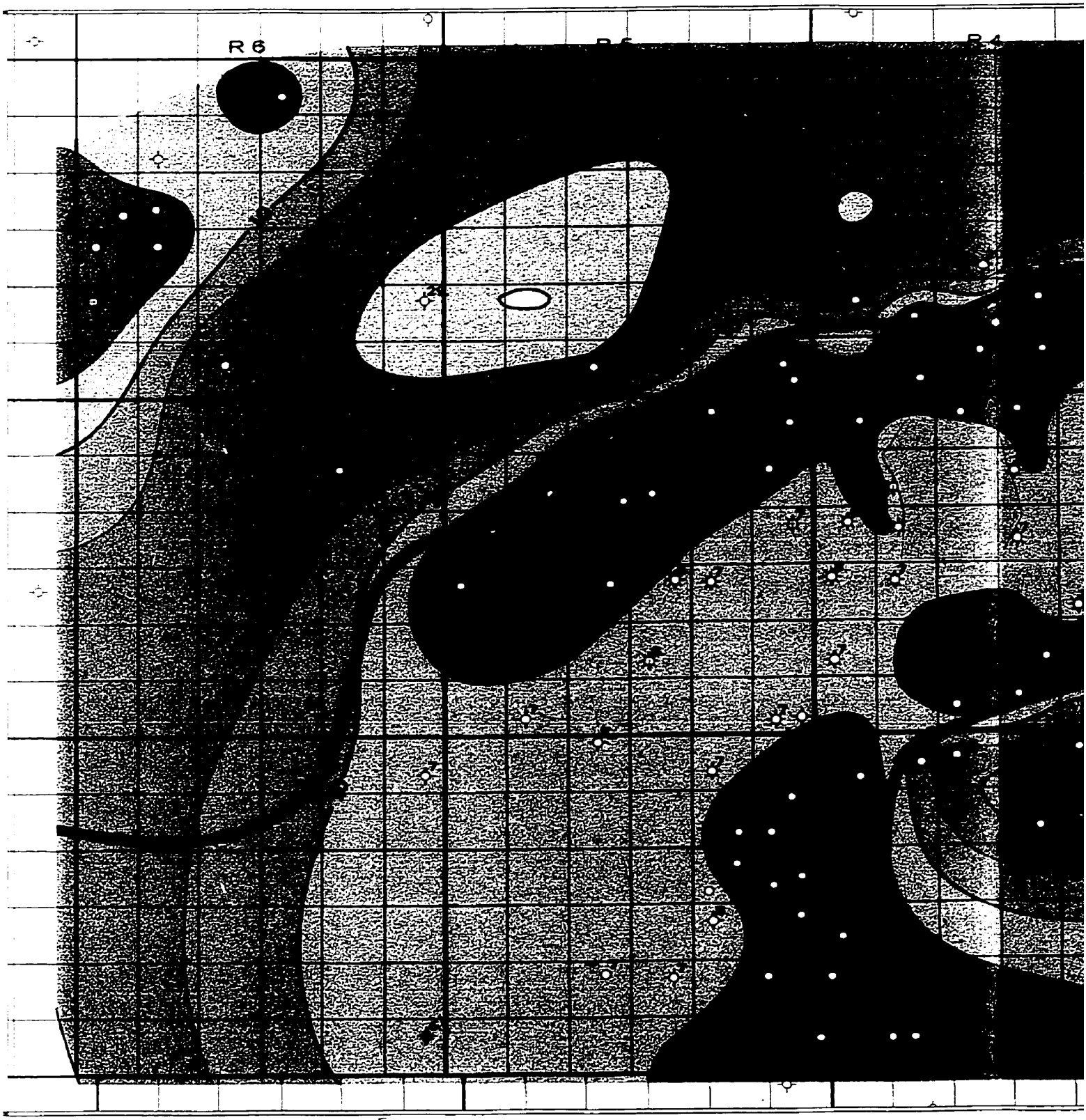

Figure 3.11. Lower Waterways isopach map. Scale
Lower Waterways onto Cycle 4 of the Upper
black line). Contour Interval is 5 m.

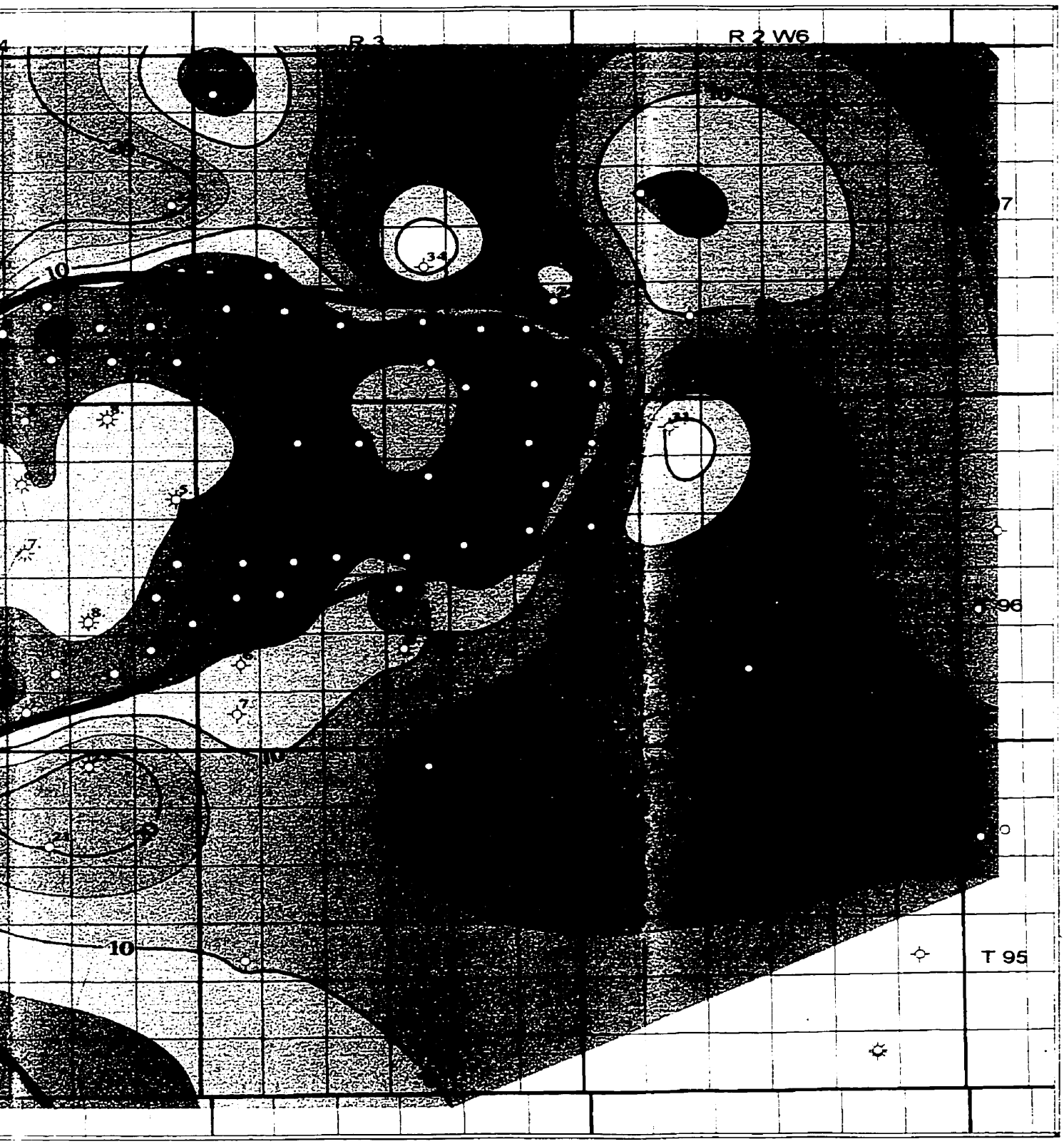

ap. Scale 1:150,000. Note the thinning of the
the Upper Slave Point 'reefal' buildup (solid

the sequential reconstruction of the Slave Point within the study area. These second order Slave Point cycles also correspond to Slave Point 'growth' stages, which are the products of various depositional events.

The evolution of the Slave Point occurred in five main 'growth' stages (oldest to youngest): 1) Lower Slave Point Basal Platform; 2) Upper Slave Point Basal Bank; 3) Upper Slave Point 'Reef'; 4) Upper Slave Point Shoal; and 5) Lower Waterways Basin Fill. These cycles of sedimentation include basinal deposition (Lower Waterways) and concomitant and reciprocal reef growth (Upper Slave Point).

A summary of the depositional model illustrating the evolution of the Slave Point Formation in the study area is shown in Figure 3.12.

Stage 1: Lower Slave Point Basal Platform

The deposition of the Lower Slave Point Basal Platform began during a rapid marine transgression across the surface of the Watt Mountain Formation (Oldale and Munday, 1996). During the transgression relatively deep water mudstones (Facies 1) and nodular brachiopod-crinoidal wackestones (Facies 2) of Cycle 1 prograded basinward over the more argillaceous sediments of the Waterways Formation. The Lower Slave Point Basal Platform stage was probably influenced by antecedent topographic highs, possibly Precambrian-related (Gosselin et. al., 1989; Tooth and Davies, 1989; Craig, 1987), in the study area. This stage forms a widespread, asymmetric, blanket-like deposit in the study area (Fig. 3.4). The stabilization of these muddy sediments by the lower foreslope fauna of *Thamnopora* occurred on paleotopographic highs, where shoaling developed. This subsequently served as a foundation for later 'reef' growth.

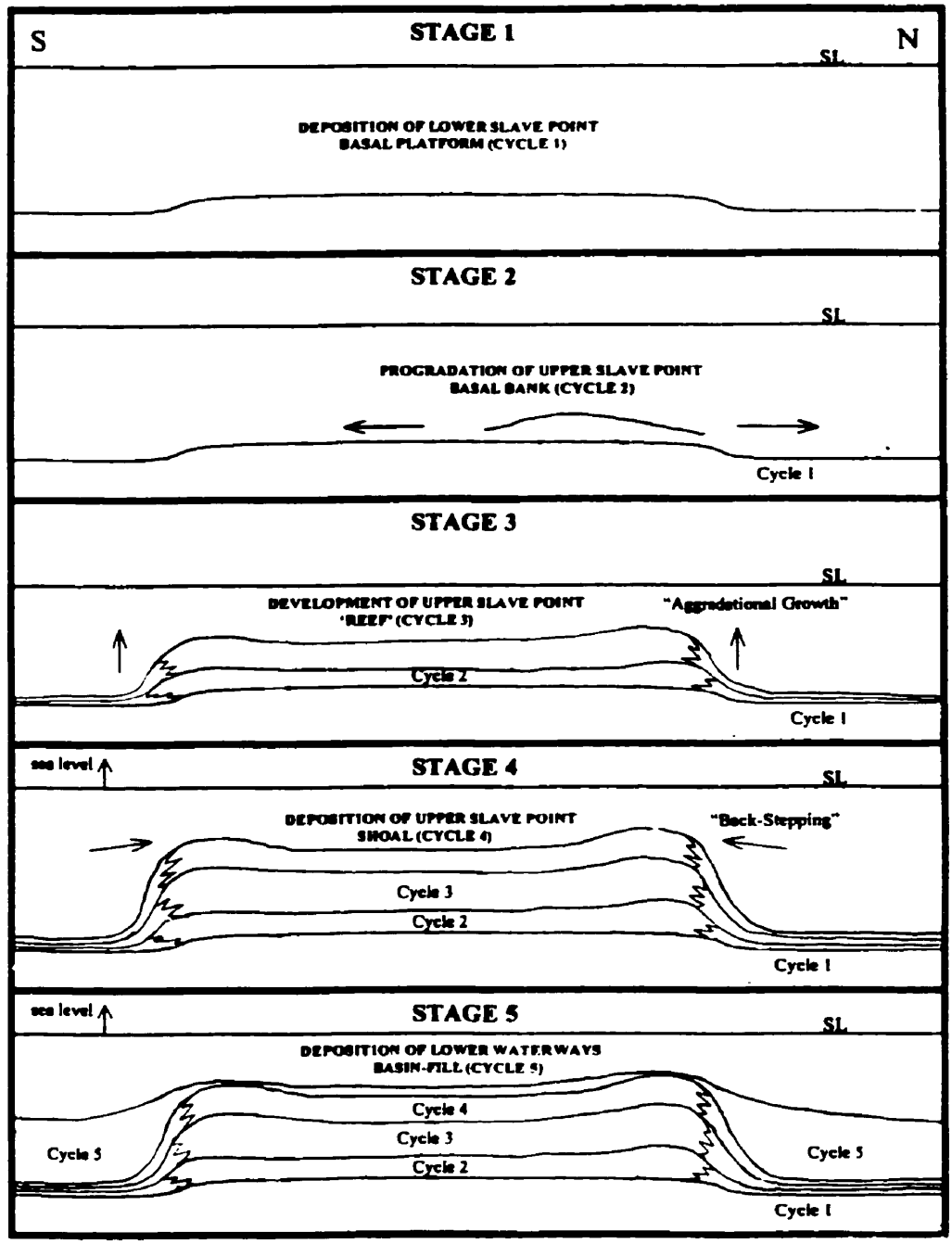

Figure 3.12. Summary of the Slave Point and Waterways Formations depositional model. Evolution occurred in 5 stages: 1) Lower Slave Point Basal Platform; 2) Upper Slave Point Basal Bank; 3)Upper Slave Point 'Reef'; 4) Upper Slave Point Shoal; and 5) Lower Waterways Basin-Fill.

Stage 2: Upper Slave Point Basal Bank

The Upper Slave Point Basal Bank was deposited following a relative sea level rise that occurred after Stage 1 sedimentation in the study area. Further colonization of Cycle 1 *Thamnopora* wackestones (Facies 3) by the *Stachyodes* and *Thamnopora* floatstones (Facies 4) of Cycle 2 occurred. Deposition of Stage 2 was progradational (Campbell, 1992) reflecting open marine conditions, shallow bathymetry and moderate to high carbonate production. As sedimentation kept pace with sea level Facies 4 (lower to middle foreslope) shoaled upward into higher energy tabular stromatoporoid floatstones and rudstones (Facies 5) in 'reefal' margin positions (see Fig. 2.38). This shoaling upward trend is indicated by the increase in faunal abundance and fragmentation and by the first appearance of tabular stromatoporoids. As this stage grew toward sea level, sedimentation outstripped sea level rise, resulting in the seaward progradation of this relatively shallow water stage over the deeper water deposits of the Lower Slave Point Basal Platform.

Stage 3: Upper Slave Point 'Reef'

The Upper Slave Point Reef was deposited following a relative sea level rise that occurred after Stage 2 sedimentation in the study area. The shallow, high energy, upper foreslope to 'reefal' margin facies (Facies 8) initially backstepped and as a result, Cycle 3 margins are typically inboard of the antecedent Cycle 2 margin (see Fig. 2.38). The remainder of Cycle 2 is dominated by aggradational sedimentation in response to continuous relative sea level rise, which characterizes the Upper Slave Point 'Reef' Stage.

This aggradational growth resulted in the formation of an elevated 'reefal margin' (see Fig. 2.38) that sheltered a low energy, lagoonal environment in the interior. In some areas, reefal margin growth continued above wave base in a high energy environment of deposition resulting in stromatoporoid fragmentation and rubble. *Amphipora* rudstones (Facies 6) and tidal laminites (Facies 7) were deposited in the low energy lagoonal environment. The contemporaneous accumulation of *Stachyodes* and *Thamnopora* wackestones (Facies 11) in the forereef positions through erosion and regeneration of the 'reefal' margin contributed skeletal debris to these forereef areas. Throughout deposition of this stage sea-level continued to rise, illustrated in the numerous third order shoaling upward cycles in the lagoon.

Stage 4: Upper Slave Point Shoal

The Upper Slave Point Shoal was deposited following a increased rate of relative sea level rise that occurred after Stage 3 sedimentation in the study area. On the 'reefal' buildups this resulted in the deposition of low energy lime packestones (Facies 9) in the interior and high energy bulbous stromatoporoids grainstones along the 'reefal' margin. Deposition was dominantly aggradational and formed pronounced elevated 'rims' along the 'reefal' margin. Backstepping also occurred and is evidenced by Facies 10 that commonly prograde in an inboard direction overtop of Facies 9. Toward the end of Upper Slave Point Shoal sedimentation a relative increase in the rate of sea level rise occurred leading to the eventual drowning of the Upper Slave Point 'reefal' buildup in the study area.

Stage 5: Lower Waterways Basin Fill

Upper Slave Point deposition was terminated by a relative increase in the rate of sea level rise. This resulted in very low rates of carbonate production and sediment stability, which allowed widespread cementation and hardground formation at the top of the Upper Slave Point Shoal. Laminated mudstones were deposited in the relatively deep water basinal areas (Facies 12), followed by nodular mudstones (Facies 13) shallowing upward into brachiopod wackestones (Facies 14) of the 'Cranberry Member'. These sediments of the Lower Waterways Formation subsequently infilled any remnant topography on the underlying surface. This stage thickens into the remnant topography of the Cycle 4 muddy shoal interior (Facies 9) and filled the basinal areas, onlapping and eventually encasing the Upper Slave Point 'reefal' buildup (Stage 2 to 4).

This initial basin-fill was then covered by a more argillaceous basin-fill of the Upper Waterways Formation, marking the final major marine transgression in the study area.

3.4 Discussion

The Slave Point in this study has been subdivided into 5 distinct depositional cycles with corresponding 'growth' stages: 1) Lower Slave Point Basal Platform (Cycle 1; Stage 1), 2) Upper Slave Point Basal Bank (Cycle 2; Stage 2), 3) Upper Slave Point 'Reef' (Cycle 3; Stage 3), 4) Upper Slave Point Shoal (Cycle 4; Stage 4), and 5) Lower Waterways Basin Fill (Cycle 5; Stage 5).

Campbell (1992) divided the Slave Point Formation in the study area into two megasequences. The basal megasequence was dominated by progradation with an upper

aggradational phase. The basal megasequence equates in this study to Cycles 1; 2 and 3. However, Cycle 3 has more affinities to the aggradational megasequence of Campbell (1992). The upper megasequence of Campbell (1992) is characterized by aggradation and backstepping, equates to Cycle 4 of this study.

Reinson et. al. (1993) divided the Fort Vermilion – Slave Point succession into four units: 1) a basal 'Slave Point Platform' overlain by, 2) a relatively thin, discontinuous 'Coral Zone', that is overlain by, 3) the Cranberry 'Slave Point Bioherm' and 4) shallow marine inter- and off reef sediments. Cycle 1 of this study correlates to the upper part of their 'Slave Point Platform', whereas Cycle 2 of this study corresponds to their 'Coral Zone'. The 'Slave Point Bioherms' equate to the buildups of Cycles 3 and 4. Finally, the shallow marine inter- and off reef strata of Reinson et. al. (1993) equate to Cycle 5 of this study.

Gosselin et. al. (1989) studied the Slave Point Formation in the Golden and Evi reef complexes. They subdivided the Slave Point Formation into 3 distinct informal growth stages: 1) Substage I, 2) Substage II, and 3) Substage III. Substage I is dominated by progradational (some aggradational growth) depositional style and equates to Cycle 2 in this study. Substage II is dominated by aggradational growth (some back-stepping) and equates to Cycle 3 in this study. Substage III is dominated by back-stepping growth (some aggradational) and roughly equates to Cycle 4 in this study, although the facies are not similar.

CHAPTER 4: DOLOMITIZATION

4.1 Introduction

Dolostones from the Devonian Slave Point Formation are important hydrocarbon reservoirs in the Western Canada Sedimentary Basin. The distribution of this dolomite and an understanding of its formation is important because of the enhanced porosity and the increased effective reservoir potential which can accompany the dolomitization process. Many mechanisms have been proposed to account for the different circumstances in which dolomitization has occurred and the testing of these hypotheses relies heavily on geochemistry, isotope studies and the use of cathodoluminescence to augment petrography.

There is no unique environment of dolomitization. Aside from the very basic chemical constraint that a solution must be oversaturated with dolomite in order to crystallize it, dolomite clearly forms in a variety of chemical environments (Land, 1985). Waters known to be capable of dolomitization include marine-derived brines (Behrens and Land, 1972; Patterson and Kinsman, 1982), continental-derived brines (von der Borsch et al., 1975; Andrews et al., 1987), mixtures of marine- and continental-derived brines (Pierre et al., 1984), normal seawater (Saller, 1984), and mixtures of seawater and meteoric water (Land, 1973). Machel and Mountjoy (1987) concluded that dolomitization may occur in waters of virtually any salinity as long as they are supersaturated with respect to dolomite.

Review articles on dolomitization by Shields and Brady (1995), Morrow (1990), Machel and Mountjoy (1987) and Land (1985) have provided excellent synopses of the dolomite problem. Various models have been proposed to explain dolomite formation

(Zenger et al., 1980). Some of the more important aspects that remain controversial are: (1) source and supply of Mg^{2+} (Land, 1985; Morrow, 1990), (2) plumbing mechanisms necessary to transport Mg-bearing solutions to the site of dolomitization (Packard et al., 1990; Mountjoy and Halim-Dihardja, 1991), (3) stoichiometry of ancient dolomite (Land, 1980), and (4) neomorphism of dolomite (Mazzullo, 1992, Smith and Dorobek, 1989).

As dolomitization is the most significant diagenetic process that occurred in the Slave Point Formation in terms of reservoir quality and because an interpretation of the entire diagenetic history of the Slave Point is beyond the scope of this Master's thesis, the emphasis is on the most significant and relevant diagenetic event, namely dolomitization.

4.2 Dolomite Petrography

This section focuses on petrographic and cathodoluminesence observations, spatial distributions, and cross-cutting relationships between depositional fabrics, cements and compactional features to aid in the identification of the various types of dolomite. In the study area, approximately 10% of the wells penetrating the Slave Point Formation in the Cranberry Field study area have been partially dolomitized, illustrating the diagenetic complexity in ancient dolostones. In the study area, the different petrographic types of dolomite are recognized and classified according to crystal-size distribution (Folk, 1972) and crystal-boundary shape (Sibley and Gregg, 1987). The classification of dolomite textures is based on petrographic and cathodoluminescence (CL) observations. In the study area, three types of dolomite are recognized: 1) Type 1 – Matrix Dolomite; 2) Type 2 - Coarse Crystalline Dolomite; and 3) Type 3 - Coarse

"Saddle" Dolomite Cement. Dolomite Types 1 and 2 are replacement dolomites and Type 3 is a dolomite cement.

4.2.1 Type 1 - Matrix Dolomite

Matrix dolomite is volumetrically unimportant and accounts for a relatively small portion of the total rock volume (≤10%). Matrix dolomite is composed of very small 10 to 30 μm crystals with planar-s and planar-e fabrics (Fig. 4.1). Crystals are typically clear and contain abundant inclusions. Under CL, matrix dolomite is non-luminescent. This dolomite type is Fe-rich (Fig. 4.1).

Matrix dolomite occurs in all facies, except those facies with grainstone matrices (Facies 4, 5, 8, 9 and 10). It preferentially occurs along dissolution seams and stylolites (Fig. 4.1).

4.2.2 Type 2 - Coarse Crystalline Dolomite

Coarse crystalline dolomite is the most common and volumetrically important textural type of dolomite comprising up to 100% of Facies 4 and 5 in the Slave Point Formation. The spatial distribution of Type 2 dolomite in the study area is shown in Figure 4.2. Type 2 dolomite is composed of 200 to 800 μm crystals with planar-s and planar-e mosaic textures (Fig. 4.3). Crystals generally have a cloudy appearance. Planar euhedral mosaics form porous zones of significant intercrystalline porosity (5% to 10%) within otherwise dense mosaics. The contact between porous and nonporous is gradational. Type 2 dolomite creates excellent reservoir rocks in previous non-porous limestones (i.e. Facies 6) because it develops secondary porosity types such as vuggy, moldic and intercrystalline porosity. The secondary porosity can be partly occluded by pyrobitumen and saddle dolomite cements. Dense mosaics of cloudy subhedral crystals

Figure 4.1. Thin-section photomicrograph of Type 1 Matrix Dolomite. Crystals have euhedral, planar-s and planar-e fabrics. Note the distribution of the dolomite parallels the distribution of the stylolites. Note the greenish color of this dolomite type, due to potassium ferricyanide staining. Plane-polarized light. Field of View is 1.4 mm. 3-1-96-5w6, 2350 m (7710 ft).

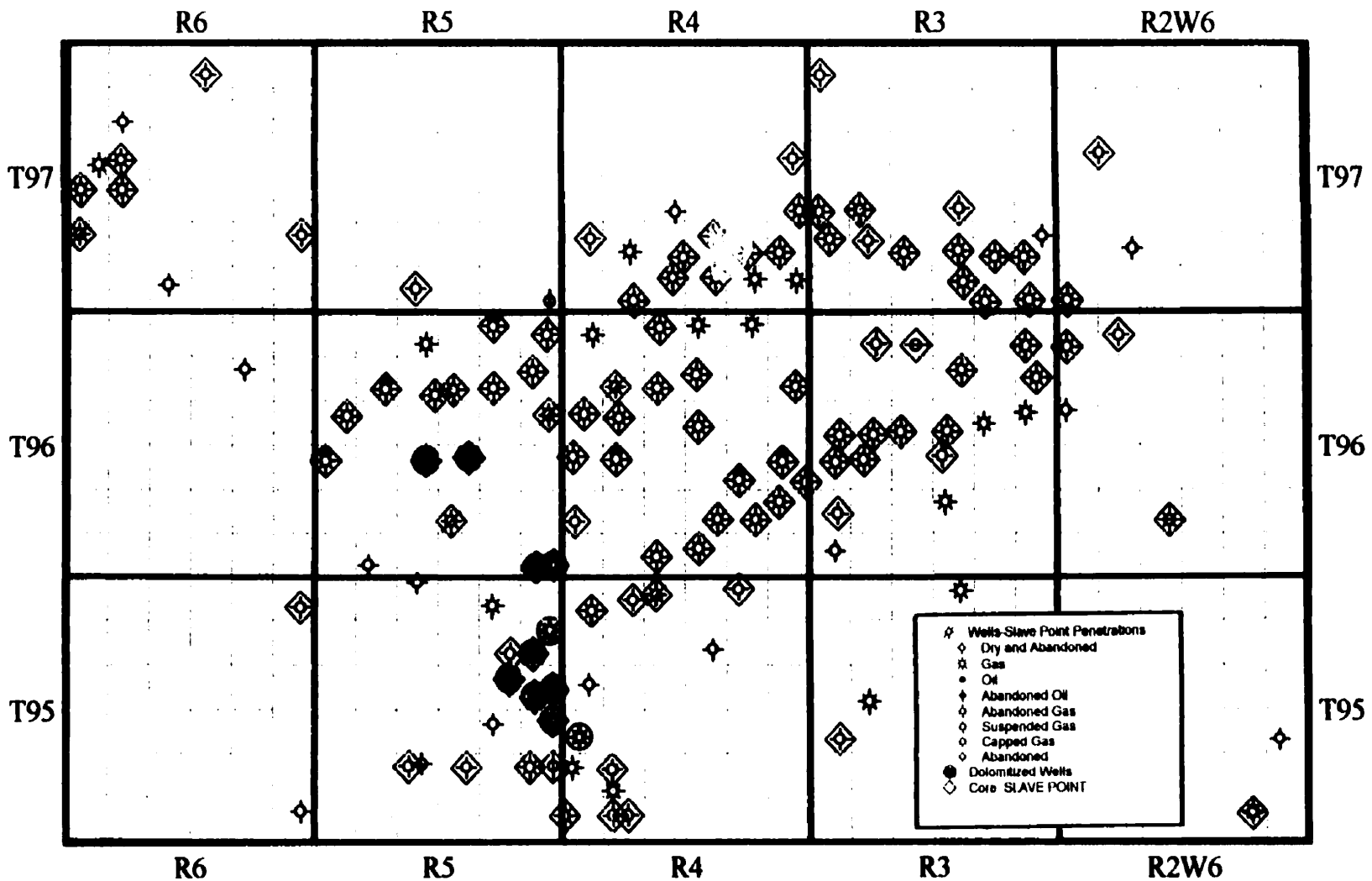

Figure 4.2. Map of the study area. Scale 1:250 000. Diamonds represent Slave Point wells with core. Circles represent wells where Type 2 dolomitization has occurred.

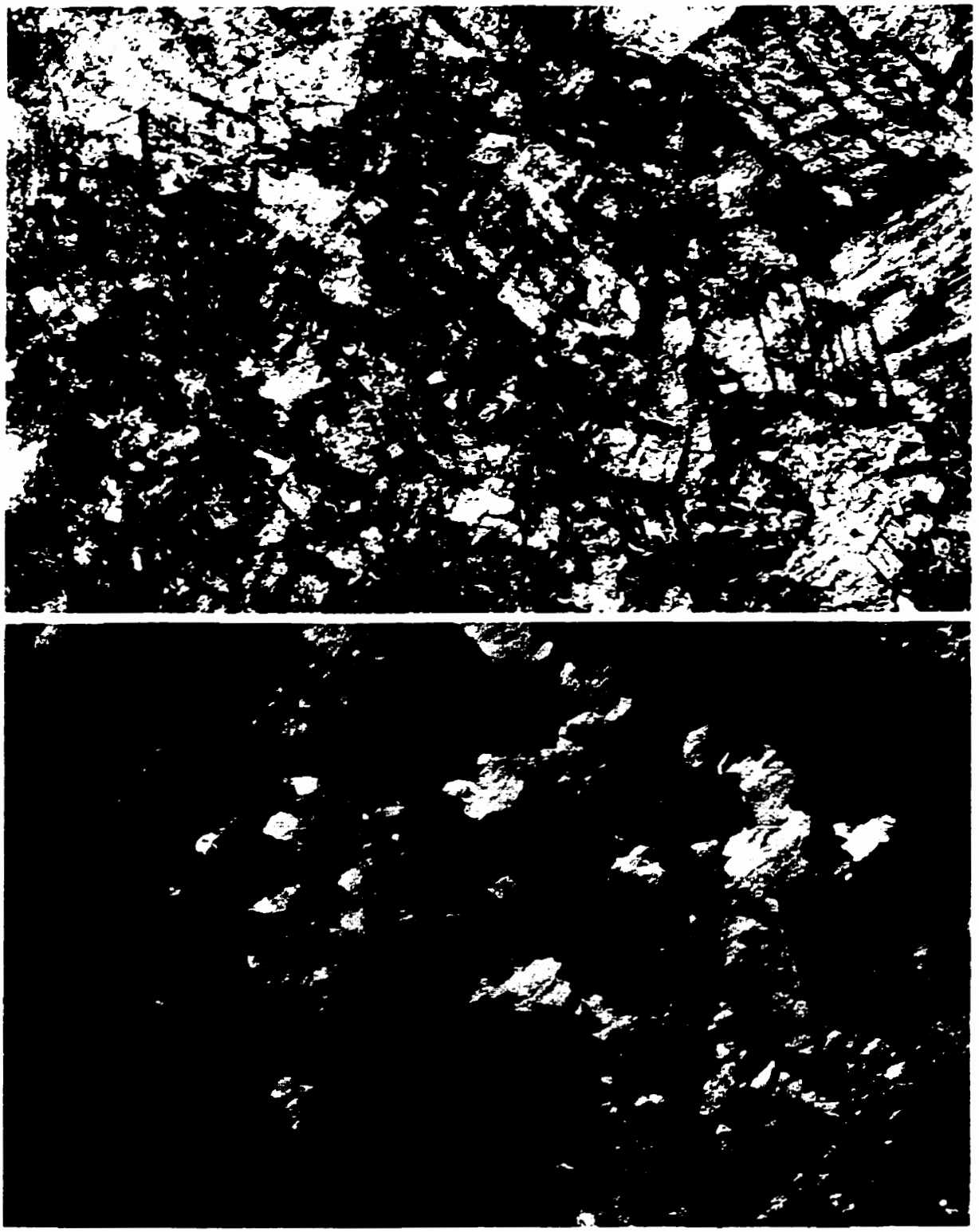

Figure 4.3. Thin-section photomicrograph of Type 2 Coarse Crystalline Dolomite. **A, B.** Plane light A and cathodoluminescent (CL) B views. Note the crystal size and p planar-e and planar-s fabrics. Under CL Type 2 dolomite shows up as bright r reddish-orange dolomite crystals in a limestone matrix (yellow). Field of View is 1.4 mm.

and porous mosaics of cloudy subhedral to euhedral crystals are characteristic for this type of dolomite. This dolomite is typically non-ferroan and often cut by fractures containing Type 3 saddle dolomite cements.

Under CL, this dolomite type typically shows a homogeneous to blotchy bright reddish-orange luminescence (Fig. 4.3). Some crystals may appear concentrically zoned, with bright reddish-orange cores and thin non-luminescent rims (Fig. 4.4). Crystals that rim primary or secondary porosity often have homogenous bright reddish-orange cores and non-luminescent (Fe-rich) rims (Fig. 4.4). It is apparent that the contact between the non-luminescent rims and the bright reddish-orange cores is straight and regular (Fig. 4.4). This suggests a change in fluid chemistry during precipitation.

Coarse crystalline dolomite is fabric-destructive and partially to completely replaces limestone matrix and fossil components in Facies 4, 5, 6 and 7, but its presence is areally restricted in the study area (Fig. 4.2). The spatial distribution of this dolomite can also vary considerably within a single well. Stratigraphically higher facies may be only partially dolomitized, whereas stratigraphically lower facies may be completely dolomitized within a single well.

4.2.3 Type 3 - Saddle Dolomite Cement

Saddle dolomite cements are the second most volumetrically abundant types of dolomite in the Slave Point Formation. Although this type of dolomite is less common than the Type 2 coarse crystalline dolomites, discussed previously, it is more widespread, occurring in all facies. Type 3 dolomites have a distinct white color in hand specimen and consist of very coarse millimeter-sized crystals (Fig. 4.5). Individual clear crystals range

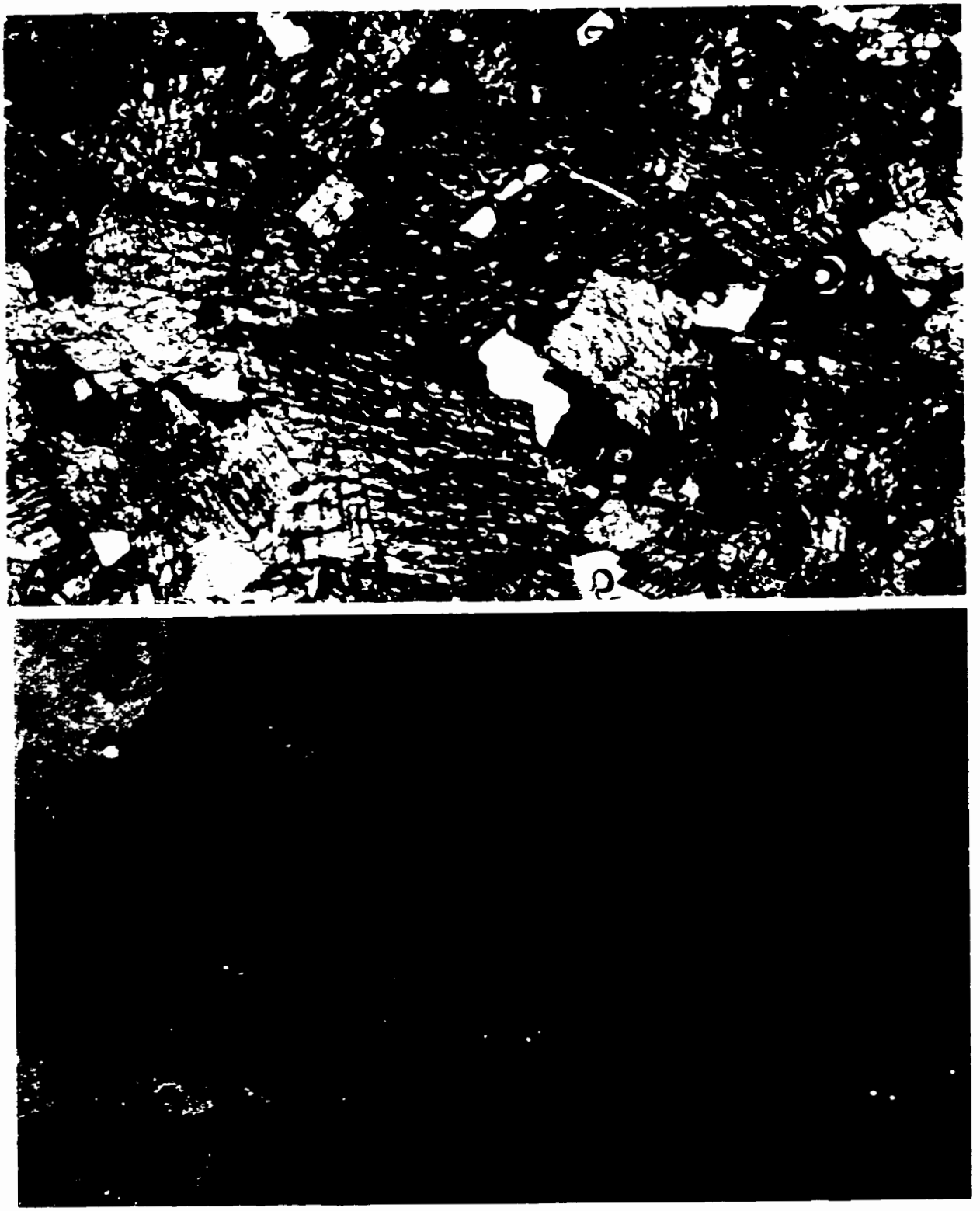

Figure 4.4. Thin-section photomicrograph of Type 2 Coarse Crystalline Dolomite. **A, B .** Plane light A and cathodoluminescent B views. Note the intercrystalline porosity (blue). Under CL Type 2 zoned crystals rim secondary porosity, later filled by Type 3 (non-luminescent) dolomite. Field of View is 1.4 mm.

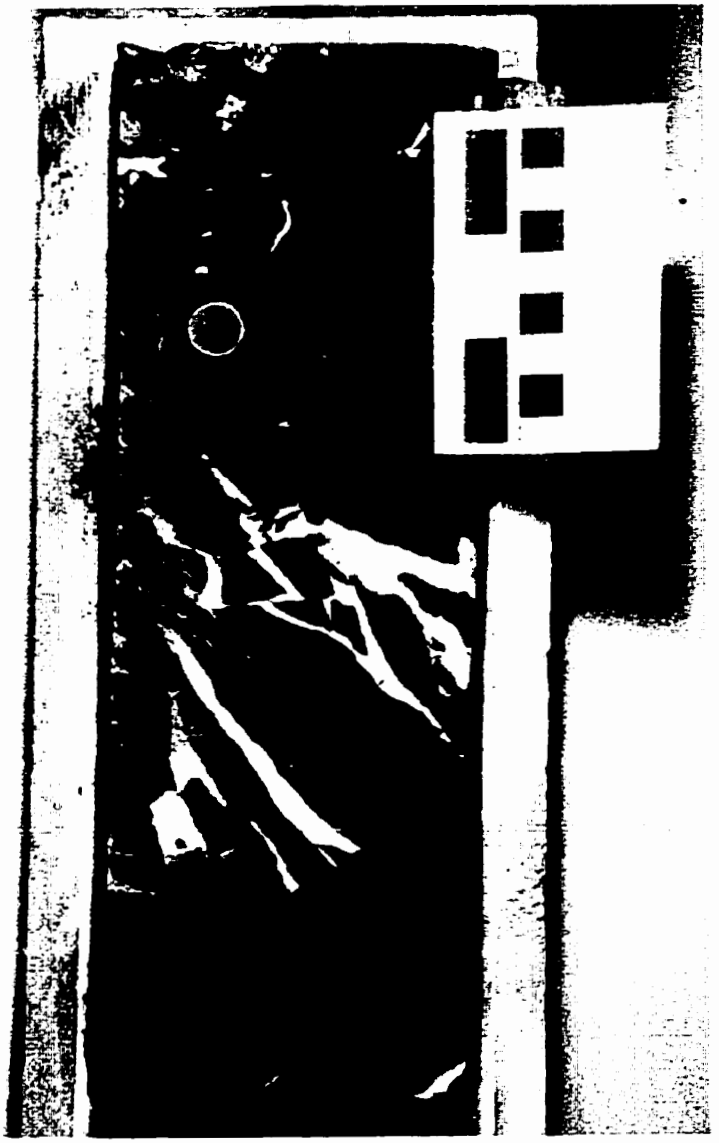

Figure 4.5. Core Photo. Note the fractures in the limestones of Facies 5 filled by Type 3 white saddle dolomite cement. 7-11-96-4w6, 2170 m (7120 ft).

in size from 500 μm to 2000 μm and exhibit euhedral planar-e fabrics with lobate or curved crystal faces (Fig. 4.6). A variety of pore types are occluded by Type 3 dolomites including intergranular, fenestral and fractures in limestones (Fig. 4.5) and intercrystalline, vuggy, moldic and fractures in dolostones (Fig. 4.7) The occurrence of this dolomite is closely associated but not restricted by the presence of Type 2. This dolomite is typically Fe-rich.

Under CL, crystals appear non-luminescent (Fig. 4.6). The contact between bright reddish-orange Type 2 dolomites and the non-luminescent Type 3 dolomites is transitional (Fig. 4.6). Some crystals exhibit a distinct complex compositional banding (Fig. 4.8), but this complex zoning is rare.

4.3 Dolomite Geochemistry

The usefulness of oxygen and carbon isotope analyses in the study of dolomite has been severely limited by the inability to precipitate dolomite at low temperatures in the laboratory (Carpenter, 1980; Land, 1980). The degree of equilibrium fractionation of oxygen isotope between dolomite-water and dolomite-calcite at low temperatures is therefore uncertain. Estimates of these fractionation factors are obtained by extrapolating from high temperature synthesis studies (Matthews and Katz, 1977). Furthermore, the possibility exists that when dealing with ancient dolomites the $\delta^{18}O$ ratios of these rocks are not those obtained during dolomitization but have been altered to varying degrees during burial and neomorphism (Land, 1980). For these reasons, interpretation of oxygen isotope ratios of dolomites must be tempered with some caution.

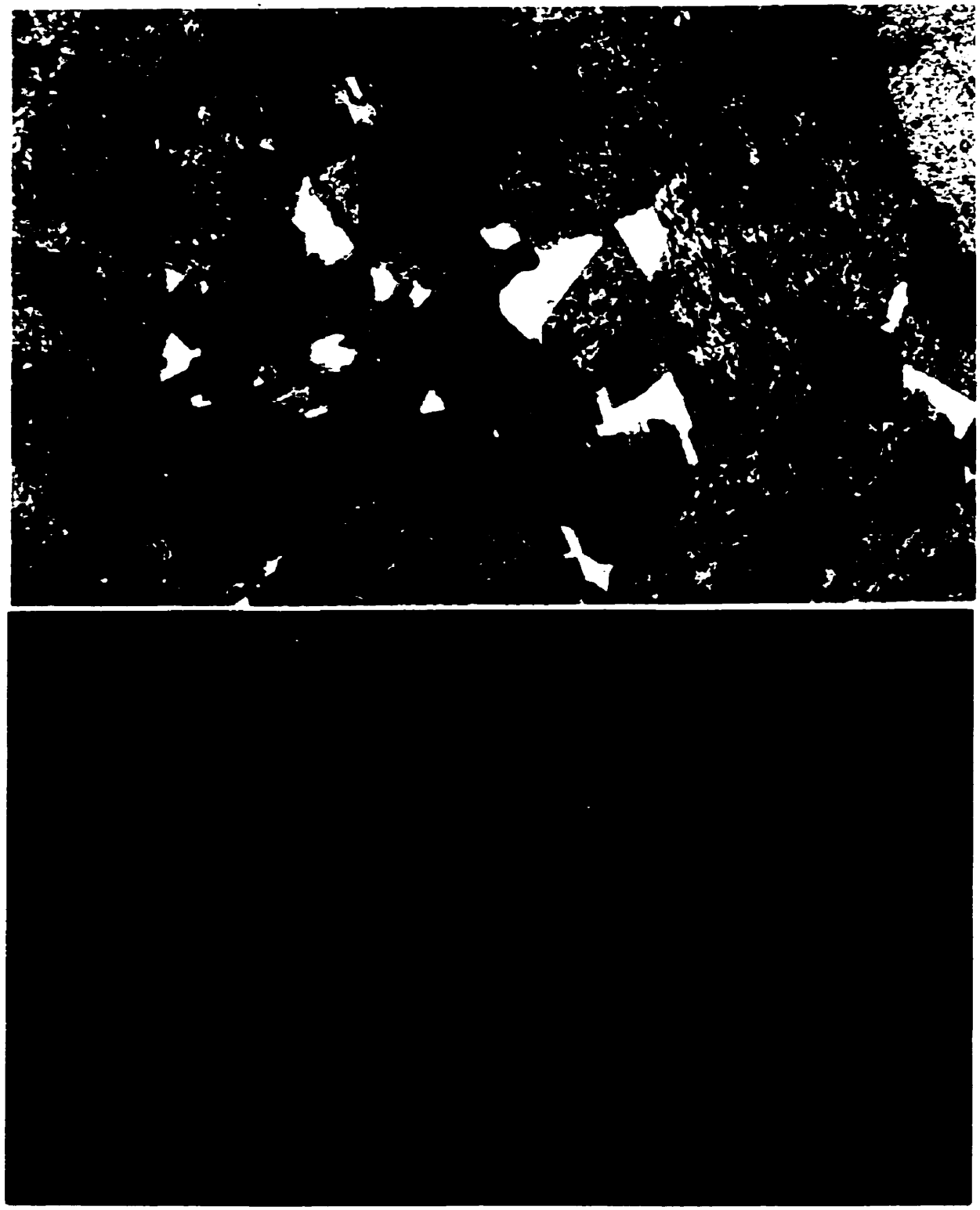

Figure 4.6. Thin-section photomicrograph of Type 3 Saddle Dolomite Cement. **A, B.** Plane light A and cathodoluminescent B views. Note the intercrystalline porosity (white). Under CL non-luminescent dolomite crystals characteristic of Type 3 and the bright reddish-orange crystals of Type 2. Field of View is 1.4 mm. 10-15-96-5w6, 2382.5 m (7817 ft).

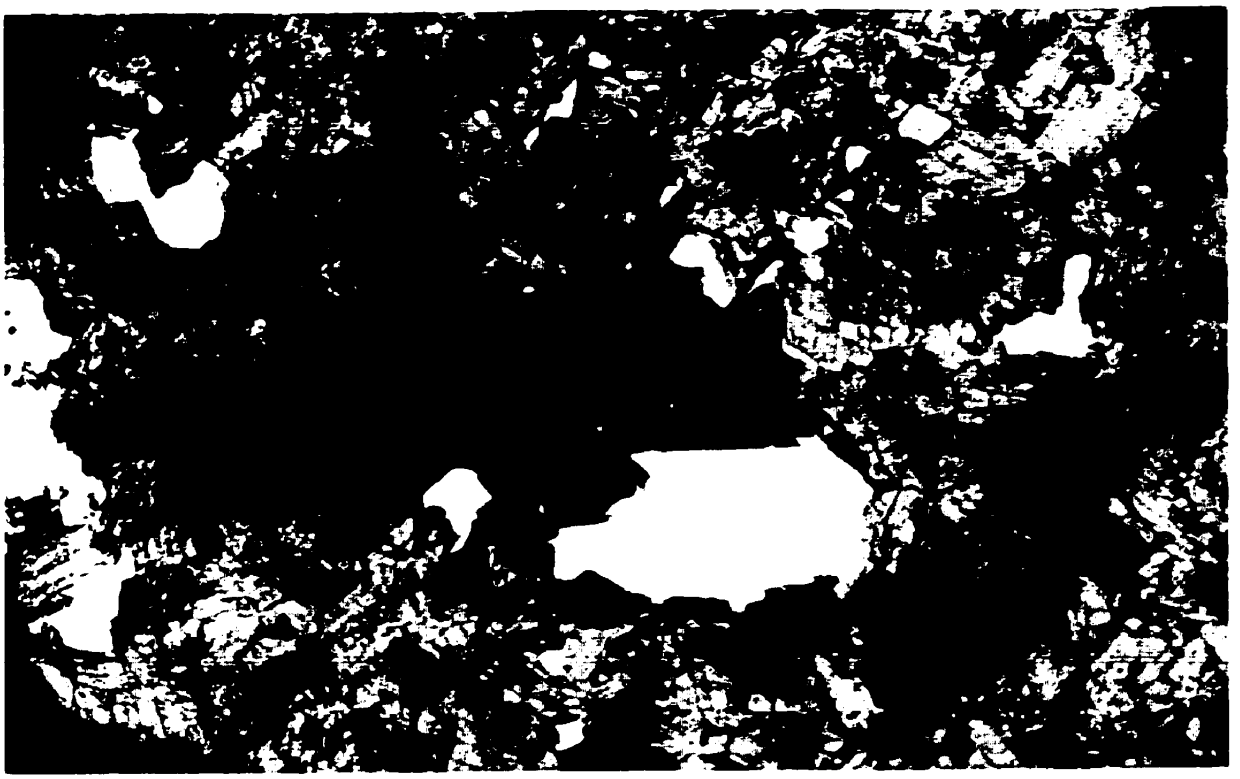

Figure 4.7. Thin-section photomicrograph of Type 3 Saddle Dolomite Cement. Note the blue-stained (indicative of Fe content) Type 3 dolomite filling what appears to be a vug or mold in a matrix that has been completely dolomitized by Type 2 dolomite (non-ferroan; unstained) Field of View is 3.5 mm. 3-1-96-5w6, 2357.5 m (7735 ft).

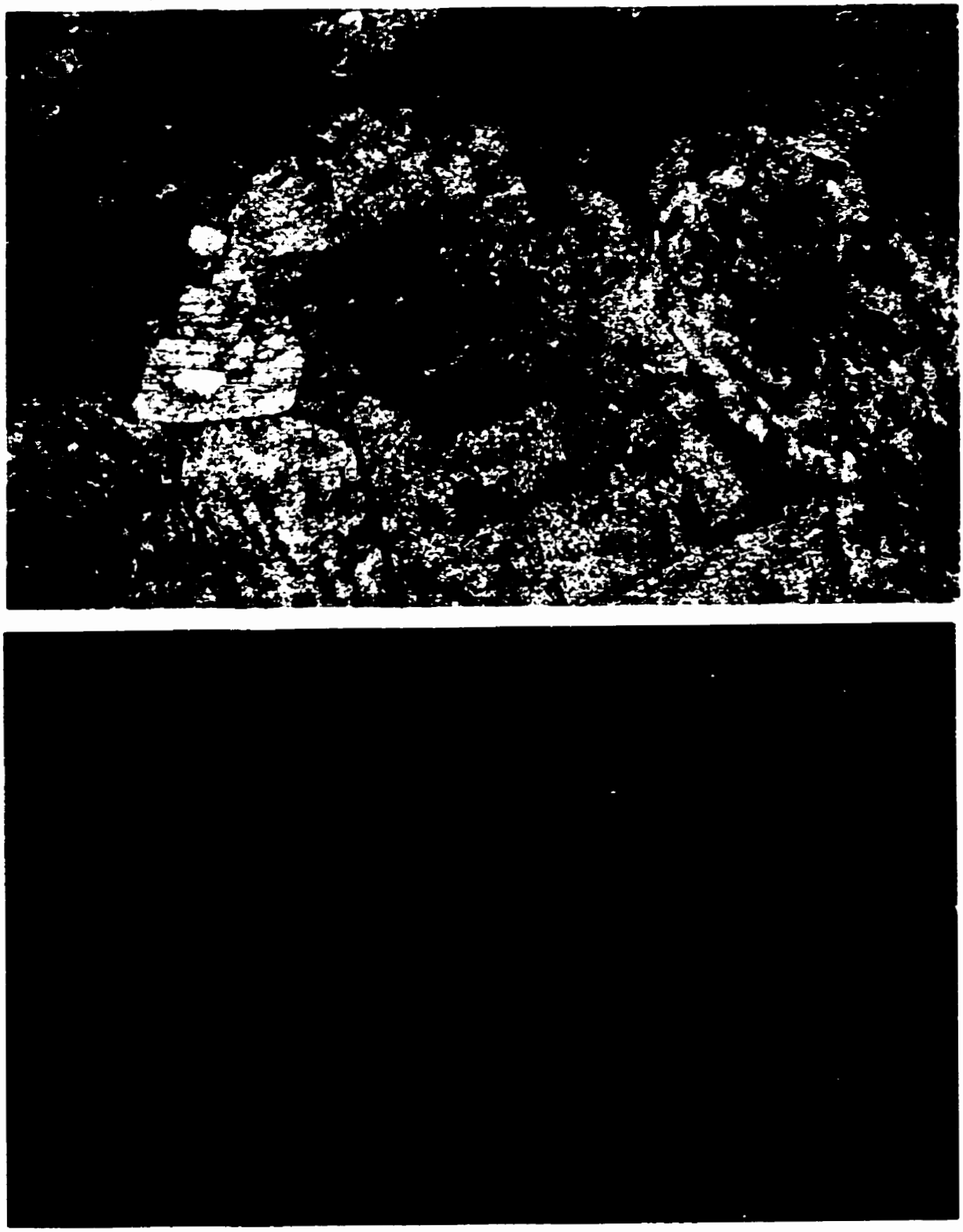

Figure 4.8. Thin-section photomicrograph of Type 3 Saddle Dolomite Cement. . **A, B.** Plane light A and cathodoluminescent B views. Note the lobate crystal faces. Under CL the complex banding of alternating bands of non-ferroan (red luminescent) and Fe-rich (nonluminescent) bands. Field of View is 1.4 mm.

Isotopic results are summarized in Table 4.1 and plotted in Figure 4.9. The isotopic measurements reported are in per mil PDB values. The trends and features of isotope analyses are discussed below. Type 1 dolomites were not analyzed because it is a volumetrically minor component in Slave Point carbonates and the crystal size (10-30 μm) and distribution restricted sampling.

4.3.1 Type 2 - Coarse Crystalline Dolomite

The non-ferroan Type 2 dolomites (n = 9) have a relatively narrow range of oxygen isotope and carbon isotope values (Figure 4.9). $\delta^{18}O$ range from -10.43 to –12.79 ‰ (mean = -11.95 ‰), and $\delta^{13}C$ values range from +2.27 to +3.19 ‰ (mean = +2.81 ‰). These values are similar to the $\delta^{18}O$ and $\delta^{13}C$ values reported for replacement dolomites at the Swan Hills, Rosevear Field (Kaufman et al., 1990). No stratigraphic trends are apparent.

4.3.2 Type 3 - Saddle Dolomite Cement

The Fe-rich Type 3 dolomites (n = 9) have a narrow range of oxygen isotope and carbon isotope values (Figure 4.9). $\delta^{18}O$ range from -10.43 to -13.35 ‰ (mean = -12.40 ‰), and $\delta^{13}C$ values range from +1.46 to +2.74 ‰ (mean = +2.32 ‰). These values are similar to the $\delta^{18}O$ and $\delta^{13}C$ values reported for saddle dolomites at the Swan Hills Field (Viau, 1986) and the Swan Hills, Rosevear Field (Kaufman et al., 1990). No stratigraphic trends are apparent.

4.4 Discussion

The stable isotopic values of Type 2 and Type 3 dolomites are similar (Figure 4.9)

Dolomite Type	N	Mean (St.D.) $\delta^{13}C$	Mean (St.D.) $\delta^{18}O$	Minimum $\delta^{13}C$	Minimum $\delta^{18}O$	Maximum $\delta^{13}C$	Maximum $\delta^{18}O$
2 Coarse Crystalline Dolomite	9	+2.49 (0.61)	-11.69 (0.90)	+1.46	-10.43	+3.19	-12.79
3 Saddle Dolomite Cement	9	+2.55 (0.26)	-12.67 (0.64)	+2.00	-11.19	+2.74	-13.35

Table 4.1. Summary of stable isotope analyses of Slave Point dolomites. St.D. is the Standard Deviation.

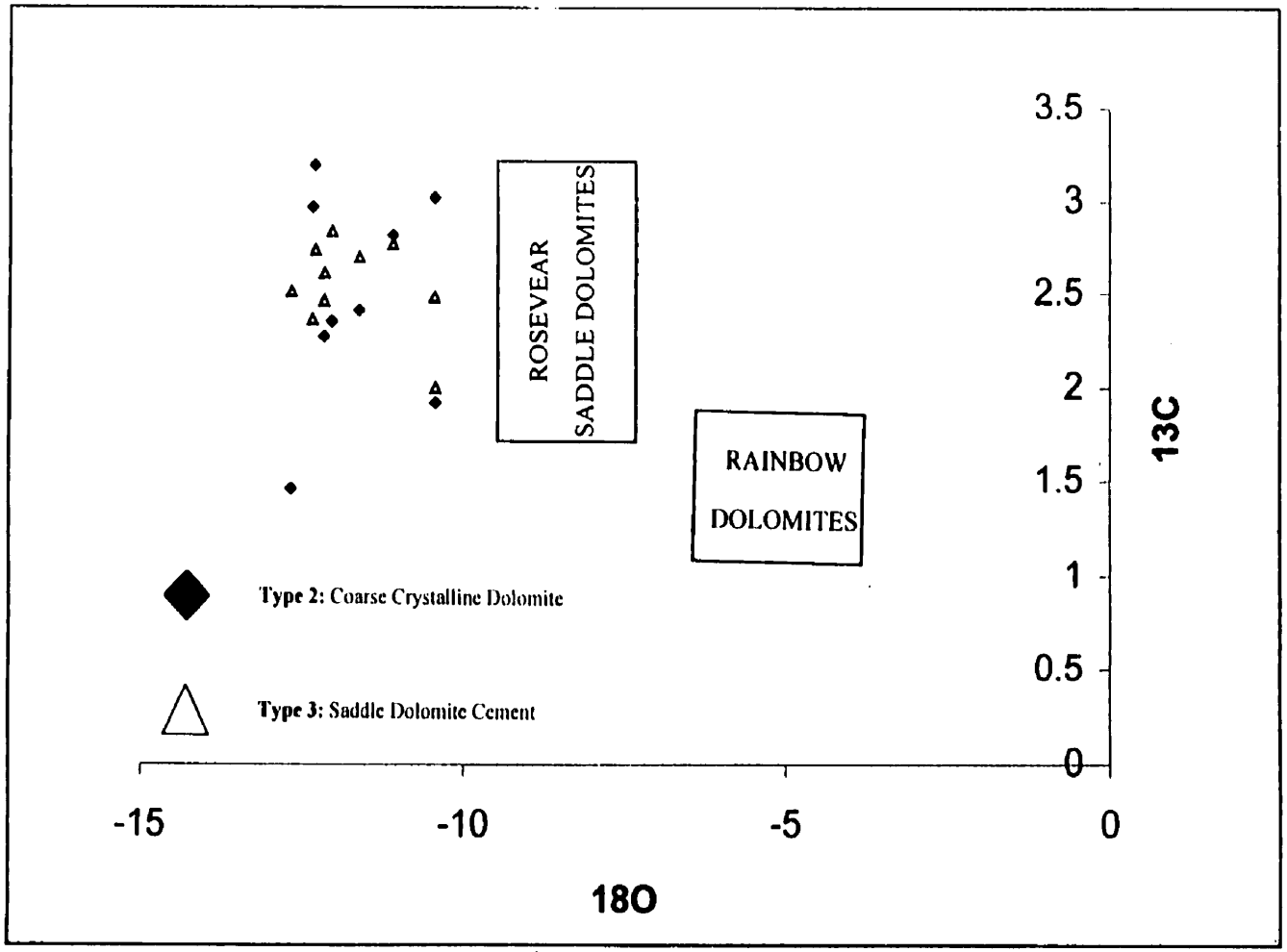

Figure 4.9. Cross plot of carbon and oxygen stable isotope compositions for Type 2 and Type 3 dolomites. Also shown are the stable isotope trends for other Middle Devonian fields in the Western Canada Sedimentary Basin (Kaufman et. al., 1996; Qing and Mountjoy, 1989a).

with $\delta^{18}O$ ranging from –10.43 to –13.35 and $\delta^{13}C$ ranging from +1.46 to +3.19. This suggests that both Type 2 and Type 3 dolomites formed from dolomitizing fluids with similar $\delta^{18}O$ and $\delta^{13}C$ values. Figure 4.10 shows that there are no apparent stratigraphic trends in the stable isotope values for dolomite Types 2 and 3 in the study area.

The $\delta^{18}O$ of both Type 2 and Type 3 dolomites are depleted in ^{18}O relative to brachiopods (-3.8 to –4.2 ‰ PDB) that appear to have preserved Middle Devonian seawater signatures (Carpenter et al., 1991). The $\delta^{13}C$ values for Type 2 and Type 3 dolomites are slightly higher (enriched) than $\delta^{13}C$ signatures of Middle Devonian seawater (1 to 2 ‰ PDB) as was determined from Devonian submarine cements and brachiopods (Popp et al., 1986; Qing and Mountjoy, 1989a).

Possible temperatures of dolomitizing fluids can be estimated assuming the dolomitizing fluids were of marine parentage with similar $\delta^{18}O$ values to Middle Devonian seawater (-3.0 to -2.0 ‰ SMOW, Carpenter et al., 1991). Figure 4.11 shows possible temperatures calculated using a temperature of 25°C and $\delta^{18}O$ values (-5.1 ‰ PDB) from Devonian submarine cements and brachiopods (Qing and Mountjoy, 1989a; Popp et al., 1986).

The $\delta^{18}O$ values constrain the temperatures and inferred depths at which dolomitization occurred. The $\delta^{18}O$ of the Type 2 dolomite ranges from –10.43 to –12.79, with an average of –11.69 (Table 4.1). From these values, a temperature range of 85 to 110°C were calculated (Land, 1985) for Type 2 using an estimate of $\delta^{18}O \leq$ -2.5 ‰ SMOW for Middle Devonian seawater (Amthor et al., 1993; Kaufman et al., 1991). The Type 3 dolomites have slightly narrower range of $\delta^{18}O$ values ranging from -11.19 to

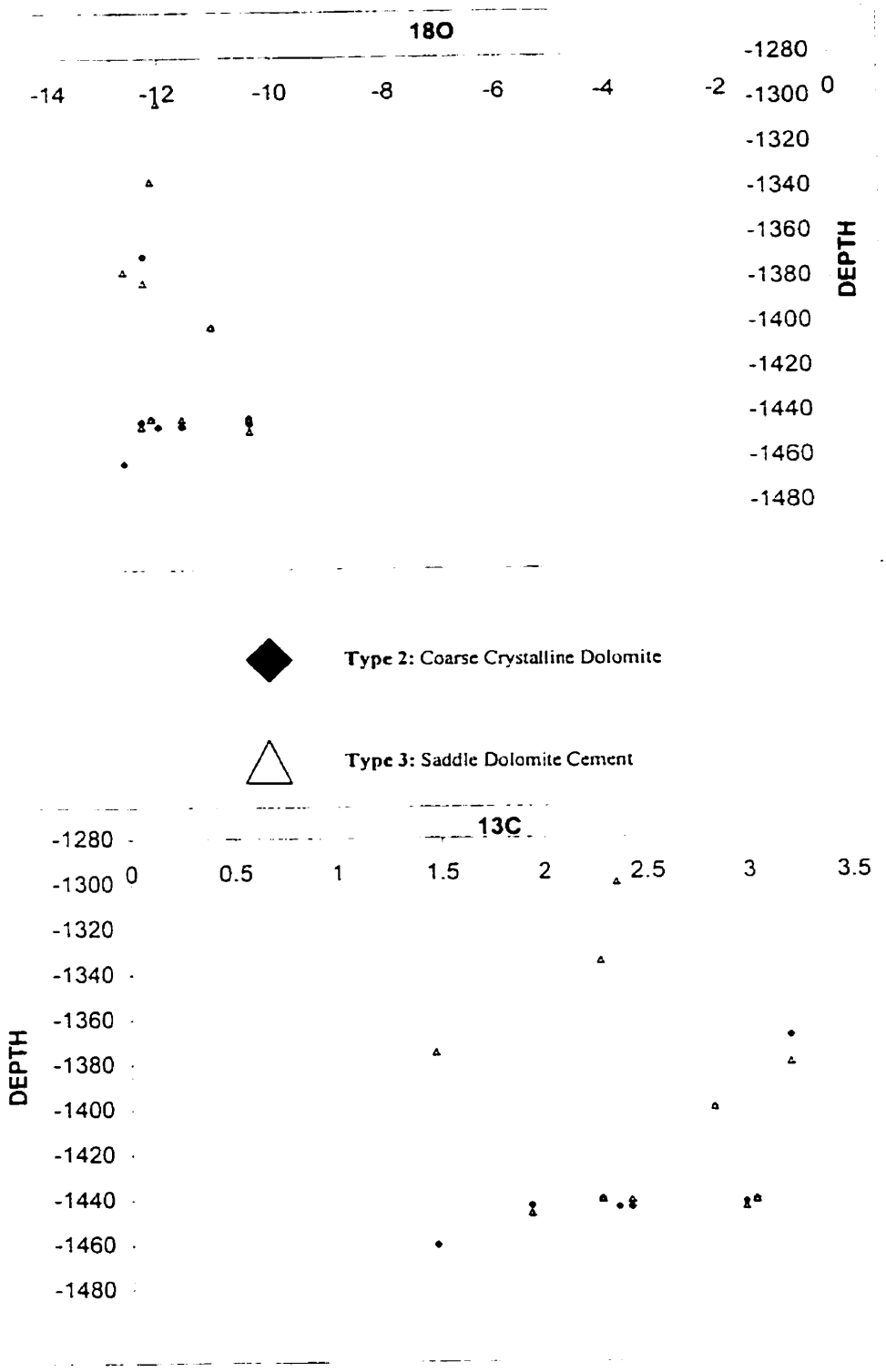

Figure 4.10. Cross plots of carbon and oxygen stable isotope compositions vs depth for Type 2 and Type 3 dolomites.

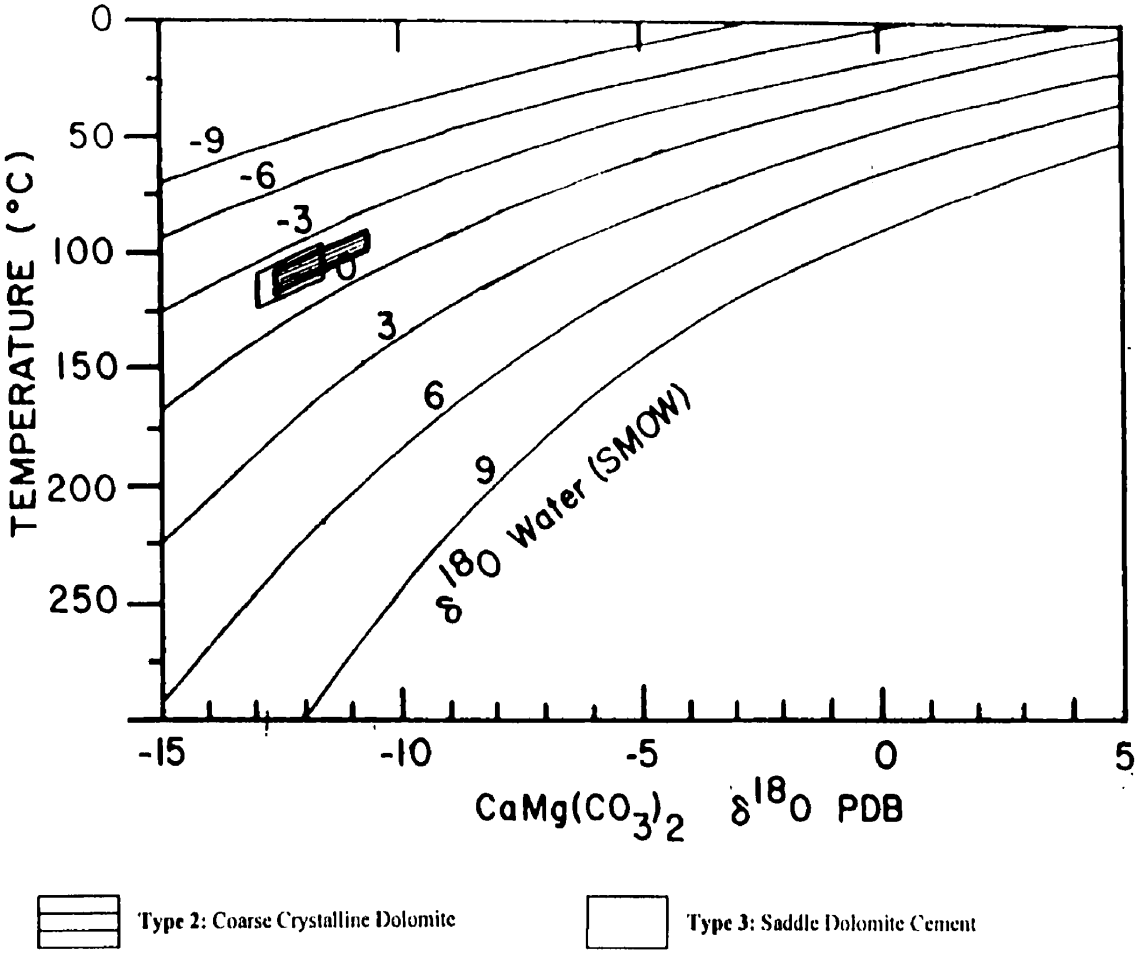

Figure 4.11. Plot of the equilibrium oxygen isotope relationships of temperature, water and dolomite (Kaufman et al., 1991). If the dolomitizing fluid had a -2.5 ‰ SMOW, then Type 2 dolomites ranging from -10.43 to -12.79 ‰ PDB could have formed at temperatures ranging from 85 to 110 °C.

-13.35, with an average of −12.67. Using these values, temperatures of approximately 100 to 120°C were calculated (Land, 1985).

Assuming normal geothermal gradients of 30°C/km and a surface temperature of 25°C (Kaufman et al., 1991), the temperatures for Type 2 dolomites correspond to depths of 2000 to 2800 m; and 2500 to 3200 m for Type 3 dolomites.

These temperatures and depths are approximations limited by uncertainties in the values for $\delta^{18}O$ of the dolomitizing fluids, paleogeothermal gradient and surface temperature. Changing the values of these parameters, within geologically reasonable limits, however, does not significantly alter the main conclusions derived from these calculations.

4.5 Dolomitization Models

Interpretations of the origin of different generations of dolomite are based on stratigraphic, petrographic and isotopic results.

4.5.1 Type 1 - Matrix Dolomite

Any model used to explain the occurrence of matrix dolomite must be able to explain its presence along pressure solution fabrics.

Hypersaline models of dolomitization can be ruled out because evaporites and/or evaporitic textures, which are closely associated with this type of dolomitization, are absent (White and Al-Aasm, 1997). Furthermore, the lack of meteoric vadose cements and moldic porosity excludes the seawater and mixing models.

The fine grained (10-30 μm) subhedral to euhedral sucrosic dolomite crystals within insoluble pressure solution seams gives the best evidence that matrix dolomite formed in a burial environment. Wanless (1979) observed similar dolomite crystals with similar grain sizes and proposed that fine crystalline euhedral dolomite can precipitate within non-sutured dissolution seams. The Mg^{2+} source comes from the clays that make up the seams, suggesting an internal source (Wanless, 1979). Dissolved $CaCO_3$ comes from the limestone host where the ions of Ca^{2+} and CO_3^{2-} are released at maximum points of stress. Type 1 dolomitization, therefore, resulted from fluid movement and ionic transport associated with pressure dissolution. During pressure dissolution, ionic transport occurs through diffusion along the water film and/or bulk pore water system (Shinn and Robbin, 1983; Baker et al., 1980). The direction of ionic transport may be either parallel or perpendicular to the imposed stress direction (Wanless, 1979). Although some stylolites may have developed in marine carbonates at burial depths of about 300 m (Qing and Mountjoy, 1994), most stylolites probably formed at depths greater than 600 to 900 m (Lind, 1993) because chemical compaction and stylolitization is a continuous process during burial. Thus, Type 1 dolomites probably formed at depths in the 600 to 900 m range. This generally corresponds to early burial depths, but precise timing cannot be determined.

4.5.2 Type 2 - Coarse Crystalline Dolomite

Any model used to explain the occurrence of coarse crystalline dolomite must be able to account for: 1) its erratic distribution in the study area, 2) dolomite post-dates early phases of pressure solution, 3) depleted oxygen isotope values (-10.43 to -12.79 ‰), and, 4) its relationship with saddle dolomite cements.

Hypersaline, seawater and mixing models cannot explain the formation of Type 2 dolomites. None of these models can explain any of the characteristics of Type 2 dolomites listed previously. The burial compaction model was used to explain the presence of Type 1 dolomites. However, the characteristics of Type 1 dolomites are different from those of Type 2 dolomites. All the characteristics of Type 2 dolomites point towards formation at deeper burial depth and probably by hydrothermal fluids. This is supported by the erratic distribution of Type 2 dolomites (Fig. 4.2), which does not appear to be stratigraphically or lithologically controlled, and the non-porous nature of laterally equivalent facies (i.e. Facies 6 and 7) indicates that dolomitization was not controlled by primary facies and/or stratigraphy.

Stoakes (1987b) suggests that the above features result from hydrothermal processes. These same types of relationships are observed in the Presqu'ile Barrier, NWT (Qing and Mountjoy, 1994), Black River and Trenton Formations of the Michigan Basin (Coniglio et al., 1994) and upper Wabamun Formation (Packard et al., 1992, Mountjoy and Halim-Dihardja, 1991). These studies observed the erratic distribution of pervasively dolomitized beds, which were not stratigraphically or lithologically controlled. In the study area there is a strong correlation betweeen the spatial distribution of Type 2 dolomites (Figure 4.2) and the pattern of faulting (Figure 1.9), suggesting that Type 2 dolomitization was probably controlled by faults, associated fracture systems and permeable zones in hydrologic continuity with them.

The model proposed for Type 2 dolomitization involves the fault-controlled, up-dip migration of deep basinal fluids in response to progressive tilting of the Western Canada Sedimentary Basin. Large-scale fluid movements were probably related to

WCSB tectonic compression and sedimentary loading (Qing and Mountjoy, 1994), which occurred at least twice, initially during early burial between the Late Devonian and Early Carboniferous and later, during deep burial between the Late Jurassic and Early Tertiary.

Based on the timing constraints placed by temperatures and depths derived from oxygen isotopes, Type 2 dolomites probably developed as basinal fluids migrated updip during the tilting of the WCSB in the Late Jurassic to Early Tertiary. The presence of a Late Devonian to Early Carboniferous age north-south trending fault system at Cranberry (Fig. 1.9) may have focused fluids updip from deep basinal sources to produce the observed linear dolomite trend.

Depending on the proximity to fluid pathways, there was preferential dolomitization of facies closest to the north-south fault system in the study area. The limestone to dolostone transition along bedding planes is easily explained by faults and/or fractures making dolomitizing fluids available for alteration of the adjacent rock. Evidence from the study area suggests that faulting occurred prior to dolomitization, allowing the incursion of dolomitizing fluids and explaining the crosscutting patterns of dolomitization and the petrographic similarity of dolomite throughout the Slave Point.

4.5.3 Type 3 - Saddle Dolomite Cement

Saddle dolomite is one of the most important types of dolomite found in the Slave Point Formation. Saddle dolomite has been attributed by various authors to indicate formation in a burial environment by hot (60 – 150°C) and saline (2 – 6 times seawater salinity) hydrothermal fluids (Radke and Mathis, 1980; Searl, 1989).

Any model explaining the formation of Type 3 saddle dolomites in the study area must be able to satisfy the following: 1) timing of saddle dolomite, occurring after the

formation of Type 2 , 2) its depleted oxygen isotope values (-11.19 to –13.35 ‰), 3) its relationship as a late-stage void-filling cement in fractures and vugs, and 4) its widespread distribution across the study area.

Type 3 dolomites in the study area probably formed under temperatures ranging from 100 to 120°C. The attainment of 100 to 120°C temperatures as the product of a 'normal' paleogeothermal gradient would require the burial of the Slave Point to much greater depths, on the order of 3200 m, than at present (2200 - 2400m). Such depths could only have been reached during the deepest phase of Slave Point burial in the Late Cretaceous – Early Tertiary (Porter et al., 1982; Hitchon, 1984).

It has been proposed by other investigators (Qing and Mountjoy, 1994; Dix, 1993; Law, 1981) studying other saddle dolomite deposits that the fluids responsible for the formation of these dolomites came from the west and are hydrothermal in nature. The flow of basinal fluids was propelled eastward by tectonic forces related to the Columbian and Laramide Orogenies that occurred during Late Jurassic to early Tertiary (Kaufman et. al., 1991; Qing and Mountjoy, 1989b). These orogenic movements produced multi-stage events of tectonic compression, sedimentary loading and uplift. Alternatively, dolomitization occurred during the Antler Orogeny from Late Devonian to Early Carboniferous. However, petrological and geochemical evidence suggest a late diagenetic stage for the formation of Type 3 dolomites under depths of several kilometers. Also, the tectonic loading and compression associated with the Antler Orogeny would not be enough to drive sufficient dolomitizing fluids (Qing and Mountjoy, 1994). Therefore, the Type 3 dolomitization probably occurred during the Laramide Orogeny because fluid

migration was the most active due to greater sediment thickness from the increased tectonic and sedimentary loading because of greater uplift.

4.6 Iron and Magnesium Source and Fluid Origin

The sources of dolomitizing fluids are important aspects in understanding the dolomitization process. In this study, the possible sources of iron (Fe) and magnesium (Mg) will be discussed.

4.6.1 Sources of Iron

There are two possible sources of iron which could explain the presence of ferroan dolomite (Type 3) in the Slave Point: (1) Fe^{2+} could have been transferred to the Slave Point from the Watt Mountain shales during dewatering and diagenesis of the shales; (2) the pre-existing limestone of the Slave Point could have been originally rich in iron (detrital Fe-oxides, clays, organics).

The Watt Mountain as a source of iron is supported by the following lines of reasoning: (a) iron may be reduced within the clay lattice and released via ion-exchange processes (Drever, 1971; Heller-Kallai and Rozenson, 1978; Irwin, 1980); (b) the reaction of smectite to illite can also release iron (Boles and Franks, 1979; McHargue and Price, 1982).

Whether or not the precursor limestone in the Slave Point acted as an internal source of iron is difficult to evaluate. Detrital iron oxides and organic matter deposited within the Slave Point probably contributed some Fe^{2+} to the formation of ferroan dolomite. It seems more likely, however, that the source of much of the Fe^{2+} was external (i.e. Watt Mountain sourced).

4.6.2 Sources of Magnesium

One of the criteria required for dolomitization is the source and transport of Mg to the site. Potential sources of magnesium are (Qing and Mountjoy, 1994): 1) cannibalization of high Mg calcites, 2) Mg absorbed on clay minerals and organic matter, 3) structurally bound Mg in clay minerals and organic compounds, 4) Mg remobilized by pressure solution from older dolomites, 5) formation waters, and 6) fluid injection through fractures and faults. Because most of these sources are only available during early burial (1 and 2) and/or cannot provide a sufficient amount of Mg (1 to 3), the most likely sources of Mg for extensive late-stage burial dolomitization (Types 2 and 3) in the Slave Point are a combination of sources 4 to 6.

Only a limited and generally insufficient amount of Mg^{2+} is available from formation waters to cause regionally pervasive dolomitization. Additional Mg^{2+} released by clay mineral reactions at depth and possibly pressure dissolution is also generally considered to result only in local cementation rather than pervasive dolomitization. The limited areal extent of dolomitization in the study area avoids the common problem of the burial compaction model in explaining regional dolomites due to insufficient Mg^{2+} available from pore waters or clay mineral diagenesis. Machel and Mountjoy (1986) point out that most burial compaction occurs early in a basin's subsidence history and is relatively ineffective at depths exceeding 1000 meters. Whether sufficient permeability in this buried, dominantly tight limestone sequence existed is unknown, although the regional fracture system is likely to have been instrumental in allowing effective transmission of burial fluids laterally and vertically through the basin.

4.7 Summary

This section focuses on the phases of dolomite formation within the Slave Point. Three different petrographic types of dolomite are identified: Type 1 - Matrix Dolomite: Type 2 - Coarse Crystalline Dolomite; and Type 3 - Saddle Dolomite Cement.

Type 1 is characterized by its small crystal size (10-30 μm) and its presence along pressure solution fabrics. Type 1 dolomites are typically Fe-rich. Type 1 dolomites only account for a minor amount of the total dolomitization that has taken place in the Slave Point Formation.

Type 2 is characterized by its coarse crystal size (200 to 800 μm) and its limited areal extent in the study area. Type 2 dolomites are typically non-ferroan but may have ferroan-rich rims where bordering secondary porosity. Type 2 dolomites form the enhanced reservoir at Cranberry and appear to be fault-related.

Type 3 dolomites are characterized by curved or lobate crystal margins and occur primarily as pore-filling cements in the study area. Where present in dolostones, saddle dolomite cements fill fractures and secondary porosity types, thus post-dating the formation of the replacive Type 2 dolomites. Type 3 dolomites are typically ferroan. . Type 3 dolomites are widespread across the study area.

Based on oxygen isotope values, Type 2 is interpreted to have formed at temperatures of 85 to 105°C and Type 3 at 100 to 120°C. In the absence of an abnormally high geothermal gradient, these temperatures of dolomitization could have been reached upon burial of the Slave Point Formation to depths of 2000 to 2800 m for Type 2 dolomites and 2500 to 3200 m for Type 3 dolomites.

Faulting appears to have played a major role on controlling the movement of dolomitizing fluid in the subsurface. The model proposed for the formation of Type 2 dolomites is by the up-dip migration of fluids in response to basin tilting during the Late Cretaceous – Early Tertiary, focussed by a north-south post-Slave Point (probably related to Antler Orogeny tectonics) trending fault system (Figure 1.9). The model for Type 3 dolomites suggests precipitation during deeper burial from deep basinal fluids. These fluids were probably expelled during the Late Cretaceous – Early Tertiary.

CHAPTER 5: SUMMARY & CONCLUSIONS

The objective of this thesis is to investigate the major depositional and diagenetic (namely, dolomitization) processes in the Slave Point Formation in the study area responsible for the formation, preservation and destruction of this complex reservoir.

The main conclusions are:

1) On the basis of an extensive core study, the Slave Point Formation is informally subdivided into a Lower Slave Point and an Upper Slave Point; similarly, the Waterways Formation has been subdivided into a Lower Waterways and an Upper Waterways.

2) The Slave Point and Waterways Formation can be subdivided into 14 depositional facies: Facies 1 to 3 comprise the Lower Slave Point; Facies 4 to 11 comprise the Upper Slave Point; and Facies 12 to 14 comprise the Lower Waterways. Each facies is associated with a specific depositional environment (Figure 5.1).

3) Porosity is strongly facies controlled in limestones, being the best in Facies 5, the highly fossiliferous basal bank deposits. To a lesser degree, limestone porosity also occurs in the 'grainy' shoal shoal margin deposits of Facies 10. The main limestone reservoir facies in the study area are Facies 5 and 10. Porosity in these facies is dominantly primary interparticle and intraparticle.

	CYCLE	FACIES		DEPOSITIONAL ENVIRONMENT
Lower Waterways	CYCLE 5	14	Nodular Brachiopod Wackestone	Basin
		13	Nodular Mudstone	Basin
		12	Laminated Mudstone	Basin
Upper Slave Point	CYCLE 4	10	Lime Packestone	Restricted Shoal
		9	Bulbous Stromatoporoid Grainstone	Open Shoal
	CYCLE 3	11	Stromatoporoid Wackestone	Forereef Debris
		8	Hemispherical Stromatoporoid Rudstone and Boundstone	Upper Foreslope (Reef Margin)
		7	Tidal Laminite	Restricted Lagoon
		6	*Amphipora* Rudstone and Floatstone	Open Lagoon
	CYCLE 2	11	Stromatoporoid Floatstone	Forereef Debris
		5	Tabular Stromatoporoid Floastone and Rudstone	Upper Foreslope (Reef Margin)
		4	*Stachyodes -Thamnopora* Floatstone	Middle Foreslope
		3	*Thamnopora* Wackestone	Lower Foreslope
Lower Slave Point	CYCLE 1	2	Nodular Brachiopod – Crinoidal Wackestone	Platform
		1	Mudstone	Platform

Figure 5.1. Summary of Slave Point and Waterways Formation depositional facies, environments and second order cycles.

4) The Slave Point and Waterways Formation can be grouped into 5 second-order cycles: Cycle 1: Lower Slave Point Basal Platform; Cycle 2: Upper Slave Point Basal Bank; Cycle 3: Upper Slave Point "Reef"; Cycle 4: Upper Slave Point Shoal and Cycle 5: Lower Waterways Basin Fill. Each cycle is associated with specific depositional facies (Figure 5.1).

5) The evolution of the Slave Point and Waterways Formations in the study area can be described in 5 main stages: 1) Lower Slave Point Basal Platform; 2) Upper Slave Point Basal Bank; 3) Upper Slave Point 'Reef'; 4) Upper Slave Point Shoal and 5) Lower Waterways Basin Fill. Stage 1 is characterized by basinward progradation of the Lower Slave Point Basal Platform and the initial colonization of subtle topographic highs by *Thamnopora*. Stage 2 is characterized by a shallowing upward cycle and the basinward progradation of the Upper Slave Point Basal Bank. Stage 3 is characterized by an initial backstepping (due to a relative sea level rise) followed by aggradation of the Upper Slave Point 'Reef'. Stage 4 is also characterized by an initial backstepping (due to a relative sea level rise) followed by aggradation of the Upper Slave Point Shoal, forming an elevated rim. Stage 5 is characterized by post-Slave Point deposits of the Lower Waterways which onlap and overlie the Slave Point Formation, creating a stratigraphic trap of considerable extent (~10 km wide and ~40 m thick).

6) The isopach of the Lower Waterways provides an important map that can be used to interpret the underlying topography of the Slave Point.

7) Slave Point sedimentation was probably influenced by antecedent topography possibly related to the Precambrian (?).

8) Facies mapping and various isopachs indicate that the transition from buildup to basin occurs over a distance of less than 1 km.

9) Three major types of dolomite occur in the Slave Point Formation in the study area based on petrographic and CL observations: Type 1 – Matrix Dolomites; Type 2 – Coarse Crystalline Dolomites; and Type 3 – Saddle Dolomite Cements.

10) Petrographic and crosscutting relationships indicate that Slave Point dolomites formed in the order: Type 1 $\Rightarrow$ Type 2 $\Rightarrow$ Type 3.

11) Type 2 dolomites probably formed at depths of 2000 to 2800 m and at temperatures of 85 to 110°C. The model for Type 2 dolomites involves the migration of burial hydrothermal fluids preferentially concentrated along a Mississippian age north-south fault system during the Late Cretaceous – Early Tertiary in the study area.

12) Type 3 dolomites probably formed at depths of 2500 to 3200 m and at temperatures of 100 to 120°C. The model for Type 3 dolomitization involves the regional eastward migration of burial hydrothermal fluids during the Late Cretaceous –Early Teritary.

5.1 Further Work

Further work should include fluid inclusion data from dolomite and calcite phases to improve the estimates of proposed depths and temperatures of formation of dolomites, thereby refining the dolomitization models. Additionally, a more detailed petrographic stable isotope analysis of the main diagenetic mineral phases would provide a more complete picture of the diagenetic history of the Slave Point Formation. Sr isotopes can provide useful information about the nature of the fluids from which the carbonates were precipitated.

REFERENCES

Allan, J.R. and Matthews, R.K., 1982. Isotope signatures associated with early meteoric diagenesis. Sedimentology, v. 29, p. 797-817.

Amthor, J.E., Mountjoy, E.W. and Machel, H.G., 1993. Subsurface dolomites in Upper Devonian Leduc Formation buildups, central part of Rimbey-Meadowbrook reef trend, Alberta, Canada. Bulletin of Canadian Petroleum Geology, v. 41, no. 2, p. 164-185.

Andrews, J.E., Hamilton, P.J. and Fallick, A.E., 1987. The geochemistry of early diagenetic dolostones from a low salinity, Jurassic lagoon. Journal of the Geological Society, v.144, p. 687-698.

Baker, P.A. Kastner, M., Byerlee, J.D. and Lockner, D.A., 1980. Pressure solution and hydrothermal recrystallization of carbonate sediments – an experimental study. Marine Geology, v. 38, p. 185-203.

Behrens, E.W. and Land, L.S., 1972. Subtidal Holocene dolomite, Baffin Bay, Texas. Journal of Sedimentary Geology, v. 42, p. 155-161.

Bell, J.S. and McCallum, R.E., 1990. *In situ* stress in the Peace River Arch area, Western Canada. Bulletin of Canadian Petroleum Geology, vol. 38A, p. 270-281.

Belyea, H. and Norris, A.W., 1971. Middle Devonian tectonic history of the Tathlina uplift, southern District of Mackenzie and northern Alberta, Canada. Geological Society of Canada, Paper 70-14.

Berner, R.A., 1981. A new geochemical classification of sedimentary environments. Journal of Sedimentary Petrology, v. 51, p. 359-365.

Bloy, G. and McKellar, R., 1992. The Slave Point Formation exploration play in the Hamburg-Cranberry area of northern Alberta. American Association of Petroleum Geologists, 1992 Annual Convention, Calgary, Alberta, Abstracts, p. 10-11.

Boles, J.R. and Franks, S.G., 1979. Clay Diagenesis in Wilcox Sandstones of Southwest Texas: Implications of smectite diagenesis on sandstone cementation. Journal of Sedimentary Petrology, v. 49, p. 55-70.

Braun, W.K., 1967. Upper Devonian ostracod faunas of Great Slave Lake and northeastern Alberta: *In* International Symposium on Devonian Systems, Oswald, D. (Ed.): Alberta Society of Petroleum Geologists, v. 2, p. 617-652.

Braun, W.K., Norris, A.W. and Uyeno, T.T., 1988. Late Givetian to Early Frasnian Biostratigraphy of western Canada: The Slave Point-Waterways Boundary and related events; *In* Devonian of the World: Proceedings of the Second International Symposium on the Devonian System, Volume III, Paleontology, Paleoecology and Biostratigraphy, N.J. McMillian, A.F. Embry, and D.J. Glass (Eds.); Canadian Society of Petroleum Geologists, Memoir 14, p. 93-111.

Budrevics, V., 1974. Detailed stratigraphy of the Slave Point Formation in the Nabesche River area, northeastern British Columbia. M.Sc. Thesis, University of Manitoba, Winnipeg, Manitoba, 118 p.

Burrowes, O.G. and Krause, F.F., 1987. Overview of the Devonian System: subsurface of Western Canada Basin; *In* Devonian Lithofacies and Reservoir Styles in Alberta, F.F. Krause and O.G. Burrowes, (eds.); Canadian Society of Petroleum Geologists, Core Conference, Calgary, Alberta, p. 1-5.

Cameron, A.E., 1918. Explorations in the vicinity of Great Slave Lake, Geological Survey of Canada, Summary Report, 1917, Part C, p. 22-28.

Cameron, A.E., 1922. Hay and Buffalo Rivers, Great Slave Lake and adjacent country, Northwest Territories. Geological Survey of Canada, Dept. of Mines 1920-21, Summary Report., 1921, Part. B., p. 1-44.

Cameron, E.M., 1966. Geochemistry of Slave Point Formation, western Canada. Geological Society America, Special Paper 87, p. 26-27.

Campbell, C.V., 1992. Beaverhill Lake Megasequence; *In* Devonian-Early Mississippian Carbonates of the Western Canada Sedimentary Basin: A Sequence Stratigraphic Framework, J.C. Wendte, F.A. Stoakes and C.V. Campbell (eds.); Society for Sedimentary Geology, Calgary, p. 163-180.

Campbell, N.L., 1950. The Middle Devonian in the Pine Point Area, N.W.T. Geological Association of Canada Proceedings., v. 3, p. 87-96.

Cant, D.J., 1988. Regional structure and development of the Peace River Arch, Alberta: A Paleozoic failed - rift system? Bulletin of Canadian Petroleum Geology, v.36, p.284-295.

Carpenter, A.B., 1980. The chemistry of dolomite formation I: the stability of dolomite. Special Publication Society Economic Paleontologists, Mineralogists, Tulsa, v. 28, p. 111-121.

Carpenter, S.J., Lohmann, K.C., Holden, P., Walter, L.M., Hoston, T. and Halliday, A.N., 1989. $\delta^{18}O$ values, 87Sr/86Sr and Sr/Mg ratios of Late Devonian abiotic

marine calcite: implications for composition of ancient seawater. Geochimica Cosmochimica Acta, v. 55, p. 1991-2010.

Choquette, P.W. and Pray, L.C., 1970. Geologic nomenclature and classification of porosity in sedimentary carbonates. American Association of Petroleum Geologists Bulletin, v. 54, p. 207-250.

Coniglio, M., Sherlock, R., William-Jones, A.E., Middleton, K. and Frape, S.K., 1994. Burial and hydrothermal diagenesis of Ordovician carbonates from the Michigan Basin, Ontario, Canada. Special Publication International Association of Sedimentology, v. 21, p. 231-254.

Craig, H., 1957. Isotopic standards for carbon and oxygen and correction factors for mass-spectrometric analysis of carbon dioxide. Geochimica et Cosmochimica Acta, v. 12, p. 272-374.

Craig, J.H., 1987. Depositional Environments of the Slave Point Formation, Beaverhill Lake Group, Peace River Arch; *In* Devonian Lithofacies and Reservoir Styles in Alberta, F.F. Krause and O.G. Burrowes (Eds.); Canadian Society of Petroleum Geologists 13th Core Conference, Calgary, Alberta, p. 181-199.

Crawford, F.D., 1972. Facies Analysis and Depositional Environments in the Middle Devonian Fort Vermilion and Slave Point Formations of northern Alberta. M.Sc. Thesis, University of Calgary, Calgary, Alberta, Canada, 86 p.

Crickmay, C.H., 1957. Elucidation of some western Canada Devonian Formations. Calgary, published by author, Imperial Oil Ltd., 15 p.

Davies, G.R. and Tooth, J.W., 1987. Middle Devonian Slave Point lithofacies, Gift Lake, North Central, Alberta: *In* Devonian Lithofacies and Reservoir Styles in Alberta, F.F. Krause and O.G. Burrowes (Eds.): Canadian Society of Petroleum Geologists 13th Core Conference, Calgary, Alberta, p. 173-180.

Dickson, J.A.D., 1965. A modified staining technique for carbonates in thin section. Nature, v. 205, p. 587.

Dix, G.R., 1993. Patterns of burial and tectonically controlled dolomitization in an upper Devonian fringing-reef complex, Leduc Formation, Peace River Arch Area , Alberta, Canada. Jounral of sedimentary Petrology, v. 63, no. 4, p. 628-640.

Douglas, R.J.W., 1959. Great Slave Lake and Trout River map-areas, N.W.T. Geological Survey of Canada, Paper 58-11.

Drever, J.L., 1971. Magnesium-iron replacement in clay minerals in anoxic marine sediments. Science, v. 172, p. 1334-1336.

Dunham, J.B. and Larter, S., 1981. Association of stylolitic carbonates and organic matter; implications for temperature control on stylolite formation. American Association of Petroleum Geologists Bulletin, v. 65, no. 5, p. 922.

Dunham, J.B., Crawford, G.A. and Panasiuk, W., 1983. Sedimentology of the Slave Point Formation (Devonian) at Slave Field, Lubicon Lake, Alberta; *In* Carbonate buildups: a core workshop, P.M. Harris, (Ed.); Society of Economic Paleontologists and Mineralogists, Core Workshop No. 4, Dallas, p. 73-111.

Dunham, R.J., 1962. Classification of carbonate rocks according to depositional texture: *In* Classification of Carbonate Rocks, W.E. Hana (Ed.); American Association of Petroleum Geologists, Memoir 1, p. 101-121.

Embry, A.F. and Klovan, J.E., 1971. A late Devonian reef tract on northeastern Banks Island, N.W.T. Bulletin Canadian Petroleum Geology, v. 19, p. 730-781.

Embry, A.F. and Klovan, J.E., 1972. Absolute water depth limits for Late Devonian paleoecological zones. Geologische Rundschau, v. 61, p. 572-686.

Epstein, S., Graf, D.L. & Degens, E.T., 1964. Oxygen isotope studies on the origin of dolomite. *In* Isotopic and Cosmic Chemistry, H. Craig (Ed.): North Holland Publishing Co., p. 169-180.

Evamy, B.D., 1963. The application of a chemical staining technique to a study of dedolomitization. Sedimentology, v. 2, p. 631-650.

Featherstone, R.P., 1982. Biostratigraphy of the Middle Devonian Salve Point and adjoining formations, northern Alberta, Canada. M.Sc. Thesis, University of Saskatchewan, Saskatoon, Saskatchewan, 196 p.

Fischbuch, N.R., 1968. Stratigraphy, Devonian Swan Hills Reef Complexes of Central Alberta. Canadian Petroleum Geology Bulletin, v. 16, p. 446-587.

Folk, R.L., 1972. Practical petrographic classification of limestones; *In* Carbonate Rocks I: Classifications, Dolomite, Dolomitization, American Association of Petroleum Geologists, Reprint Series no. 4, p. 11-48.

Fong, G., 1959. Type section Swan Hills Member of the Beaverhill Lake Formation. Alberta Society of Petroleum Geologists Journal, v. 7, no. 5, p. 95-108.

Fong, G., 1960. Geology of the Devonian Beaverhill Lake Formation, Swan Hills area, Alberta, Canada. American Association of Petroleum Geologists Bulletin, v. 44, no. 4, p. 195-209.

Galloway, W.E., 1989. Genetic sequences in basin analysis 1: Architecture and genesis of flooding surface bounded by depositional units. American Association of Petroleum Geologists Bulletin, v. 73, no. 2, p. 125-142.

Given, R.K. and Lohmann, K.C., 1986. Isotopic evidence for the early diagenesis of the reef facies, Permian reef complex of west Texas and New Mexico. Journal of Sedimentary Petrology, v. 56, p. 158-169.

Goldsmith, J.R. and Graf, D.L., 1958a. Structural and compositional variations in some natural dolomites. Journal of Geology, v. 66, p. 678-693.

Goldsmith, J.R. and Graf, D.L., 1958b. Relation between lattice constants and composition of the Ca-Mg carbonates. American Mineralogist, v. 43, p. 84-101.

Gosselin, E.G., 1990. Geology of the Middle Devonian Slave Point Formation, northwestern Alberta, Canada. M.Sc. Thesis, Queens University, Kingston, Ontario, Canada, 224 p.

Gosselin, E.G., Smith, L. and Mundy, D.J.C., 1989. The Golden and Evi reef Complexes, Middle Devonian, Slave Point Formation, northwestern Alberta; *In* Reefs: Canada and adjacent areas, H.H.J. Geldsetzer, N.P. James, and G.E. Tebbutt, (Eds.): Canadian Society of Petroleum Geologists, Memoir 13, p. 440-447.

Gray, F.F. and Kassube, J.R., 1963. Geology and stratigraphy of Clarke Lake gas field, northeastern British Columbia, American Association of Petroleum Geologists, Bulletin, v. 47, no. 3, p. 467-483.

Griffin, D.L., 1965. The Devonian Slave Point, Beaverhill Lake, and Muskwa Formations of northeastern British Columbia and adjacent areas. British Columbia Dept.Mines and Petroleum Resources Bulletin, 5090 p.

Hadley, M.G. and Jones, B., 1990. Lithostratigraphy and nomenclature of Devonian Strata in the Hay River area, N.W.T. Bulletin Canadian Petroleum Geology, v. 38, no. 3. p. 332-356.

Halim-Dihardja, M.K., 1986. Diagenesis and sedimentology of the Late Devonian (Famennian) Wabamun Group in the Tangent, Normandville and Eaglesham fields, north-central Alberta. M.Sc. Thesis, McGill University, Montreal, Quebec, 173 p.

Heller-Kallai, L. and Rozenson, I., 1978. Removal of magnesium from interstitial waters in reducing environments: the problem reconsidered. Geochimica Cosmochimica Acta, v. 42, p. 1907-1909.

Hiscock, R.G., 1984. Stratigraphy, lithofacies and diagenesis of the Slave Point Formation in the Evi-Cadotte Lake area of northern Alberta. B.Sc. Thesis, Memorial University, St. John's, Newfoundland, Canada.

Hitchon, B., 1984. Geothermal gradients, hydrodynamics and hydrocarbon occurences, Alberta, Canada. American Association of Petroleum Geologists Bulletin, v. 68, p., 713-743.

Hutton, A.N., 1994. Textural evidence for the origin of dolomitization in the Slave Point Hamburg to Clarke Lake. Canadian Society of Petroleum Geologists Annual Meeting, Program with Abstracts, p. 342-343.

Irwin, H., 1980. Early Diagenetic precipitation and pore fluid mineralization in the Kimmeridge clay of Dorset England. Sedimentology, v. 27, p. 577-591.

James, N.P., 1984. Reefs: In Facies Models, R.G. Walker (Ed.). Geological Association of Canada, GeoScience Canada, Reprint Series 1, Kitchener, Ontario, p. 229-244.

Jamieson, E.R., 1971. Paleoecology of Devonian Reefs in western Canada. *In* Reef organisms through time. Istituto Veneto di Science. Lettere ed Arti. Classe di Scienze Mathematiche e Naturali, p. 1300-1340.

Johnson, J.G., 1970. Taghanic Onlap and the End of North American Devonian Provinciality. Geological Society of America Bulletin., v. 81, p. 2077-2106.

Keith, J.W., 1990. The influence of the Peace River Arch on Beaverhill Lake sedimentation. Bulletin of Canadian Petroleum Geology, v.38A, p.55-65.

Kaufman, J., Hanson, G.N. and Meyers, W.J., 1991. Dolomitization of the Swan Hills Formation, Rosevear Field, Alberta, Canada. Sedimentology, v. 38, p. 41-66.

Kaufman, J., Meyers, W.J. and Hanson, G.N., 1990. Burial cementation in the Swan Hills Formation (Devonian) Rosevear Field, Alberta, Canada. Journal of Sedimentary Petrology, v. 60, no. 6, p. 918-939.

Klovan, J.E., 1964. Facies Analysis of the Red Water Reef Complex, Alberta, Canada. Bulletin Canadian Petroleum Geology, v. 14, p. 241-265.

Kramers, J.W. and Lerbekmo, J.K., 1967. Petrology and mineralogy of Watt Mountain Formation, Mitsue – Nippisi Area, Alberta. Bulletin Canadian Petroleum Geology, v. 15, p. 346-378.

Kwiatkowski, M., 1985. Diagenesis of Middle Devonian Slave Point Formation in the Red Earth area of Alberta, Canada. Geological Association of Canada/Mineralogical Association of Canada, joint annual meeting, Fredericton, NB, Programs with Abstracts, v. 10, p. A32.

Land, L.S., 1985. The origin of massive dolomite. Journal of Geological Education, v. 33, p. 112-125.

Land, L.S., 1980. The isotopic and trace element geochemistry of dolomite: the state of the art: *In* Concepts and Models of Dolomitization, D.H. Zenger, J.B. Dunham and R.L. Ethington (Eds.): Society of Economic Paleontologists and Mineralogists Special Publication, v. 28, p. 87-110.

Land, L.S., 1973. Holocene meteroic dolomitization of Pleistocene limestones, North Jamaica. Sedimentology, v. 70, p. 411-424.

Law, J., 1981. Mississippian correlations, northeastern British Columbia and implications for oil and gas exploration. Bulletin of Canadian Petroleum Geology, v. 29, p. 378-398.

Law, J., 1955. Geology of northwestern Alberta and adjacent areas. American Association of Petroleum Geologists Bulletin, v. 39, p. 1927-1975.

Leavitt, E.M. and Fischbuch, N.R., 1968. Devonian nomenclatural changes, Swan Hills area, Alberta, Canada. Canadian Petroleum Geology Bulletin, v. 16, p. 288-297.

Lecompte, M., 1958. Les recifs Paleozoiques en Belgique. Geologische Rundschau, v. 47, no.1, p. 384-401.

Lind, I.L., 1993. Stylolites in chalk from Leg 130, Ontong Java plateau. In W.H. Berger, J.W. Kroenke and L.A. Mayer (eds.): Proceedings of the Ocean Drilling Program, Scientific Results, v. 130, p. 445-447.

Logan, B.W., 1969. Carbonate Sediments and Reefs, Yucatan Shelf, Mexico: *In* Yucatan - Bonacca, B.W. Logan and A. McBirney (Eds.): American Association Petroleum Geologists Memoir 11, p. 129-198.

Machel, H.G. and Anderson, J.H., 1989. Pervasive subsurface dolomitization of the Nisku Formation in central Alberta. Journal of Sedimentary Petrology, v. 59, p. 891-911.

Machel, H.G. and Mountjoy, E.W., 1987. General constraints on extensive pervasive dolomitization and their application to the Devonian carbonates of Western Canada. Bulletin of Canadian Petroleum Geology, v. 35, p. 143-158.

Machel, H.G. and Mountjoy, E.W., 1986. Chemistry and environment of dolomitization - a reappraisal. Earth Sciences Review, v. 23, p. 175-222.

Matthews, A. and Katz, A., 1977. Oxygen isotope fractionation during dolomitization of calcium carbonate. Geochimica Cosmochimica Acta, v. 41, p. 1431-1438.

Mazzullo, S.J.J., 1992. Geochemical and neomorphic alteration of dolomite: A review. Carbonates and Evaporites, v. 7, p. 21-37.

McCamis, J.G. and Griffith, L.S., 1967. Middle Devonian facies relationships, Zama Area, Alberta, Bulletin Canadian Petroleum Geology, v.15, no. 4, p. 434-467.

McCrea, J.M., 1950. On the isotopic chemistry of carbonates and a paleotemperature scale. Journal of Chemical Physics, v. 18, p. 849-857.

McGill, P., 1963. Upper and Middle Devonian ostracods from the Beaverhill Lake Formation, Alberta, Canada. Bulletin Canadian Petroleum Geology, v.2, p. 1-26.

McGill, 1966. Ostracods of probable Late Givetian age from the Slave Point Formation, Alberta. Bulletin Canadian Petroleum Geology, v. 14, p. 104-133.

McHargue, T.R. and Price, R.C., 1982. Dolomite from clay in argillaceous or shale-associated marine carbonates. Journal of Sedimentary Petrology, v. 52, p. 873-886.

Meijer-Drees, N.C., 1986. Evaporite deposits of Western Canada. Geological Society of Canada, Paper 85-20, 118 p.

Moore, P.F., 1989. The Lower Kaskaskia Sequence - Devonian; *In* Western Canada Sedimentary Basin: A Case History, B.D. Ricketts, (ed.): Canadian Society of Petroleum Geologists, Calgary, Alberta, p. 139-164.

Morrow, D.W., 1990. Dolomite - Part 2: dolomitization models and ancient dolostones: *In* Diagenesis, I.A. McIlreath and D.W. Morrow (Eds.); Geoscience Canadian Reprint Series, v. 4, p. 125-139.

Mountjoy, E.W. and Halim-Dihardja, M.K., 1991. Multiple phase fracture and fault-controlled burial dolomitization, Upper Devonian Wabamun Group. Journal of Sedimentary Petrology, v. 61, p. 590-612.

Murray, J.W., 1965. Stratigraphy and carbonate petrology of the Waterways Formation, Judy Creek, Alberta, Canada. Bulletin Canadian Petroleum Geology, v. 13, no. 2, p. 303-326.

Murray, J.W., 1966. An oil-producing reef-fringed carbonate bank in the Upper devonian Swan Hills Member, Judy Creek, Alberta. Bulletin Canadian Petroleum Geology, v. 14, no. 1, p. 1-103.

Norris, A.W., 1963. Devonian Stratigraphy of northeastern Alberta and northwestern Saskatchewan. Geological Survey of Canada, Memoir 313.

Norris, A.W., 1965. Stratigraphy of Middle Devonian and older Paleozoic rocks of the Great Slave Lake region, Northwest Territories. Geological Survey of Canada, Memoir 322.

Norris, A.W. and Uyeno, T.T., 1981. Stratigraphy and paleontology of the lowermost Upper Devonian Slave Point Formation on Lake Claire and the lower Upper Devonian Waterways Formation on Birch River, northeastern Alberta. Geological Survey Canada, Bulletin 334, 53 p.

Norris, A.W. and Uyeno, T.T., 1983. Biostratigraphy and paleontology of Middle-Upper Devonian boundary beds, Gypsum Cliffs area, northeastern Alberta. Geological Survey Canada, Bulletin 313.

O'Connell, S.C., Dix, G.R. and Barclay, J.F., 1990. The origin, history and regional structural development of the Peace River Arch, Western Canada. Bulletin of Canadian Petroleum Geology, v. 38A, p. 4-24.

Oldale, H.S. and Munday, R.J., 1994. Chapter II: Devonian Beaverhill Lake Group of the Western Canada Sedimentary Basin, *In* Geological Atlas of the Western Canada Sedimentary Basin, G.D. Mossop and I. Shetsen (eds.), Canadian Society of Petroleum Geologists and Alberta Research Council, Calgary, Alberta, p. 149-163.

Packard, J.J., Pellegrin, G.J., Al-Asam, I.S., Samson, I. And Gagnon, J., 1992. Diagenesis and dolomitization associated with hydrothermal karst in Famennian upperWabamun ramp sediments, northwestern Alberta: *In* The Development of Porosity in Carbonate Reservoirs, G.R. Bloy and M.G. Hadley (Eds.), Canadian Society of Petroleum Geologists Continuing Education Short Course, Section 9.

Patterson, R.J. and Kinsmen, D.J.J., 1982. Formation of diagenetic dolomites in coastal sabkas along the Arabian Persian Gulf. American Association of Petroleum Geologists, v. 66, p. 28-43.

Park, D.G. and Jones, B., 1985. Nature and genesis of breccia bodies in Devonian strata, Pine Point area, Wood Buffalo Park, northeastern Alberta. Bulletin of Canadian Petroleum Geology, v. 33, no. 3, p. 275-294.

Pierre, C., Ortlieb, L. and Person, A., 1984. Supratidal evaporitic dolomite at Ojo de Liebre Lagoon: mineralogical and isotopic arguments for primary crystallization. Journal of Sedimentary Petrology, v. 54, p. 1049-1061.

Podruski, J.A., Barclay, J.E., Hamblin, A.P., Lee, P.J., Osadetz, K.G., Proctor, R.M. and Taylor, G.C., 1988. Conventional Oil resources of Western Canada (Light & Medium), Part I: Resource Endowment. Geological Survey of Canada, Paper 87-26, 125 p.

Popp, B.N., Anderson, T.F. and Sandberg, P.A., 1986. Textural, elemental and isotopic variations among constituents in Middle Devonian limestones, North America. Journal of Sedimentary Petrology, v. 56, p. 715-727.

Porter, J.W., Price, R.A. and McCrossan, R.G., 1982. The Western Canada Sedimentary Basin. Phil. Trans., Royal Society of London, v. 305, p. 169-192.

Qing, H. and Mountjoy, E., 1994. Formation of Coarsely Crystalline hydrothermal dolomite reservoirs in the Presqu'ile Barrier, Western Canada Sedimentary Basin. American Assoication of Petroleum Geology Bulletin, v. 78, no. 1, p. 55-77.

Qing, H. and Mountjoy, E., 1991. Dolomitization of Middle Devonian Presqu'ile Facies in western Canada. Geological Association of Canada/Mineralogical Association of Canada with the Society of Economic Geologists, joint annual meeting, Toronto, Ontario, Programs with Abstracts, v. 16, p. 103.

Qing, H. and Mountjoy, E., 1989a. Dolomitization of Middle Devonian Presqu'ile barrier at Pine Point: an indication of open-system diagenesis. Geological Association of Canada /Mineralogical Association of Canada, joint annual meeting, Montreal, PQ, Programs with Abstracts, v. 14, p. 64.

Qing, H. and Mountjoy, E., 1989b. Multistage dolomitization in Rainbow buildups, Middle Devonian Keg River Formation, Alberta, Canada. Journal of Sedimentary Petrology, v. 59, p. 114-126.

Radke, B.M. and Mathis, R.L., 1980. On the formation and occurrence of saddle dolomite. Jounral of Sedimentary Petrology, v. 50, p. 1149-1168.

Reinson, G.E. and Lee, P.J., 1993. Study finds Devonian gas resources of western Canada attractive target. Oil & Gas Journal, v. 91, p. 80-83

Reinson, G.E., Lee, P.J., Barclay, J.E., Bird, T.D. and Osadetz, K.G., 1993a. Western Canada basin conventional gas resources estimated at 232 tcf. Oil & Gas Journal, v. 91, p. 92-95.

Reinson, G.E., Lee, P.J., Warters, W., Osadetz, K.G., Bell, L.L., Price, P.R., Trollope, F., Campbell, R.I. and Barclay, J.E., 1993b. Devonian Gas Resources of Western Canada Sedimentary Basin. Part 1: Geological Play Analysis and Resource Assessment. Geological Survey Canada Bulletin 452, Ottawa, p. 10-102.

Rosenthal, L.R., 1988. The Winnipegosis Formation (Middle Devonian) of the northeastern margin of the Williston Basin, Canada; *In* Devonian of the World: Proceedings of the Second International Symposium on the Devonian System,

Volume II. Sedimentation. N.J. McMillan. A.F. Embry and D.J. Glass (Eds.). Canadian Society of Petroleum Geologists. Memoir 14. p. 463-475.

Saller. A.H.. 1984. Petrologic and geochemical constraints in the origin of subsurface dolomite. Enewetak Atoll: An example of dolomitization by normal seawater. Geology. v. 12. p. 217-220.

Searl. A.. 1989. Saddle Dolomite: a new view . its nature and origin. Mineralogic Magazine. v. 53. p. 547-555.

Shields. M.J. and Brady. P.V.. 1995. Mass balance and fluid flow constraints on regional scale dolomitization. Late Devonian Western Canada Sedimentary Basin. Bulletin of Canadian Petroleum Geology. v. 43. no. 4. p. 371-392.

Shinn. E.A. and Robbin. D.M.. 1983. Mechanical and chemical compaction in fine-grained shallow-water limestones. Journal of Sedimentary Petrology. v. 53. p. 595-618.

Shinn. E.A.. 1968. Practical significance of birdseye structures in carbonate rocks. Journal of Sedimentary Petrology. v. 38. p. 215-223.

Sibley. D.F. and Gregg. J.M.. 1987. Classification of Dolomite Rock Textures. Journal of Sedimentary Petrology. v. 57. no. 6. p. 967-975.

Sikabonyi. L.A.. 1958. Magnesium-Calcium ratio examinations from the Slave Point Formation. Alberta Society of Petroleum Geologists Journal. v. 6. no. 10. p. 249-251.

Skall. H.. 1975. The paleoenvironment of the Pine Point lead-zinc district. Economic Geology. v.70. p. 22-45.

Smith. T.M. and Dorobek. S.L.. 1989. Dolomitization of the Devonian Jefferson Formation. south-central Montana. The Mountain Geologist. v. 26. p. 81-96.

Stoakes. F.A.. 1987a. Evolution of the Upper Devonian of Western Canada: *In* Canadian Reef Inventory Project: Principles and Concepts for the Exploration and Exploitation of Reefs in the Western Canada Sedimentary Basin. G.R. Bloy and M. Charest (Eds.): Canadian Society of Petroleum Geologists. Short Course Notes. section 3.

Stoakes. F.A.. 1987b. Fault controlled dolomitization of the Wabamun Group. Tangent Field. Peace River Arch. Alberta; *In* Devonian Lithofacies and Reservoir Styles in Alberta. F.F. Krause and O.G. Burrrowes (Eds.); Canadian Society of Petroleum Geologists 13th Core Conference. Calgary. Alberta. p. 73-85.

Stoakes, F.A., 1992. Nature and Succession of Basin Fill Strata; *In* Devonian-Early Mississippian Carbonates of the Western Canada Sedimentary Basin: A Sequence Stratigraphic Framework, J. Wendte, F.A. Stoakes and C.V. Campbell (Eds.): SEPM Short Course, no. 28, Calgary, p. 127-144.

Tebbutt, G.E., Conley, C.D. and Rodes, D.W., 1965. Lithogenesis of a distinctive Carbonate rock fabric: Contributions to Geology, University of Wyoming, Laramie, v. 4, no. 1, 13 p.

Thomas, G.E. and Rhodes, H.S., 1961. Devonian Limestone bank-atoll reservoirs of the Swan Hills area, Alberta. Alberta Society of Petroleum Geologists Journal, v. 9, no. 2, p. 29-38.

Tooth, J.W. and Davies, G.R., 1987. The Gift Slave Point Field, northern Alberta: a geologic model for enhanced oil recovery; *In* Canadian Reef Inventory Project: Principles and Concepts for Exploration and Exploitation of Reefs in the Western Canada Basin, G.R. Bloy and M. Charest (Eds.); Canadian Society of Petroleum Geologists, Short Course Notes, section ?.

Tooth, J.W. and Davies, G.R., 1988. Gift Lake Slave Point Reef, Middle Devonian, Alberta; *In* Reefs: Canada and adjacent areas, H.H.J. Geldsetzer, N.P. James and G.E. Tebbutt (Eds.): Canadian Society of Petroleum Geologists, Memoir 13, p. 528-534.

Torrie, J.E., 1973. Northeastern British Columbia. *In* The Future Petroleum Provinces of Canada: Their Geology and Potential. Canadian Society of Petroleum Geologists, Calgary, Alberta, p. 151-186.

Uyeno, T.T., 1974. Conodonts of the Waterways Formation (Upper Devonian) of northeastern and central Alberta. Geological Survey Canada, Bulletin 232.

Uyeno, T.T., 1979. Devonian conodont biostratigraphy of Powell Creek and adjacent areas, western District of Mackenzie: *In* Western and Arctic Canadian Biostratigraphy, C.R. Stelck, & B.D.E. Chatterton (Eds.); Geological Association of Canada, Special Paper 18, p. 233-256.

Viau, C.A., 1986. Diagenesis, sedimentology and structure of the Swan Hills Formation, Swan Hills Field, central Alberta, Canada (unpublished Ph.d dissertation), Calgary, Alberta, University of Calgary 574 p.

Von der Borsch, C.C., Lock, D. and Schwebel, D., 1975. Groundwater formation of dolomite in the Coorong region of South Australia, Geology, v. 3, p. 283-285.

Walters, L.J., Jr., Claypool, G.E. and Choquette, P.W., 1972. Reaction rates and $\delta^{18}O$ variation for the carbonate-phosphoric acid preparation method. Geochimica et Cosmochimica Acta, v. 36, p. 129-140.

Wanless, H.R., 1979. Limestone response to pressure solution and dolomitization. Journal of Sedimentary Petrology, v. 49, p. 437-462.

Warren, P.S., 1933. The age of the Devonian limestone at McMurray. Canada Field Naturalist, v. 47, no. 8, p. 148-149.

Warren, P.S. and Stelck, C.R., 1950. Succession of Devonian faunas in western Canada. Transactions of the Royal Society of Canada 44, p. 61-78.

Wendte, J.C., 1992a. Overview of the Devonian of the Western Canada Sedimentary Basin. *In* Devonian-Early Mississippian Carbonates of the Western Canada Sedimentary Basin: A Sequence Stratigraphic Framework, J.C. Wendte, F.A. Stoakes and C.V. Campbell (Eds.): Society for Sedimentary Geology, Short Course No. 28, Calgary, p. 1-21.

Wendte, J.C., 1992b. Platform Evolution and its control on reef inception and localization: *In* Devonian-Early Mississippian Carbonates of the Western Canada Sedimentary Basin: A Sequence Stratigraphic Framework, J.C. Wendte, F.A. Stoakes and C.V. Campbell (Eds.); Society for Sedimentary Geology, Short Course No.28, Calgary, p. 41-87.

Wendte, J.C., 1992c. Cyclicity of Devonian Strata in the Western Canada Sedimentary Basin: *In* Devonian-Early Mississippian Carbonates of the Western Canada Sedimentary Basin: A Sequence Stratigraphic Framework, J.C. Wendte, F.A. Stoakes and C.V. Campbell (Eds.): Society for Sedimentary Geology, Short Course No.28, Calgary, p. 27-40.

Wendte, J.C., 1992d. Evolution of the Judy Creek Complex, a late Middle Devonian isolate platform-reef complex in west-central Alberta: *In* Devonian-Early Mississippian Carbonates of the Western Canada Sedimentary Basin: A Sequence Stratigraphic Framework, J.C. Wendte, F.A. Stoakes and C.V. Campbell (Eds.): Society for Sedimentary Geology, Short Course No.28, Calgary, p. 27-40.

White, K.E., 1995. A Petrophysical Evaluation of the Slave Point Formation, Cranberry Field, Alberta, In Exploration, Evaluation and Exploitation, Canadian Society of Petroleum Geologists Core Session Abstracts, Calgary.

White, T. and Al-Aaasm, I.S., 1997. Hydrothermal dolomitization of the Mississippian Upper Debolt Formation, Sikanni gas field, northeastern British Columbia, Canada. Bulletin of Canadian Pteroleum Geology, v. 45, no. 3, p. 297-316.

Williams, G.K., 1977. The Hay River Formation and its relationship to adjacent formations, Slave River map-area, N.W.T. Geological Survey of Canada Paper 75-12.

Wilson, J.L., 1975. Carbonate Facies in Geologic History. Springer-Verlag, New York, 471 p.

Zenger, D.H., Dunham, J.B. and Etherington, R.L., 1980. Concepts and models of dolomitization. Society of Economic Paleontologists and Mineralogists, Special Publication 28, 308 p.

APPENDIX A

Formation Tops

UWI	KB (m)	MUSKWA (mKB)	BIHLK (mKB)	CRANBERRY MEMBER (mKB)	UPPER SLAVE POINT (mKB)	LOWER SLAVE POINT (mKB)	WATT MOUNTAIN (mKB)	MUSKEG (mKB)
100-10-02-095-02w6/00	766.9	1958	1973.9	2114.1	-	2123	2165.4	2230.5
102-10-02-095-02w6/00	770.5	1958.6	1976.6	2115	-	2126.3	2167.1	2227.5
100-06-13-095-02w6/00	762.3	1935	1952.5	2095.8	-	2116.5	2147.6	2208.6
100-07-18-095-03w6/00	751.8	2010	2026	2147	-	2166	2212	2254
100-10-34-095-03w6/00	725.7	1929	1943.4	2069	-	2088	2139.1	2183
100-10-05-095-04w6/00	869.3	2179	2192	2307	2310	2337	2367	2407
100-12-05-095-04w6/00	857.6	2169	2183	2298	2298	2330	2356	2391
100-12-06-095-04w6/00	853.9	2180	2193	2308	2309	2339	2365	2398
100-12-07-095-04w6/00	833.2	-	2147	2276	2278	2306	2333	-
100-06-18-095-04w6/00	847.7	2158	2172	2289	2290	2318	2347	2379
100-07-27-095-04w6/00	837.9	-	-	2237.8	2258.6	2259	2305.5	2347
100-02-31-095-04w6/00	841.9	2119	2133	2251	2252	2282.5	2319	2359
100-07-32-095-04w6/00	856.8	2128	2141.5	2258.6	2271.4	2292	2328.7	2365.9
100-11-33-0095-4w6/00	843.7	2107	2120.8	2238.5	2256.7	2272	2307.3	2350
100-11-35-095-04w6/00	829	2081	2095	2216	2239	2263	2283	2332
100-15-09-095-05w6/00	964.9	2303	2315	2428.5	2436	2464	2487	2514
100-10-10-095-05w6/00	931	2265	2277	2391	2398	2426	2443	2483
100-12-12-095-05w6/00	861.6	2177	2190	2304	2307	2340	2356	2392
100-16-13-095-05w6/00	897.4	2205	2218	2334.5	2335	2365	2385	-
100-11-14-095-05w6/00	946.3	2260	2272	2387	2395	2423	2447	2477
100-04-23-095-05W6/00	875.1	-	-	-	-	-	-	-
100-10-23-095-05w6/00	875.1	-	-	2303.1	2304.9	2338.4	2362.8	2394.5
100-06-24-095-05w6/00	895.3	2196	2208	2324	2325	2357	2383	2414
100-08-24-095-05w6/00	859.4	2168	2189	2305	2306	2341	-	-
100-03-25-095-05w6/00	834.1	2132	2145	2261	2262	2297	2322	2356
100-15-25-095-05w6/00	822.3	2110	2125	2245	2246	2280	2309	-
100-07-26-095-05w6/00	844	2144	2157	2272	2275	2306	-	-
100-14-33-095-05w6/00	917.8	2225	2236.5	2355	2362	2387	2419	2446
100-06-35-095-05w6/00	838.5	2134	2145.8	2261	2267.7	2292.7	2324.4	2349.4
100-10-01-095-06w6/00	981.7	2359	2372	2488	2494	2523	2540	2572

UWI	KB (m)	MUSKWA (mKB)	BIILK (mKB)	CRANBERRY MEMBER (mKB)	UPPER SLAVE POINT (mKB)	LOWER SLAVE POINT (mKB)	WATT MOUNTAIN (mKB)	MUSKEG (mKB)
100-07-36-095-06w6/00	910.2	2253	2265	2381	2388	2414	2444	2470
100-07-09-096-02w6/00	691.5	1849	1865	1993	2011	2015	2059	2116
100-13-19-096-02w6/00	745	1898	1914	2045	2067	2082	2112	-
100-04-31-096-02w6/00	754.2	1901	1918	2047	2052	2080	2120	-
100-06-32-096-02w6/00	785.2	1922	1938	2069	2100	2110	2142	-
100-10-06-096-03w6/00	740.1	1968	1982.4	2106.2	2113	2126	2178.1	2224
100-07-07-096-03w6/00	747	1967	1980.5	2107	2113	2127	2177	-
100-11-10-096-03w6/00	727.3	1926	1940.5	2070	2078	2090	2138	-
100-13-15-096-03w6/00	756.9	1946	1961	2087	2100	2117	-	-
100-11-17-096-03w6/00	769	1977	1990.5	2117	2120	2149	2191	2240
100-10-18-096-03w6/00	750.5	1959	1974	2098	2099	2135	2167	-
100-02-19-096-03w6/00	780.8	1988	2002.5	2130	2133	2159	2200	2250
100-02-20-096-03w6/00	782.6	1987	2002	2129	2130	2160	2200	2248
100-05-21-096-03w6/00	782	1983	1999	2126	2128	2152	2198	-
100-06-22-096-03w6/00	765.4	1956	1971	2099	2101	2134	2172	-
100-05-23-096-03W6/00	755.1	1946	1961	2089.5	2090.5	2124	-	-
100-12-24-096-03w6/00	744.5	1912	1927	2056	2058	2087	-	-
100-10-25-096-03w6/00	768.3	1923	1939	2069	2070	2101	-	-
100-10-27-096-03w6/00	812.7	1987	2000.7	2130	2135	2163	2200.4	2249
100-07-32-096-03w6/00	909.8	2089	2106	2233	2237	2263	-	-
100-07-33-096-03w6/00	923.3	2098	2112	2242	2246	2274	2312	2357.5
100-04-36-096-03w6/00	791.9	1944	1960	2092	2094	2125	-	-
100-11-03-096-04w6/00	824.2	2078	2101.3	2211.6	2212.8	2243.9	2281	2328.7
100-06-04-096-04w6/00	867.5	2128	2140.9	2259.2	2260.4	2288.4	2332	2372
100-06-07-096-04w6/00	873.7	2149	2163.5	2286	2293.3	2318.9	2347.6	2394.5
100-08-10-096-04w6/00	797.6	2041	2055	2179	2181.5	2210	-	-
100-07-11-096-04w6/00	774.8	2002	2016	2136	2137	2172	2206	2259
100-11-12-096-04w6/00	763.8	1989	2003	2129	2131	2162	2200	2251
100-01-13-096-04w6/00	754.9	2042	2058	2196	2197	2232	2270	-
100-11-13-096-04w6/00	752.3	1973	1987	2114	2118	2147	2182	2229

UWI	KB (m)	MUSKWA (mKB)	BIILK (mKB)	CRANBERRY MEMBER (mKB)	UPPER SLAVE POINT (mKB)	LOWER SLAVE POINT (mKB)	WATT MOUNTAIN (mKB)	MUSKEG (mKB)
100-03-14-096-04w6/00	787	2024	2038	2163.5	2171	2197	2232	2278
100-11-17-096-04w6/00	814.1	2073	2087.9	2210.4	2217.1	2245	2274.4	2325.6
100-11-18-096-04w6/00	849.7	2125	2140	2262	2270	2297	2333	2378
100-10-19-096-04w6/00	870.9	2131	2142.7	2265.9	2272	2305	2339.7	2384.8
100-11-20-096-04w6/00	825.1	2075	2088.5	2211.6	2217	2249	2277.5	2337.5
100-06-22-096-04w6/00	770.1	2003	2018	2141	2147.5	2177	2206	2261
100-05-23-096-04w6/00	755.1	-	1962	2090	2091	2117	2159	-
100-07-25-096-04w6/00	828.8	2032	2047	2174.4	2179.3	2210	2245	2287.8
100-11-27-096-04w6/00	789.4	2016	2031	2155	2161	2191	2239	2273
100-06-28-096-04w6/00	865.6	2102	2117.8	2241.5	2248.2	2276	2312	2363
100-06-29-096-04w6/00	865.7	2109	2149	2249	2256	2284	2332	2363
100-10-31-096-04w6/00	871.3	2114	2128	2255	2259	2290	-	-
100-11-33-096-04w6/00	803.7	2027	2040	2167	2170	2199	2252	2287
100-11-34-096-04w6/00	798.3	2006	2020.8	2146.4	2148.8	2178.9	2219	-
100-10-35-096-04w6/00	820.8	2024	2039	2165	2173	2199	2237	-
100-03-01-096-05w6/00	928.7	2207	2221	2337	2344	2368	2400	2442
100-08-01-096-05w6/00	911.9	2220	-	2355	2358	-	-	-
100-06-05-096-05w6/00	933.6	2244	2255.5	2375.6	2382.9	2407.3	2438.4	2468.3
100-06-10-096-05w6/00	950.9	2252	2266	2387	2395	2420	2450	2488
100-11-14-096-05w6/00	944.3	2222	2235.4	2357.3	2364	2395	2426.2	2475
100-10-15-096-05w6/00	943.1	2225	2237	2359	2365	2392	2423	2455
100-10-16-096-05w6/00	923	2217	2229	2350	2352	2383	2415	2453
100-11-18-096-05w6/00	978.5	2293	2305	2424	2425	2460	2491	2520
100-09-19-096-05w6/00	932.8	2236	2249	2365	2366	2394	2439	2486
100-10-24-096-05w6/00	885.6	2155	2171	2292	2299	2331	2365	2407
100-11-25-096-05w6/00	926	2174	2187	2310.5	2314	2349	2374	2430
100-06-26-096-05w6/00	961.9	2240	2254	2377	2380	2417	2454	-
100-06-27-096-05w6/00	946.1	2240	2254	2378	2381	2421	2456	2494
100-01-28-096-05w6/00	956.2	2232	2245.2	2364.6	2365.2	2407	2429	2473.8
100-07-29-096-05w6/00	973.4	2254	2271	2389	2390	2410	2462	2497

UWI	KB (m)	MUSKWA (mKB)	BHLK (mKB)	CRANBERRY MEMBER (mKB)	UPPER SLAVE POINT (mKB)	LOWER SLAVE POINT (mKB)	WATT MOUNTAIN (mKB)	MUSKEG (mKB)
100-07-33-096-05w6/00	935.1	2203	2217	2337.5	2338	2365	2422	-
100-11-35-096-05w6/00	883.6	2134	2148	2273	2275	2297	2345	2398
100-10-36-096-05w6/00	869.9	2118	2132	2256	2259	2294	-	-
100-11-26-096-06w6/00	924.2	-	-	2372	-	2399	-	-
100-06-06-097-02w6/00	786.7	1918	1934	2063	2065	2099	2152	-
100-08-08-097-02w6/00	767.3	1885	1901	2034	-	2062	2121	2164
100-12-20-097-02w6/00	778.5	1886	1903	2034.2	2038	2053	2121	2133
100-06-01-097-03W6/00	825.4	1969	1980	2116	2117	2157	2192	-
100-03-02-097-03w6/00	889.9	2038	2054	2186	2190	2225	-	-
100-10-03-097-03w6/00	873.6	2025	2041	2173	2178	2206	-	-
100-10-07-097-03w6/00	941.5	2119	2134	2263	2265	2299	2351	2384
100-11-08-097-03w6/00	914.4	2078	2093.4	2223	2225	2260	2308	2331.7
100-06-09-097-03w6/00	906.5	2063	2078.1	2207	2210.4	2243.3	2293	-
100-07-10-097-03w6/00	845.7	1987	2004	2134	2136	2170	-	-
100-02-11-097-03w6/00	835.5	1978	1994	2124	2125	2160	2211	2245
100-04-12-097-03w6/00	851.2	1986	2003	2130	2132	2169	2222	-
100-10-12-097-03w6/00	798.5	1929	1945	2076	2100	2107	2165	2203
100-07-15-097-03w6/00	838.8	-	-	2122	2156	2163.5	2201.3	-
100-04-18-097-03w6/00	946.3	2118	2133	2260	2261	2286	2353	2382
100-06-31-097-03w6/00	846.1	2001	2016	2144	2146	2175	2240.3	2269
100-10-01-097-04w6/00	885.8	2072	2087	2215.5	2217	2231	-	-
100-10-02-097-04w6/00	858.6	2054	2068	2197	2199	2231	-	-
100-15-03-097-04w6/00	830	2028	2043	2170	2172	2205	-	-
100-10-04-097-04w6/00	813.7	2020	2035	2164	2167	2201	-	-
100-07-05-097-04w6/00	812.7	2039	2053	2174.5	2176.5	2221	-	-
100-10-07-097-04w6/00	837.8	2066	2080.5	2207	2224	2234	-	-
100-07-08-097-04w6/00	828.5	2049	2063.5	2190	2192	2211	2283.6	2312.8
100-01-09-097-04w6/00	830.3	2032	2047	2176	2178	2217	-	-
100-10-10-097-04w6/00	842.5	2039	2069.3	2183	2184.5	2220.8	2272.6	2301.9
100-07-11-097-04w6/00	863.1	2052	2067	2195	2197	2231	2282	2313

UWI	KB (m)	MUSKWA (mKB)	BIHLK (mKB)	CRANBERRY MEMBER (mKB)	UPPER SLAVE POINT (mKB)	LOWER SLAVE POINT (mKB)	WATT MOUNTAIN (mKB)	MUSKEG (mKB)
100-06-12-097-04w6/00	883.5	2069	2085	2214	2216	2250	2301	2330
100-01-13-097-04w6/00	951.5	2122.2	2138	2265	2266	2307	-	-
100-01-16-097-04w6/00	860.6	2057	2071	2200	2220	2238	2285	2320
100-07-24-097-04w6/00	953	2120	2135	2264	2286	2296	2357	2386
100-02-01-097-05w6/00	846.6	2089	2104	2229	2231	2255	-	-
100-10-01-097-05w6/00	846.6	2088	2103.1	2228	2229	2256	2324	2353.1
100-11-04-097-05w6/00	890	2146	2159	2281	2304	2313	2373	2409
100-11-04-097-06w6/00	812.6	2127	2136.7	2257.3	2280	2289	2335	2361.6
100-11-07-097-06w6/00	703.5	2021	2032.4	2151.3	2153.1	2184	-	-
100-10-12-097-06w6/00	792.5	2074	2086.1	2208	2237	2240	2299	2318.9
100-11-17-097-06w6/00	717.5	2016	2026.9	2147.6	2149.1	2173.2	2237	2252.5
100-11-18-097-06w6/00	696.8	2005	2015.4	2133.6	2136.3	2171	2220	2234.2
100-01-19-097-06w6/00	701.8	1998	2010	2130	2132	2156	-	-
100-06-20-097-06w6/00	701.8	2001	2010	2132	2134	2166	2216	2235
100-06-34-097-06w6/00	682.4	-	-	2087.3	2089.7	2112.9	2172.6	2203.1

APPENDIX B

Stratigraphic Cross Sections

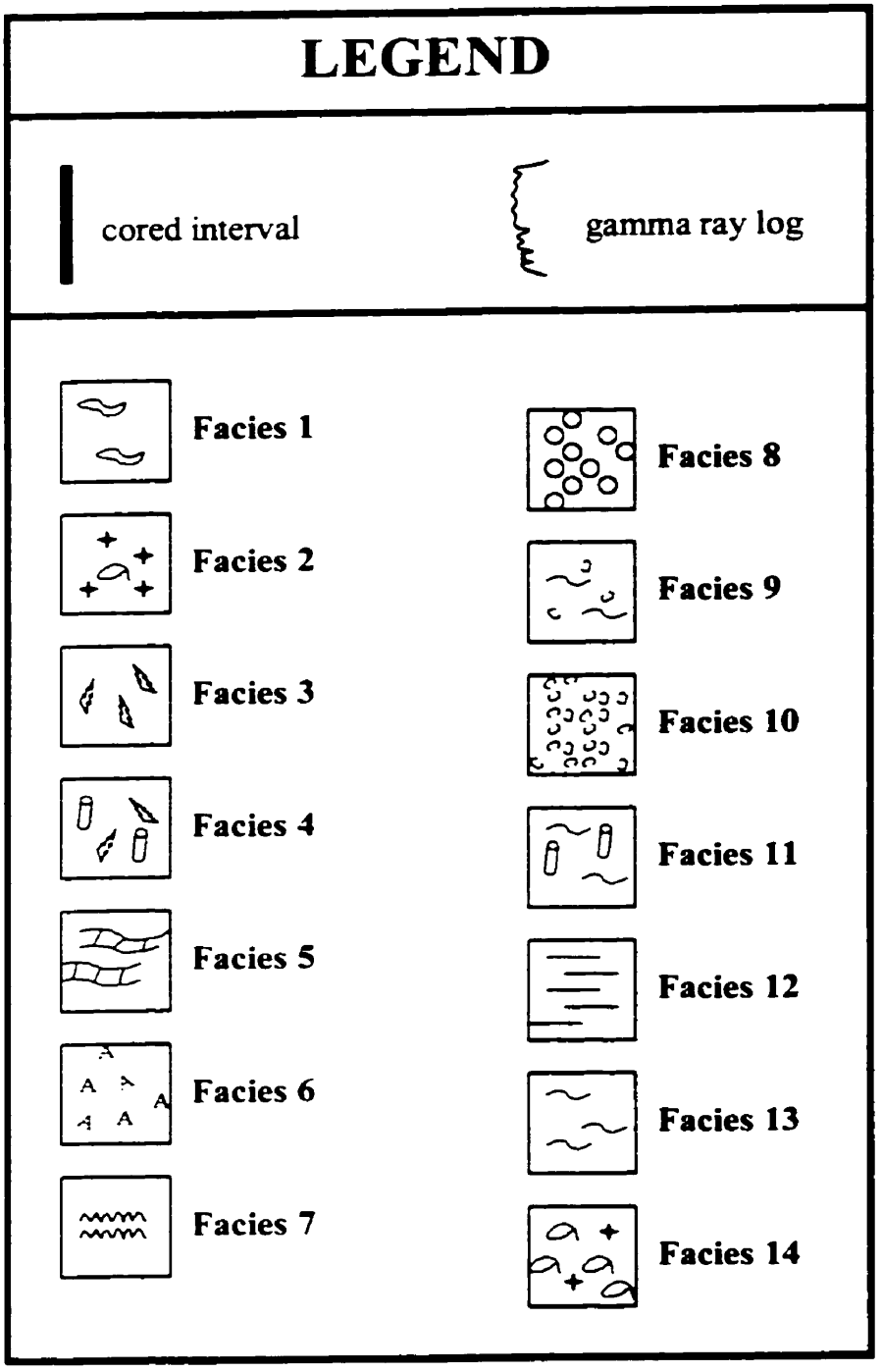
LEGEND
cored interval
gamma ray log
Facies 1
Facies 2
Facies 3
Facies 4
Facies 5
Facies 6
Facies 7
Facies 8
Facies 9
Facies 10
Facies 11
Facies 12
Facies 13
Facies 14

A

STRATIGRAPHIC CROSS-SECTION

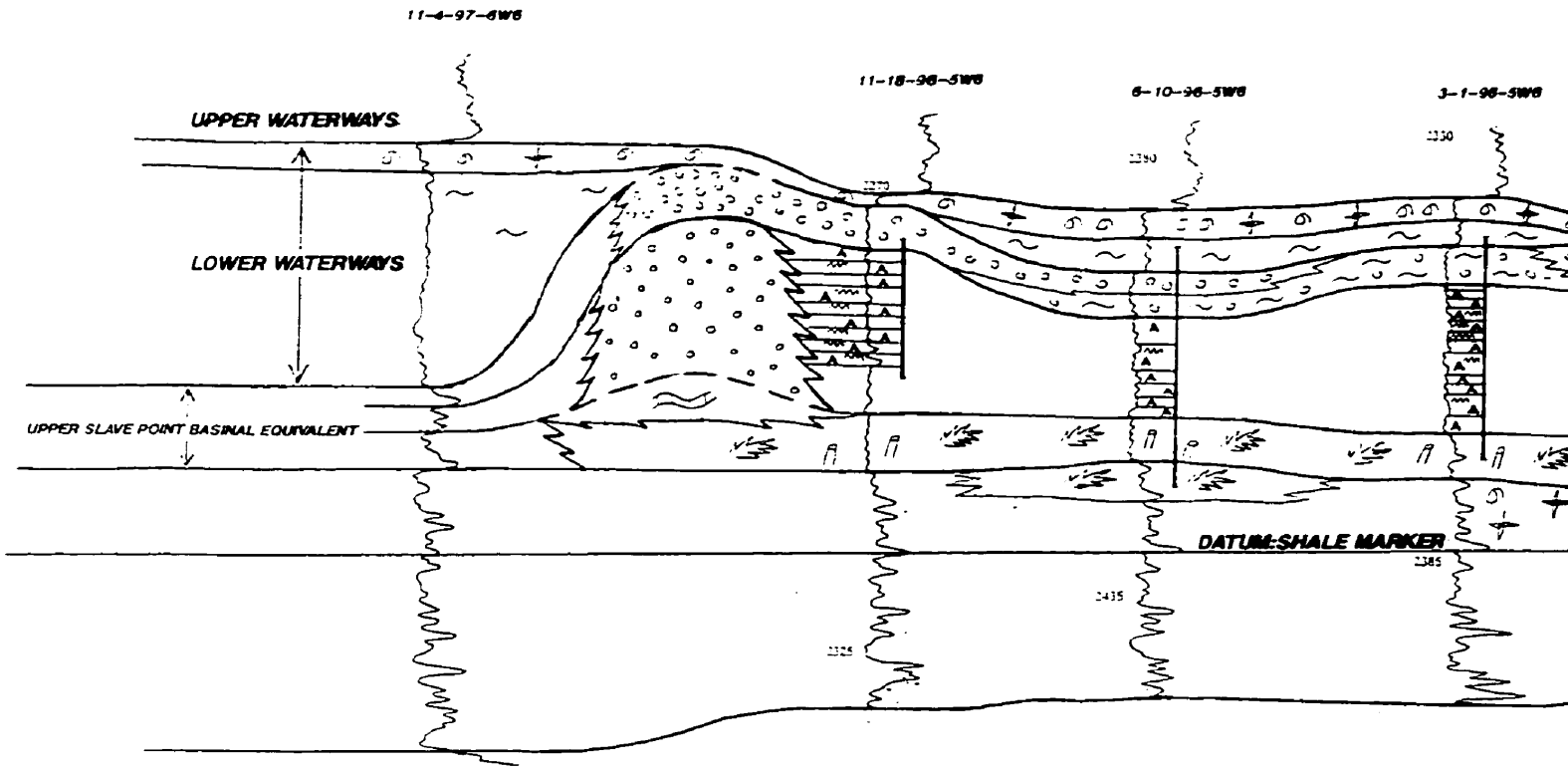

STRATIGRAPHIC CROSS–SECTION

A'

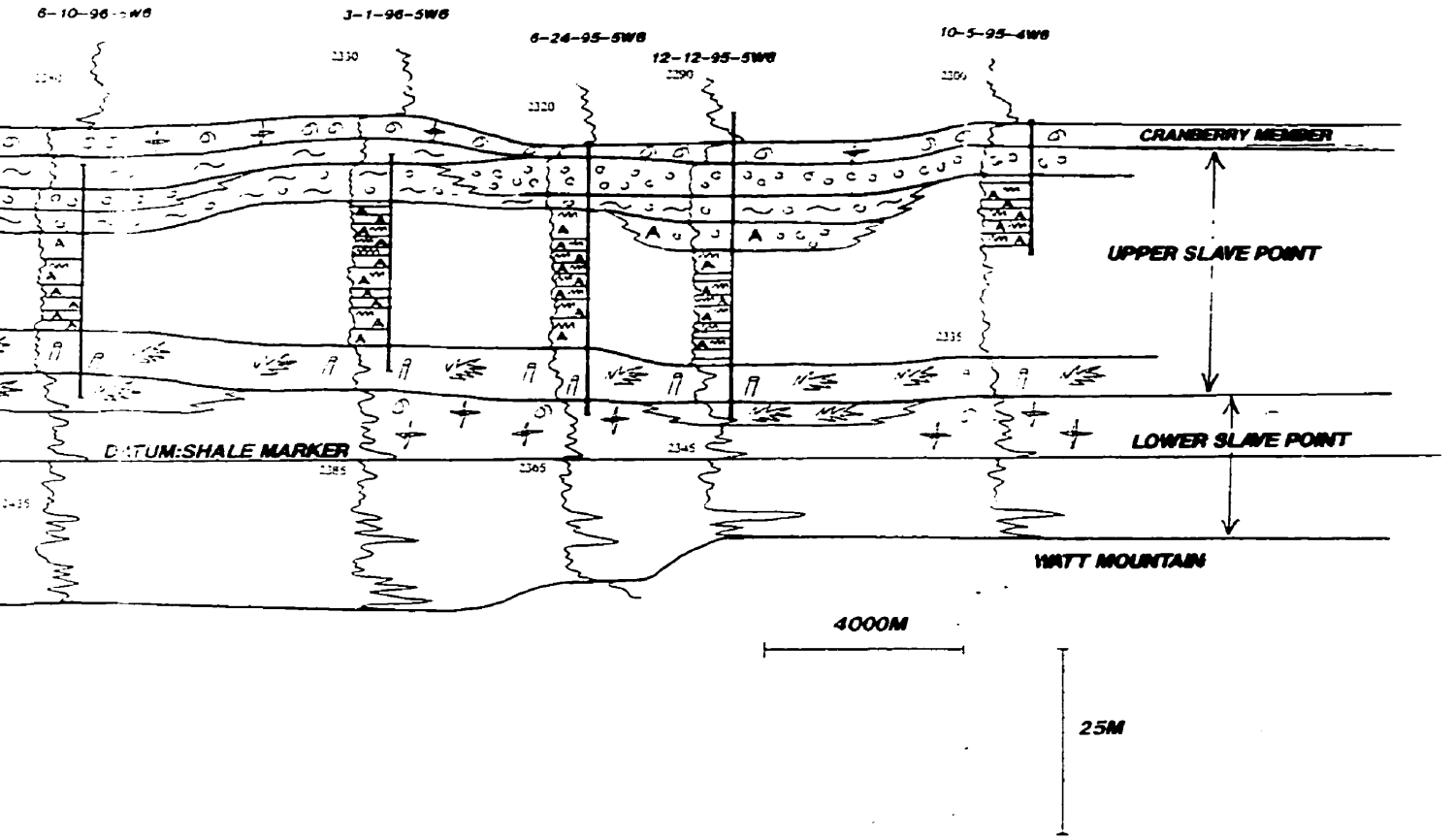

B

STRATIGRAPHIC CROSS-SECTION

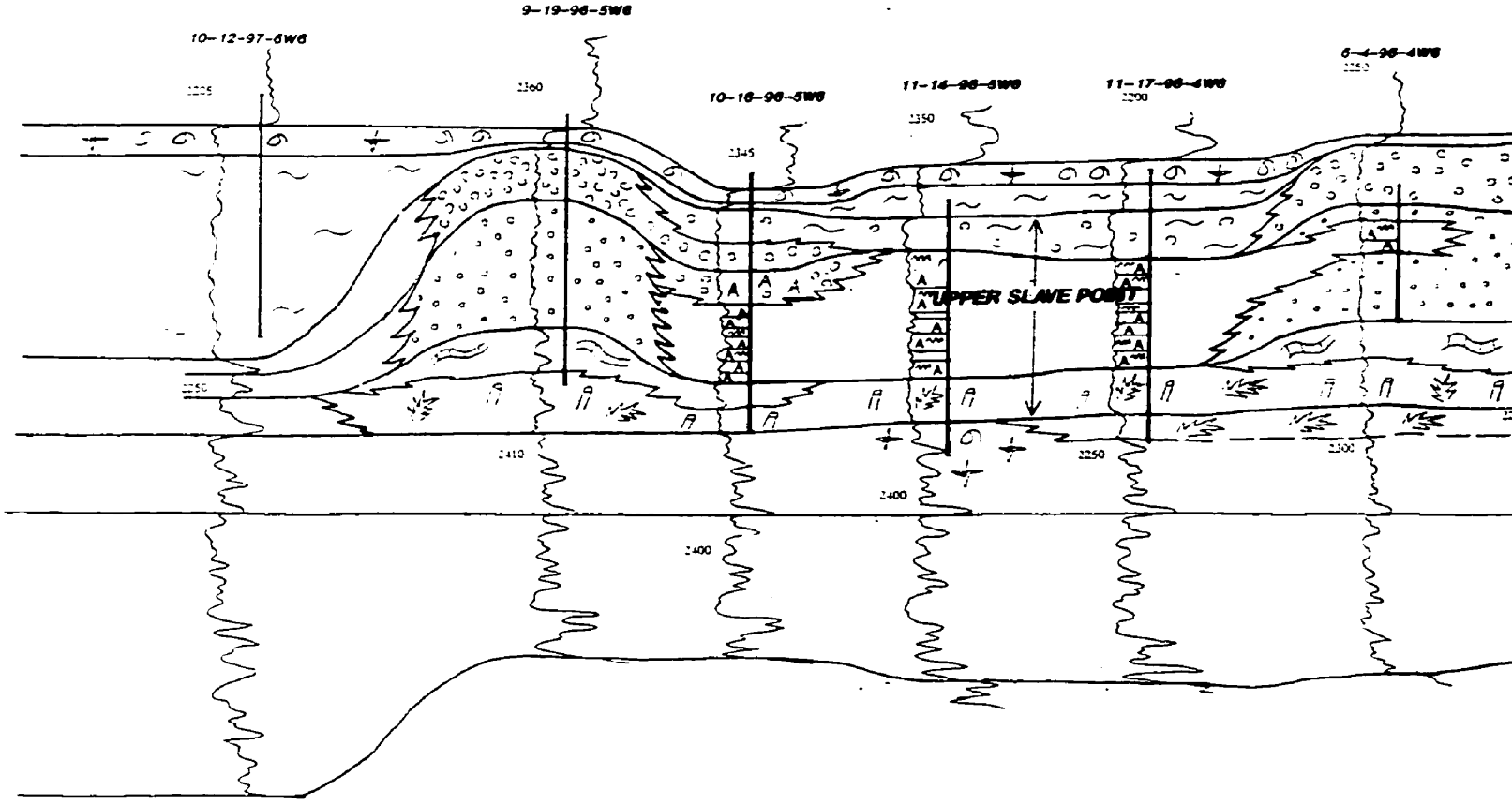

B'

-SECTION

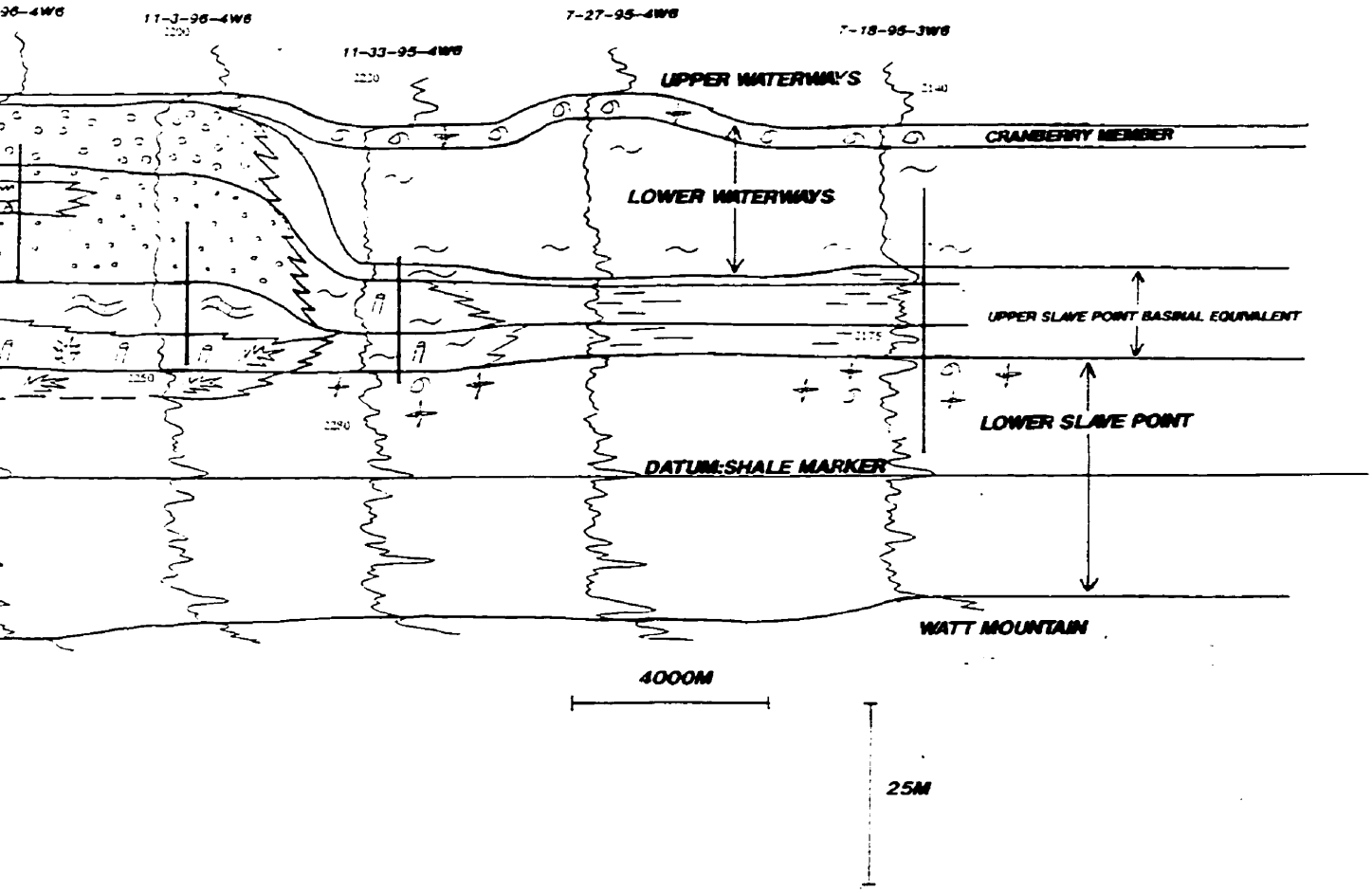
96-4W6
11-3-96-4W6
11-33-95-4W6
7-27-95-4W6
7-18-95-3W6
UPPER WATERWAYS
CRANBERRY MEMBER
LOWER WATERWAYS
UPPER SLAVE POINT BASINAL EQUIVALENT
LOWER SLAVE POINT
DATUM:SHALE MARKER
WATT MOUNTAIN
4000M
25M

STRATIGRAPHIC CROSS–SECTION

C

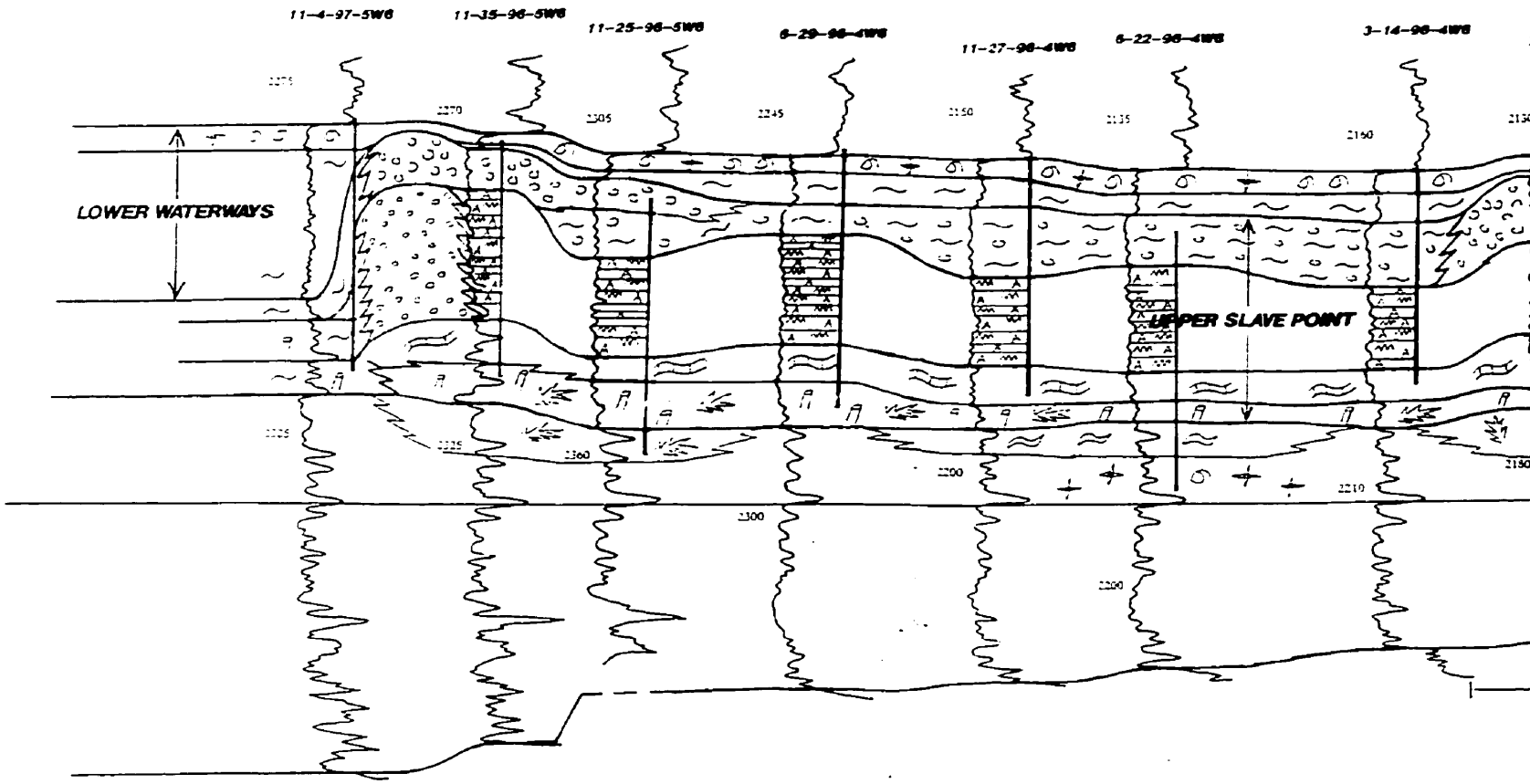

APHIC CROSS–SECTION

C'

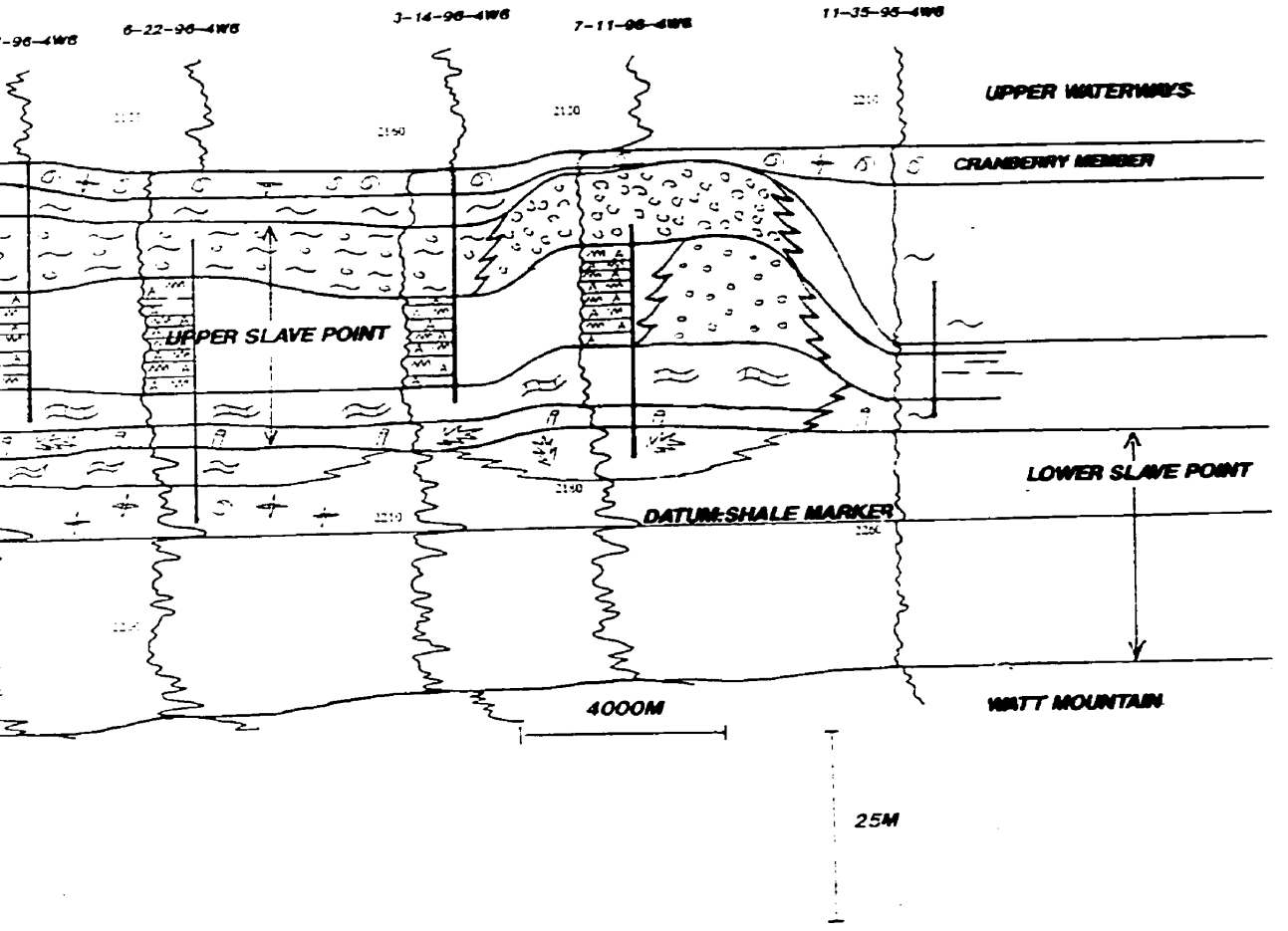

STRATIGRAPHIC CROSS-SECTION

D

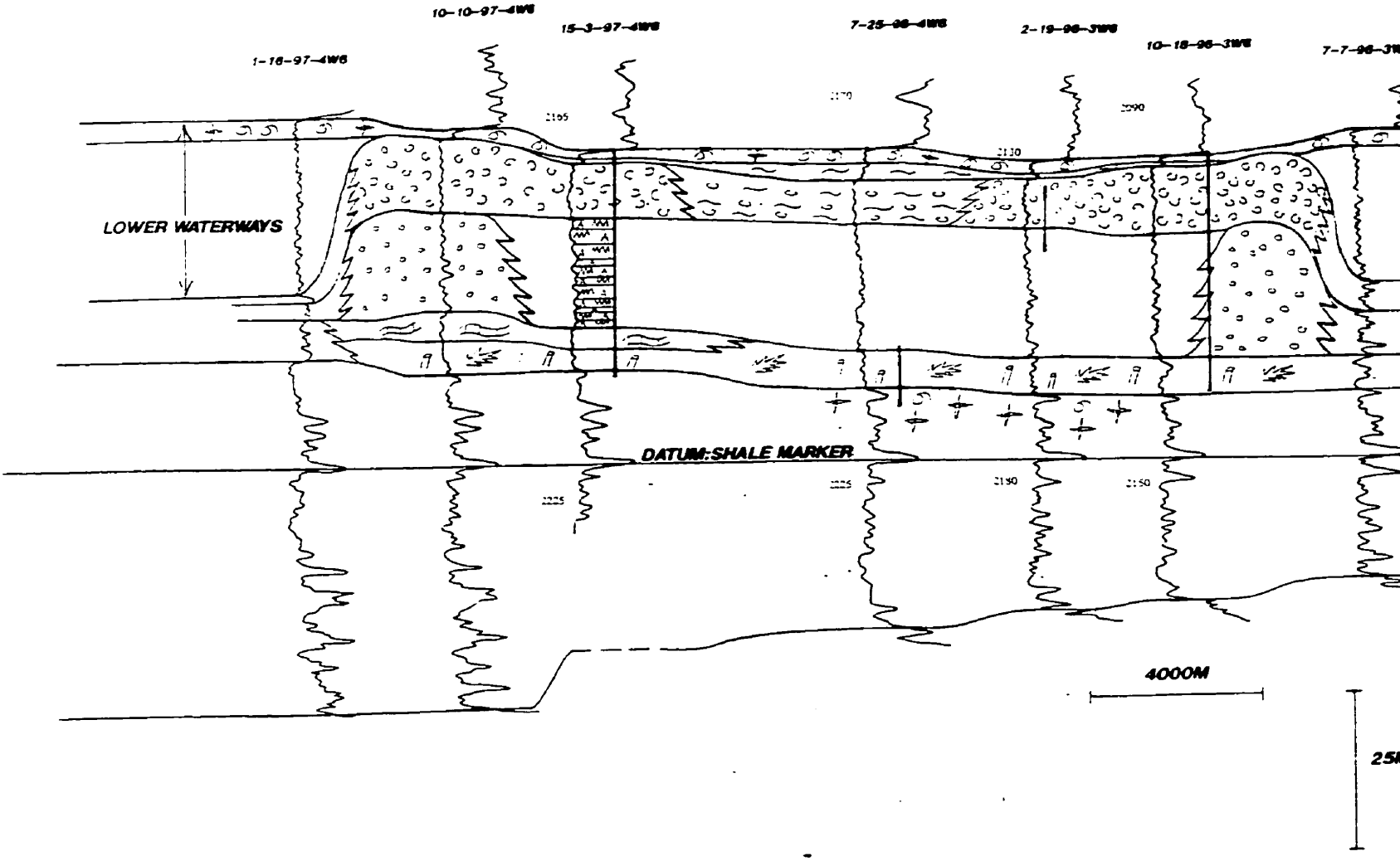

RAPHIC CROSS-SECTION

D'

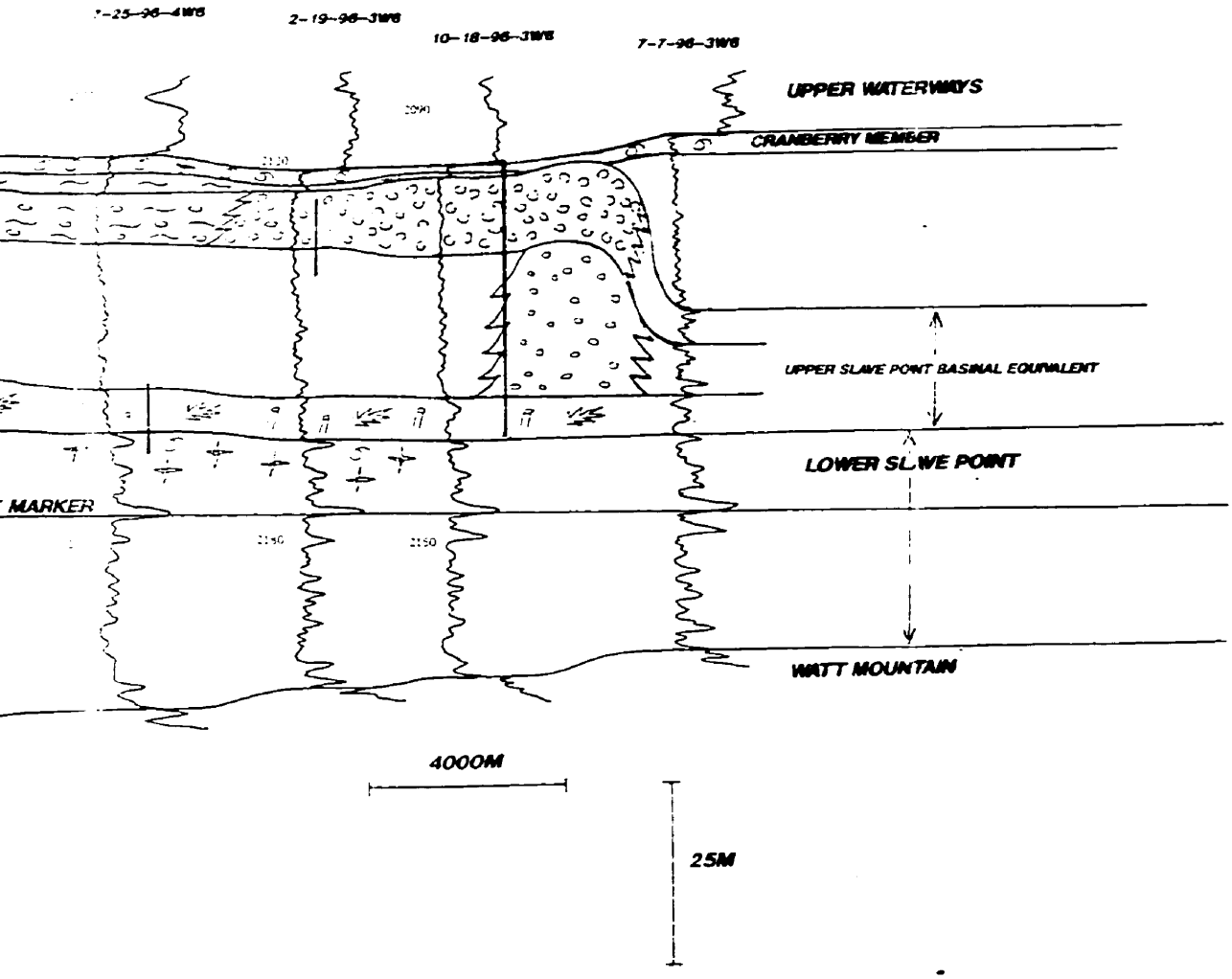

STRATIGRAPHIC CROSS-SECTION

E

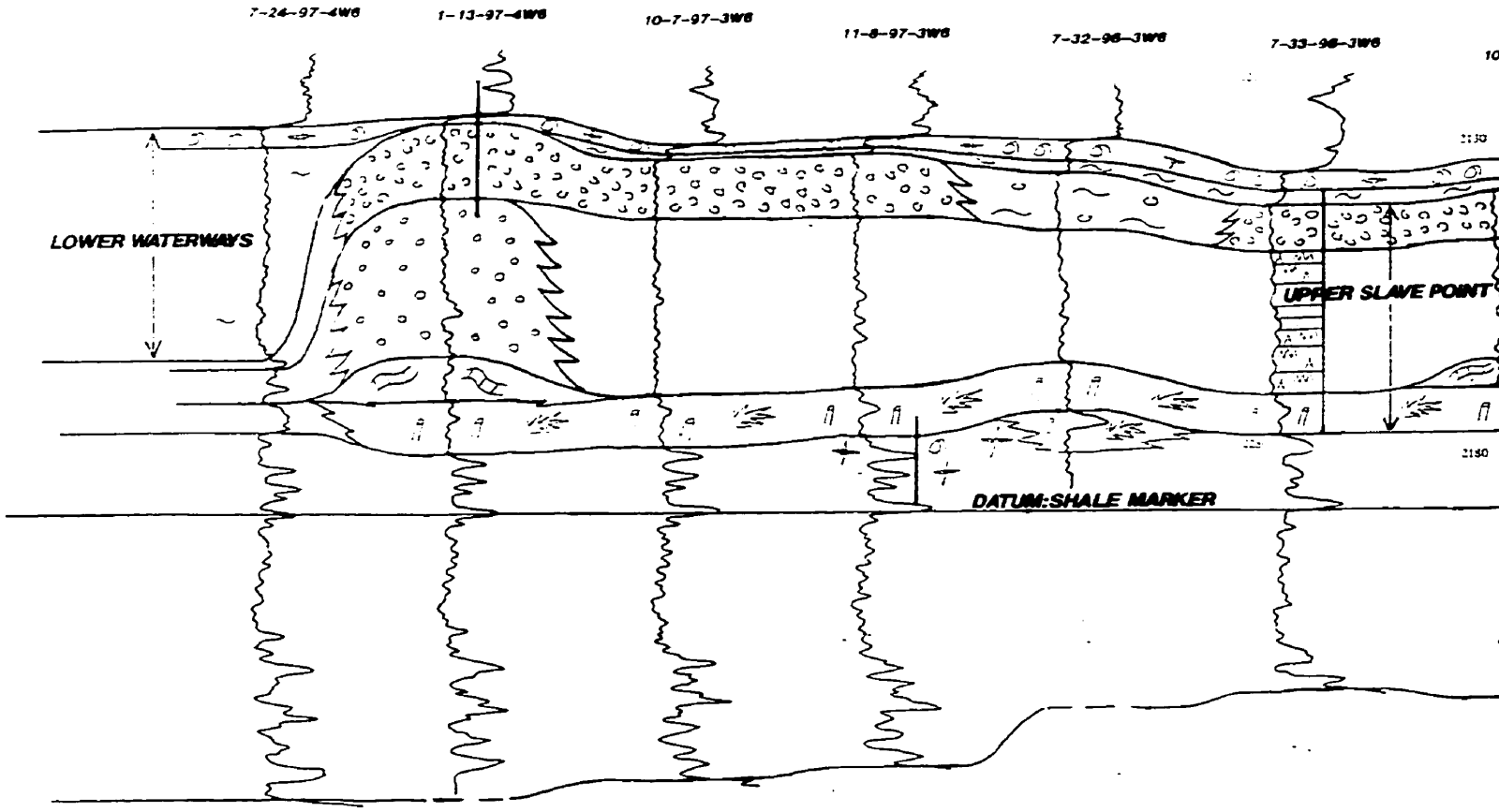

C CROSS-SECTION

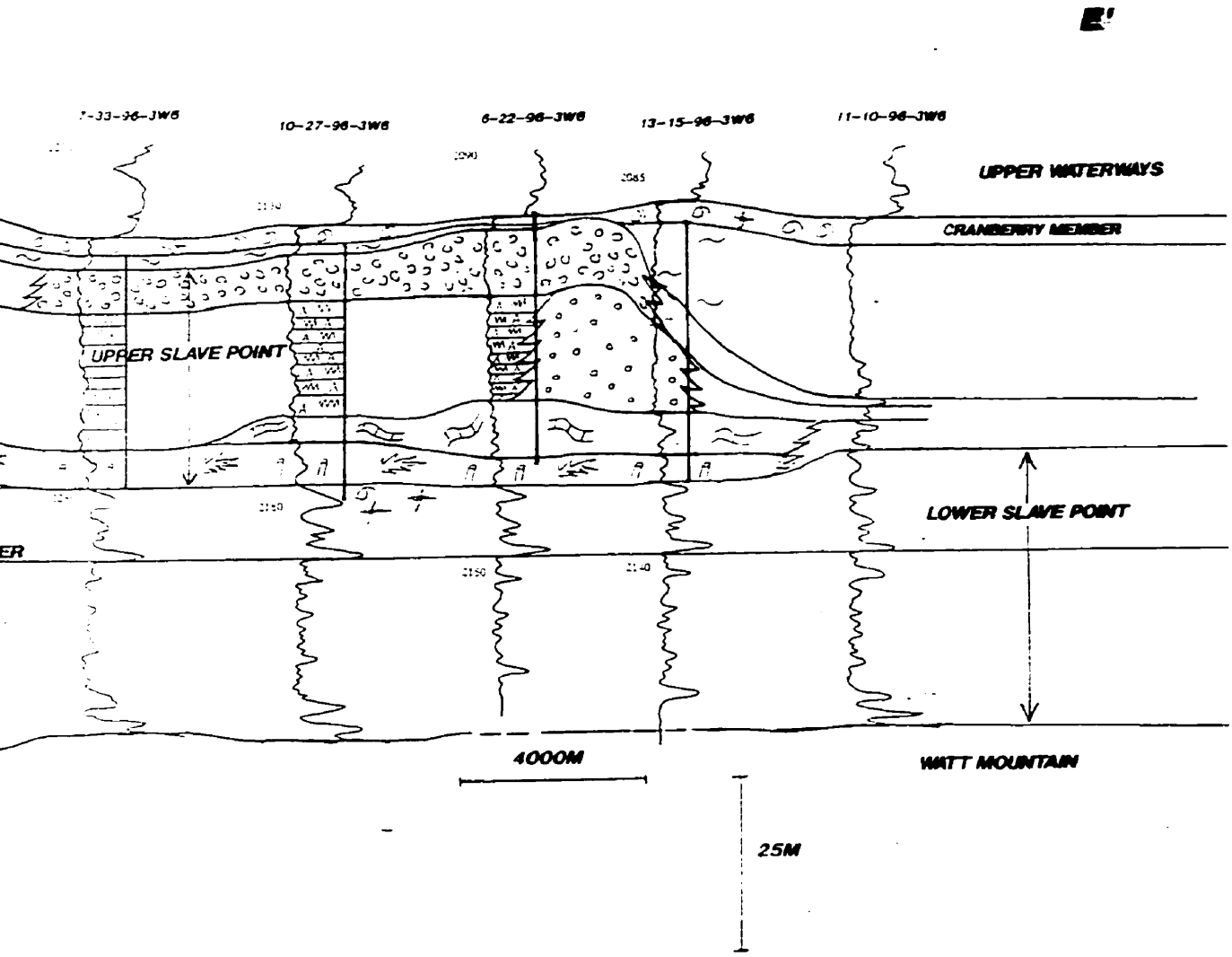

STRATIGRAPHIC CROSS-SECTION

F

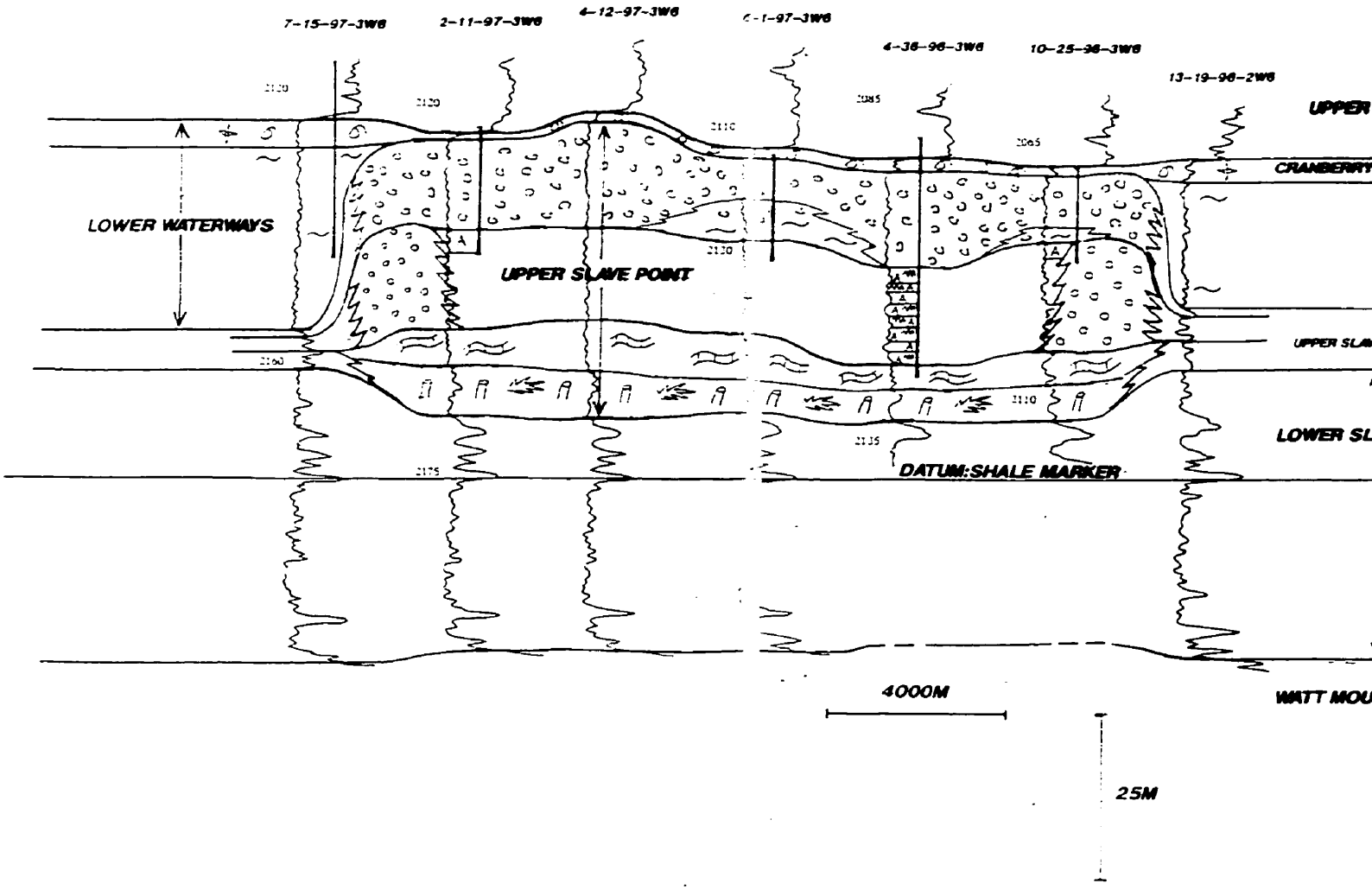

GRAPHIC CROSS-SECTION

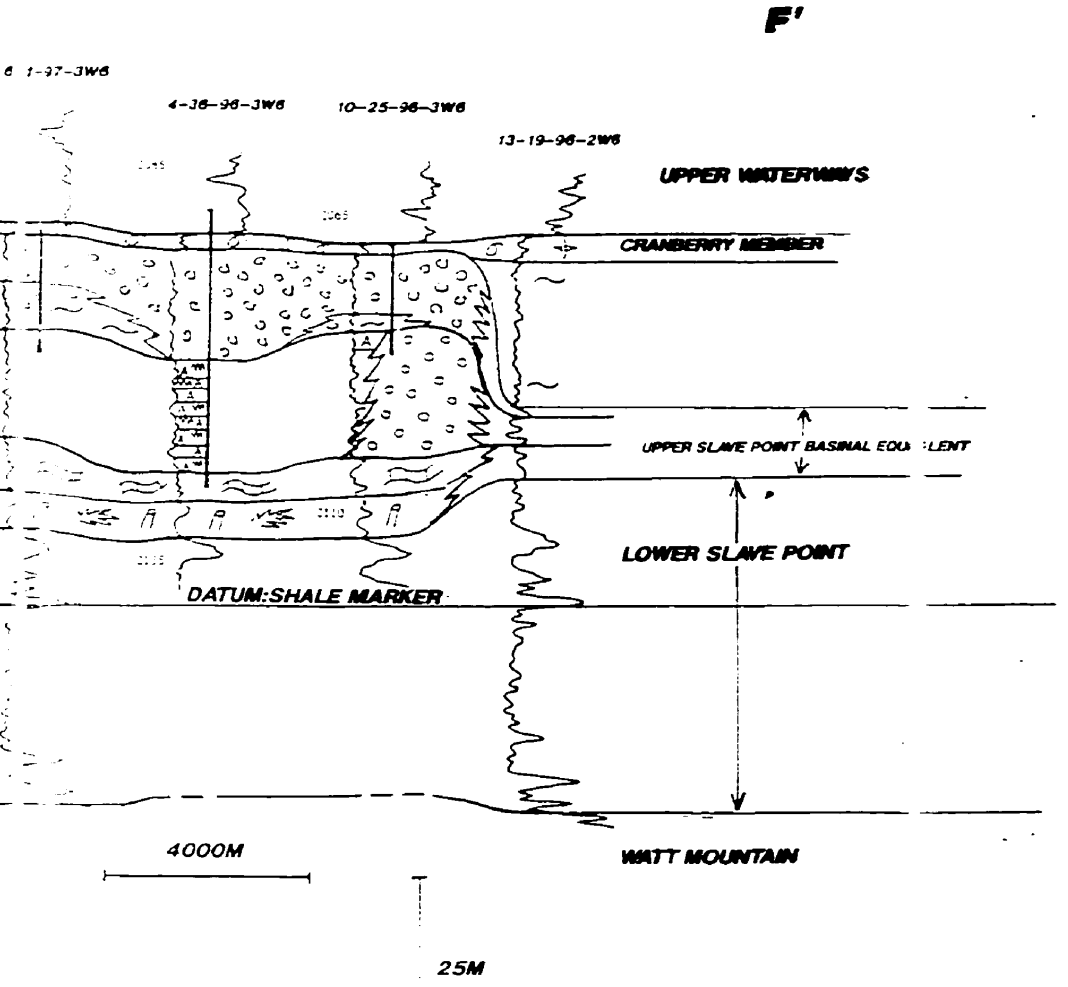

STRATIGRAPHIC CROSS-SECTION

G

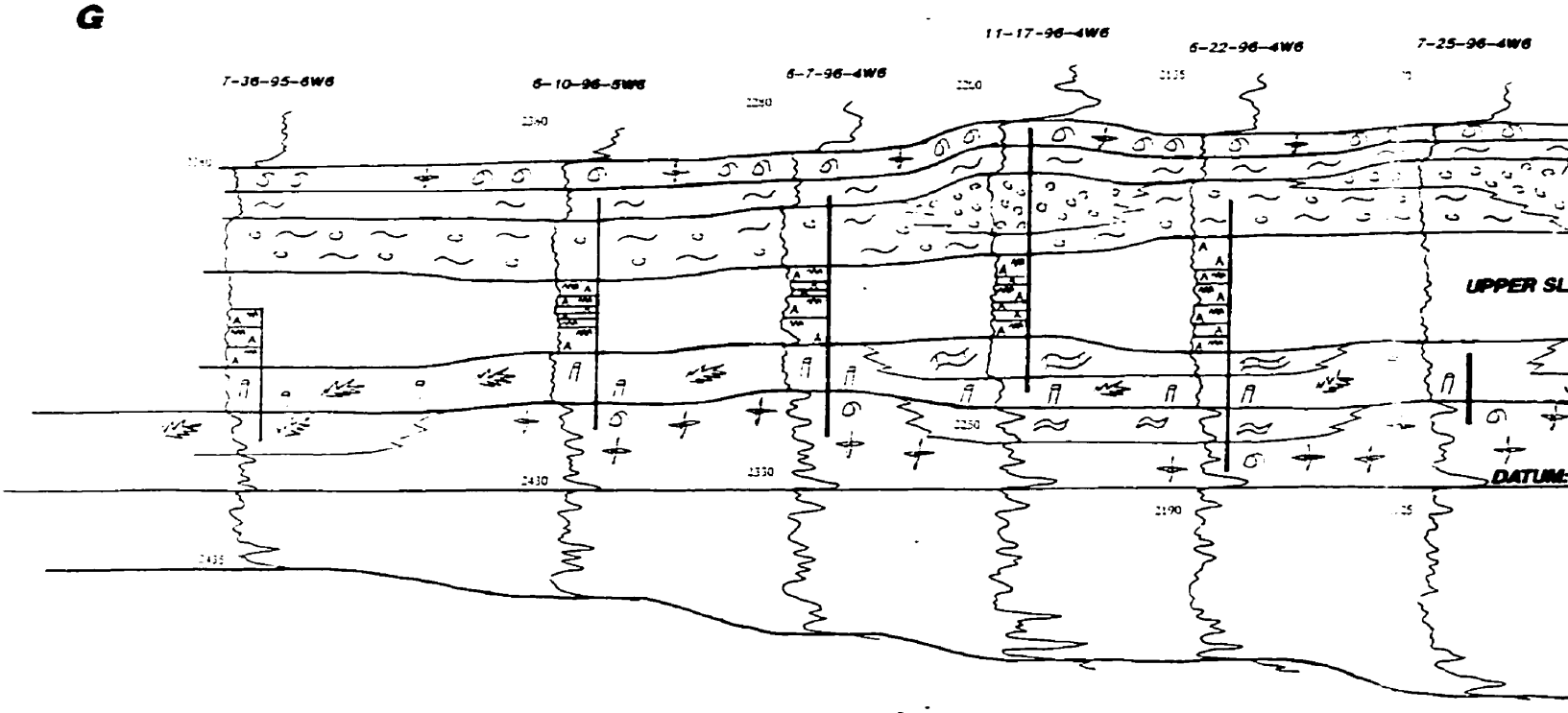

S-SECTION

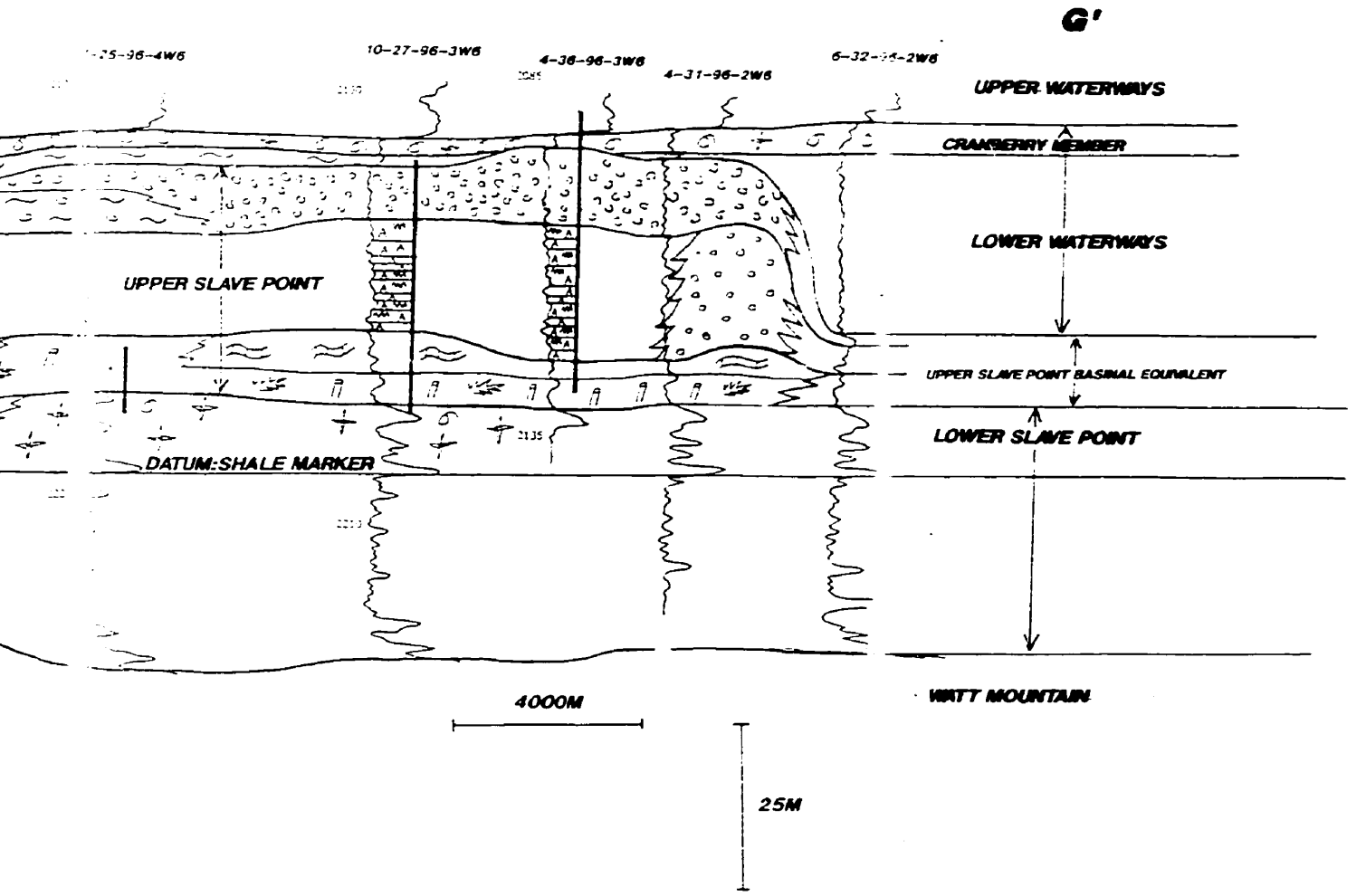
G'
10-27-96-3W6
4-36-96-3W6
4-31-96-2W6
UPPER WATERWAYS
CRANBERRY MEMBER
LOWER WATERWAYS
UPPER SLAVE POINT
UPPER SLAVE POINT BASINAL EQUIVALENT
LOWER SLAVE POINT
DATUM:SHALE MARKER
WATT MOUNTAIN
4000M
25M

APPENDIX C

Core Descriptions

LEGEND

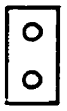
Perforated Interval

B.D. (Bioclastic Debris)

Encrustor


Stachyodes


Crinoid

Amphipora


Brachiopod


Bulbous
Stromatoporoid


Gastropod


Tabular
Stromatoporoid


Pelecypod

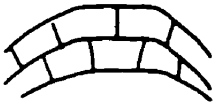
Hemispherical
Stromatoporoid


Thamnopora


Nodular
Stromatoporoid


Tidal Laminite

A - Abundant (>60%)

VC - Very Common (40-60%)

C - Common (20-40%)

P - Present (10-20%)

R - Rare (<10%)

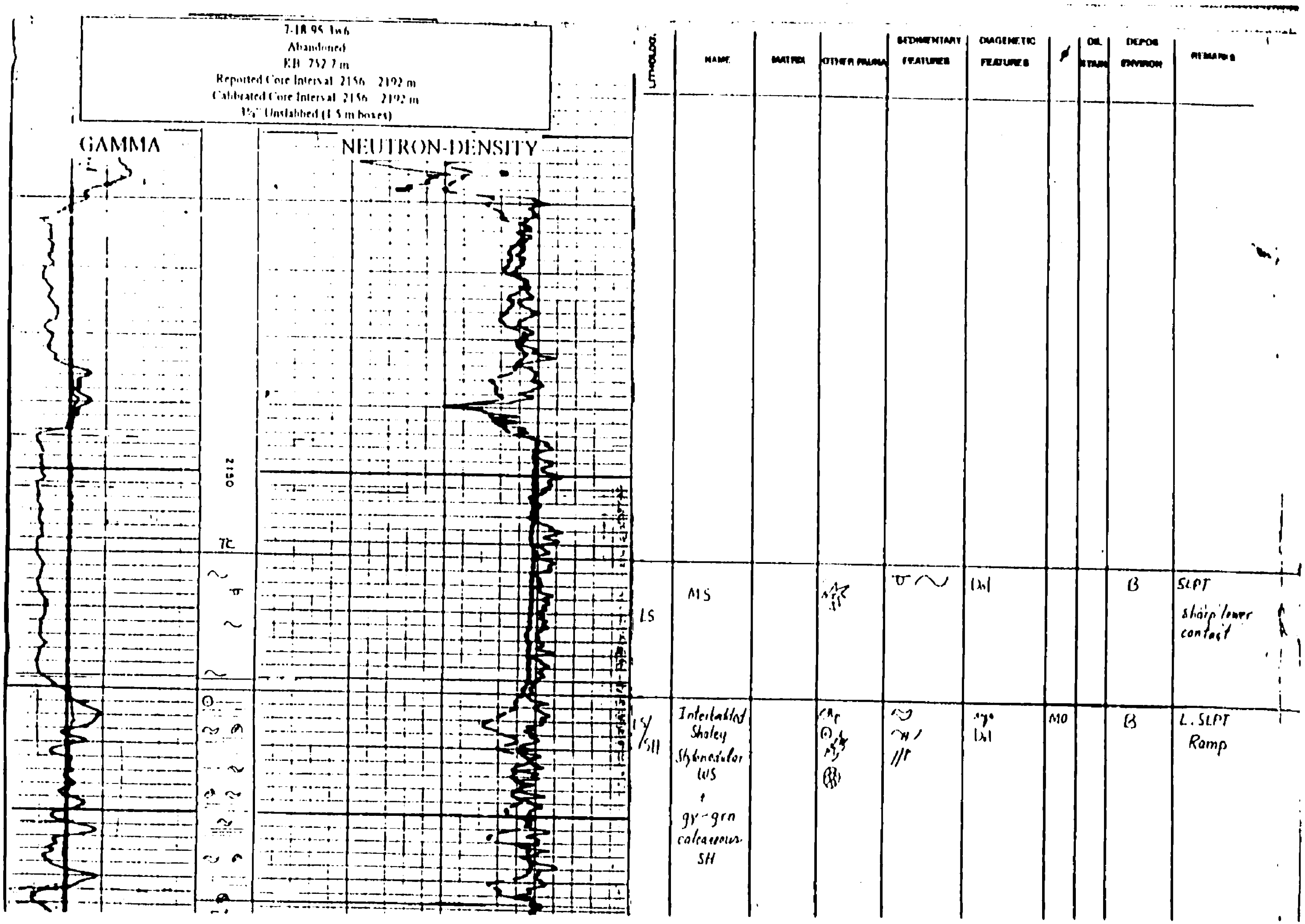

7-18-95-1w6
Abandoned
KB 752.7 m
Reported Core Interval 2156 - 2192 m
Calibrated Core Interval 2156 - 2192 m
1½" Unslabbed (1.5 m boxes)
GAMMA
NEUTRON-DENSITY
2150
LITHOLOG.
NAME
MATRIX
OTHER FAUNA
SEDIMENTARY FEATURES
DIAGENETIC FEATURES
OIL STAIN
DEPOS ENVIRON
REMARKS
LS
MS
B
SLPT
sharp lower contact
Interbedded Shaley Skeletal WS
+
gy-grn calcareous SH
MO
B
L. SLPT
Ramp

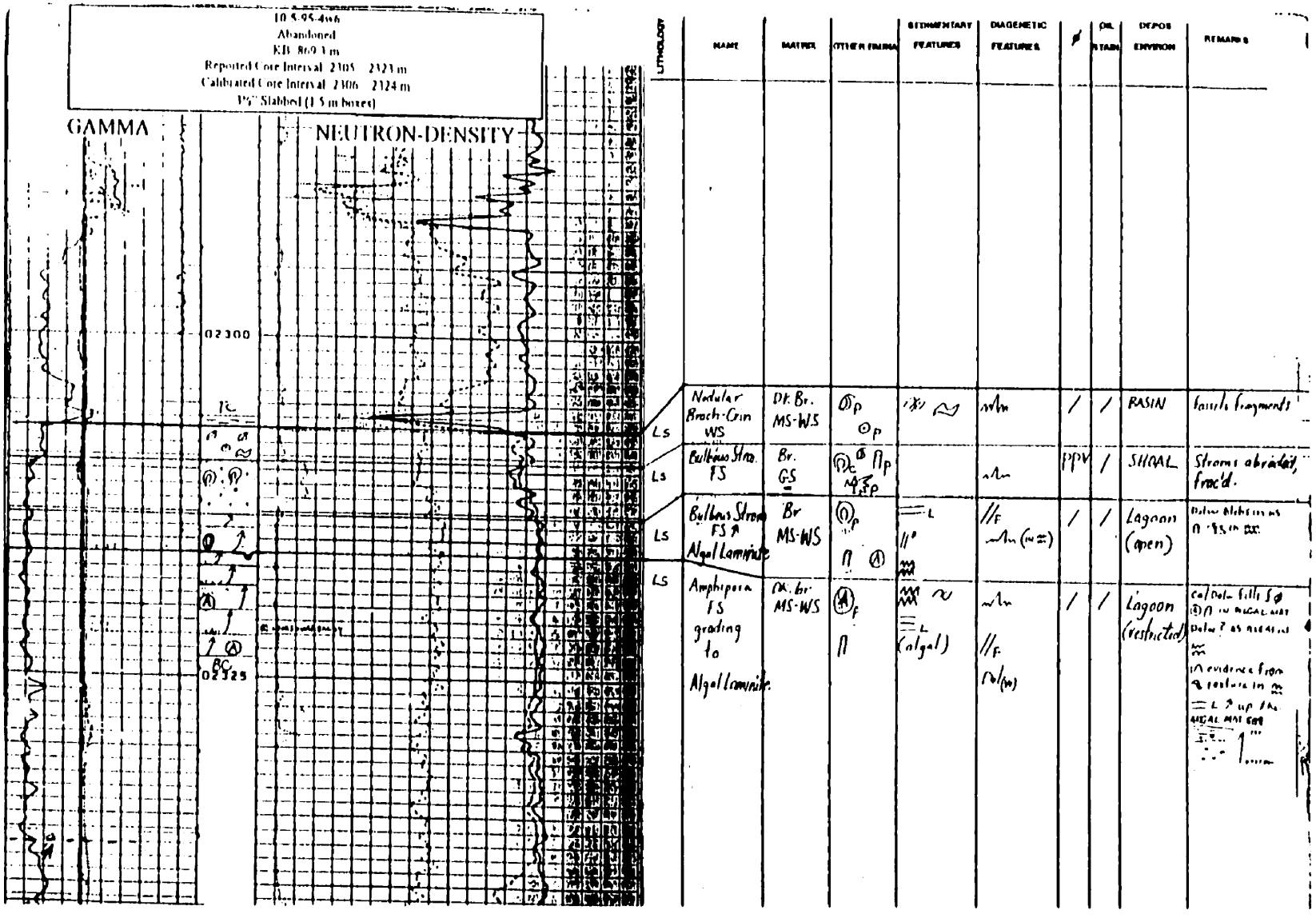
10 5-95-4wb
Abandoned
KB 869.3 m
Reported Core Interval 2305 2323 m
Calibrated Core Interval 2306 2324 m
3½" Slabbed (1.5 m boxes)
GAMMA
NEUTRON-DENSITY
02300
TC
BC
02325
LITHOLOGY
NAME
MATRIX
OTHER FRAMA
SEDIMENTARY FEATURES
DIAGENETIC FEATURES
OIL STAIN
DEPOS ENVIRON
REMARKS
Nodular Brach-Crin WS
Dk. Br. MS-WS
LS
FAIRLY fragments
Bulbous Strom. FS
Br. GS
LS
PPV
SHOAL
Stroms abraded, frac'd.
Bulbous Strom FS ↑ Algal Laminite
Br MS-WS
LS
Lagoon (open)
Amphipora FS grading to Algal Laminite
Dk. br MS-WS
LS
Lagoon (restricted)

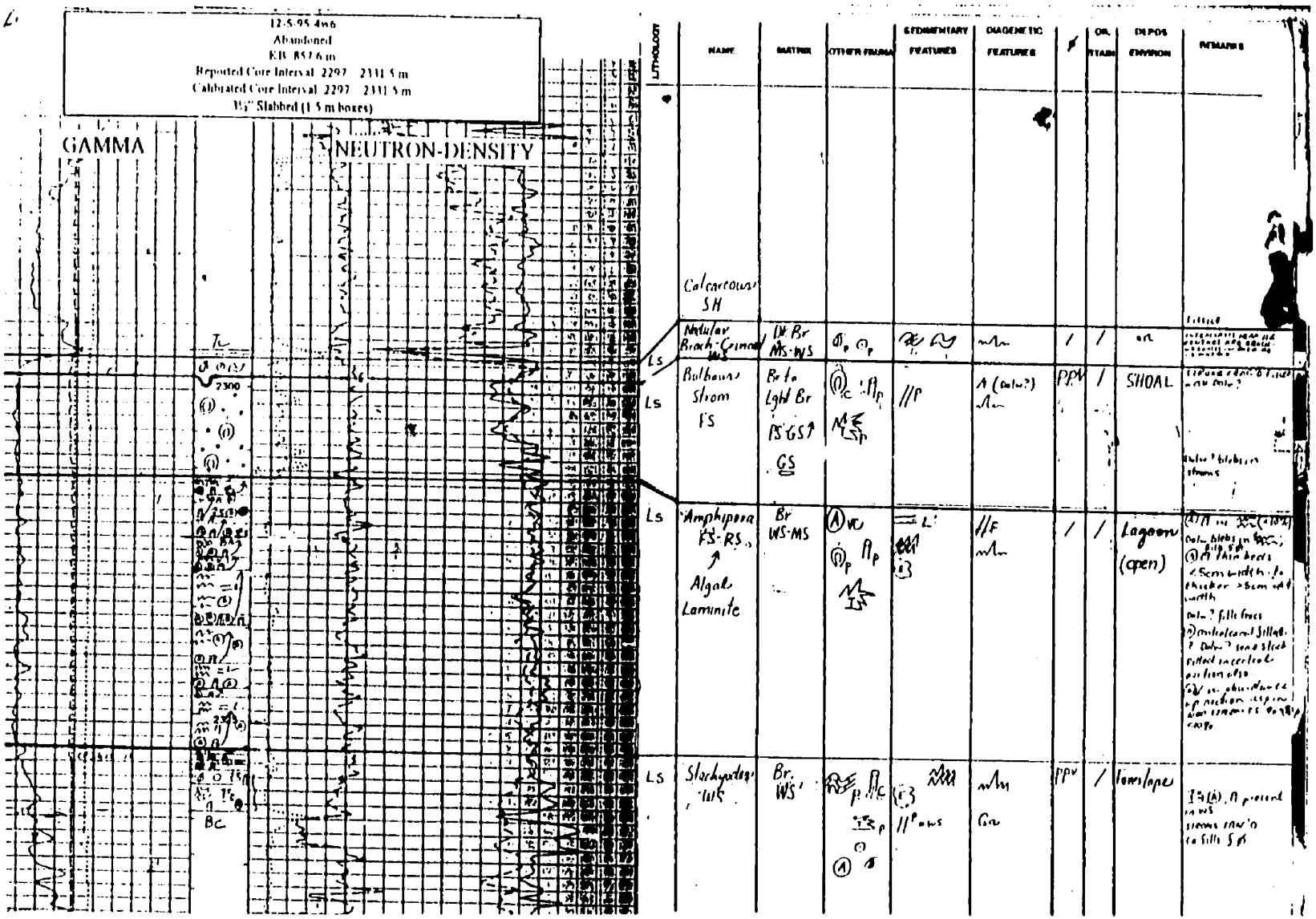
12-5-95 4m6
Abandoned
KB 85.7 m
Reported Core Interval 2297 - 2331.5 m
Calibrated Core Interval 2297 - 2331.5 m
3½" Slabbed (1.5 m boxes)
GAMMA
NEUTRON-DENSITY
LITHOLOGY
NAME
MATRIX
OTHER FAUNA
SEDIMENTARY FEATURES
DIAGENETIC FEATURES
POR
OIL STAIN
DEPOS ENVIRON
REMARKS
Calcareous SH
Nodular Brach-Grnst WS
LW Br MS-WS
Ls
Bulbous Strom FS
Br to Lght Br PS GS
Ls
Amphipora FS-RS
Algal Laminite
Br WS-MS
Lagoon (open)
Ls
Stachyodes WS
Br. WS
Bc
Tc
2300

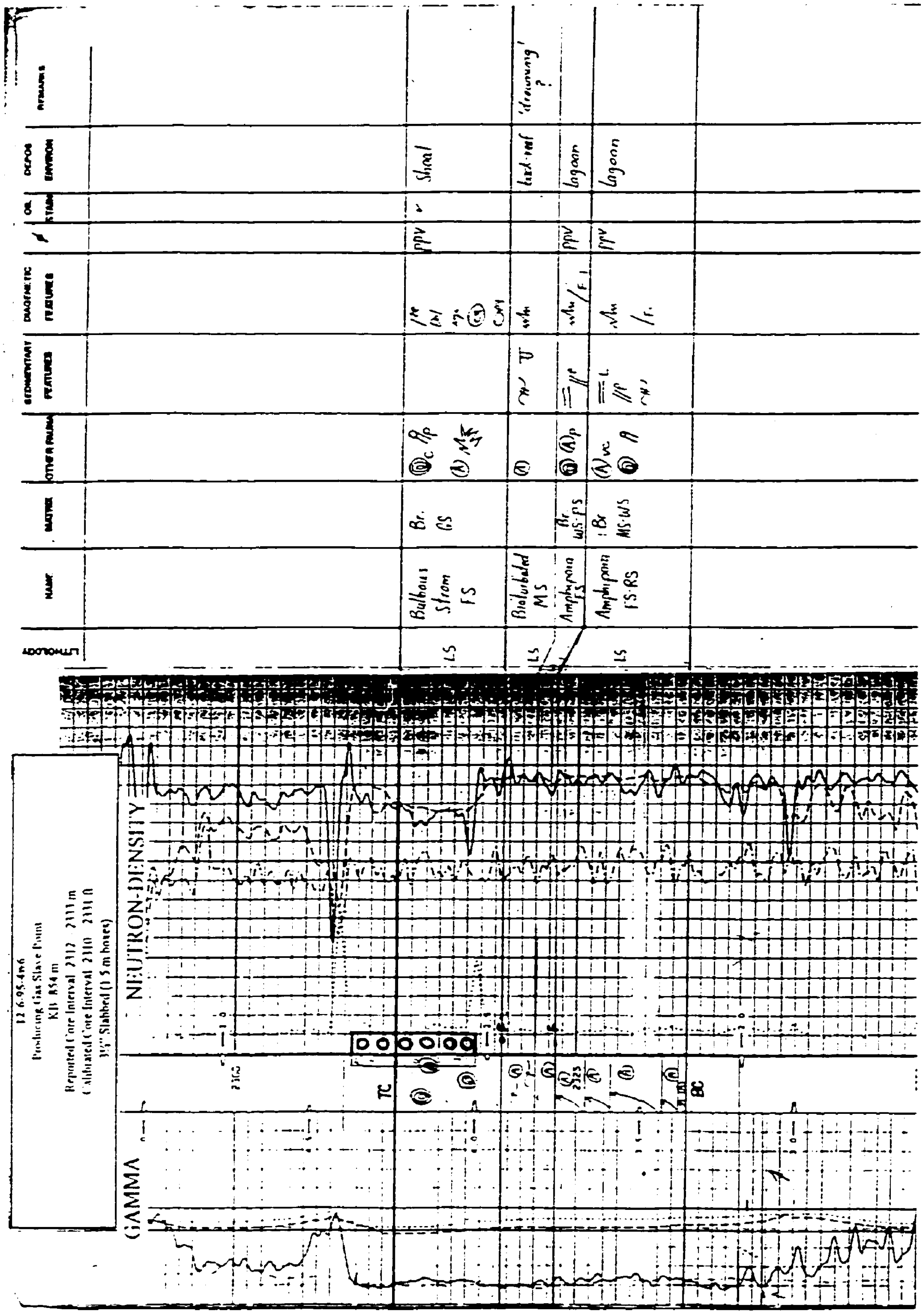
12-6-95-4w6
Producing Gas Slave Point
KB 854 m
Reported Core Interval 2312 - 2333 m
Calibrated Core Interval 2310 - 2331 m
3½" Slabbed (1.5 m boxes)
GAMMA
NEUTRON-DENSITY
TC
BC
LITHOLOGY
NAME
MATRIX
OTHER FAUNA
SEDIMENTARY FEATURES
DIAGENETIC FEATURES
OIL STAIN
DEPOS ENVIRON
REMARKS
LS
Bulbous Strom FS
Br. GS
PPV
Shoal
LS
Bioturbated MS
back-reef
'drowning' ?
Amphipora FS
Br. WS-PS
PPV
lagoon
LS
Amphipora FS-RS
Br MS-WS
PPV
lagoon

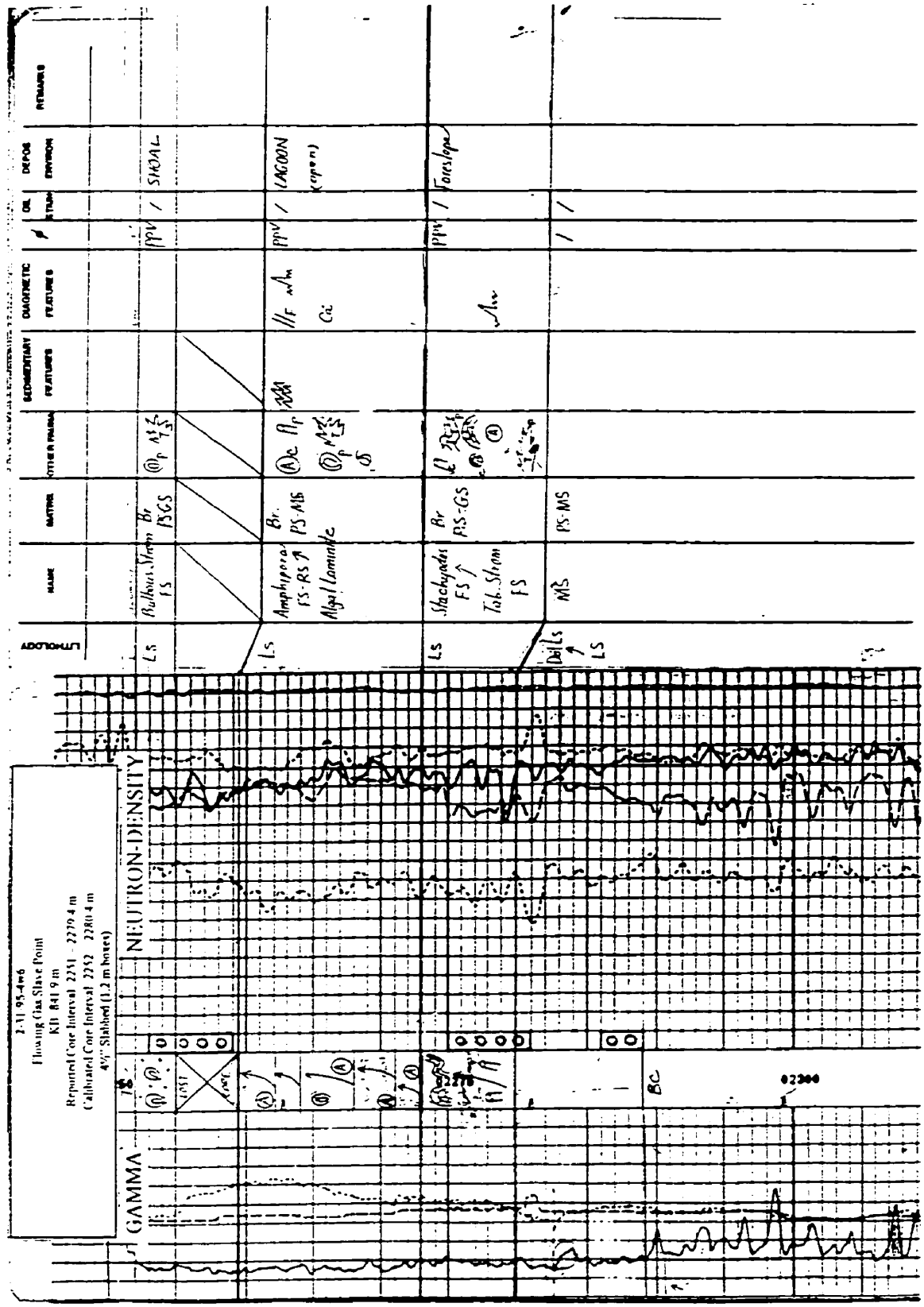
F.11 95-4w6
Flowing Gas Slave Point
KB 841.9 m
Reported Core Interval 2251 – 2279.4 m
Calibrated Core Interval 2252 – 2280.4 m
4½" Slabbed (1.2 m boxes)
GAMMA
NEUTRON-DENSITY
LITHOLOGY
LS
Bulkhead Stream FS
Amphipora FS-RS
Algal Laminite
Stackpole FS
Tab. Stream FS
MS
DEPOSITIONAL FEATURES
DIAGENETIC FEATURES
OTHER PHASES
MATRIX
NAME
DEPOSITION
OIL STAIN
REMARKS
LAGOON
SHOAL
Foreslope
BC
02300

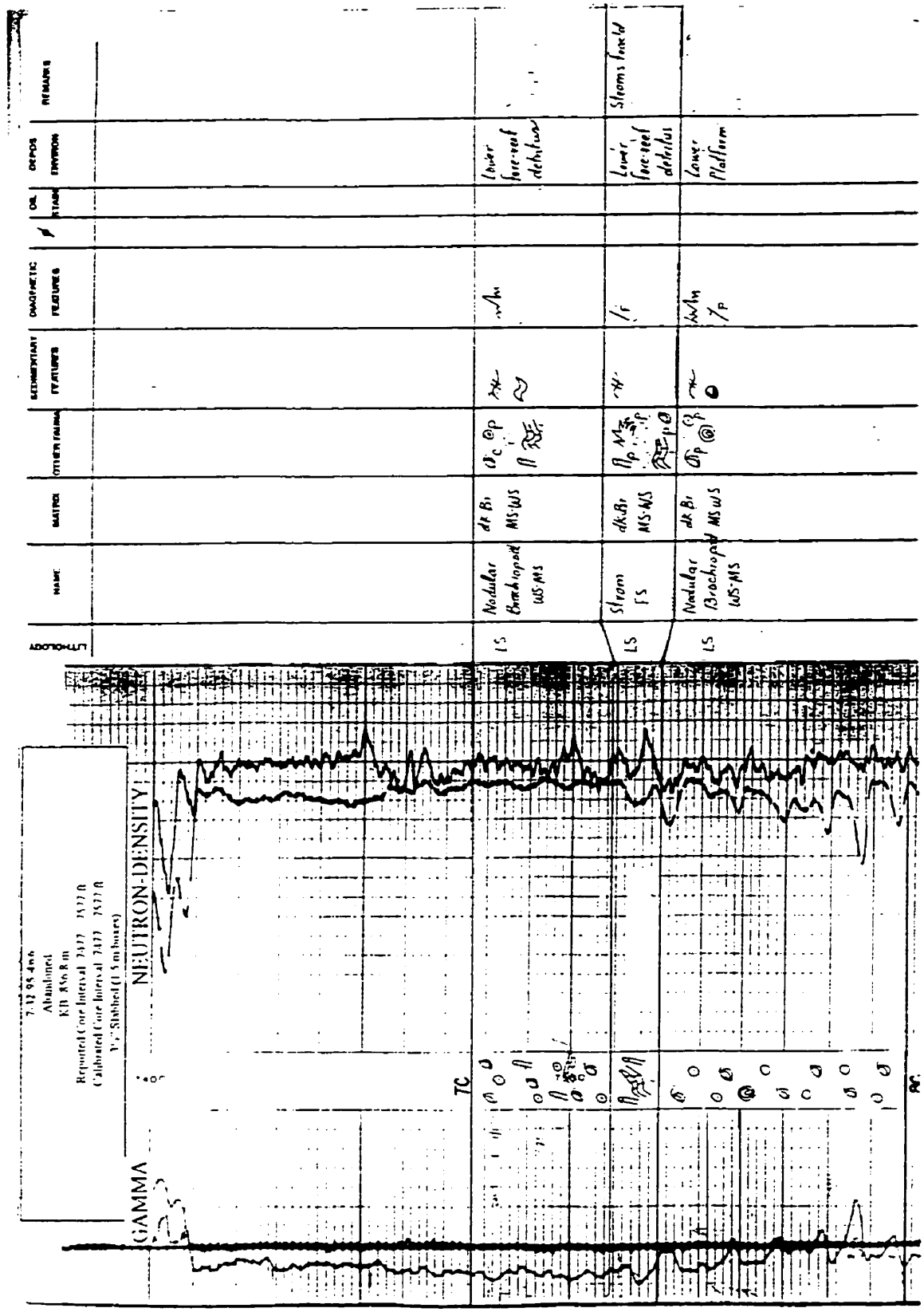
LITHOLOGY
NAME
BASIS
OTHER FAUNA
SEDIMENTARY FEATURES
DIAGENETIC FEATURES
OIL STAIN
DEPOS ENVIRON
REMARKS
Nodular Bmkhiopod WS-MS
dk Br MS-WS
LS
Lower fore-reef detritus
Strom LS
dk Br MS-WS
LS
Lower fore-reef detritus
Strom s limited
Nodular Brachiopod WS-MS
dk Br MS WS
LS
Lower Platform
NEUTRON-DENSITY
GAMMA
TC

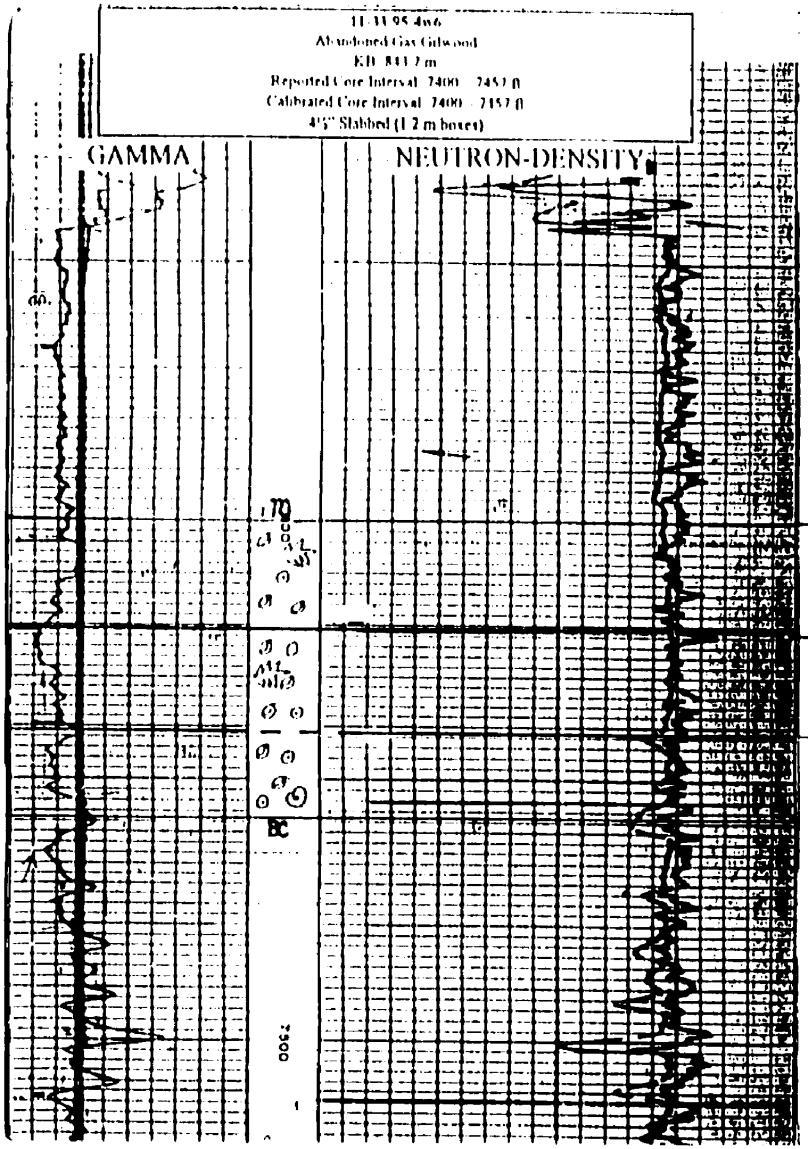

LITHOLOGY	NAME	MATRIX	OTHER FAUNA	SEDIMENTARY FEATURES	DIAGENETIC FEATURES	ϕ	OIL STAIN	DEPOS ENVIRON	REMARKS
LS	Nodular WS	dk Br MS			/F	-	-	Basin fill	Lower fore slope debris
LS	Nodular MS-WS	dk Br to dk Grey MS				-	-	Basin fill	Lower fore slope debris
LS	Nodular WS	dk Br. MS				-	-	Basin fill ?	Ca in gastropod shell.

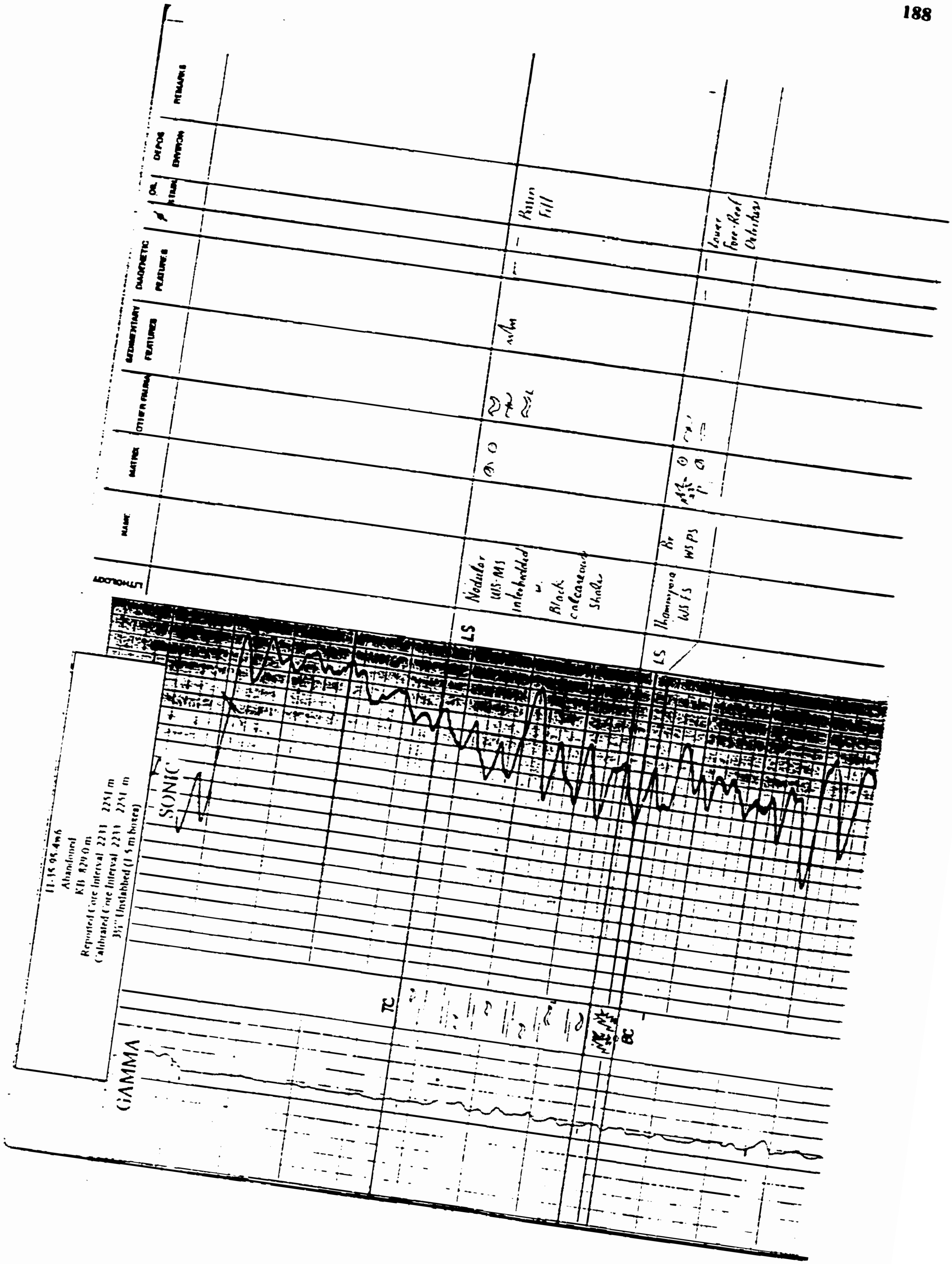
LITHOLOGY
NAME
MATRIX
OTHER FAUNA
SEDIMENTARY FEATURES
DIAGENETIC FEATURES
OIL STAIN
DEPOS. ENVIRON.
REMARKS
SONIC
GAMMA
Abandoned
Reported Core Interval 2231 - 2251 m
Calibrated Core Interval 2231 - 2251 m
LS
TC
BC
Basin Fill
Lower Fore-Reef Detritus

GAMMA
NEUTRON-DENSITY
10 10 95 5m6
Abandoned
KB 911 m
Reported Core Interval 2191 6 2409 6 m
Calibrated Core Interval 2193 2411 m
1" Undubbed (1 5 m bases)
LITHOLOGY
NAME
MATRIX
OTHER FRAM
SEDIMENTARY FEATURES
DIAGENETIC FEATURES
OIL STAIN
DEPOS ENVIRON
REMARKS
Nodular Bioturbated MS WS
dk Br
Basin Fill
upper marine assemblage
Bathurst Storm FS
Br.
Inshore Back-Bar
Amphipora FS RS
dk Br MS-WS
Lagoon
S.V.S.
TC
BC
2425

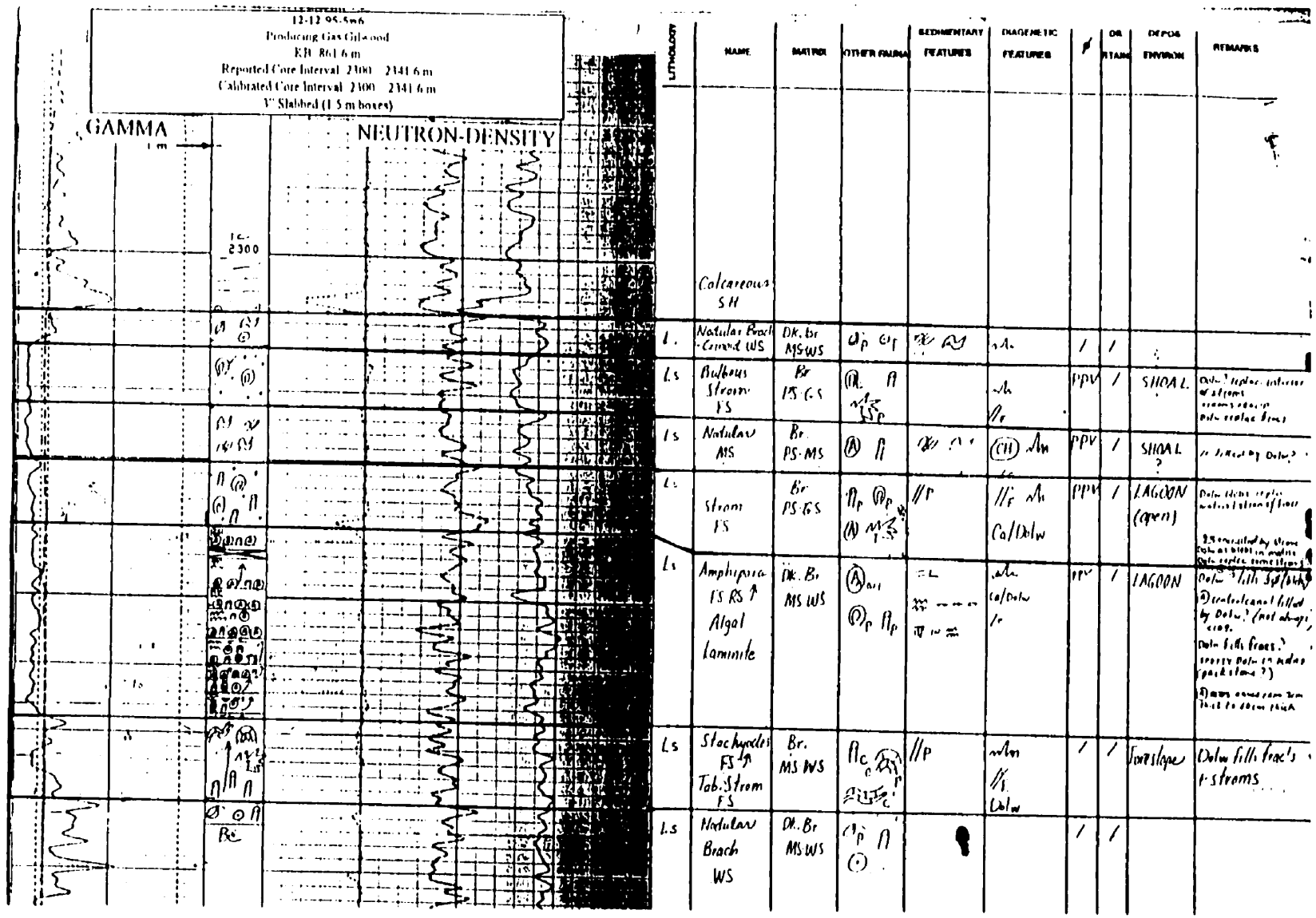
12-12 95-5w6
Producing Gas Gilwood
KB 861.6 m
Reported Core Interval 2300 2341.6 m
Calibrated Core Interval 2300 2341.6 m
3" Slabbed (1.5 m boxes)
GAMMA
1 m
NEUTRON-DENSITY
LITHOLOGY
NAME
MATRIX
OTHER FAUNA
SEDIMENTARY FEATURES
DIAGENETIC FEATURES
POR
OIL STAIN
DEPOS ENVIRON
REMARKS
Calcareous SH
Nodular Beach + Ramp WS
Dk. br MS-WS
Ls
Bulbous Stroms FS
Br PS-GS
SHOAL
Nodular MS
Br PS-MS
Ls
Stroms FS
Br PS-GS
LAGOON (open)
Ls
Amphipora FS RS
Algal laminite
Dk. Br MS WS
LAGOON
Ls
Stachyodes FS
Tab. Strom FS
Br. MS WS
Forslope
Ls
Nodular Beach WS
Dk. Br MS WS

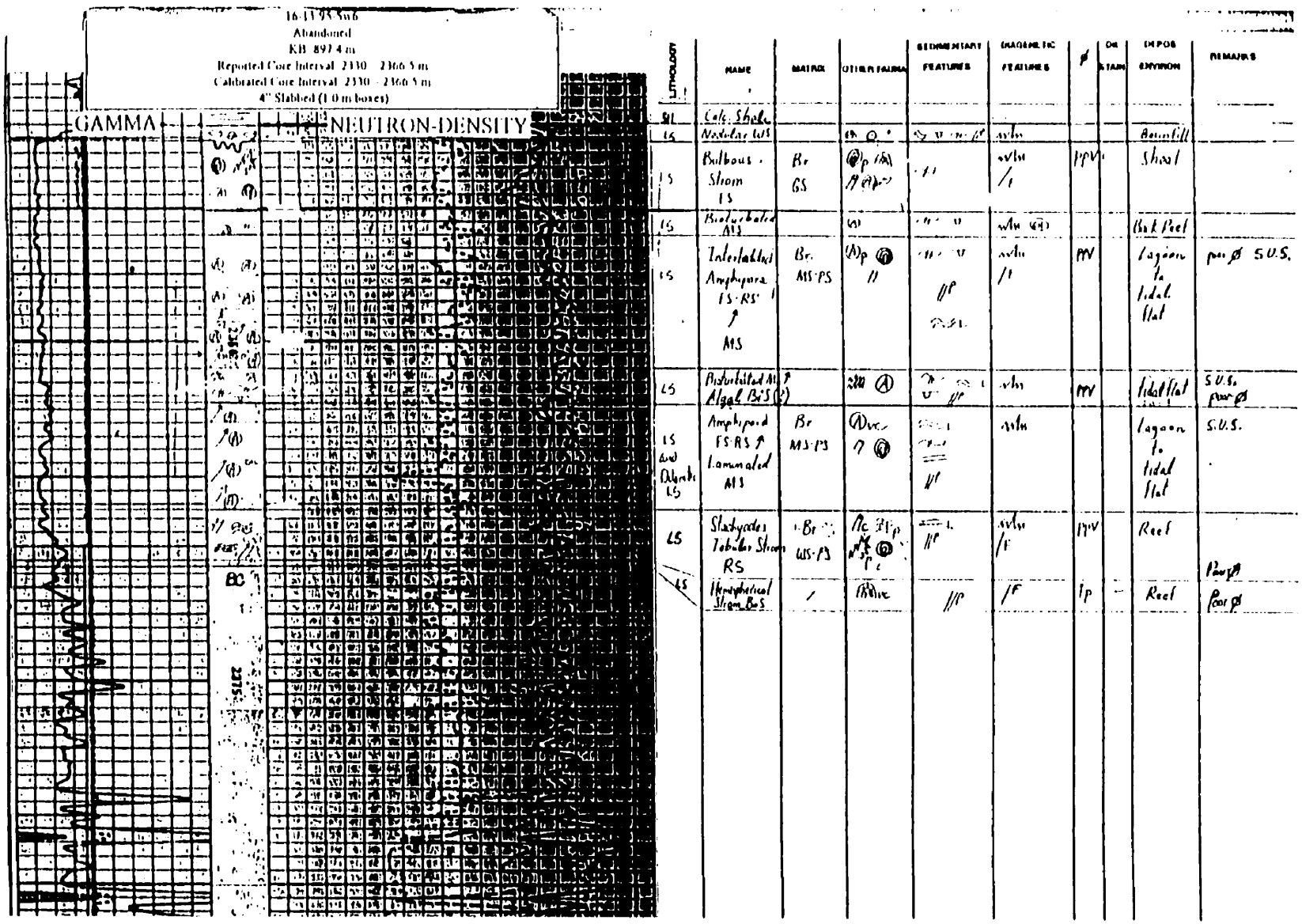
16-11-95 Sw6
Abandoned
KB 897.4 m
Reported Core Interval 2330 - 2366.5 m
Calibrated Core Interval 2330 - 2366.5 m
4" Slabbed (1.0 m bones)
GAMMA
NEUTRON-DENSITY
LITHOLOGY
NAME
MATRIX
OTHER FAUNA
SEDIMENTARY FEATURES
DIAGENETIC FEATURES
DEPOS ENVIRON
REMARKS
Calc. Shale
Nodular WS
Bulbous Strom LS
Br
GS
Bioturbated MS
Interlabbed Amphipora FS-RS MS
Br.
MS-PS
Bioturbated MS Algal BrS
Amphipod FS-RS Laminated MS
Br
MS-PS
Stachycides Tabular Strom RS
Br
WS-PS
Hemispherical Strom BrS
Lagoon to tidal flat
S.U.S.
Reef
Reef

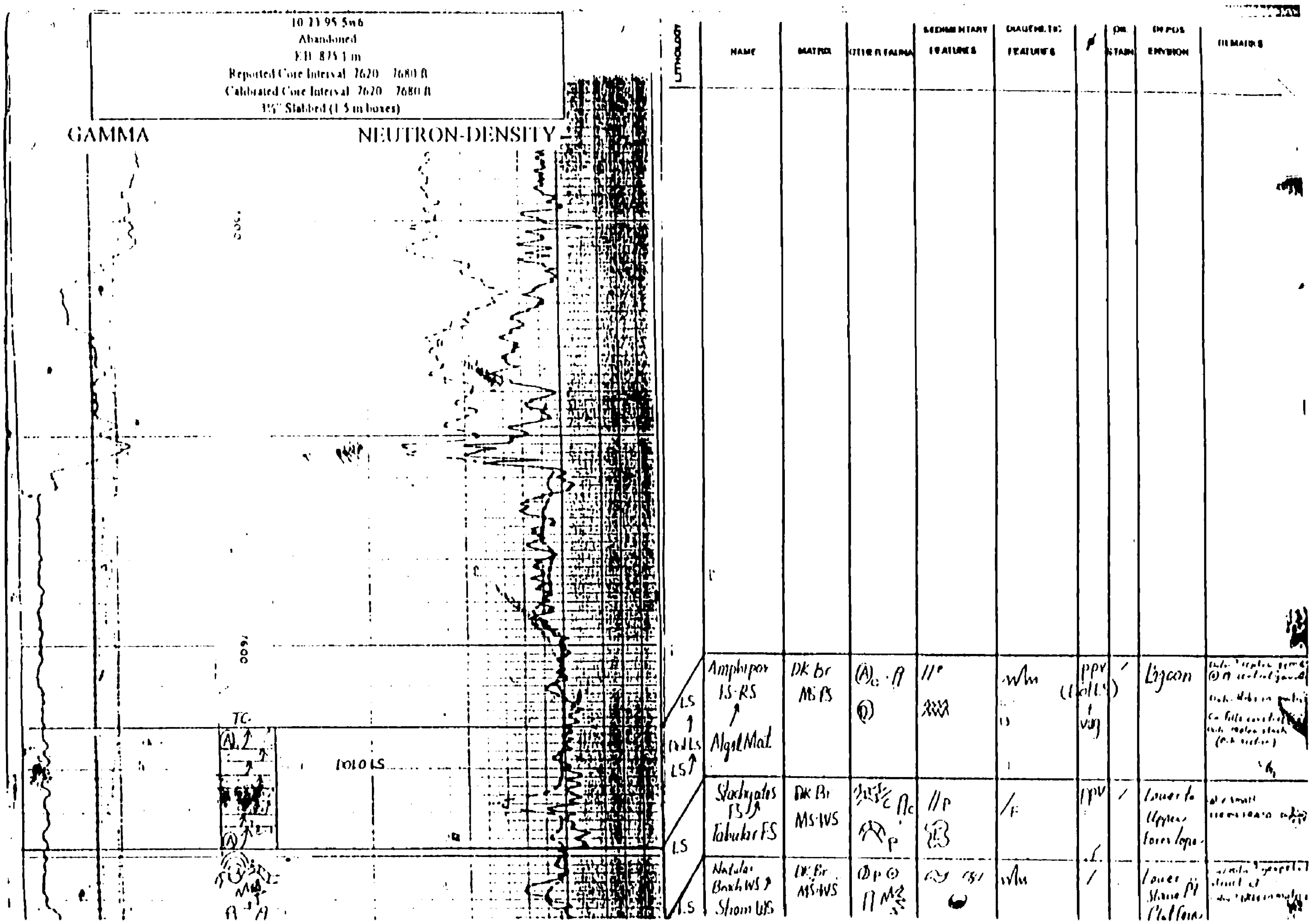
10 11 95 5w6
Abandoned
EII 875 1 m
Reported Core Interval 7620 – 7680 ft
Calibrated Core Interval 7620 – 7680 ft
3½" Slabbed (1.5 m boxes)
GAMMA
NEUTRON-DENSITY
7500
7600
LITHOLOGY
NAME
MATRIX
OTHER FAUNA
SEDIMENTARY FEATURES
DIAGENETIC FEATURES
OIL STAIN
DEPOS ENVIRON
REMARKS

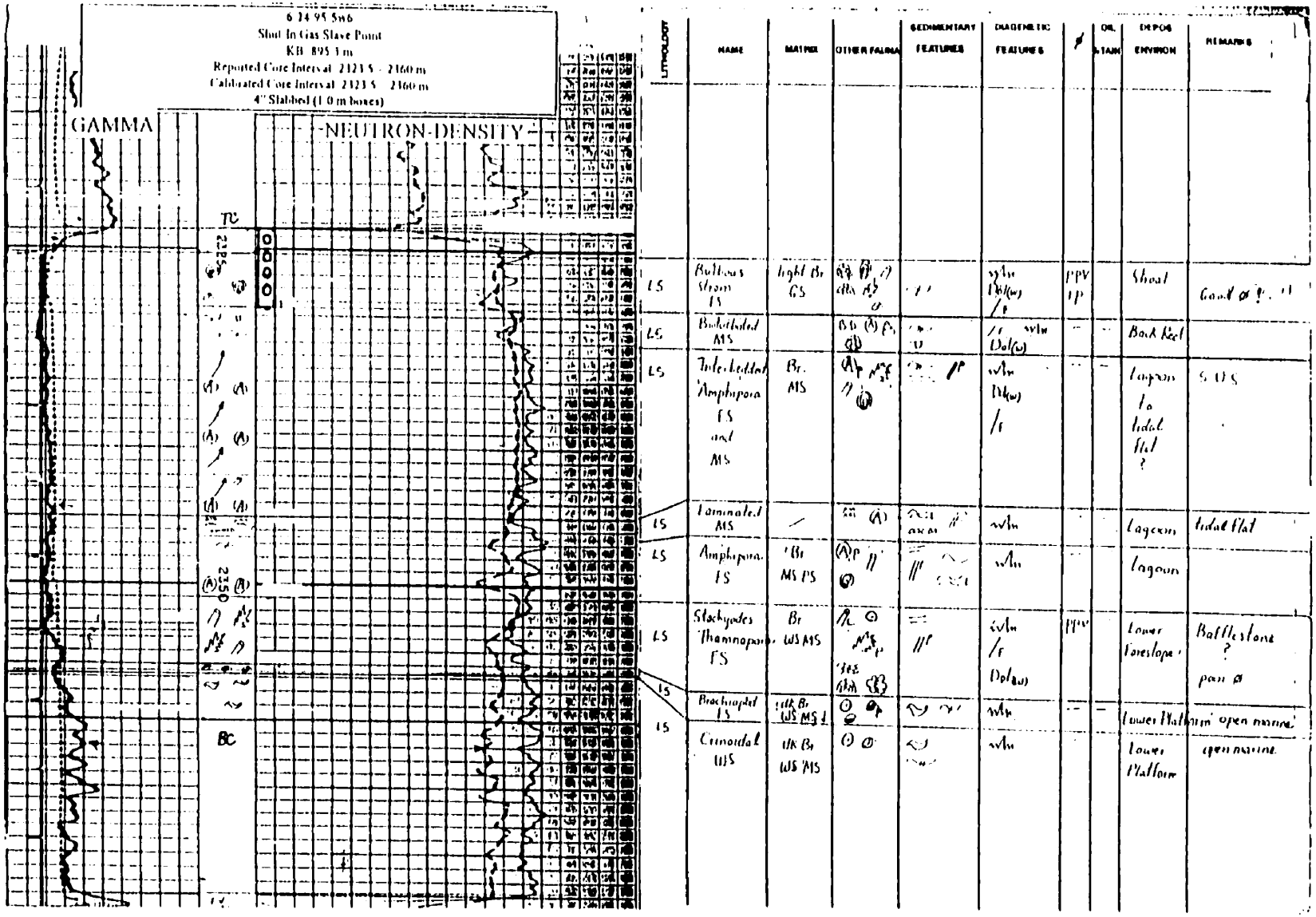
6 24 95 Sw6
Shut In Gas Slave Point
KB 895.3 m
Reported Core Interval 2123.5 - 2160 m
Calibrated Core Interval 2123.5 - 2160 m
4" Stabbed (1.0 m bones)
GAMMA
NEUTRON-DENSITY
TC
2125
2150
BC
LITHOLOGY
NAME
MATRIX
OTHER FAUNA
SEDIMENTARY FEATURES
DIAGENETIC FEATURES
OIL STAIN
DEPOS ENVIRON
REMARKS
LS
Bulbous Stram FS
light Br GS
LS
Bioturbated MS
LS
Interbedded Amphipora FS and MS
Br. MS
LS
Laminated MS
LS
Amphipora FS
Br MS FS
LS
Stachyodes Thamnopora FS
Br WS MS
LS
Brachiopod FS
dk Br WS MS
LS
Crinoidal WS
dk Br WS MS
Shoal
Back Reef
Lagoon to tidal flat ?
Lagoon
Lower foreslope
Lower Platform
tidal flat
Baffle stone ?
open marine
open marine

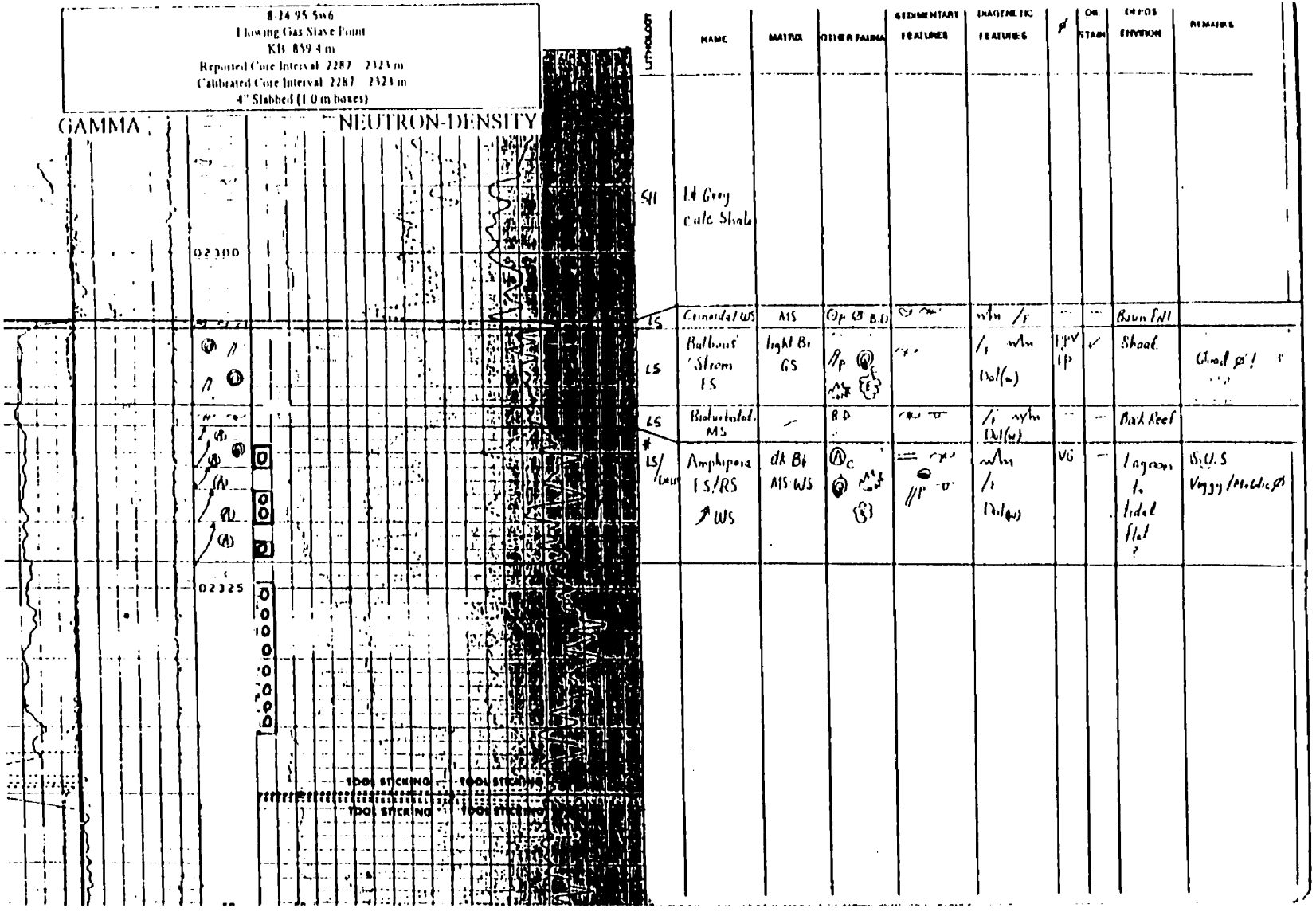
8-24-95 Sw6
Flowing Gas Slave Point
KB 859.4 m
Reported Core Interval 2287 - 2323 m
Calibrated Core Interval 2287 - 2323 m
4" Slabbed (1.0 m boxes)
GAMMA
NEUTRON-DENSITY
02300
02325
TOOL STICKING
TOOL STICKING
TOOL STICKING
TOOL STICKING
LITHOLOGY
NAME
MATRIX
OTHER FAUNA
SEDIMENTARY FEATURES
DIAGENETIC FEATURES
ϕ
OIL STAIN
DEPOS ENVIRON
REMARKS
Lt Grey calc Shale
Crinoidal WS
MS
Bioturbated MS
Amphipora FS/RS
WS
dk Brn
MS WS
Lagoon to tidal flat ?
Shoal
Back Reef

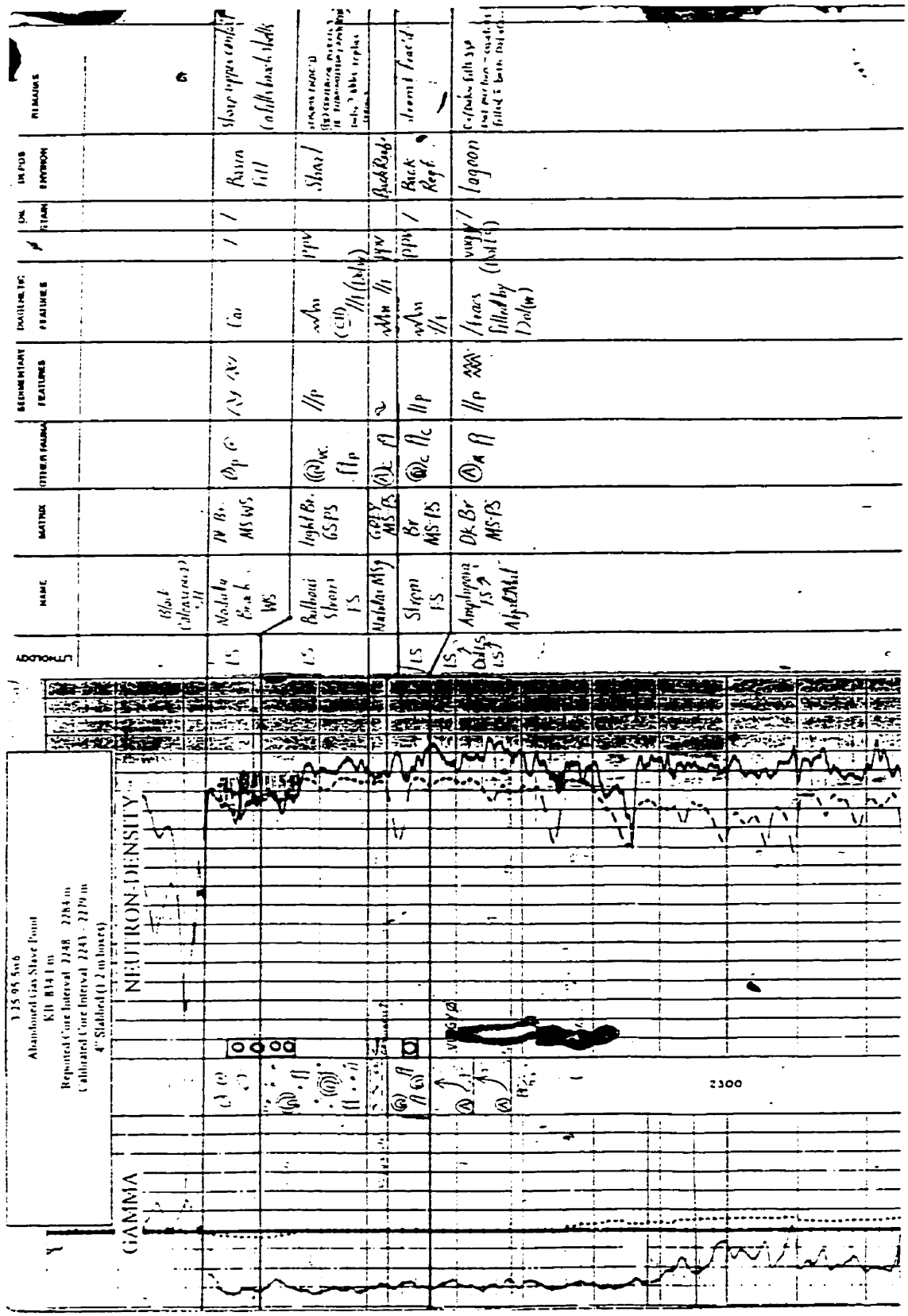
GAMMA
NEUTRON-DENSITY
2300

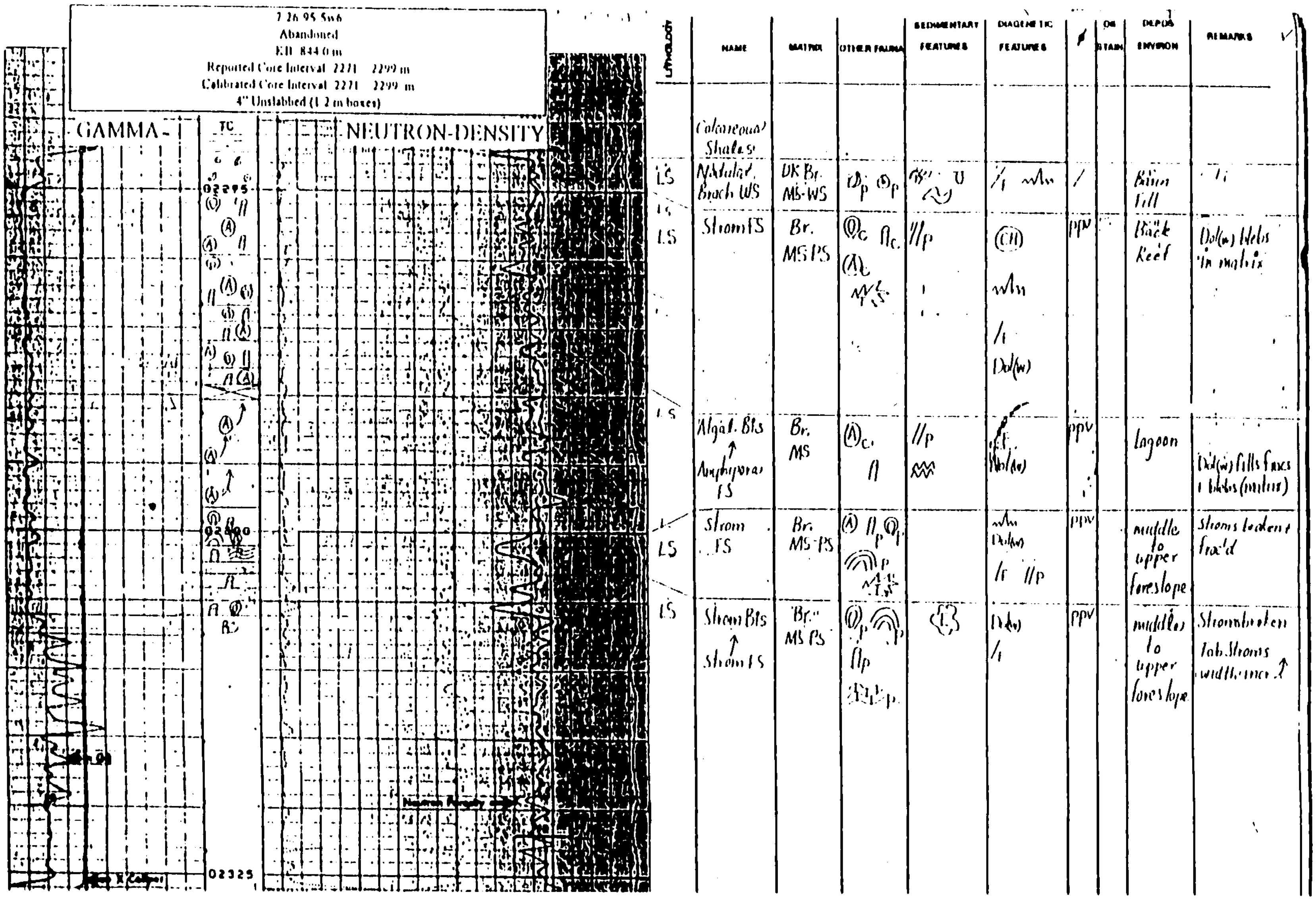
7-26-95-5w6
Abandoned
KB 844.0 m
Reported Core Interval 2271 - 2299 m
Calibrated Core Interval 2271 - 2299 m
4" Unslabbed (1.2 m boxes)
GAMMA-
NEUTRON-DENSITY
02295
02300
02325
LITHOLOGY
NAME
MATRIX
OTHER FAUNA
SEDIMENTARY FEATURES
DIAGENETIC FEATURES
OIL STAIN
DEPOS ENVIRON
REMARKS
Calcareous Shales
LS
Nodular Brach WS
DK Br. MS-WS
Basin Fill
Strom FS
Br. MS PS
Back Reef
Dol(w) blebs in matrix
Dol(w)
Algal Bls
Amphipora FS
Br. MS
Lagoon
Dol(w) fills fracs & blebs (matrix)
Strom FS
Br. MS-PS
middle to upper foreslope
Stroms broken frac'd
Strom Bls
Strom FS
Br. MS PS
Stroms broken
Tab. Stroms
ppv

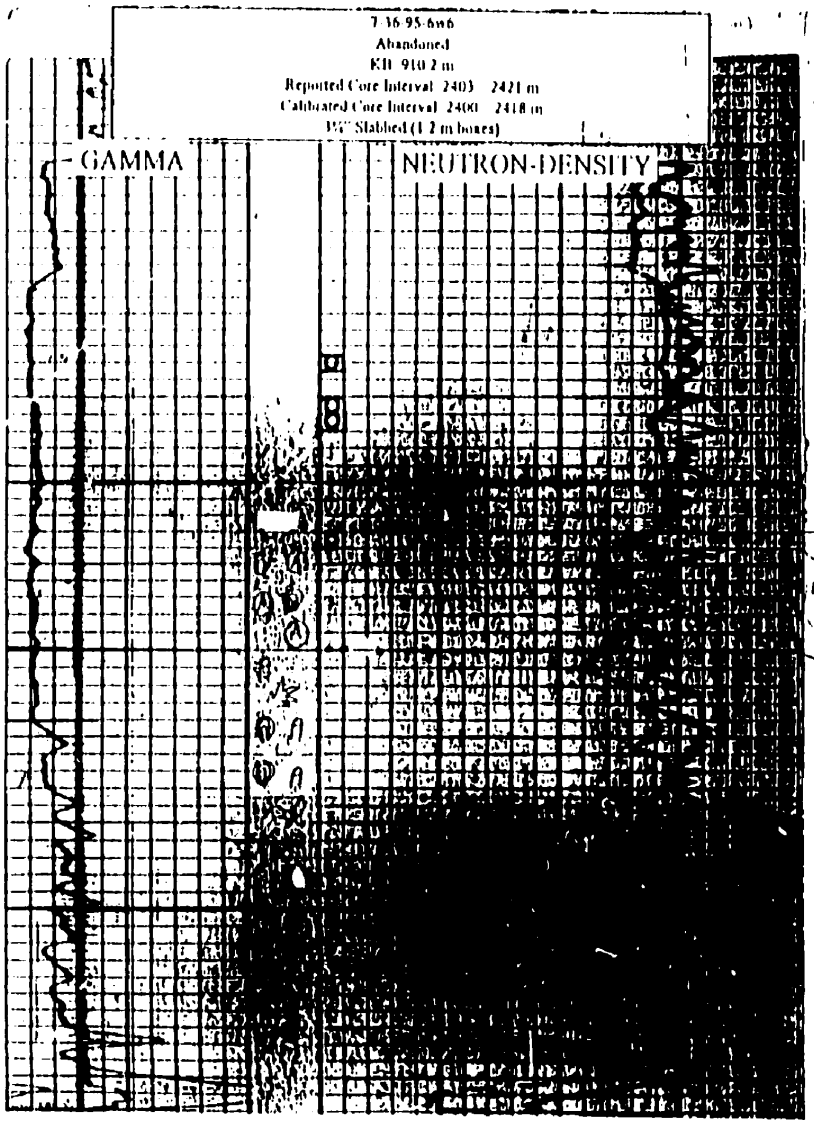

LITHOLOGY	NAME	MATRIX	OTHER FAUNA	SEDIMENTARY FEATURES	DIAGENETIC FEATURES	φ	OIL STAIN	DEPOS ENVIRON	REMARKS
LS	Stromi FS	Br. MS	Ⓐp A Ⓐp			ppv		Back Reef	
LS	Amphipora FS	Br. WS-MS	Ⓐc A	≡ ≋	/F	—		Lagoon	
LS	Strom FS	PS GS	Ⓐp Ⓐc Ⓐp		Mn Dol(m)	ppv		Lower to Upper fore/sh.	Stroms frac'd Dol(m) fills ↓ Mgs. Baffle/Low Reef ?

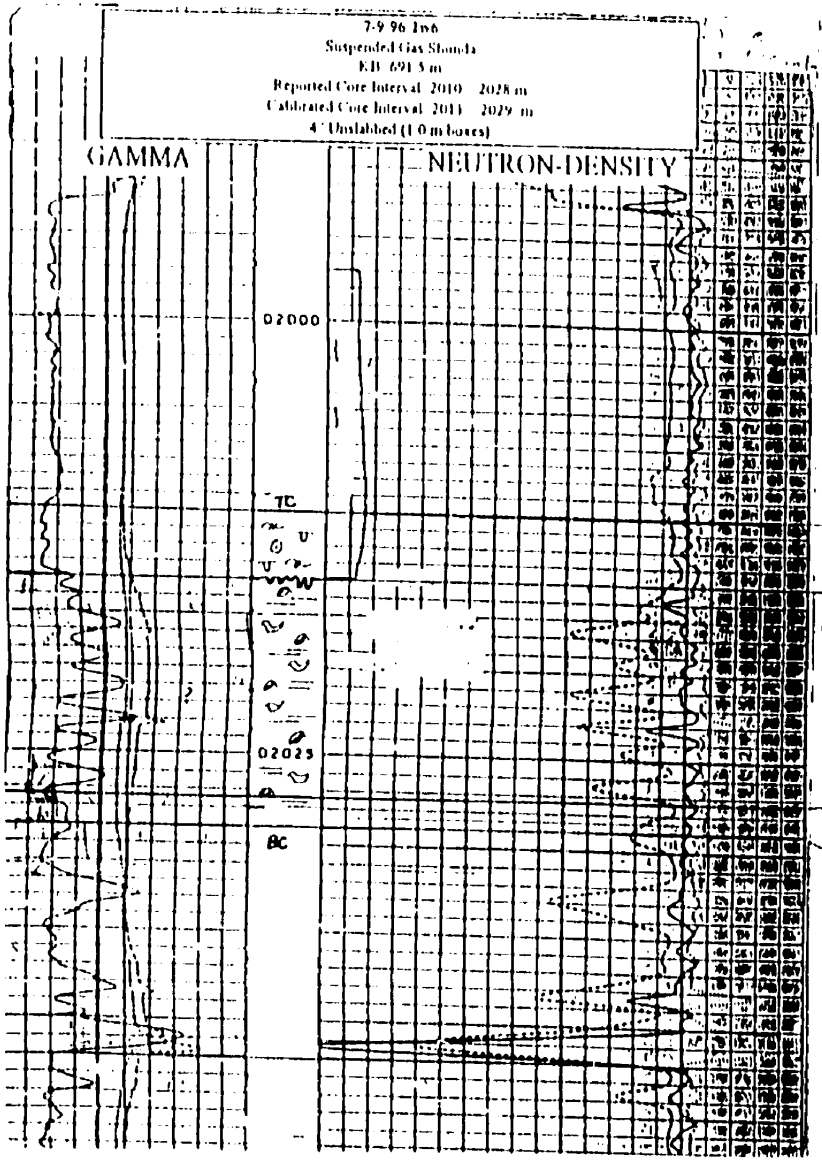

LITHOL	NAME	MATRIX	OTHER FAUNA	SEDIMENTARY FEATURES	DIAGENETIC FEATURES	✗	OIL STAIN	DEPOS ENVIRON	REMARKS
LS	Bioturbated MS				wkly Dol(ω)			Basin Fill	post - Slave Pt
LS	Nodular WS ↑ Brachiopod FS	dk Br MS-WS (Shaley)			wkly			Basin Fill	Shale partings common syn Upper Slave Pt ?
LS	Thamnopora FS	dk Br MS-WS			wkly			Lower Foreslope Debris ?	Lower Slave Pt

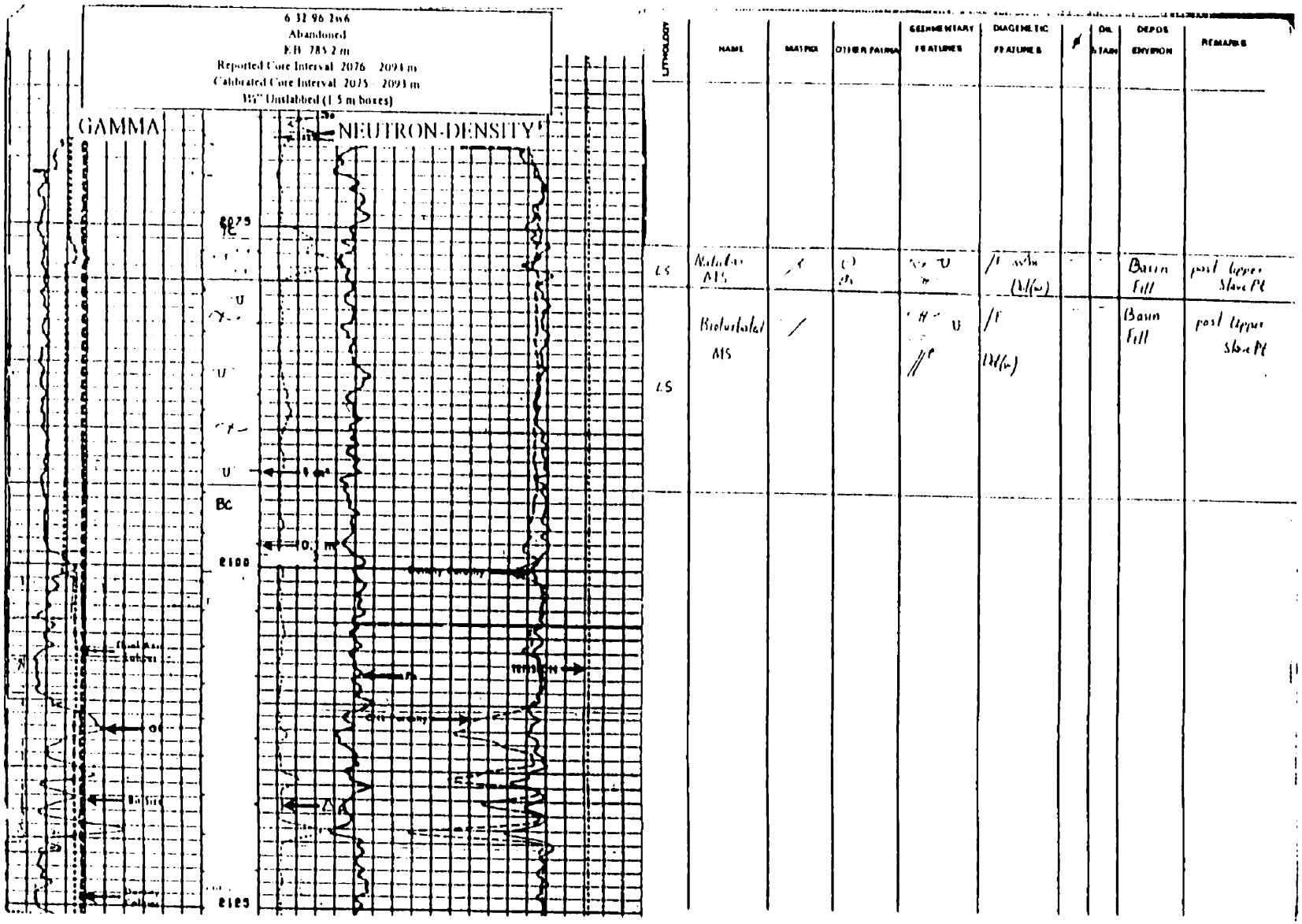
6 32 96 2w6
Abandoned
KB 785.2 m
Reported Core Interval 2076 - 2094 m
Calibrated Core Interval 2075 - 2093 m
3½" Unslabbed (1.5 m boxes)
GAMMA
NEUTRON-DENSITY
LITHOLOGY
NAME
MATRIX
OTHER FAUNA
SEDIMENTARY FEATURES
DIAGENETIC FEATURES
OIL STAIN
DEPOS ENVIRON
REMARKS
LS
LS
Bc
2075
2100
2125

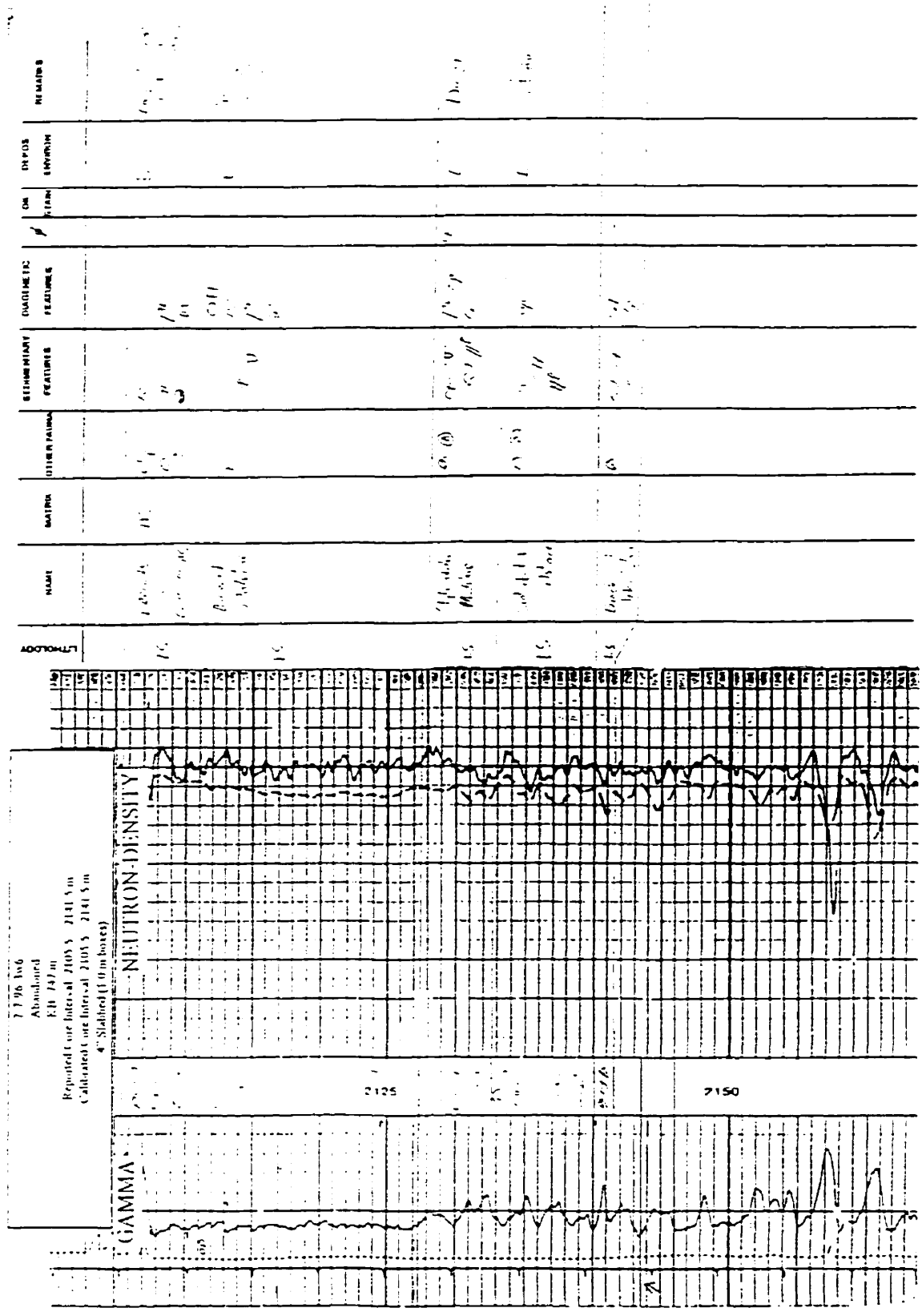
REMARKS
DEPOS ENVIRON
OIL STAIN
DIAGENETIC FEATURES
SEDIMENTARY FEATURES
OTHER FAUNA
MATRIX
NAME
ADDITIONAL
NEUTRON-DENSITY
GAMMA
2125
2150

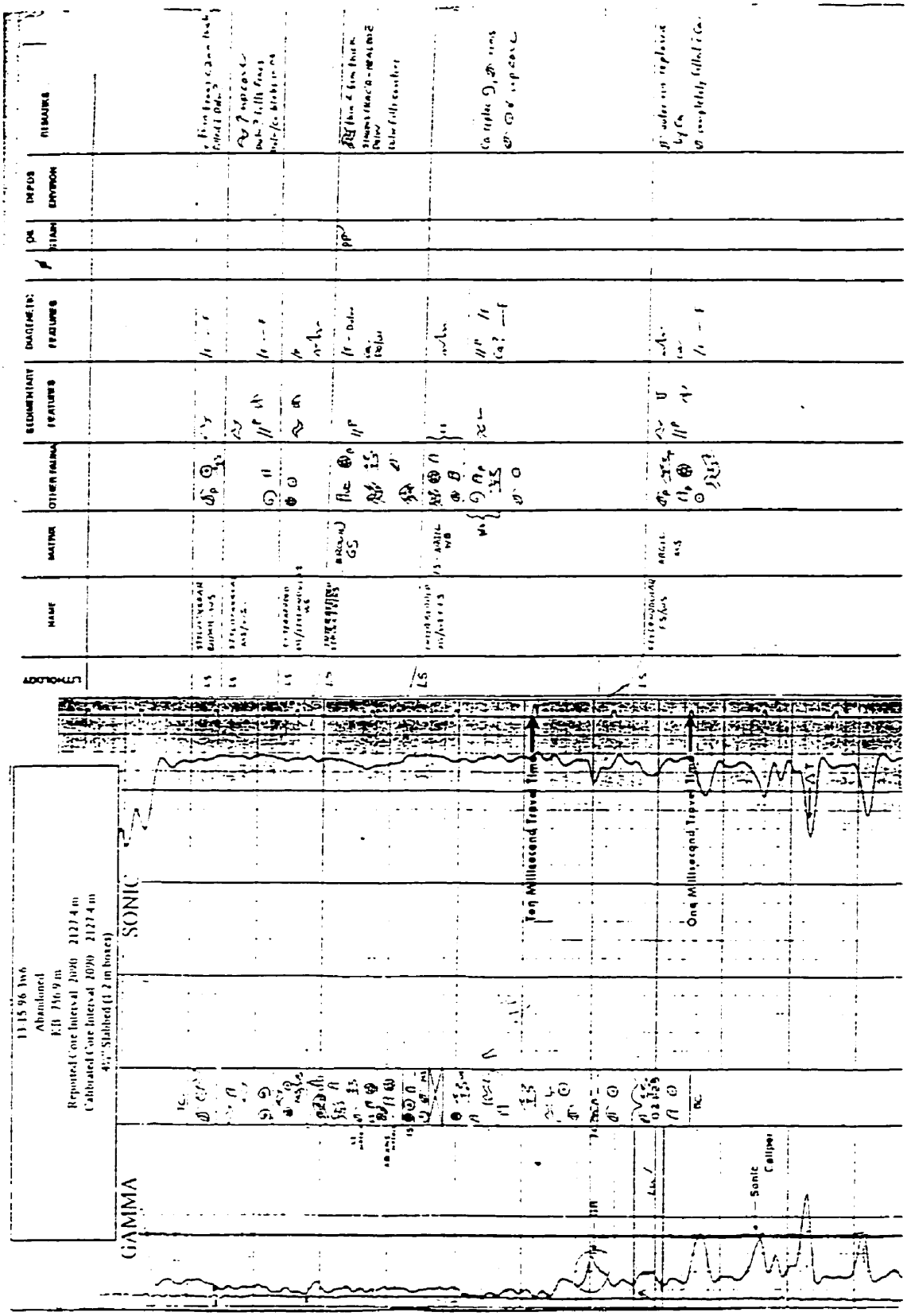
ADDITIONAL
NAME
MATRIX
OTHER FAUNA
SEDIMENTARY FEATURES
DIAGENETIC FEATURES
OIL STAIN
DEPOS ENVIRON
REMARKS
11 15 96 Inc
Abandoned
KB 336 9 m
Reported Core Interval 2090 2127 4 m
Calibrated Core Interval 2090 2127 4 m
4½" Slotted (1 2 m Bore)
SONIC
GAMMA
Ten Millisecond Travel Time
One Millisecond Travel Time
Sonic
Caliper

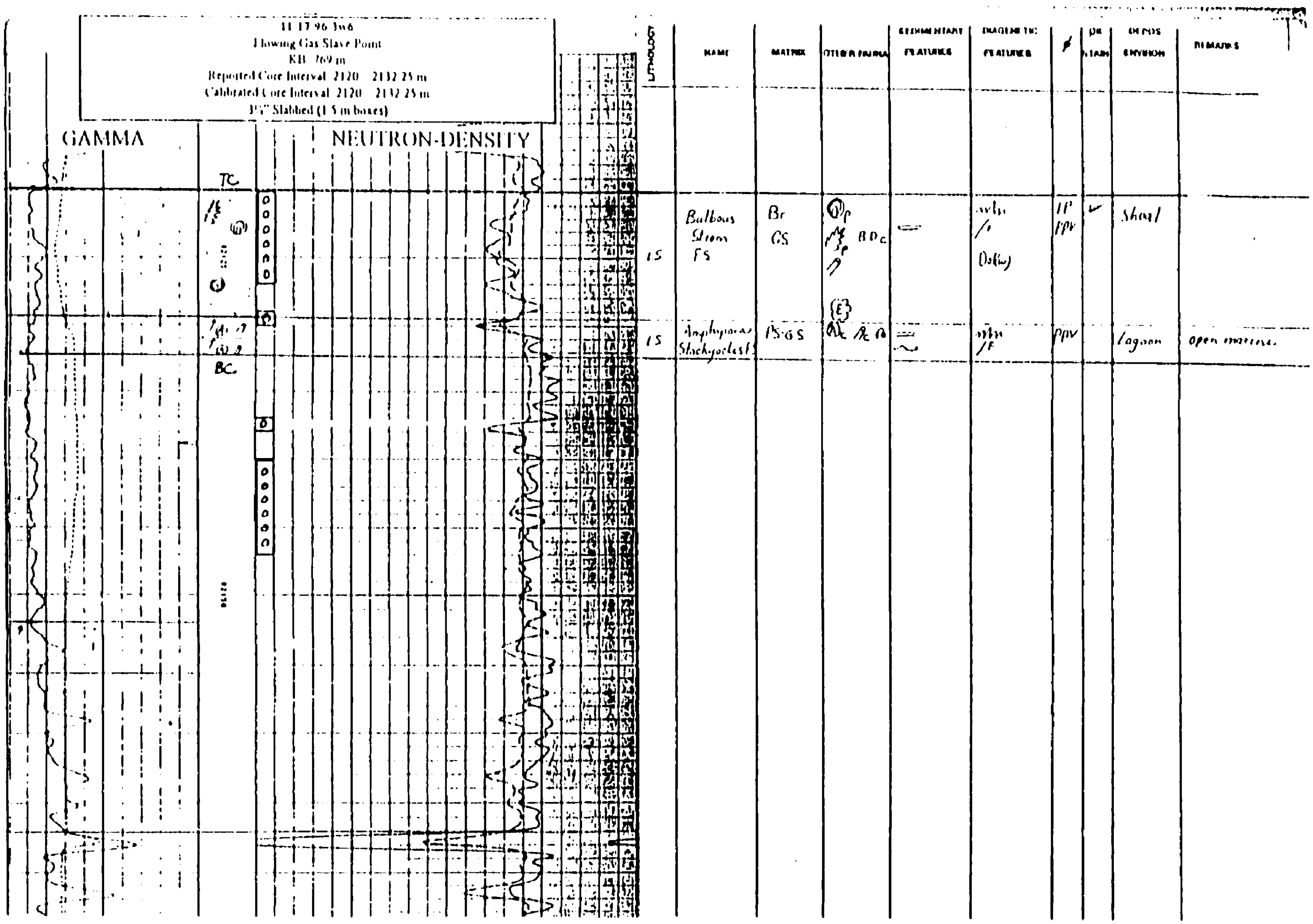
11-17-96-3w6
Flowing Gas Slave Point
KB 769 m
Reported Core Interval 2120 - 2132.25 m
Calibrated Core Interval 2120 - 2132.25 m
3½" Slabbed (1.5 m boxes)
GAMMA
NEUTRON-DENSITY
TC
BC
LITHOLOGY
NAME
MATRIX
OTHER FAUNA
SEDIMENTARY FEATURES
DIAGENETIC FEATURES
STAIN
DEPOS ENVIRON
REMARKS
LS
Bulbous Strom FS
Br
GS
BPc
Dol(w)
IP
PPV
Shoal
LS
Amphipora Stachyodes FS
FS-GS
PPV
lagoon
open marine

10 18 96 1m6
Flowing Gas Slave Point
KB 750 5 m
Reported Core Interval 2098 25 2134 5 m
Calibrated Core Interval 2098 25 2134 5 m
4" Stabbed (1 0 m Intvls)
GAMMA
SONIC
One Millisecond Travel Time
02100
02150
LITHOLOGY
NAME
BIOTICS
OTHER FAUNA
SEDIMENTARY FEATURES
DIAGENETIC FEATURES
OIL FLASH
DEPOS ENVIRON
REMARKS

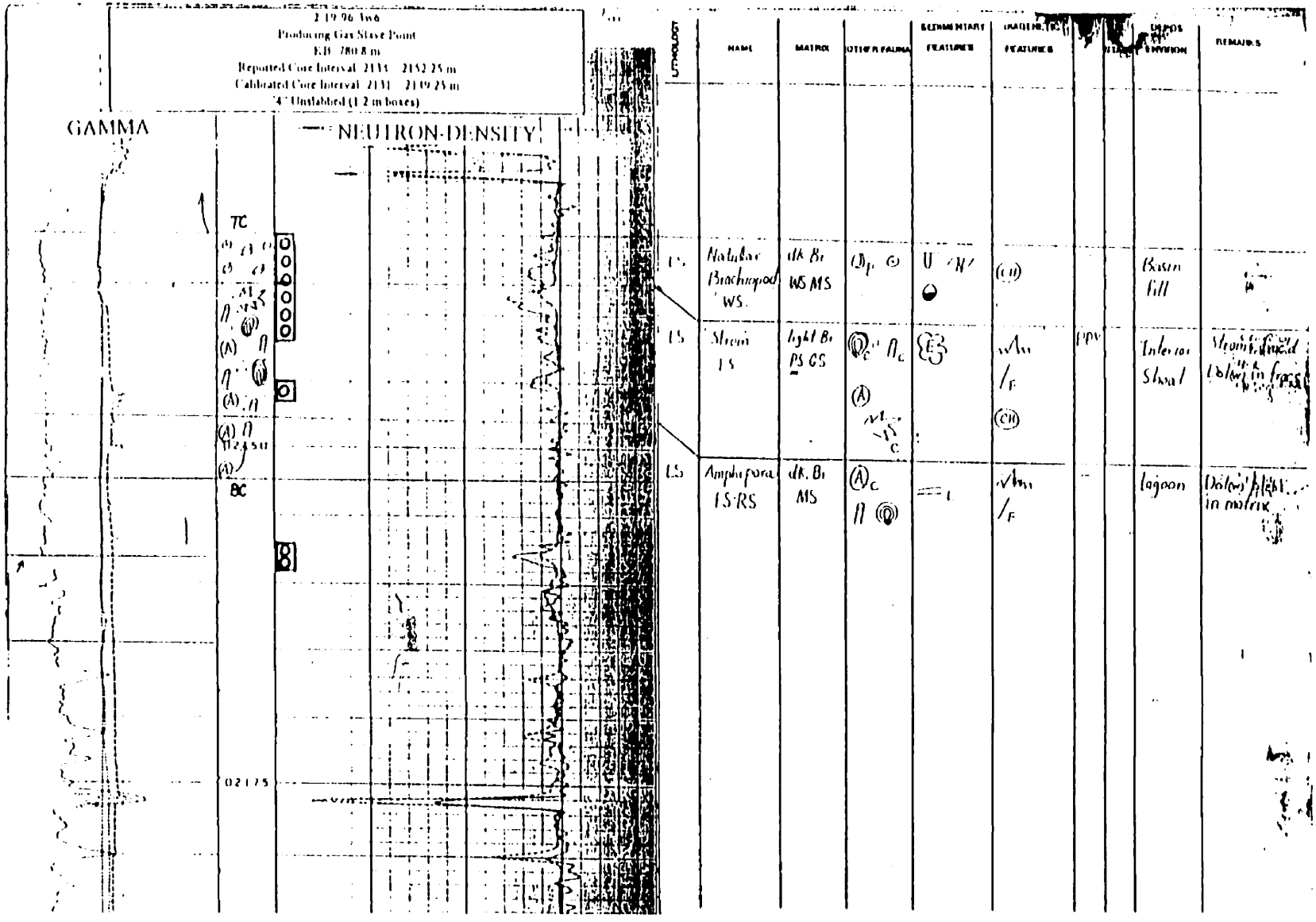
2-19-96 Iwa
Producing Gas Stave Point
KB 780.8 m
Reported Core Interval 2133 2152.25 m
Calibrated Core Interval 2131 2149.25 m
4" Unslabbed (1.2 m boxes)
GAMMA
NEUTRON-DENSITY
TC
BC
02175
LITHOLOGY
NAME
MATRIX
SEDIMENTARY FEATURES
REMARKS
Natalina Brachiopod WS.
dk. Br
WS MS
Basin fill
Strom LS
light Br
PS GS
Interior Shoal
Strom. fined
Amphipora LS-RS
dk. Br
MS
lagoon

LITHOLOGY
NAME
MATRIX
OTHER FAUNA
SEDIMENTARY FEATURES
DIAGENETIC FEATURES
ϕ
OIL STAIN
DEPTH ENVIRON
REMARKS
GAMMA
NEUTRON-DENSITY
08178

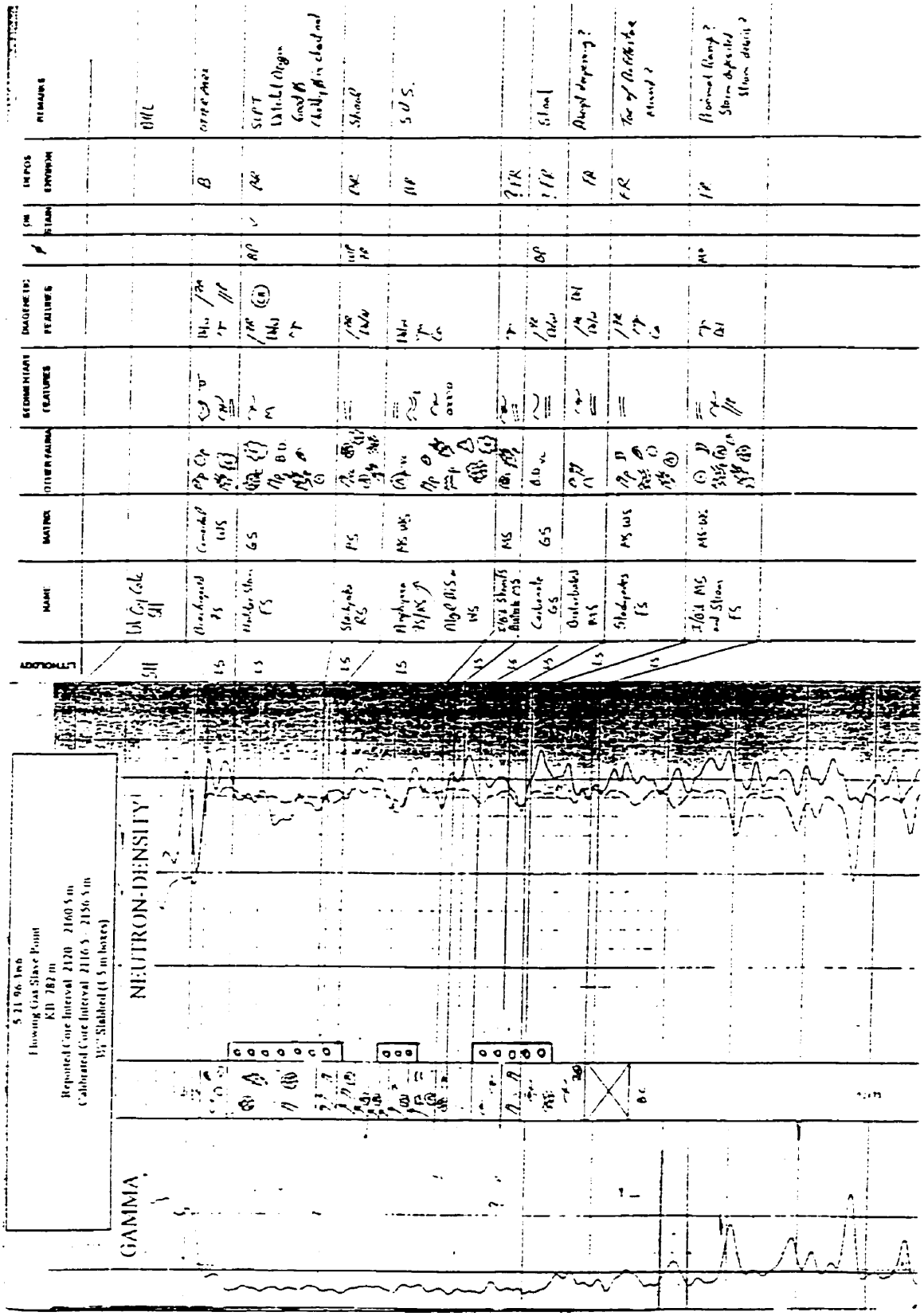
NEUTRON-DENSITY
GAMMA
5 21 96 Ireb
Flowing Gas Slave Point
KB 782 m
Reported Core Interval 2120 - 2160 S m
Calculated Core Interval 2116 5 - 2156 S m
Bit Slabbed (1 5 m loss)
NAME
MATRIX
OTHER FAUNA
SEDIMENTARY FEATURES
DIAGENETIC FEATURES
PORE TYPE
SW RESIS
DEPOS ENVIRON
REMARKS

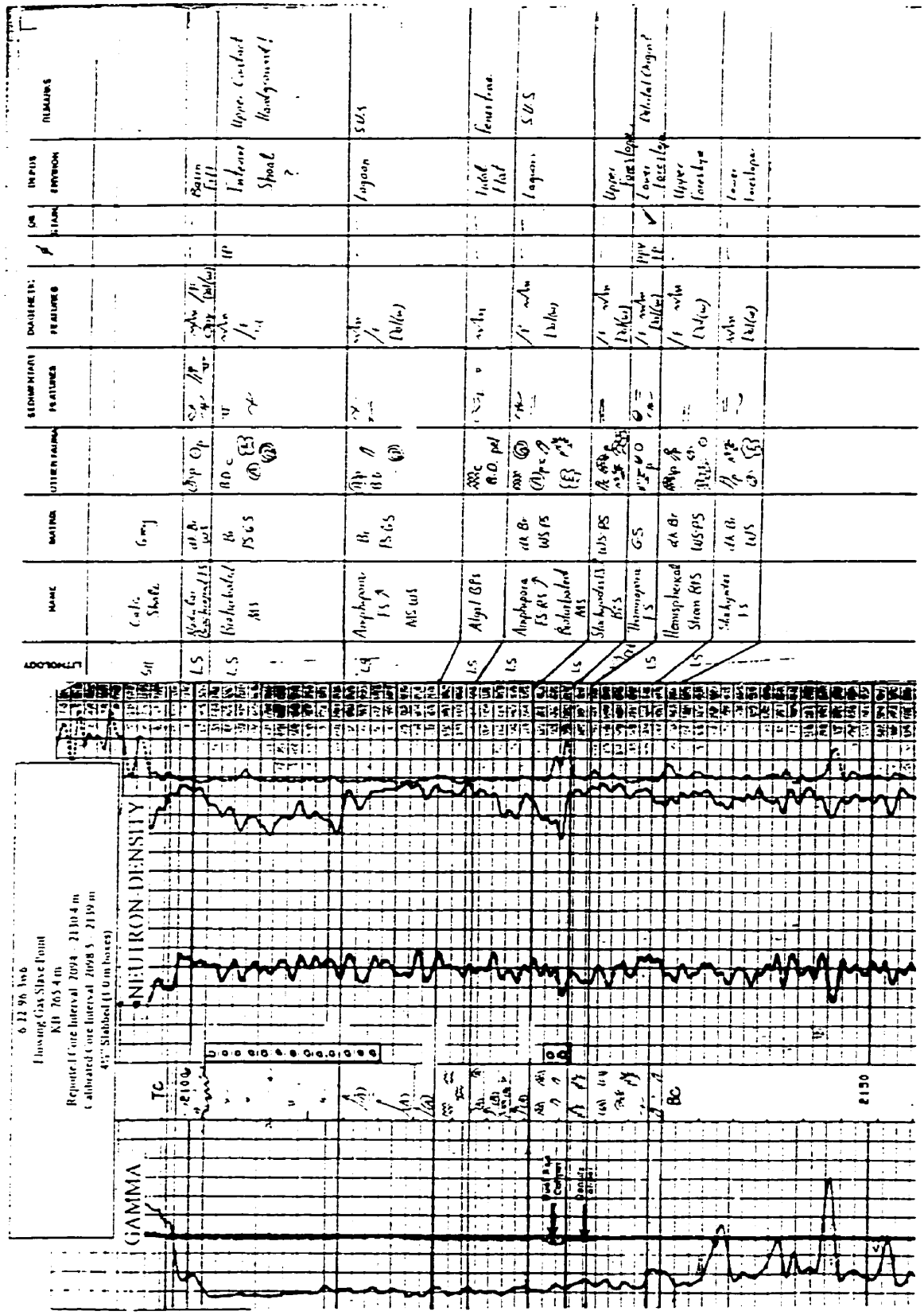
GAMMA
NEUTRON-DENSITY

NEUTRON-DENSITY
GAMMA
2100

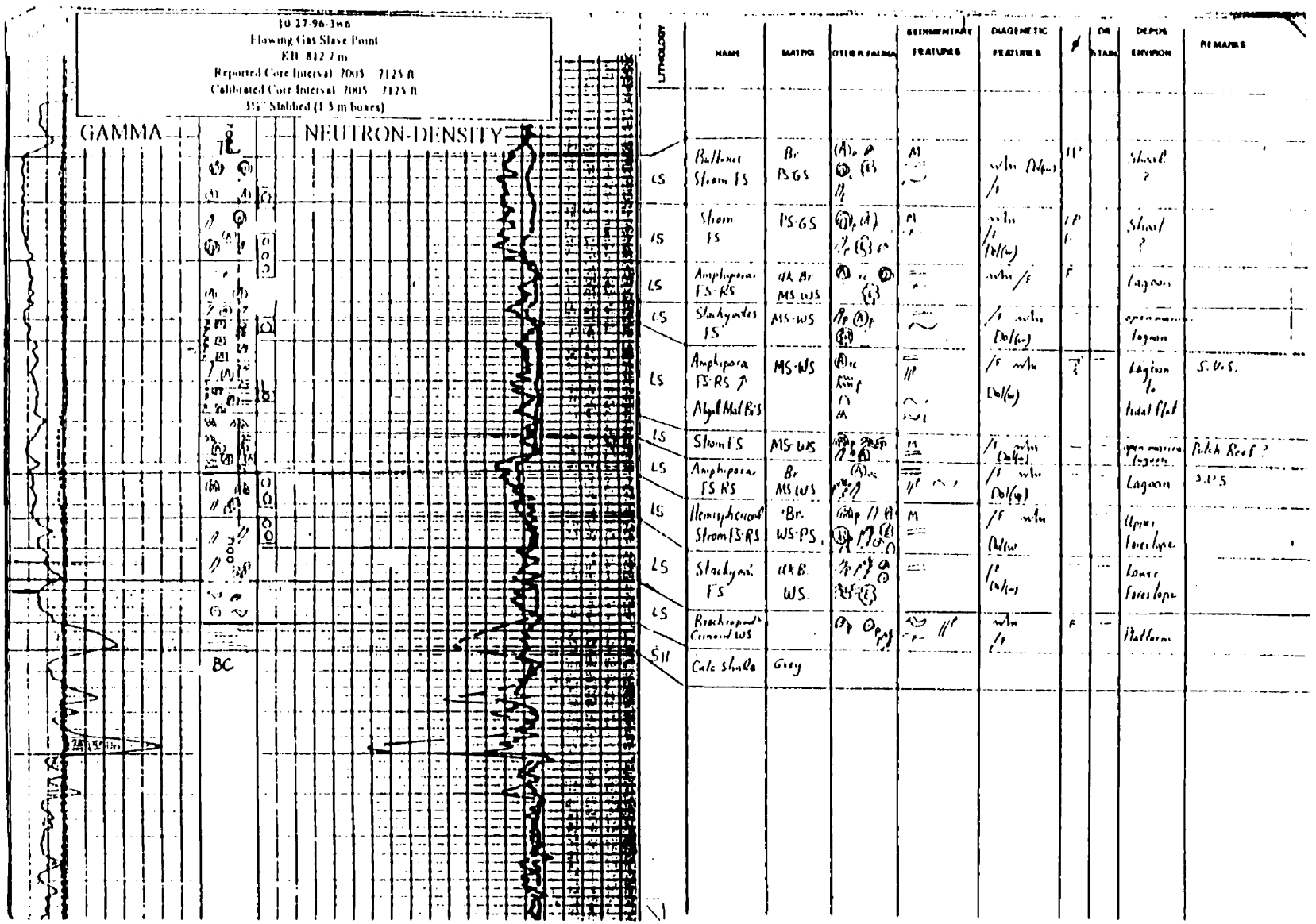
10-27-96-3w6
Flowing Gas Slave Point
KB 812.7 m
Reported Core Interval 7005 - 7125 ft
Calibrated Core Interval 7005 - 7125 ft
3½" Slabbed (1.5 m boxes)
GAMMA
NEUTRON-DENSITY
BC
LITHOLOGY
NAME
MATRIX
OTHER FAUNA
SEDIMENTARY FEATURES
DIAGENETIC FEATURES
POR
STAIN
DEPOS ENVIRON
REMARKS
LS
Shale
Sh

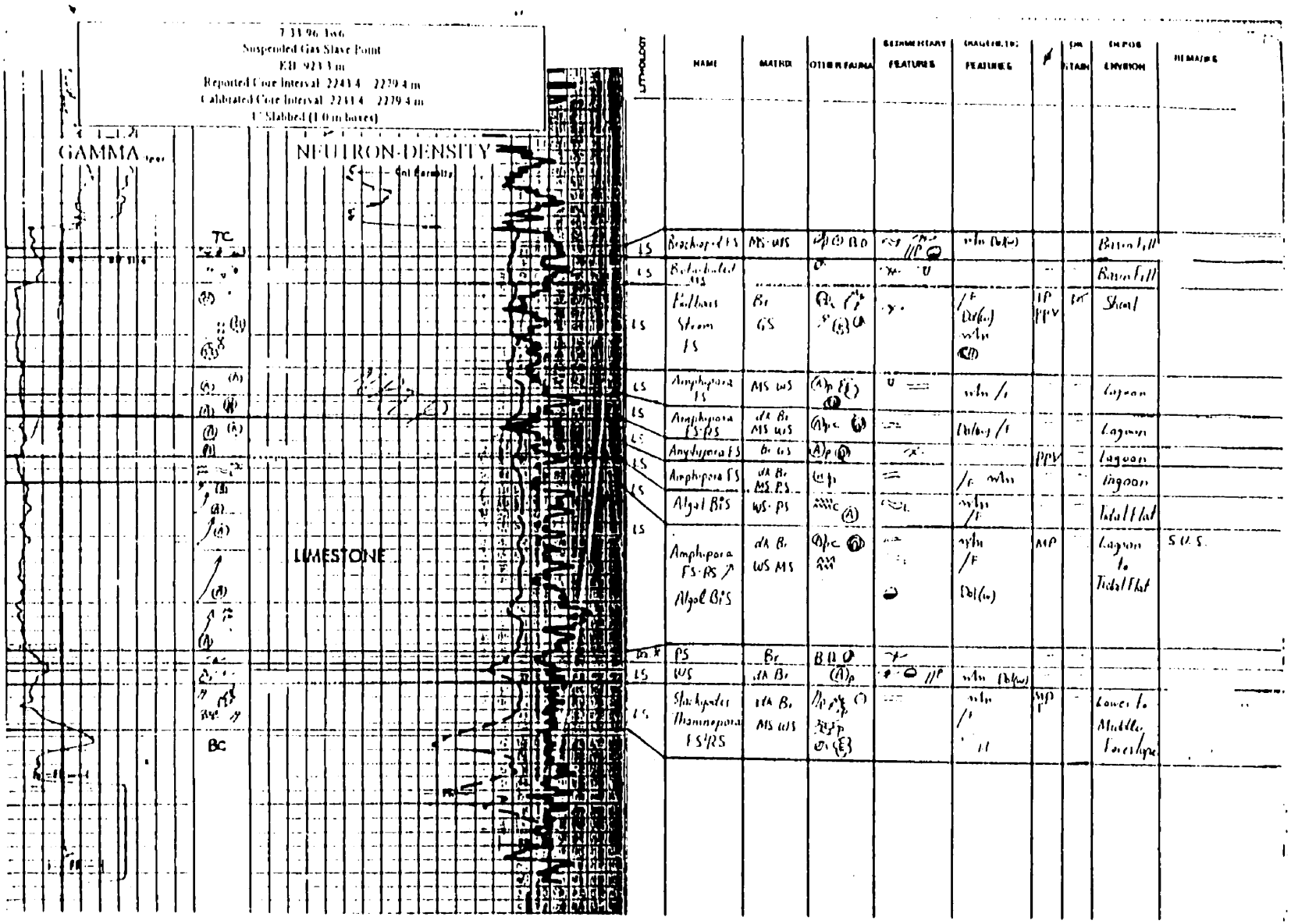
7-33-96 1x6
Suspended Gas Slave Point
KB 923.3 m
Reported Core Interval 2243.4 - 2279.4 m
Calibrated Core Interval 2243.4 - 2279.4 m
Slabbed (1.0 m boxes)
GAMMA
NEUTRON-DENSITY
TC
LIMESTONE
BC
LITHOLOGY
NAME
MATRIX
OTHER FAUNA
SEDIMENTARY FEATURES
DIAGENETIC FEATURES
POROSITY
STAIN
DEPOS ENVIRON
REMARKS
Backstone/FS
MS-WS
Bahamas Fill
Subtidal
WS
Bahamas Fill
Shoal
Fallbacks
Stream
FS
Br
GS
Lagoon
Amphipora FS
MS WS
Amphipora FS-RS
dA Br
MS WS
Amphipora FS
Algal BFS
WS-PS
Tidal Flat
Amphipora FS-RS
Algal BFS
dA Br
WS MS
Lagoon to Tidal Flat
S.U.S.
PS
Br
WS
dA Br
Stackpoles
Thamnopora FS/RS
dA Br
MS WS
Lower to Middle Lagoon

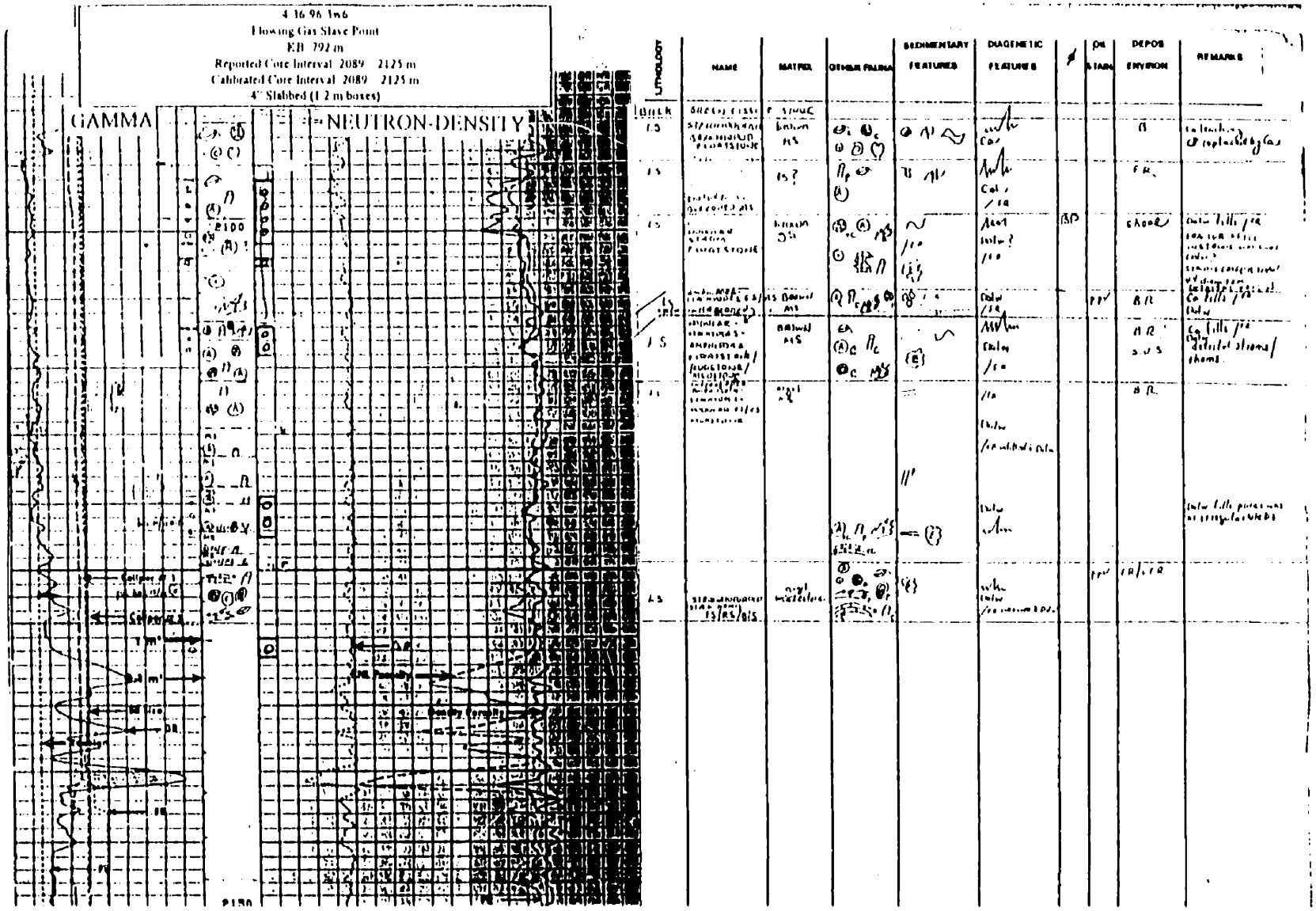
4-16-96 3m6
Flowing Gas Slave Point
KB 792 m
Reported Core Interval 2089 - 2125 m
Calibrated Core Interval 2089 - 2125 m
4" Slabbed (1.2 m boxes)
GAMMA
NEUTRON-DENSITY
LITHOLOGY
NAME
MATRIX
OTHER FILLING
SEDIMENTARY FEATURES
DIAGENETIC FEATURES
DEPOS ENVIRON
REMARKS

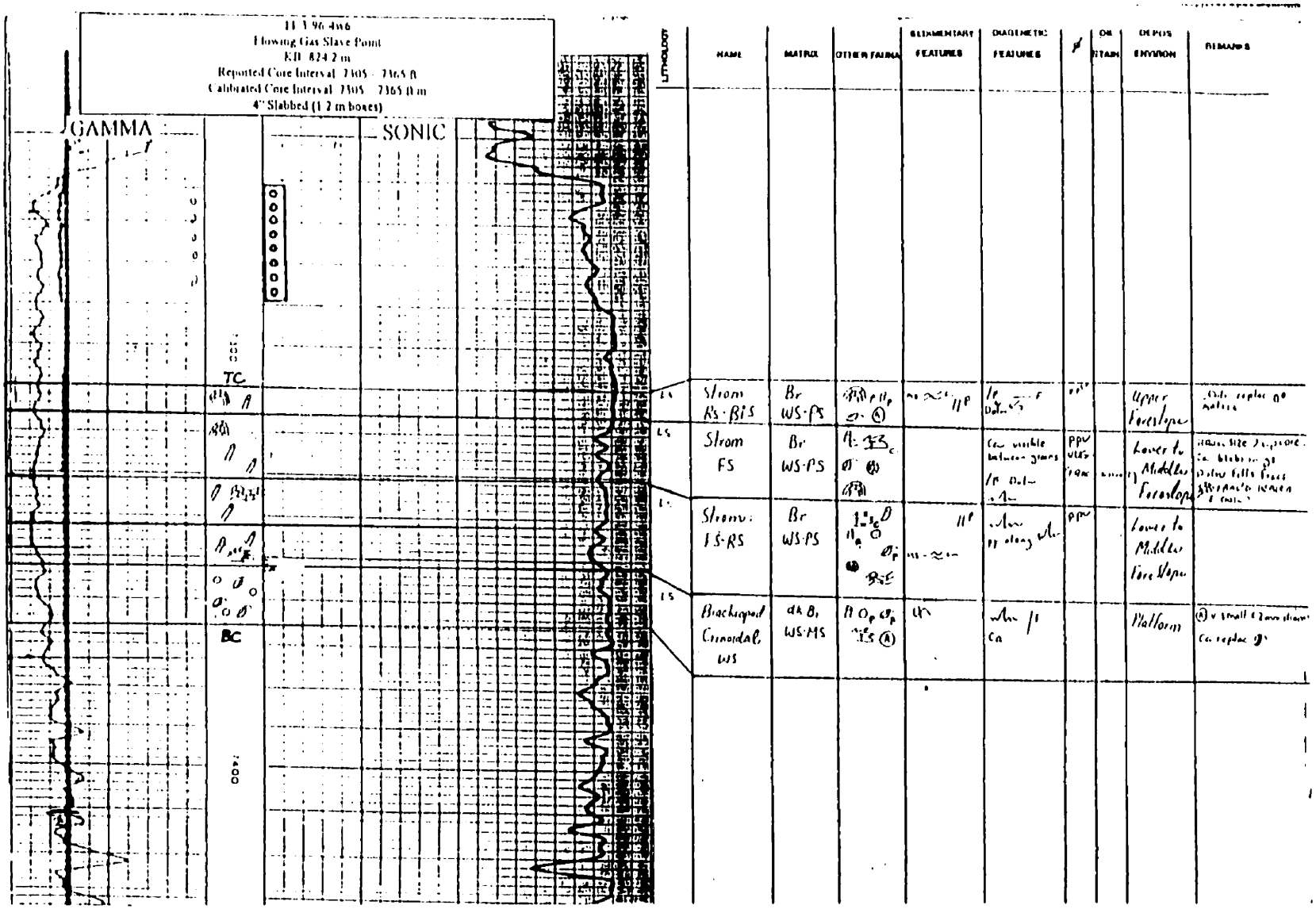
11-3 96-4w6
Flowing Gas Slave Point
KB 824.2 m
Reported Core Interval 7305 – 7365 ft
Calibrated Core Interval 7305 – 7365 ft m
4" Slabbed (1.2 m boxes)
GAMMA
SONIC
TC
BC
LITHOLOGY
NAME
MATRIX
OTHER FAUNA
SEDIMENTARY FEATURES
DIAGENETIC FEATURES
DEPOS ENVIRON
REMARKS
Strom Bs-BIS
Br WS-PS
Strom FS
Br WS-PS
Strom: FS-RS
Br WS-PS
Brachiopod Crinoidal WS
dk Br WS-MS
Upper Foreslope
Lower to Middle Foreslope
Lower to Middle Fore Slope
Platform

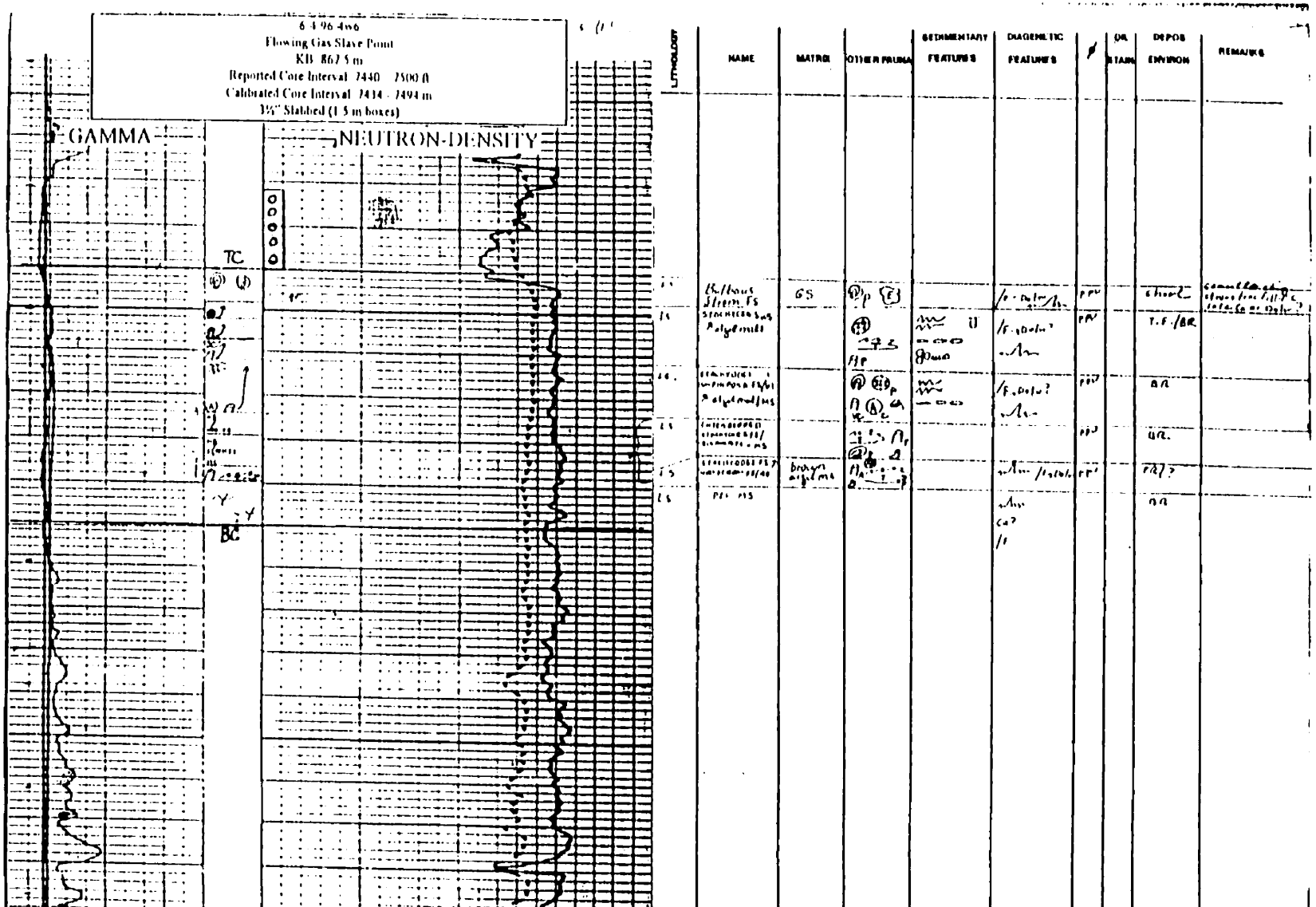
6-4-96-4w6
Flowing Gas Slave Point
KB 867.5 m
Reported Core Interval 7440 - 7500 ft
Calibrated Core Interval 7434 - 7494 m
3½" Slabbed (1.5 m boxes)
GAMMA
NEUTRON-DENSITY
TC
BC
LITHOLOGY
NAME
MATRIX
OTHER PRIMARY
SEDIMENTARY FEATURES
DIAGENETIC FEATURES
OIL STAIN
DEPOS ENVIRON
REMARKS

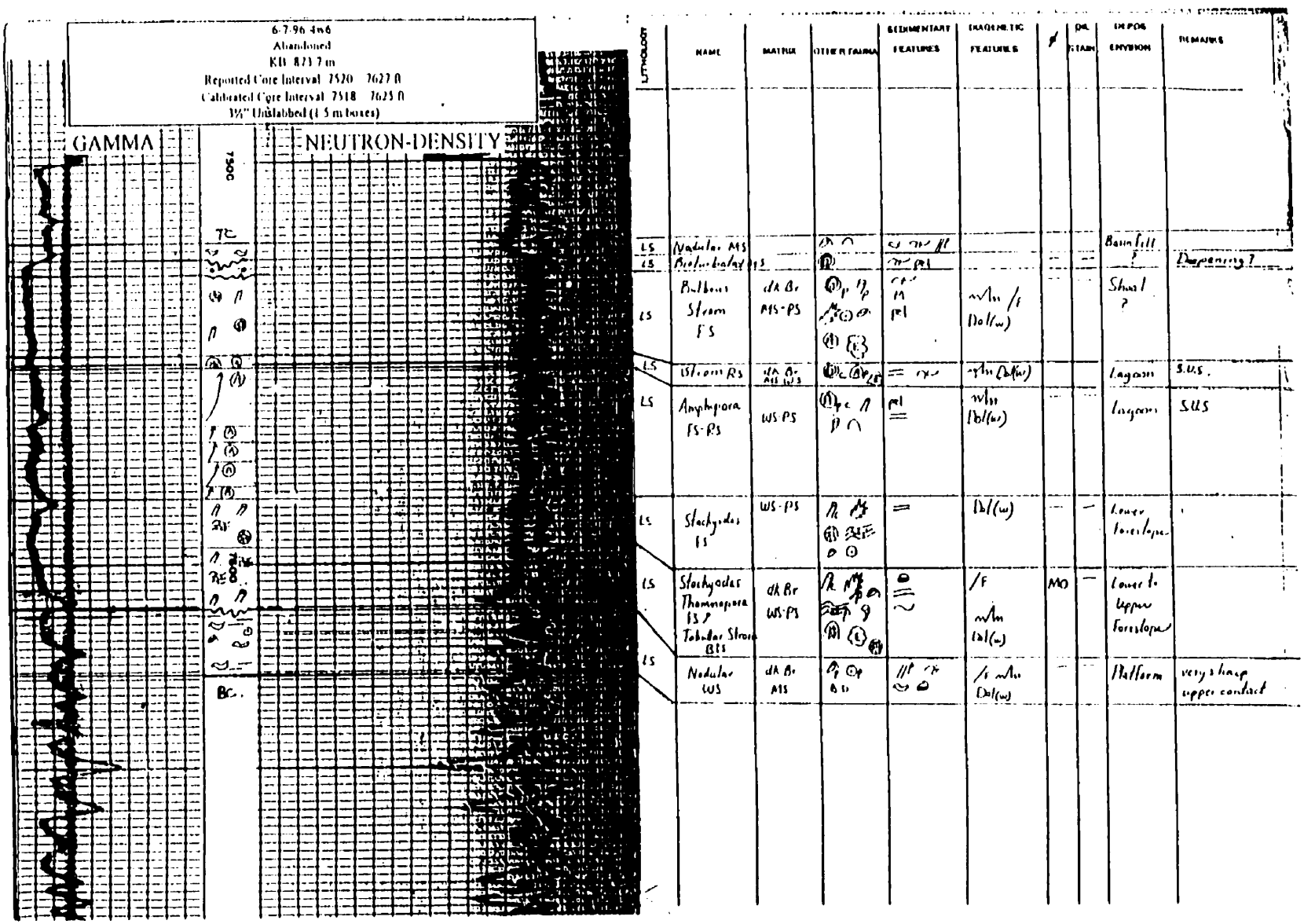
6-7-96 4w6
Abandoned
KB 873.7 m
Reported Core Interval 7520 7627 ft
Calibrated Core Interval 7518 7625 ft
3½" Unslabbed (1.5 m boxes)
GAMMA
NEUTRON-DENSITY
7500
TC
BC
LITHOLOGY
NAME
MATRIX
OTHER FAUNA
SEDIMENTARY FEATURES
DIAGENETIC FEATURES
DEPOSITION
REMARKS
LS Nodular MS Baumgill
LS Bioturbated WS ? Deepening ?
LS Bulbous Stromatoporoid FS dk Br MS-PS Shoal ?
LS Stromatoporoid RS dk Br MS WS Lagoon S.U.S.
LS Amphipora FS-RS WS PS Lagoon S.U.S
LS Stachyodes FS WS-PS Lower foreslope
LS Stachyodes Thamnopora FS ? Tabular Stromatoporoid BFS dk Br WS-PS MO Lower to Upper Foreslope
LS Nodular WS dk Br MS Platform very sharp upper contact

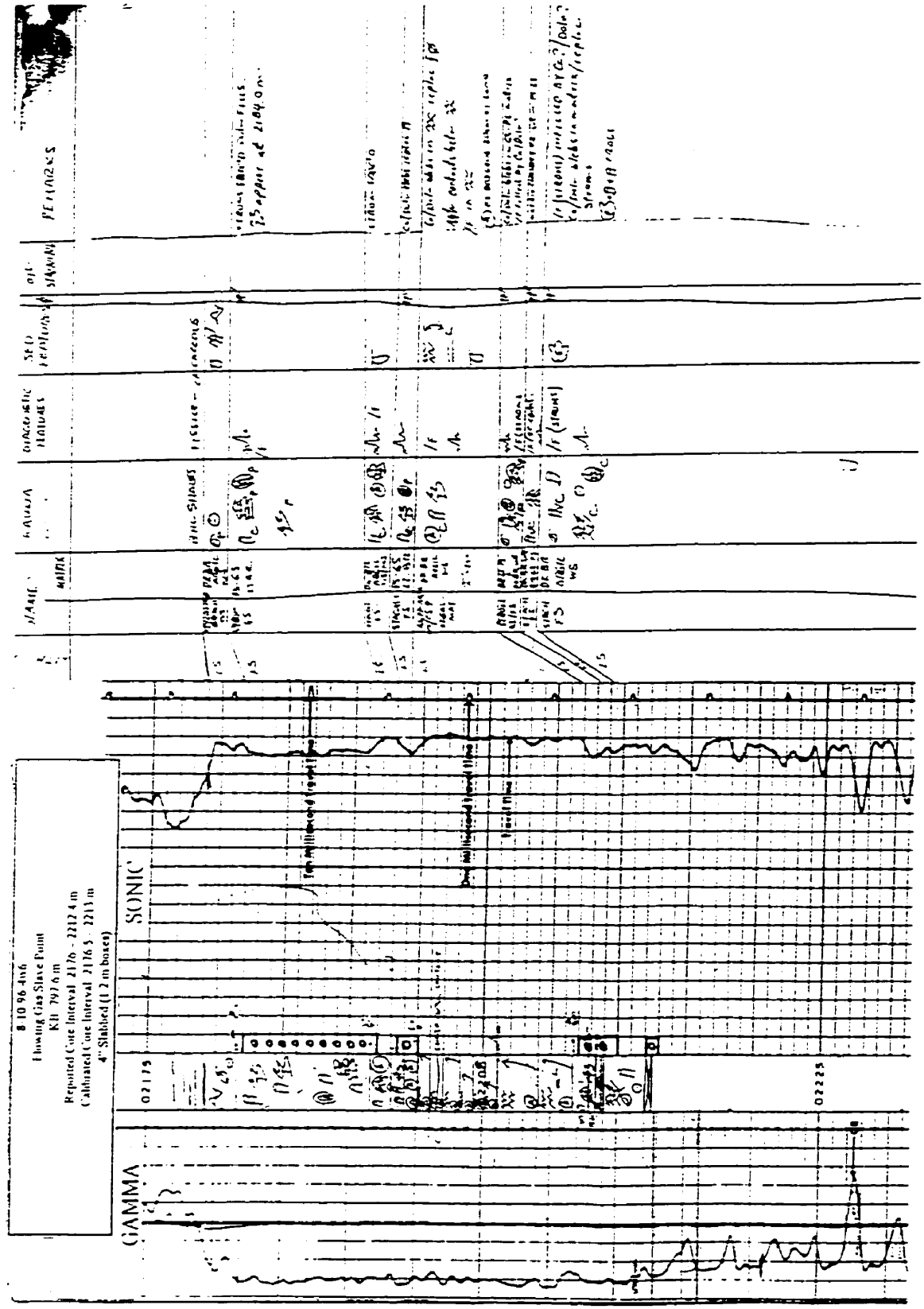
SONIC
GAMMA
02175
02225

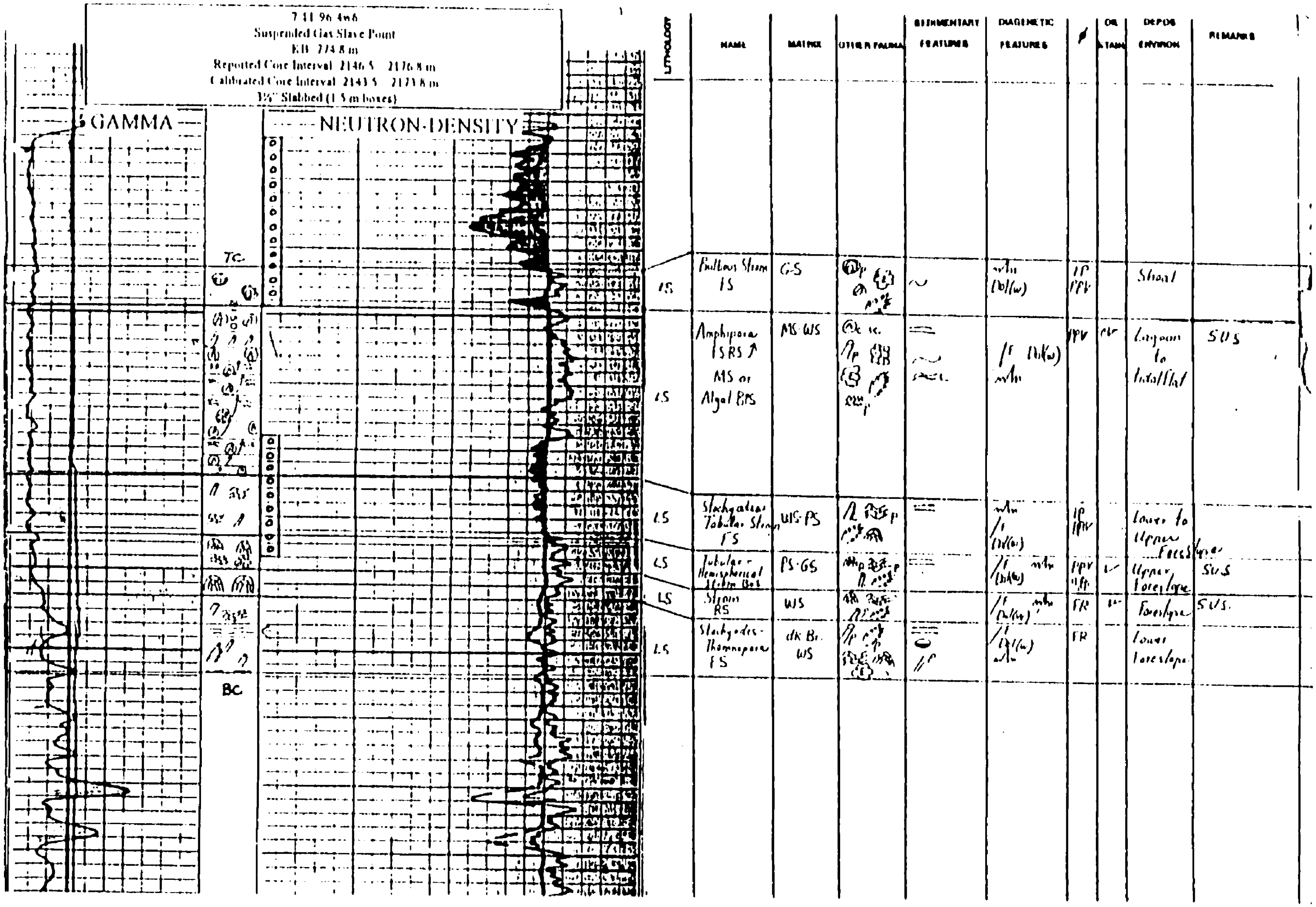
7-11-96-4w6
Suspended Gas Slave Point
KB 774.8 m
Reported Core Interval 2146.5 – 2176.8 m
Calibrated Core Interval 2143.5 – 2173.8 m
3½" Slabbed (1.5 m boxes)
GAMMA
NEUTRON-DENSITY
LITHOLOGY
NAME
MATRIX
OTHER FAUNA
SEDIMENTARY FEATURES
DIAGENETIC FEATURES
OIL STAIN
DEPOS ENVIRON
REMARKS
TC
BC
LS
Bulbous Strom FS
GS
Shoal
Amphipora FS RS
MS or Algal BtS
MS-WS
Lagoon to Intertidal
SUS
Stachyodes Tabular Strom FS
WS-PS
Lower to Upper Foreslope
Tabular-Hemispherical Strom Bds
PS-GS
Upper Foreslope
Strom RS
WS
Foreslope
Stachyodes-Thamnopora FS
dk Br. WS
Lower Foreslope

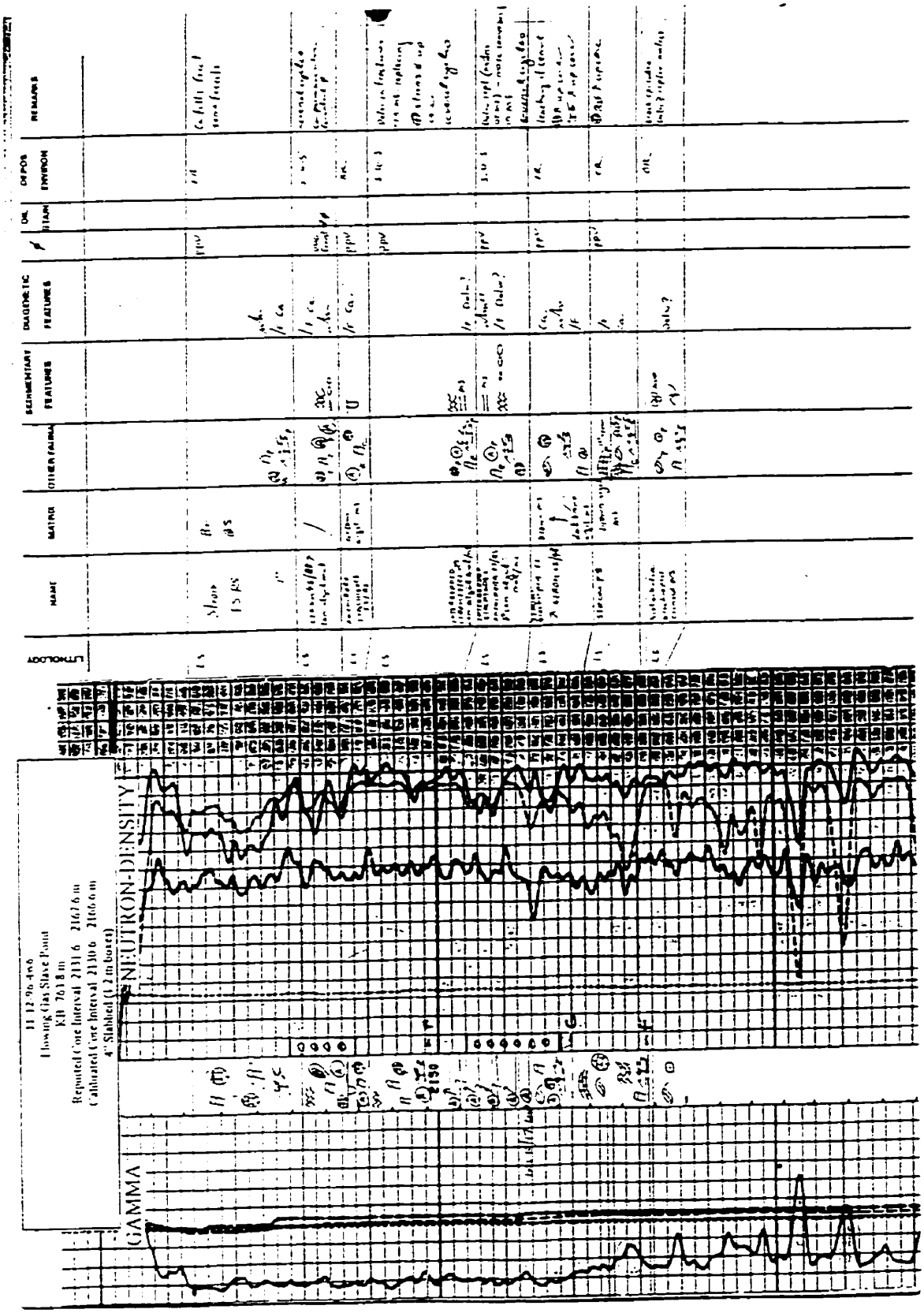
GAMMA
NEUTRON-DENSITY

1 11 96 4n6
Lowing Gas Slave Point
Kb 754.9 m
Reported Core Interval 2198 2214 ft
Calculated Core Interval 2193 2213 m
4" Slabbed (12 inchers)
GAMMA
SONIC
LITHOLOGY
NAME
MATRIX
OTHER FAUNA
SEDIMENTARY FEATURES
DIAGENETIC FEATURES
OIL STAIN
DEPOS ENVIRON
REMARKS

GAMMA
NEUTRON-DENSITY
2150

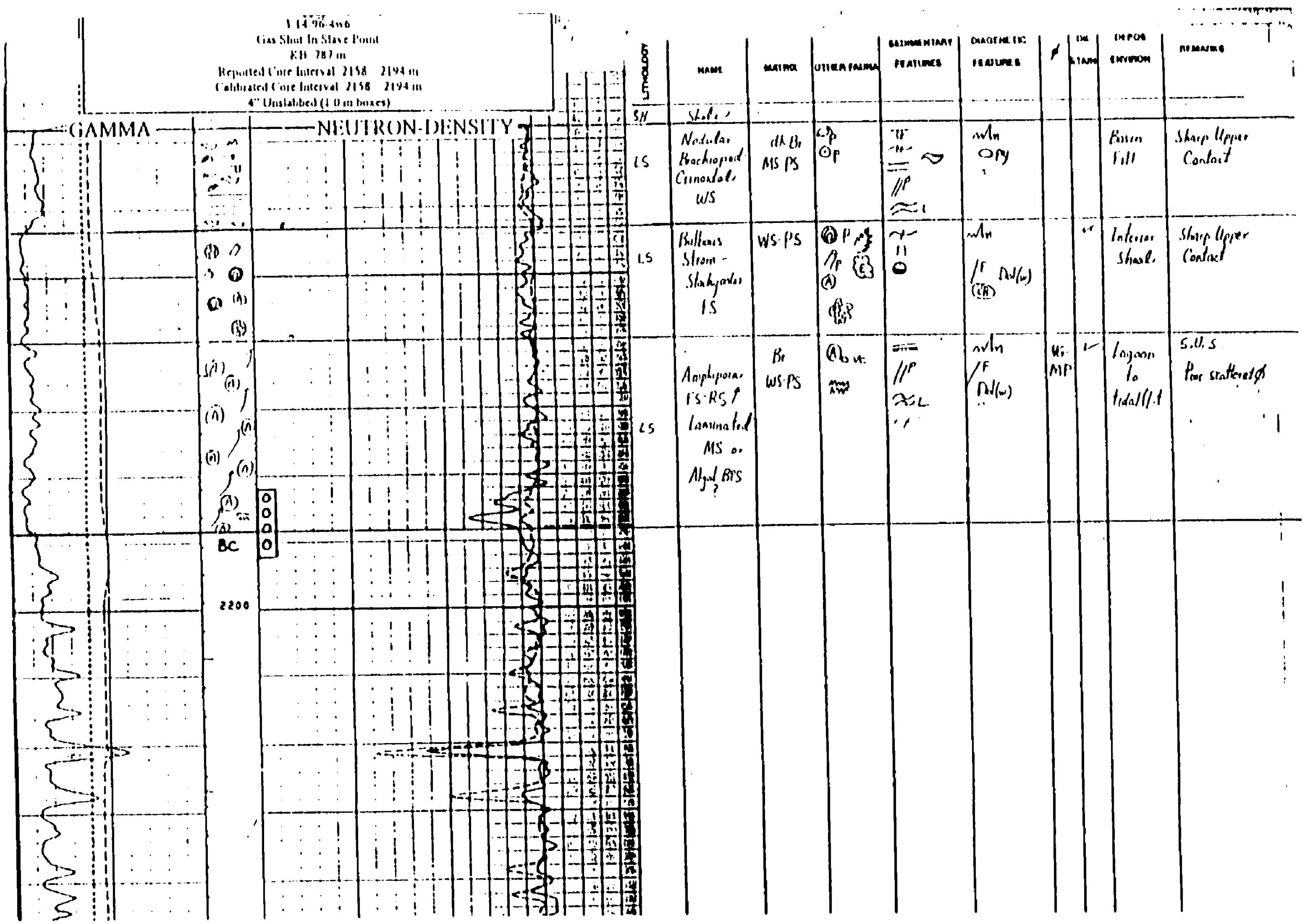
1-14-96-4w6
Gas Shut In Slave Point
KB 787 m
Reported Core Interval 2158 - 2194 m
Calibrated Core Interval 2158 - 2194 m
4" Unslabbed (1.0 m boxes)
GAMMA
NEUTRON-DENSITY
LITHOLOGY
NAME
MATRIX
OTHER FAUNA
SEDIMENTARY FEATURES
DIAGENETIC FEATURES
DEPOS ENVIRON
REMARKS
BC
2200
SH
Shale ?
LS
Nodular Brachiopod Crinoidal WS
dk Br MS PS
Basin Fill
Sharp Upper Contact
LS
Bullous Strom - Stachyodes FS
WS-PS
Interior Shoal
Sharp Upper Contact
LS
Amphipora FS-RS ? Laminated MS or Algal BTS ?
Br WS-PS
Lagoon to Tidal Flat
S.U.S
Poor scattered ø

GAMMA RAY
NEUTRON-DENSITY
11-17-96 4m6
Gas Shut In Slave Point
KB 814.1 m
Reported Core Interval 7250 - 7270 ft
Calibrated Core Interval 7256 - 7276 ft
4" Slabbed (1.2 m bases)
7400

GAMMA
NEUTRON-DENSITY
11-18 96 4m6
Flowing Gas Slave Point
AB 849 7 m
Repeated Core Interval 2270 - 2290.6 m
Calibrated Core Interval 2270 - 2290.6 m
4" Slabbed (1.2 m boxes)
2300

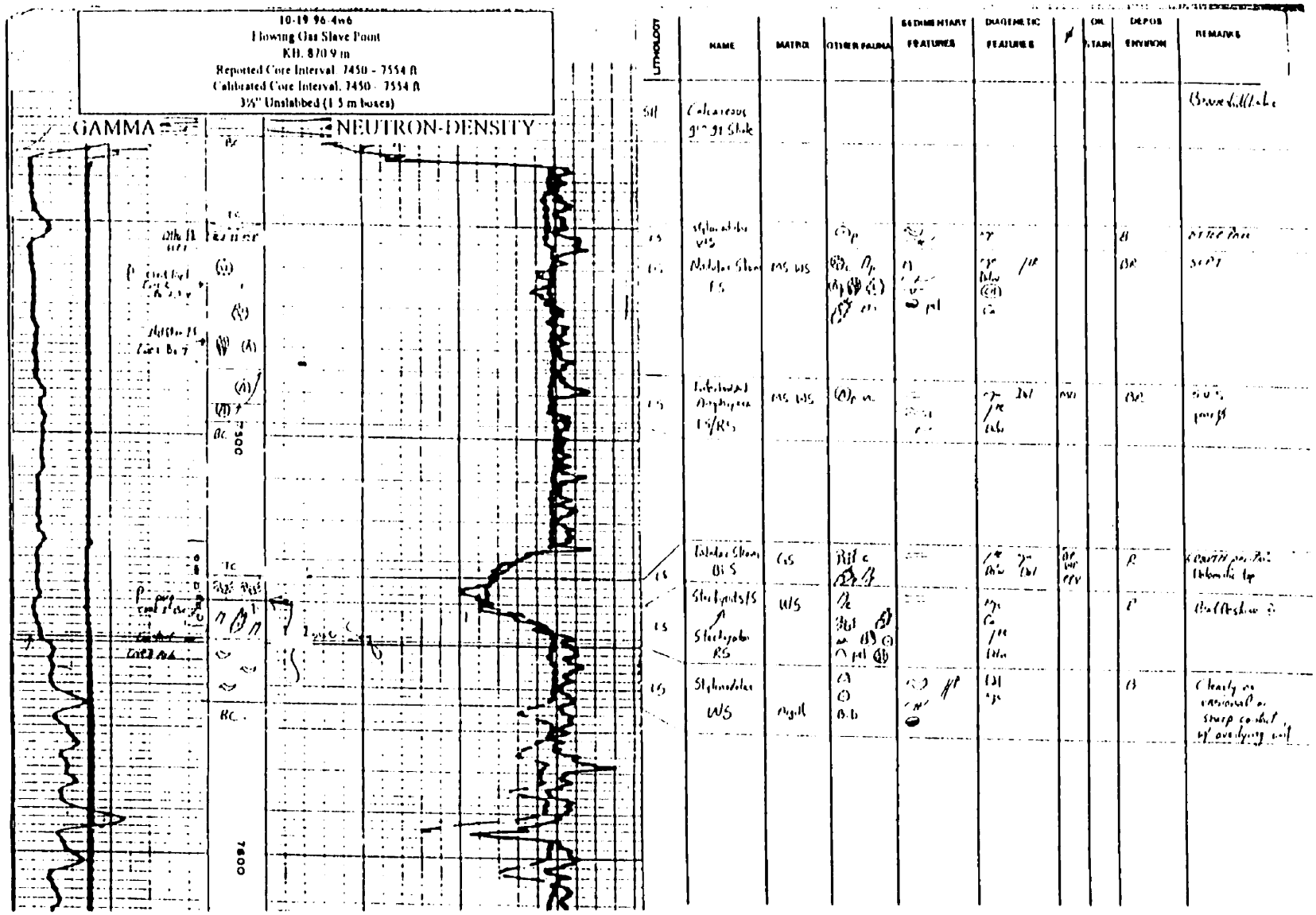
10-19-96-4w6
Flowing Gas Slave Point
KB. 870.9 m
Reported Core Interval: 7450 - 7554 ft
Calibrated Core Interval: 7450 - 7554 ft
3½" Unslabbed (1.5 m boxes)
GAMMA
NEUTRON-DENSITY
LITHOLOGY
NAME
MATRIX
OTHER FAUNA
SEDIMENTARY FEATURES
DIAGENETIC FEATURES
POROSITY
OIL STAIN
DEPOS ENVIRON
REMARKS
7500
7600

11-20 96-4w6
Flowing Gas Slave Point
KB. 825.1 m
Reported Core Interval 7281 - 7400 ft
Calibrated Core Interval 7281 - 7400 ft
3½" Slabbed (1.5 m lost)
GAMMA
NEUTRON-DENSITY
LITHOLOGY
NAME
MATRIX
OTHER FAUNA
SEDIMENTARY FEATURES
FRACTURE INDUCED FEATURES
DEPOS ENVIRON
REMARKS
7400

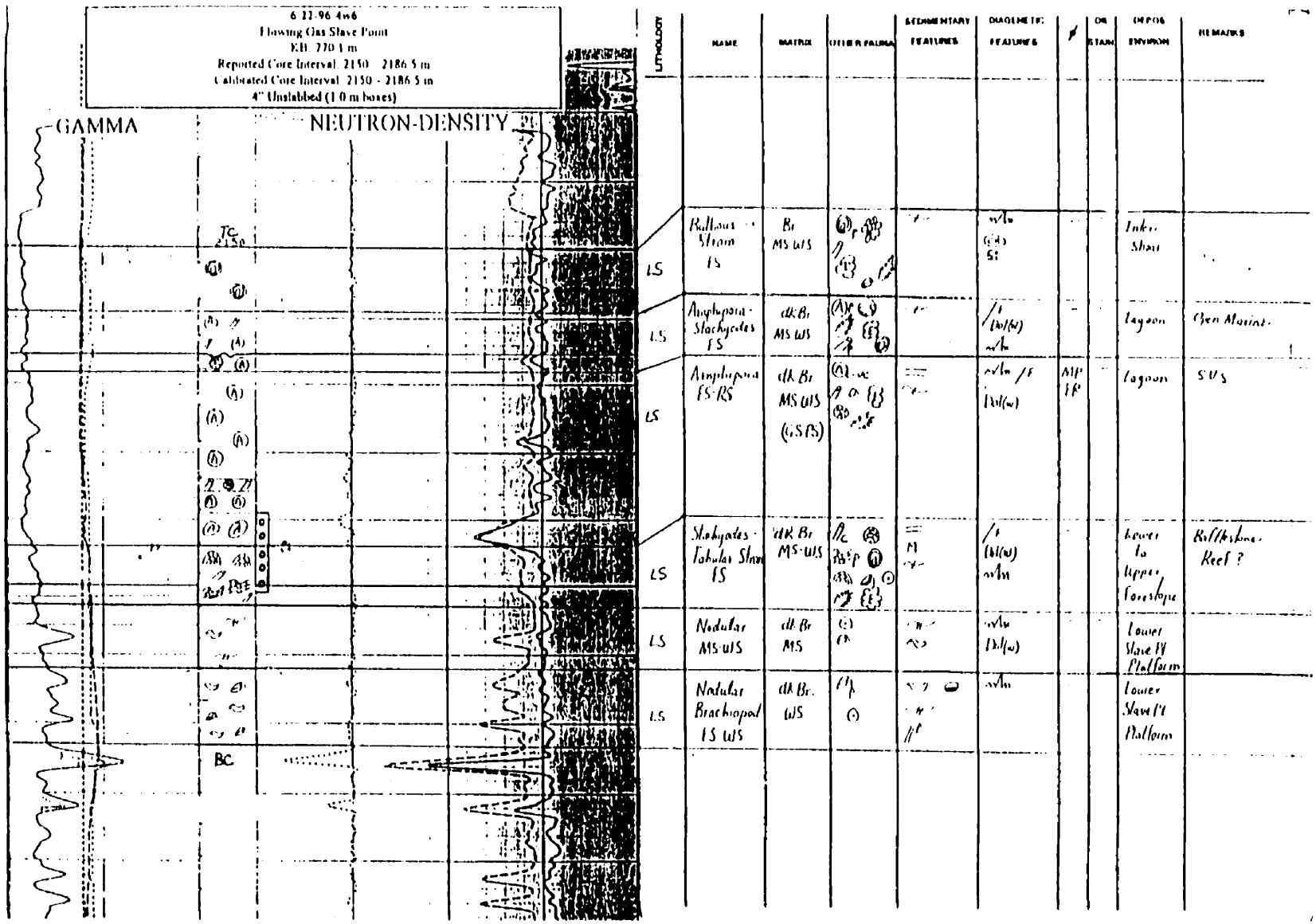
6-22-96 4w6
Flowing Gas Slave Point
KB: 770.1 m
Reported Core Interval: 2150 - 2186.5 m
Calibrated Core Interval: 2150 - 2186.5 m
4" Unslabbed (1.0 m boxes)
GAMMA
NEUTRON-DENSITY
Tc
2150
BC
LITHOLOGY
NAME
MATRIX
OTHER PARTS
SEDIMENTARY FEATURES
DIAGENETIC FEATURES
DEPOS ENVIRON
REMARKS
LS
Ballous - Strom FS
Br MS WS
Inter. Shal
Amphipora - Stachycides FS
dk Br MS WS
Lagoon
Open Marine
Amphipora FS-RS
dk Br MS WS (GSPS)
MP HP
Lagoon
SVS
Stachycides - Tabular Shm FS
dk Br MS-WS
lower to upper Foreslope
Reef Rubble Reef ?
Nodular MS-WS
dk Br MS
Lower Slave Pt Platform
Nodular Brachiopod FS WS
dk Br. WS
Lower Slave Pt Platform

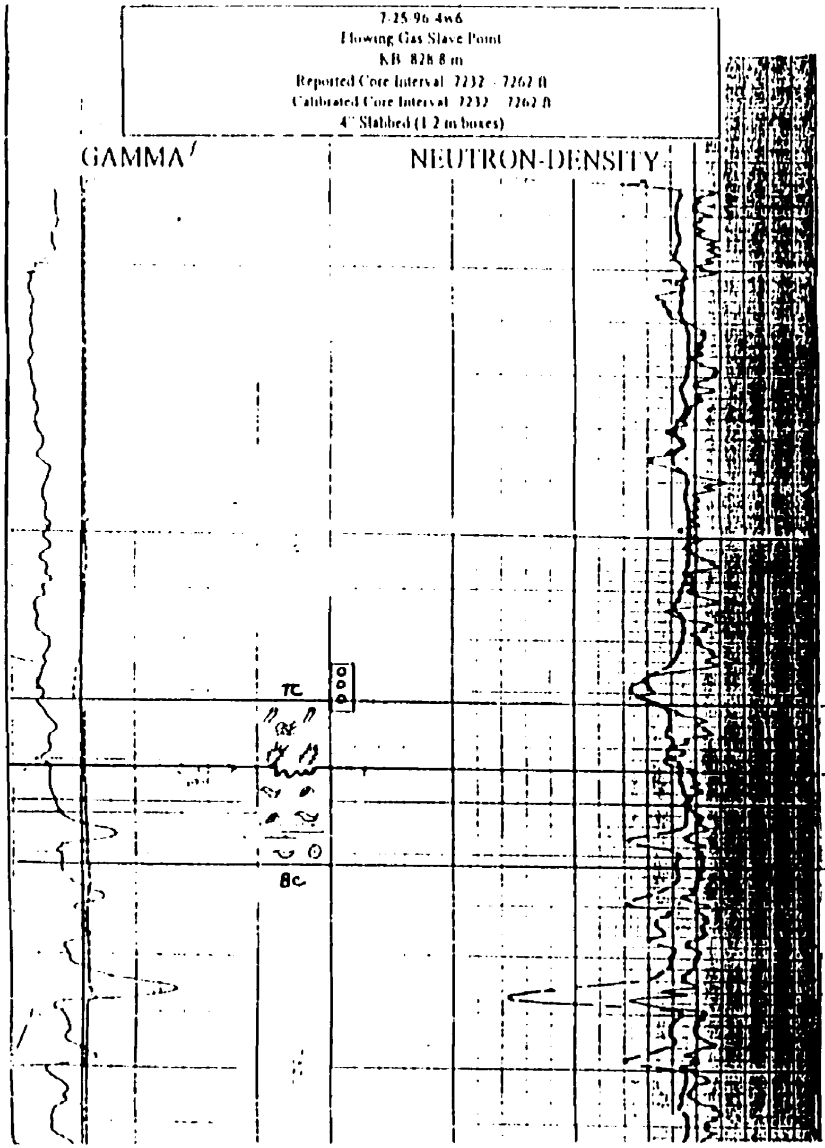

LITHOLOGY	NAME	MATRIX	OTHER FAUNA	SEDIMENTARY FEATURES	DIAGENETIC FEATURES	ø	OIL STAIN	DEPOS ENVIRON	REMARKS
LS	Stachyodes Thamnopora FS	dk Br MS WS		//P	/F	IR LG	—	Lower foreslope	Rubblestone, 'Reef'?
LS	Nodular, Brachiopod Crinoid FS	dk Br MS WS		//P	Dol(w)	—	—	Lower Slave Pt Platform	

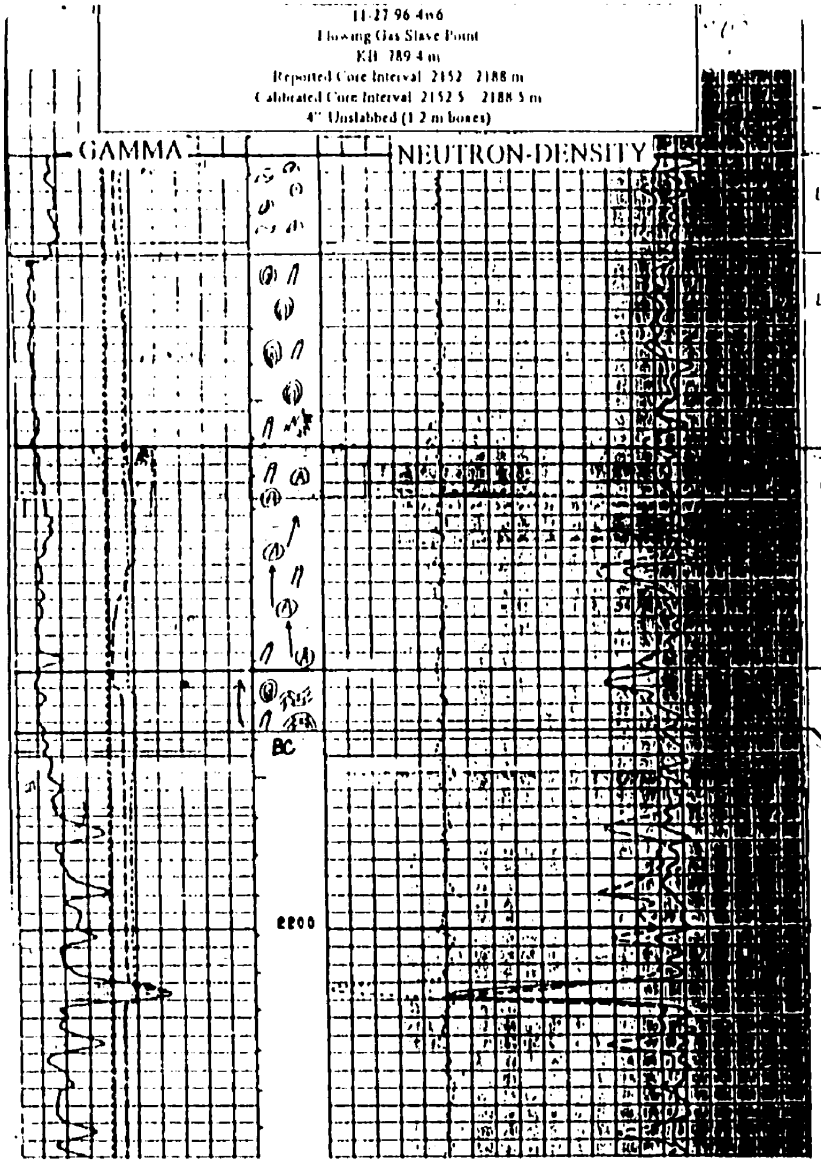

LITHOLOGY	NAME	MATRIX	OTHER FAUNA	SEDIMENTARY FEATURES	DIAGENETIC FEATURES	φ	OIL STAIN	DEPOS ENVIRON	REMARKS
LS	Nodular Brachiopod WS	dl Br MS WS						Basin fill	pool Upper Slave Pt
LS	Strom IS RS (B.Shower)	Br MS PS						Interior Shelf	
LS	Amphipora IS-RS / Laminated MS	Br MS PS						Lagoon / Tidal flat ?	
LS	Strom RS BFS	Br MS-WS						Lower to Upper Foreslope	

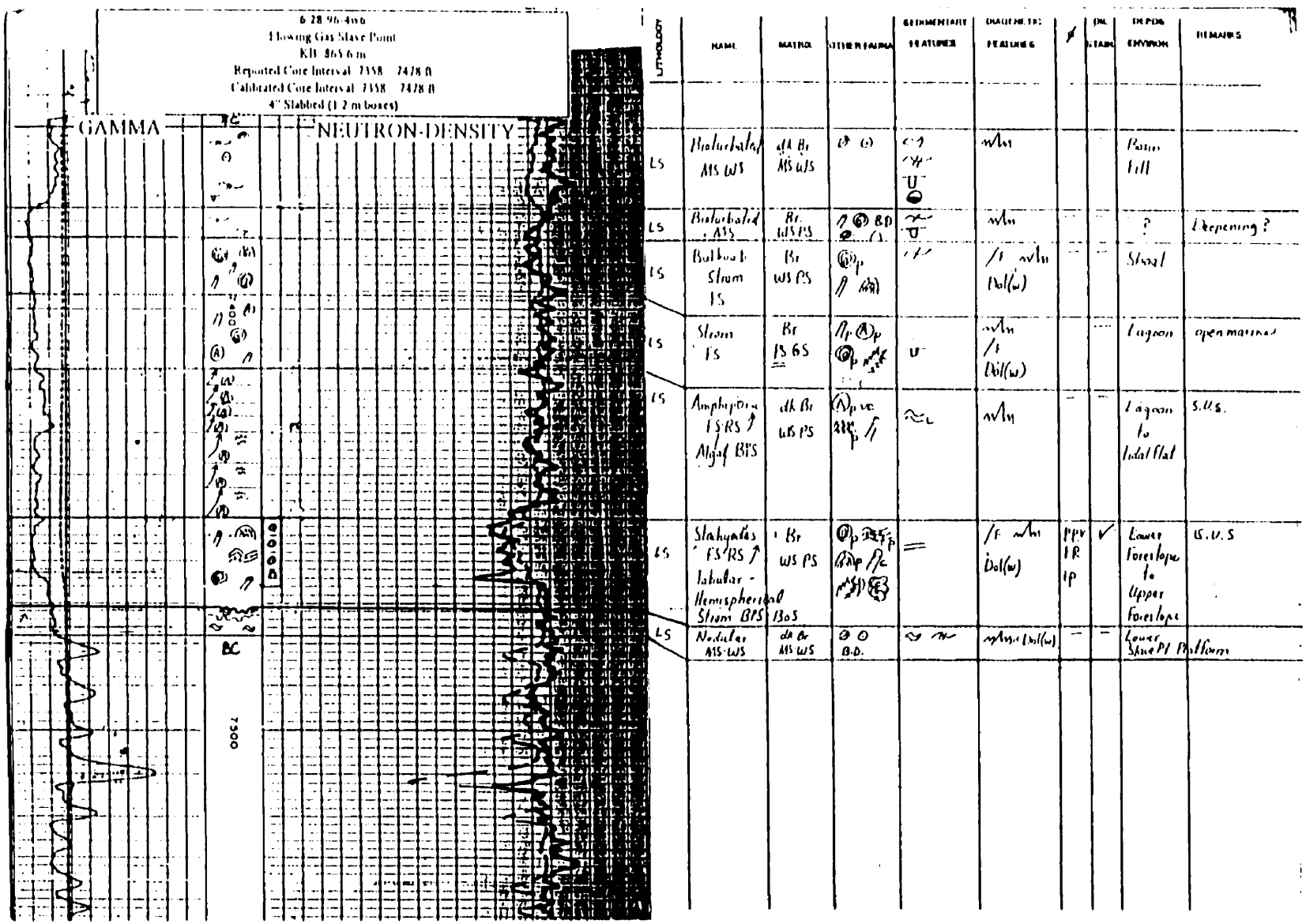
6 28 96-4w6
Flowing Gas Slave Point
KB 965.6 m
Reported Core Interval 7358 7478 ft
Calibrated Core Interval 7358 7478 ft
4" Slabbed (1.2 m bones)
GAMMA
NEUTRON-DENSITY
BC
7500
LITHOLOGY
NAME
MATRIX
OTHER FAUNA
SEDIMENTARY FEATURES
DIAGENETIC FEATURES
POR. STAIN
DEPOS. ENVIRON
REMARKS
LS
Bioturbated MS WS
dk Br MS WS
B.D.
Palm Hill
LS
Bioturbated MS
Br WS PS
B.D.
?
Deepening?
LS
Bulbous Stram FS
Br WS PS
Shoal
LS
Stram FS
Br FS GS
Lagoon
open marine
LS
Amphipora FS/RS ↑ Algal BFS
dk Br WS PS
S.U.S.
Lagoon to Intidal flat
LS
Stahyatles FS/RS ↑ Tabular - Hemispherical Stram BPS
Br WS PS
Bio S
PPP IP
Lower Foreslope to Upper Foreslope
U.S.S
LS
Nodular MS-WS
dk Br MS WS
B.D.
Lower Shoal/Platform

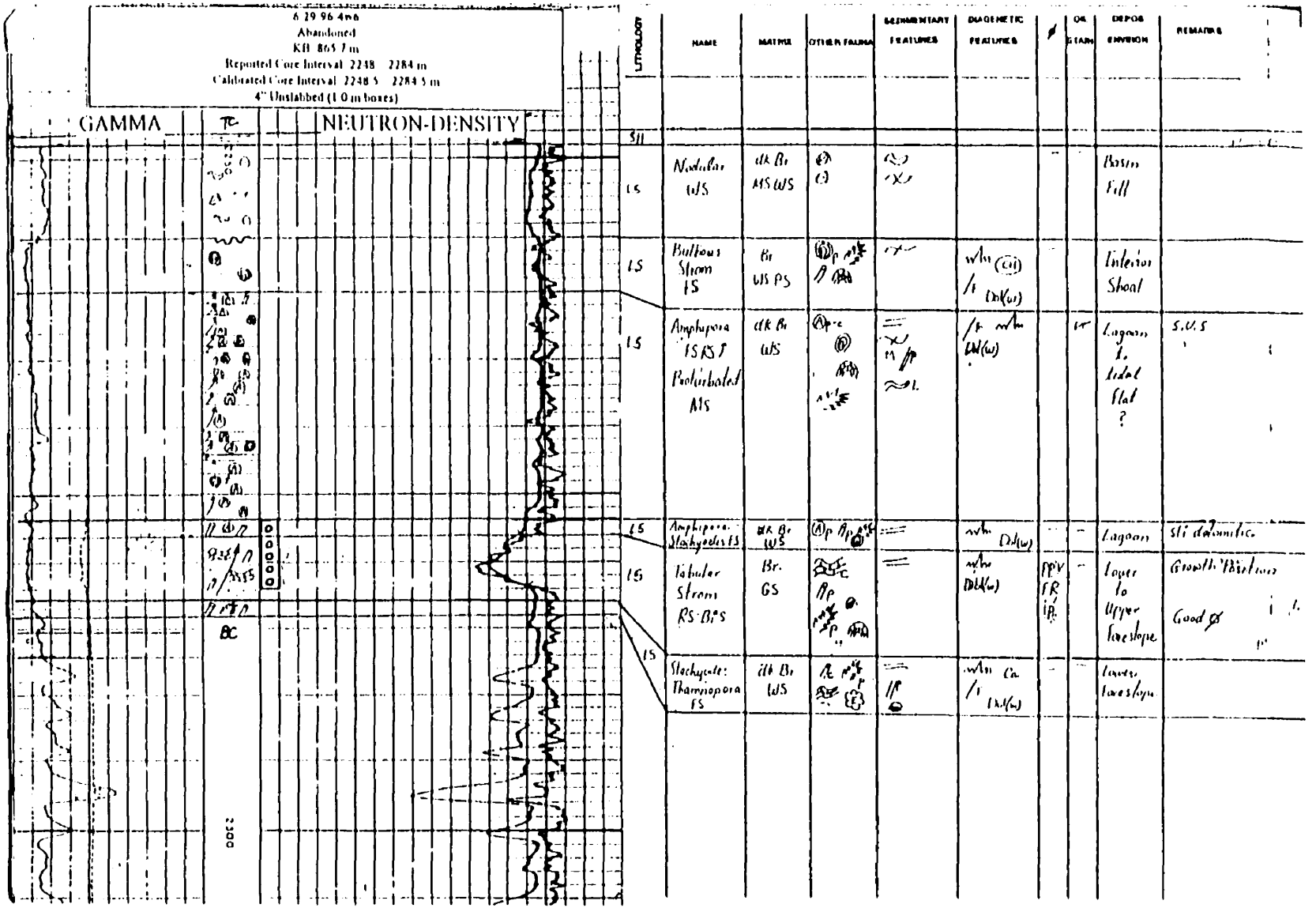
6 29 96 4n6
Abandoned
KB 865.7 m
Reported Core Interval 2248 - 2284 m
Calibrated Core Interval 2248.5 - 2284.5 m
4" Unslabbed (1.0 m boxes)
GAMMA
NEUTRON-DENSITY
LITHOLOGY
NAME
MATRIX
OTHER FAUNA
SEDIMENTARY FEATURES
DIAGENETIC FEATURES
POR
OIL STAIN
DEPOS ENVIRON
REMARKS
SH
LS
Nodular WS
dk Br MS WS
Basin Fill
Bulbous Stram FS
Br WS PS
Inferior Shoal
Amphipora FS/S T Prolirbated MS
dk Br WS
Lagoon L. Tidal Flat ?
S.U.S
Amphipora Stachyodes FS
dk Br WS
Lagoon
sli dolomitic
Tabular Stram RS-BrS
Br. GS
Lower to Upper foreslope
Growth Platform
Good
Stachyodes Thamnopora FS
dk Br WS
Lower foreslope

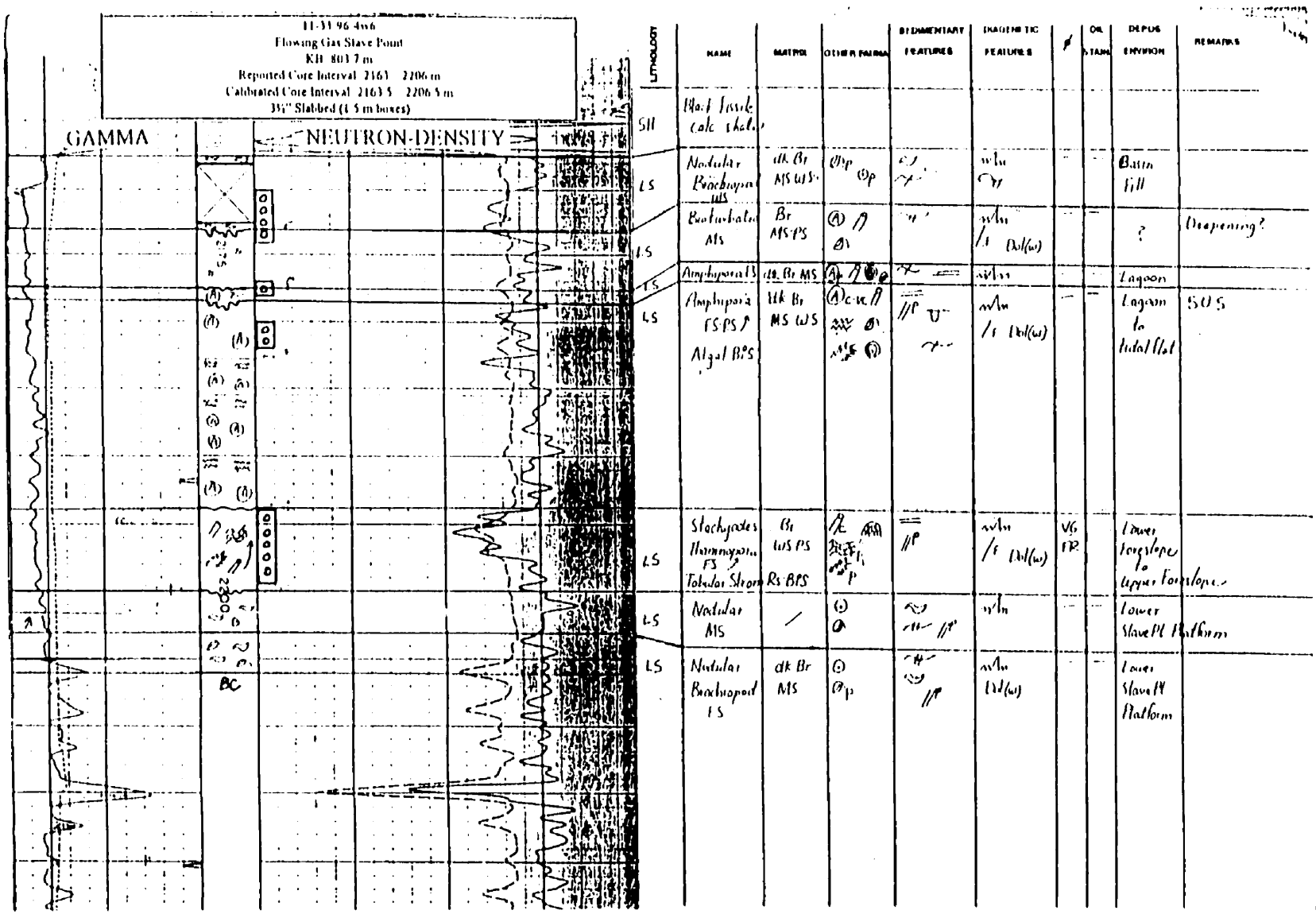
11-31 96-4w6
Flowing Gas Slave Point
KB 801.7 m
Reported Core Interval 2163 2206 m
Calibrated Core Interval 2163.5 2206.5 m
3½" Slabbed (1.5 m boxes)
GAMMA
NEUTRON-DENSITY
LITHOLOGY
NAME
MATRIX
OTHER PARMS
SEDIMENTARY FEATURES
DIAGENETIC FEATURES
OIL STAIN
DEPOS ENVIRON
REMARKS
SH
LS
Nodular Bioturbated MS
Amphipora FS-PS
Algal BPS
Stachyodes Hermanyoa FS
Tabular Strom
Nodular MS
Nodular Brachiopod FS
BC

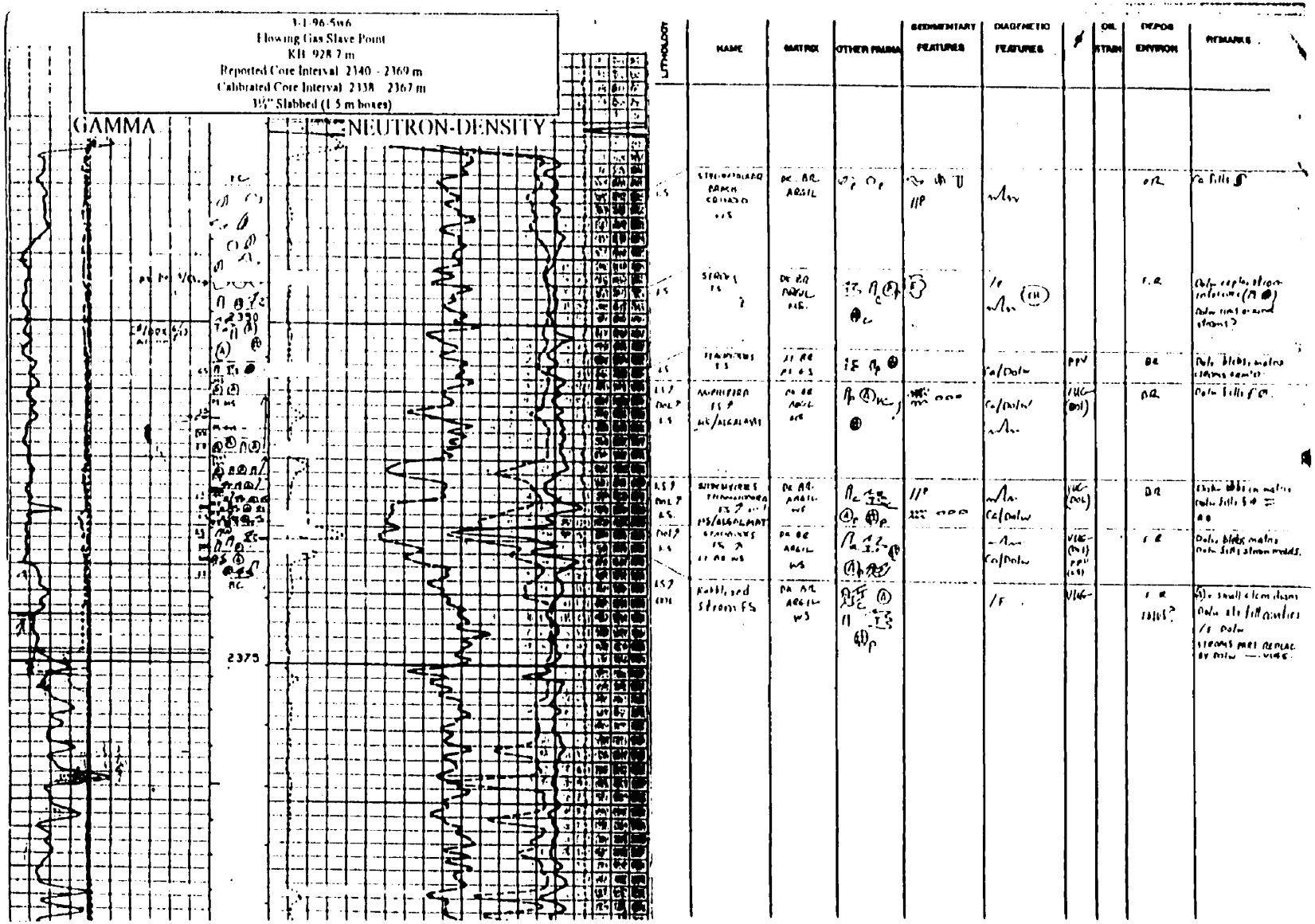
3-1-96-5w6
Flowing Gas Slave Point
KB 928.7 m
Reported Core Interval 2340 - 2369 m
Calibrated Core Interval 2338 - 2367 m
3½" Slabbed (1.5 m boxes)
GAMMA
NEUTRON-DENSITY
LITHOLOGY
NAME
MATRIX
OTHER PHASE
SEDIMENTARY FEATURES
DIAGENETIC FEATURES
OIL STAIN
DEPOS ENVIRON
REMARKS
2375

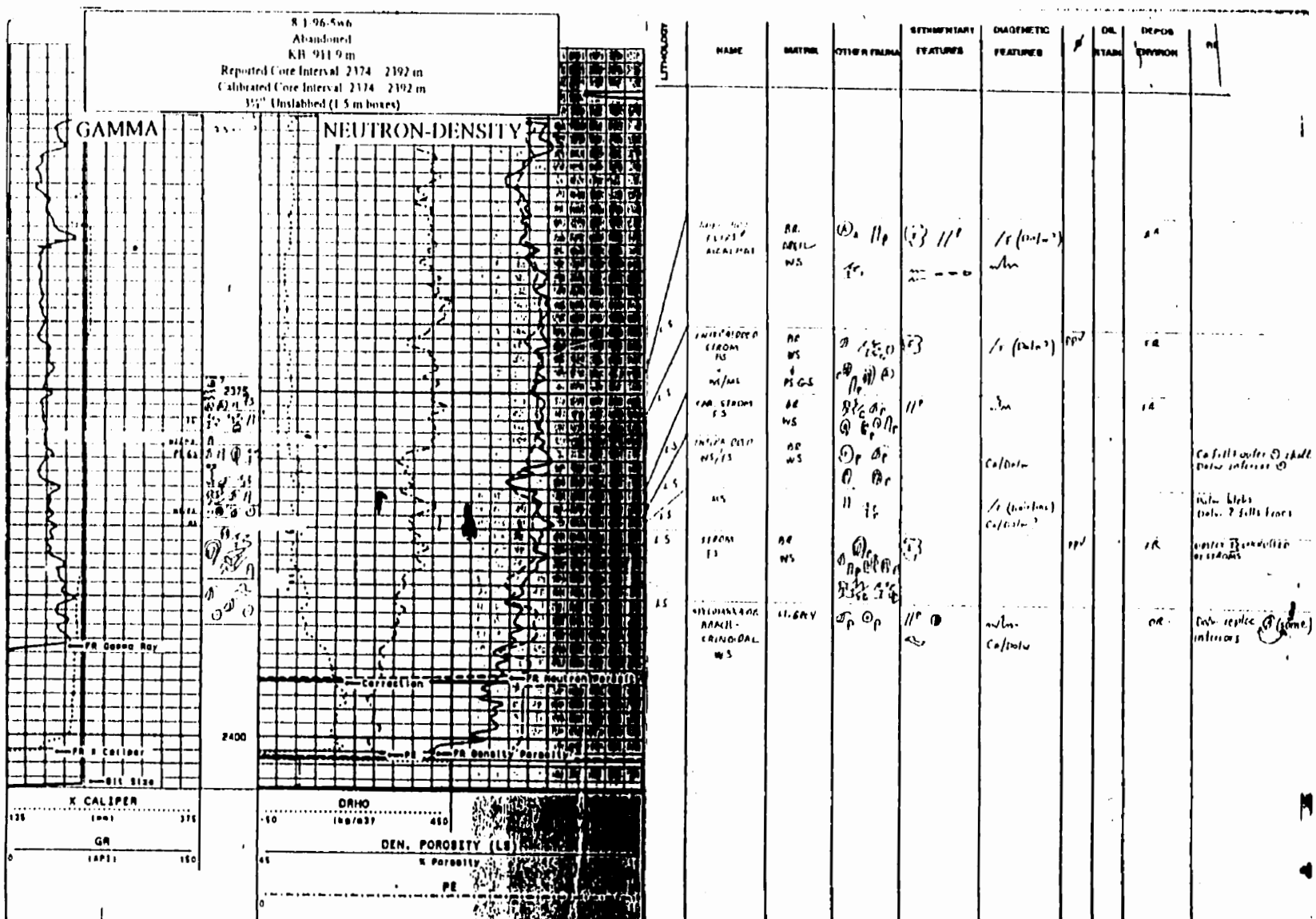
8 J 96-5wb
Abandoned
KB 911.9 m
Reported Core Interval 2374 - 2392 m
Calibrated Core Interval 2374 - 2392 m
3½" Unslabbed (1.5 m boxes)
GAMMA
NEUTRON-DENSITY
2375
2400
FR Gamma Ray
FR X Caliper
Bit Size
Correction
FR Neutron Porosity
FR Density Porosity
X CALIPER
GR
DRHO
DEN. POROSITY (LS)
PE
LITHOLOGY
NAME
MATRIX
OTHER FILLING
SEDIMENTARY FEATURES
DIAGENETIC FEATURES
DEPOS ENVIRON

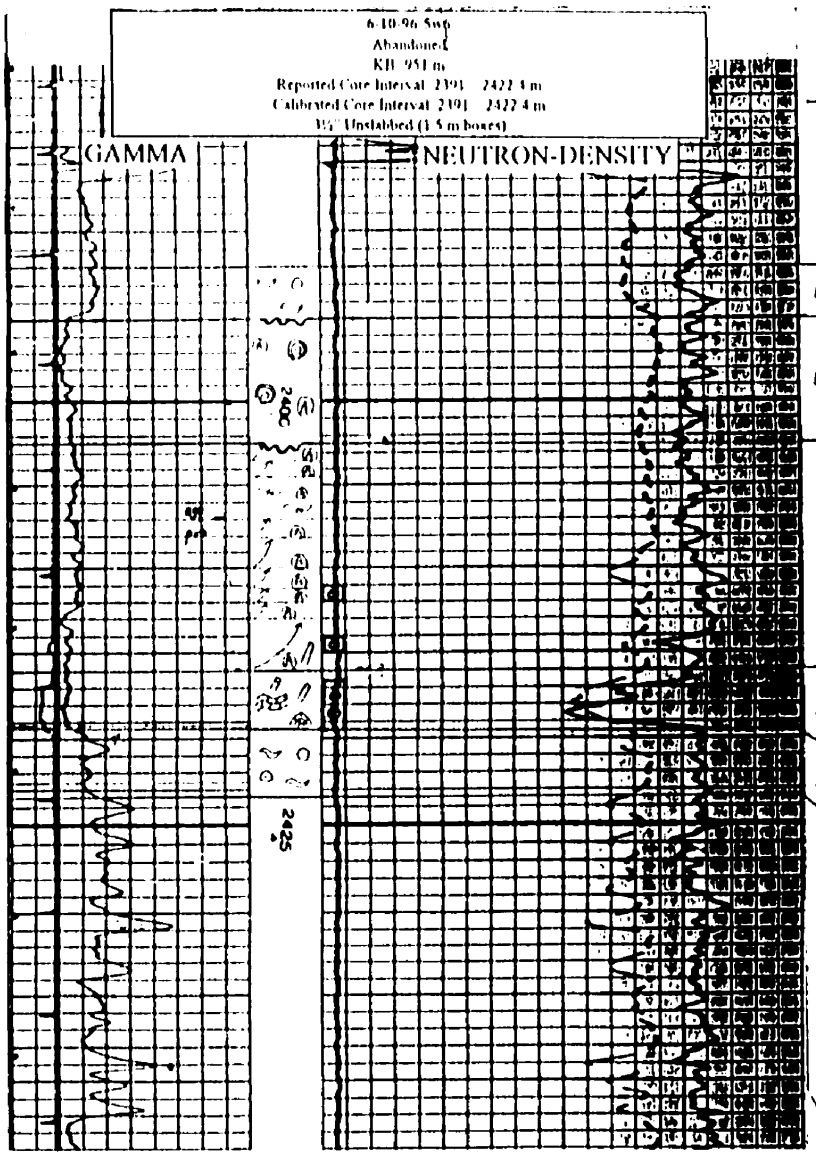

LITHOLOGY	NAME	MATRIX	OTHER FAUNA	SEDIMENTARY FEATURES	DIAGENETIC FEATURES	ϕ	OIL STAIN	DEPOS ENVIRON	REMARKS
LS	Nodular MS				w/m	–	–	Basin Fill	
LS	Bulbous Stem FS	w/c			w/m / F (Dol(w))	–	–	Interior Shoal	No ϕ
LS	Amphipora FS-RS ? Laminated MS	dk Br MS			w/m / F Dol(w)		✓	Lagoon ↑ Tidal flat ?	S.U.C. No ϕ
LS	Stachyodes - Tabular Stem FS-RS	Br. - US GS			w/m / F Dol(w)	PPV IP FR	–	Lower ↑ Upper Forereef	Good ϕ, k Baffle/Framework?
LS	Nodular Crinoidal WS	dk Br MS WS			w/m	–	–	Lower Slope Pl Platform	Sharp Upper Contact

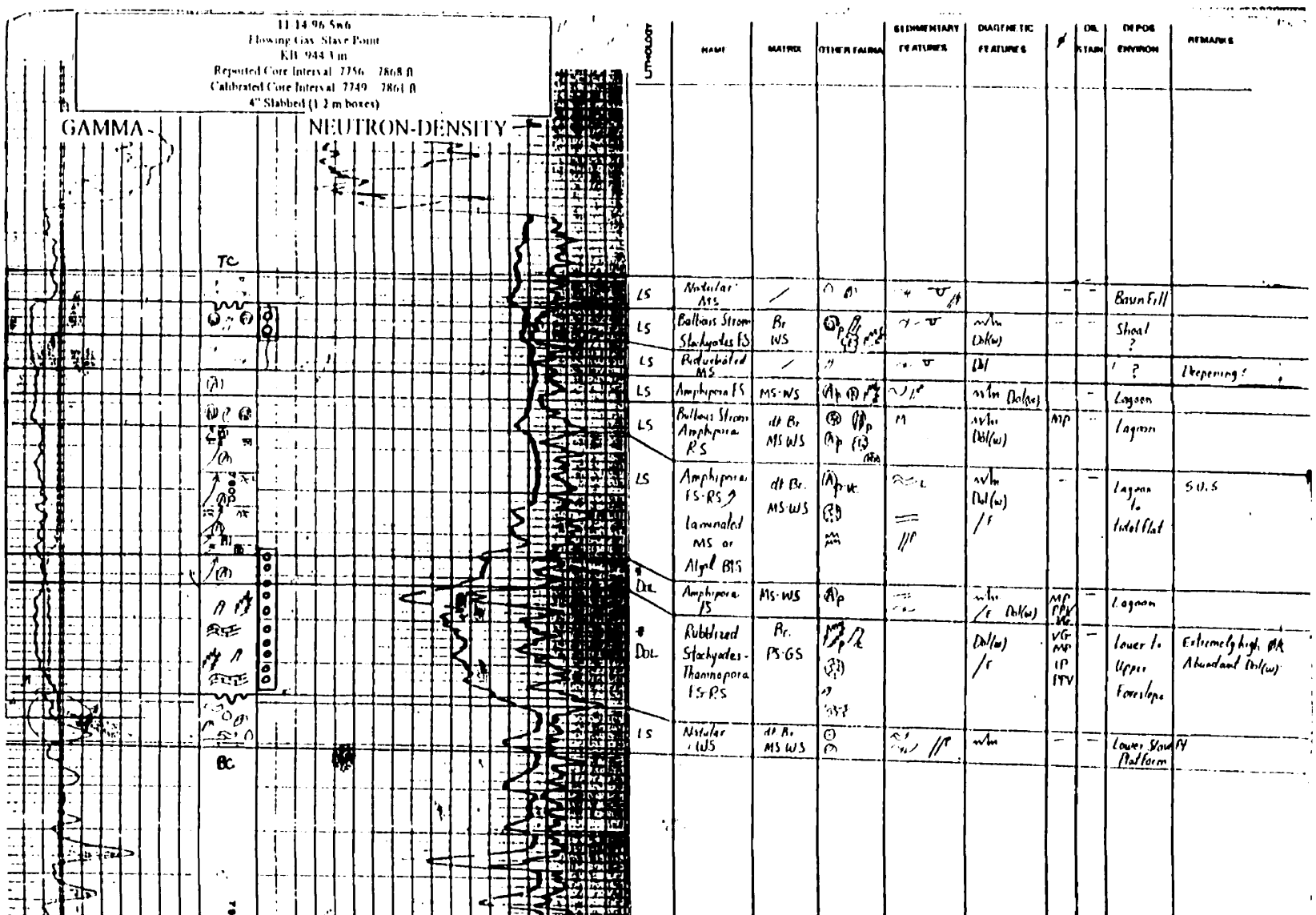
11-14-96 Sw6
Flowing Gas Slave Point
KB 944.3 m
Reported Core Interval 7756 - 7868 ft
Calibrated Core Interval 7749 - 7861 ft
4" Slabbed (1.2 m boxes)
GAMMA
NEUTRON-DENSITY
TC
BC
LITHOLOGY
NAME
MATRIX
OTHER FAUNA
SEDIMENTARY FEATURES
DIAGENETIC FEATURES
OIL STAIN
DEPOS ENVIRON
REMARKS
LS
Nodular MS
Basin Fill
LS
Balbiani Strom Stachyodes FS
Br WS
Shoal ?
LS
Redeposited MS
? ?
Deepening ?
LS
Amphipora FS
MS-WS
Lagoon
LS
Balbiani Strom Amphipora RS
dt Br MS WS
MP
Lagoon
LS
Amphipora FS-RS laminated MS or Algal BS
dt Br. MS-WS
Lagoon to Tidal Flat
S.U.S
DOL
Amphipora FS
MS-WS
MP FPF MG
Lagoon
DOL
Rubblized Stachyodes-Thamnopora FS-RS
Br. PS-GS
VG MP IP ITV
Lower to Upper Foreslope
Extremely high ØR Abundant Dol(w)
LS
Nodular WS
dt Br. MS WS
Lower Slope Platform
PF

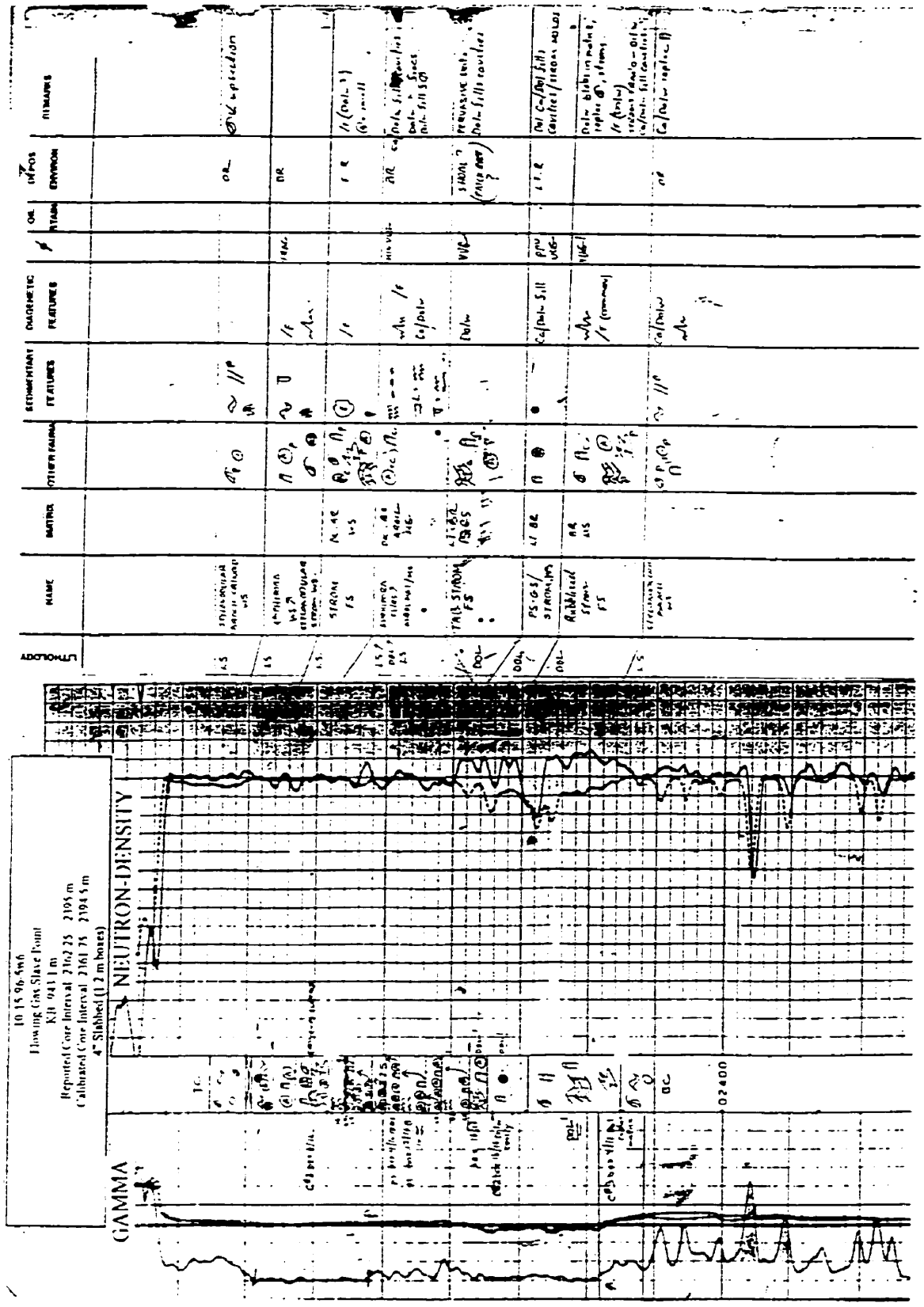
NEUTRON-DENSITY
GAMMA
10 15 96 5m6
Flowing Gas Slave Point
Kit 941 1 m
Reported Core Interval 2162 25 2195 m
Calibrated Core Interval 2161 75 2194 5 m
4" Slabbed (1 2 m boxes)
02400

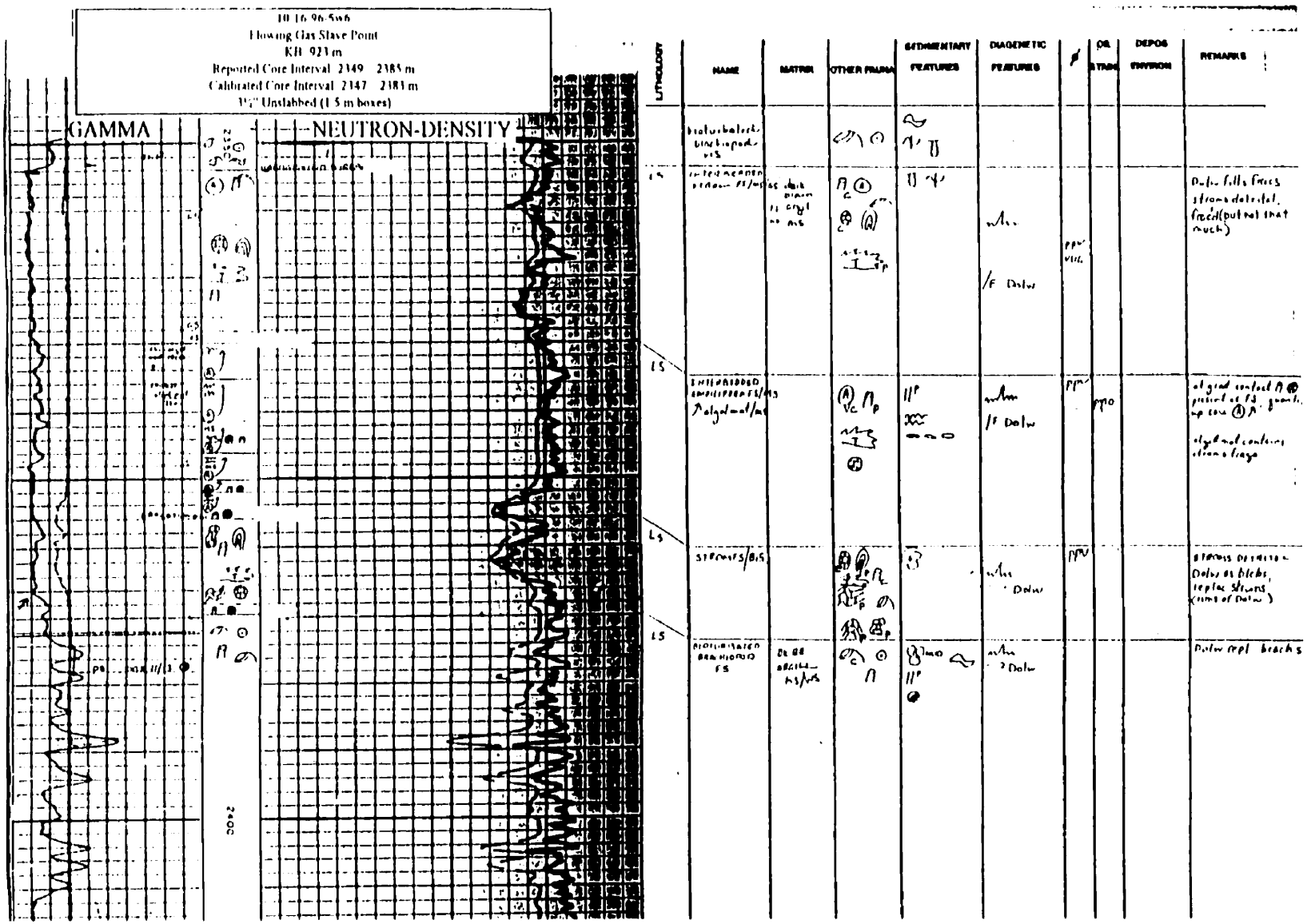
10-16-96:Sw6
Flowing Gas Slave Point
KB 923 m
Reported Core Interval 2149 2185 m
Calibrated Core Interval 2147 2183 m
3½" Unslabbed (1.5 m boxes)
GAMMA
NEUTRON-DENSITY
LITHOLOGY
NAME
MATRIX
OTHER FAUNA
SEDIMENTARY FEATURES
DIAGENETIC FEATURES
POR
OIL STAIN
DEPOS ENVIRON
REMARKS
LS
LS
LS
LS

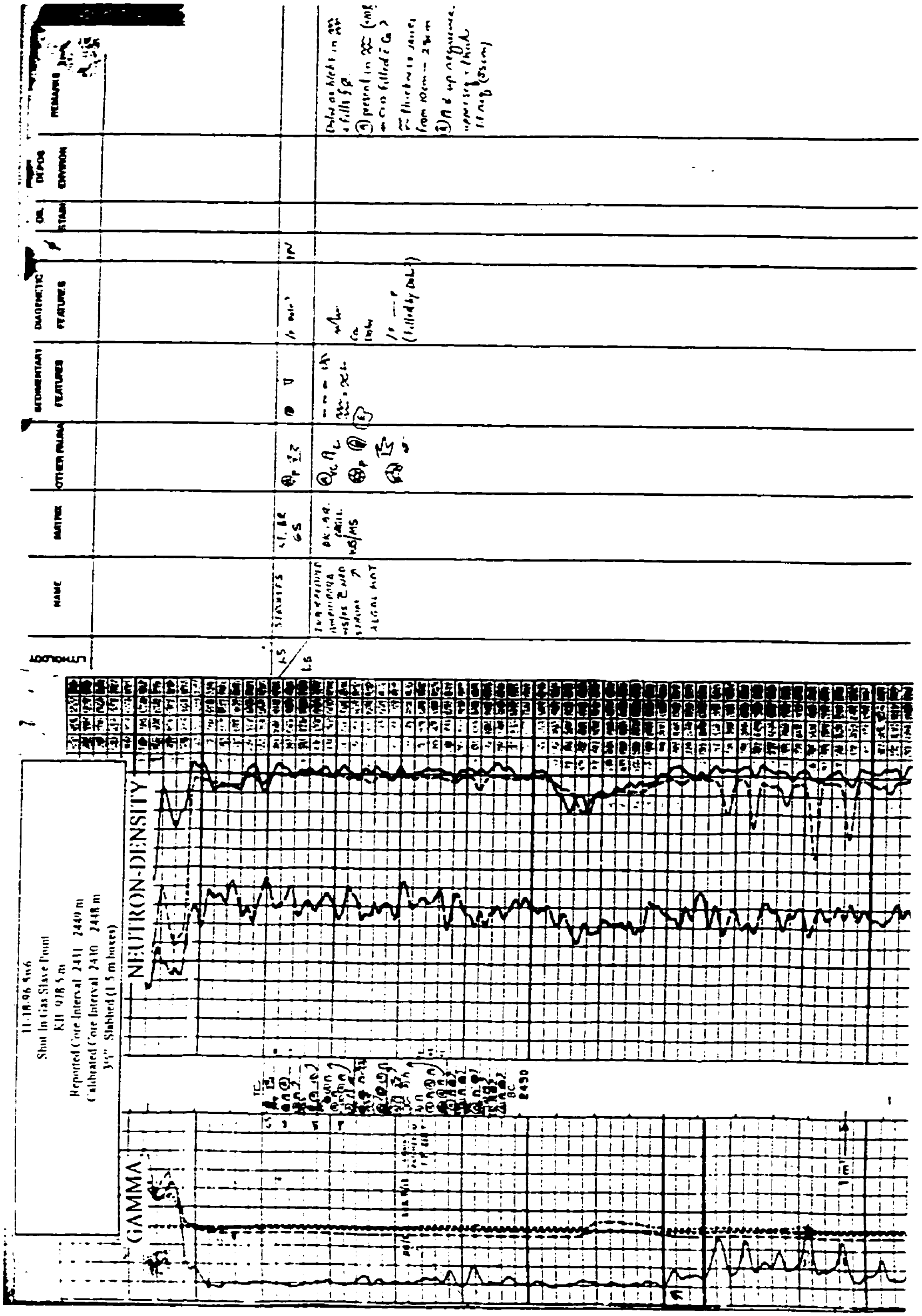

11-18-96 9w6
Shut In Gas Slave Point
KB 978.5 m
Reported Core Interval 2431 2449 m
Calibrated Core Interval 2430 2448 m
3½" Slabbed (1.5 m boxes)
NEUTRON-DENSITY
GAMMA
LITHOLOGY
NAME
MATRIX
OTHER FAUNA
SEDIMENTARY FEATURES
DIAGENETIC FEATURES
OIL STAIN
DEPOS ENVIRON
REMARKS

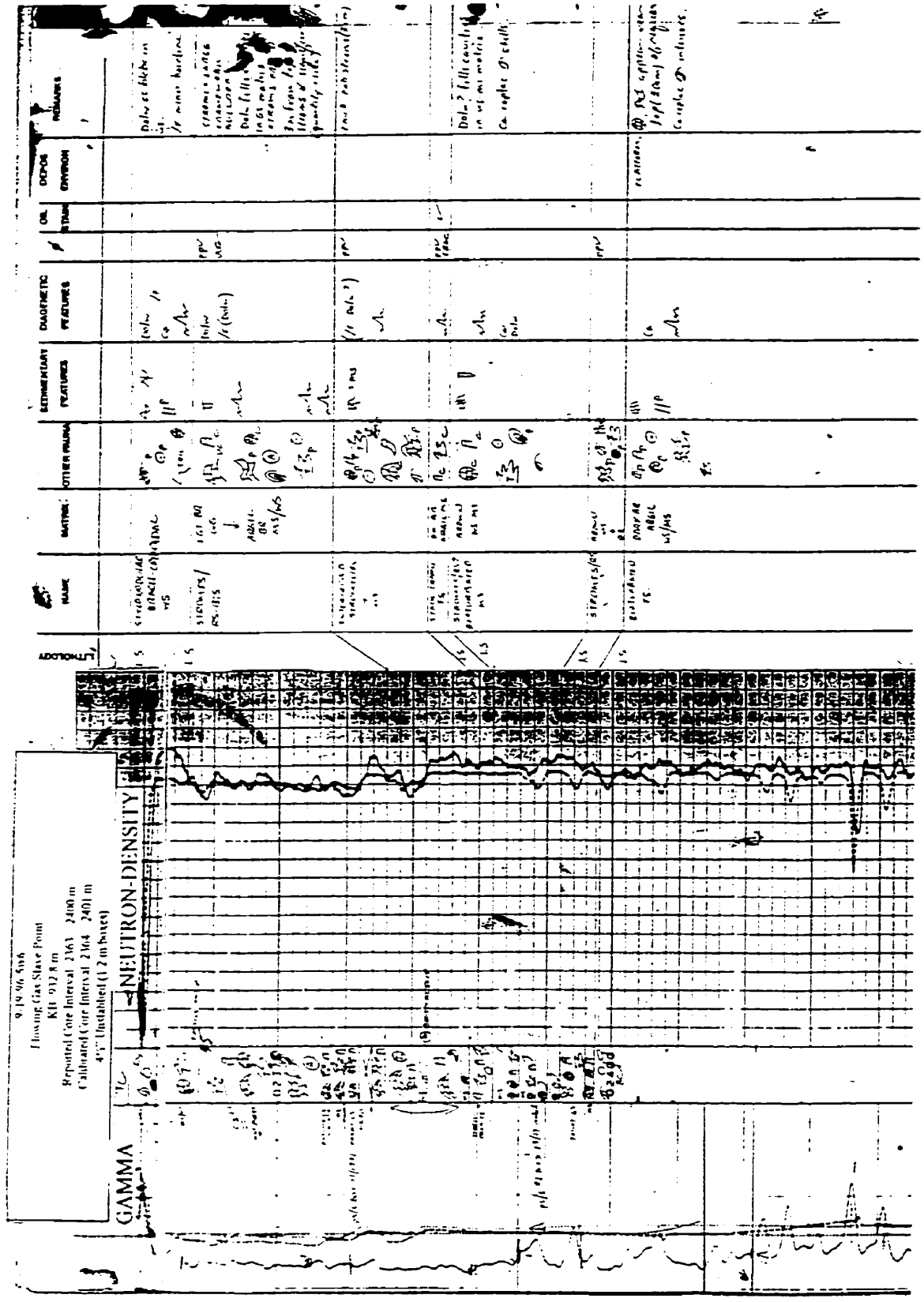
GAMMA
NEUTRON-DENSITY
Flowing Gas Slave Point
Reported Core Interval 2363 2400 m
Calibrated Core Interval 2364 2401 m
4½" Unstabilized (1.2 m Bores)

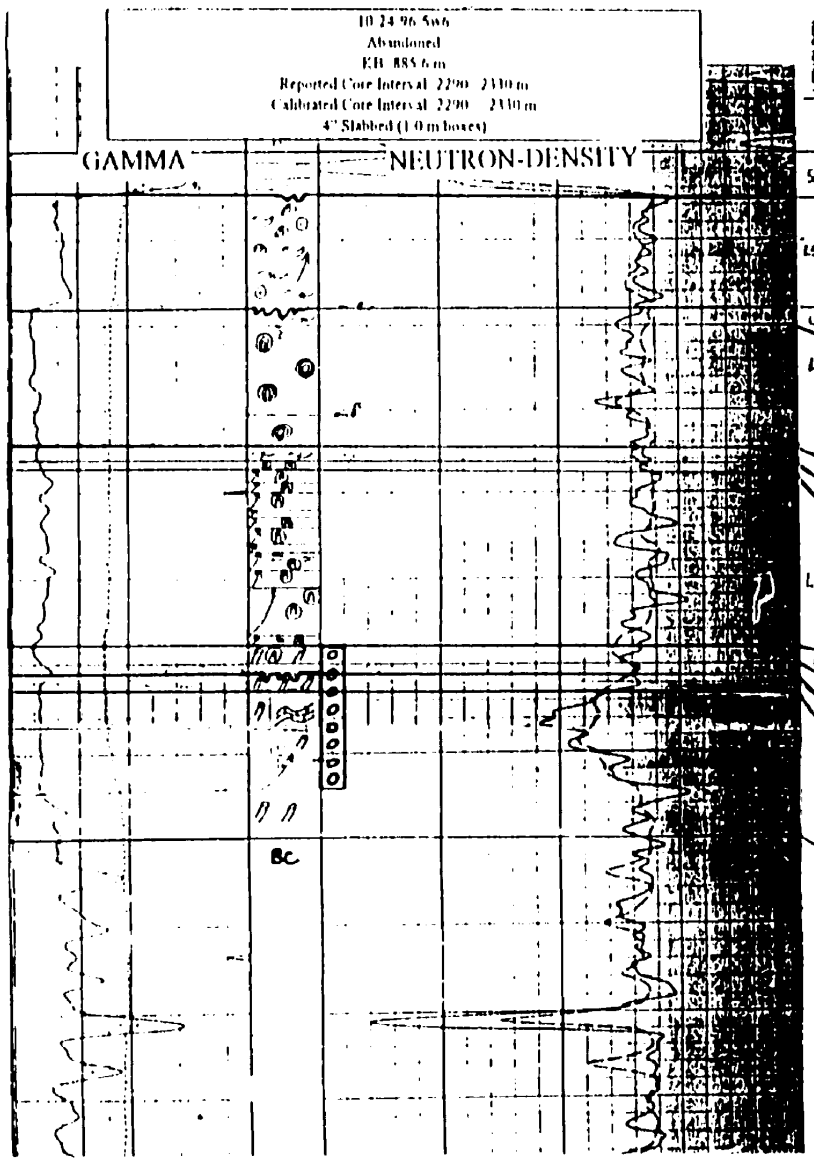

LITHOLOGY	NAME	MATRIX	OTHER FAUNA	SEDIMENTARY FEATURES	DIAGENETIC FEATURES	ϕ	OIL STAIN	DEPOS ENVIRON	REMARKS
SH	CALC. SH	DK GRY MS							
LS	Nodular MS ? Bioclasted WS	dk Br WS MS			Py		—	Basin Fill	Sharp, pyritized upper contact
LS	Bioturbated MS	MS PS	B.D		/F Dol(w)	tp	—	?	Deepening ?
LS	Bulbous Stem FS	Br WS PS			/F Dol(w)	tpv tp	—	Shoal	Stems fract'd + fragmented
LS	Bioturbated WS	WS PS	B.D		/F	—	—	Back Reef	Deepening ?
LS	Amphipora FS	WS PS			/F Dol(w)	—	—	Lagoon	open marine fauna
LS	Amphipora FS RS ↗ Algal B-S	dk Br MS WS			/F Dol(w)	mp	—	Lagoon to tidal flat	S.U.S
LS	Amphipora-FS	PS-GS			Dol(w)	—	—	Lagoon	
LS	MS	PS GS	B.D		/F Dol(w)	—	—	" ?	Detrital ?
LS	Stachyodes FS/RS	PS GS			/F Dol(w)	tp fr	—	Lower foreslope	
LS	Stachyodes FS ↗ Tabular Stro BPS	dk Br WS-PS ? light Br GS			/F Dol(w)	tpv tp fr	✓	Lower to upper foreslope	S.U.S Good ϕ

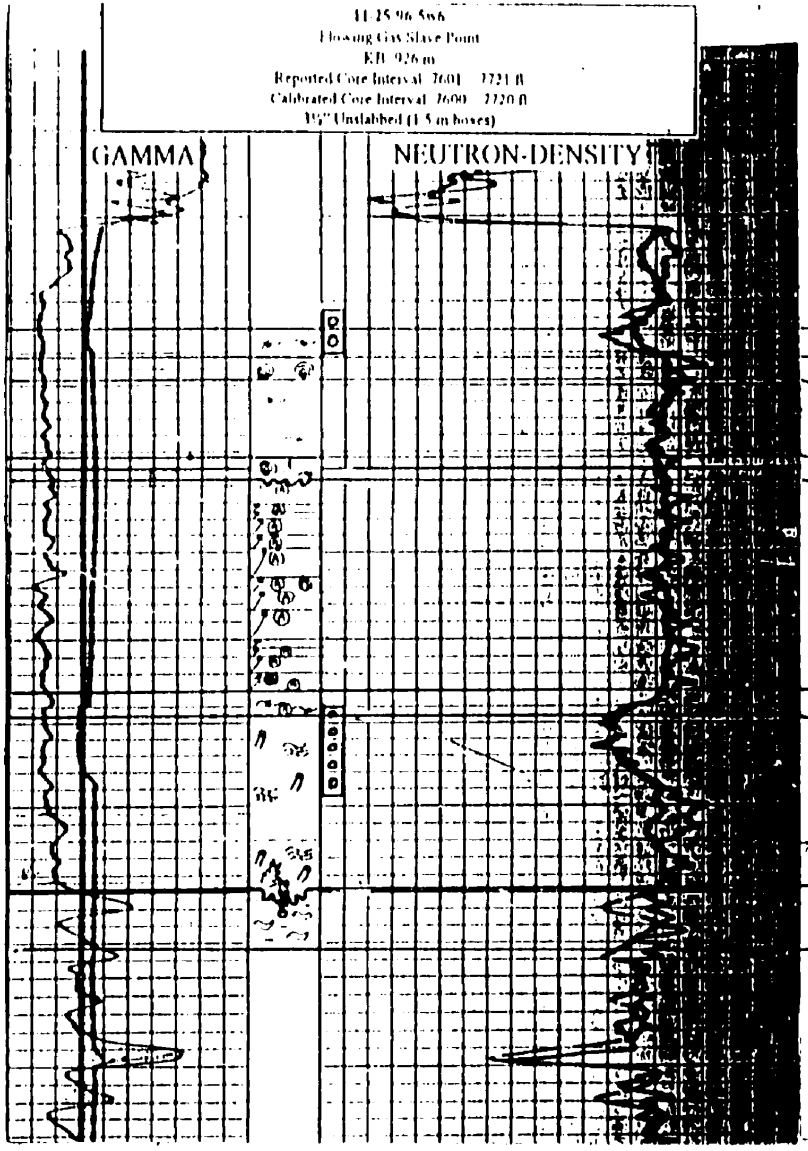

LITHOLOGY	NAME	MATRIX	OTHER FAUNA	SEDIMENTARY FEATURES	DIAGENETIC FEATURES	ϕ	OIL STAIN	DEPOS ENVIRON	REMARKS
LS	Bioturbated MS	Br MS			/F (Dol(ω))	PPV	—	Slope?	
LS	Pelloid Stromb FS	Br WS FS	p		Dol(ω)	—	—	Shoal?	
LS	Bioturbated MS-WS	Br WS FS	B.D. A		/F (Dol(ω))	—	—	Lagoon	
LS	Bioturbated to Stromb FS	Br Bk WS PS	A		/F (Dol(ω))	—	—	Lagoon	SDS open marine
LS	Amphipora FS-RS ? Laminated MS	Br MS WS	A p vc		/F Dol(ω)	—	—	Lagoon to tidal flat	S.U.S. Sharp Upper Contact. (Erosional)
LS	Bioturbated MS-WS	Br MS	A		/F Dol(ω)	—	—	Lagoon	
LS	Stachyodes FS? Tabular Stromb FS-RS	dk Br WS PS	fc p P		/F Dol(ω)	PPV		Lower Foreslope to Upper Foreslope	Baffle stone Reef? poor PS
LS	Nodular WS	dk Br MS-WS	A B.D.			—	—	Lower Shelf/Platform	

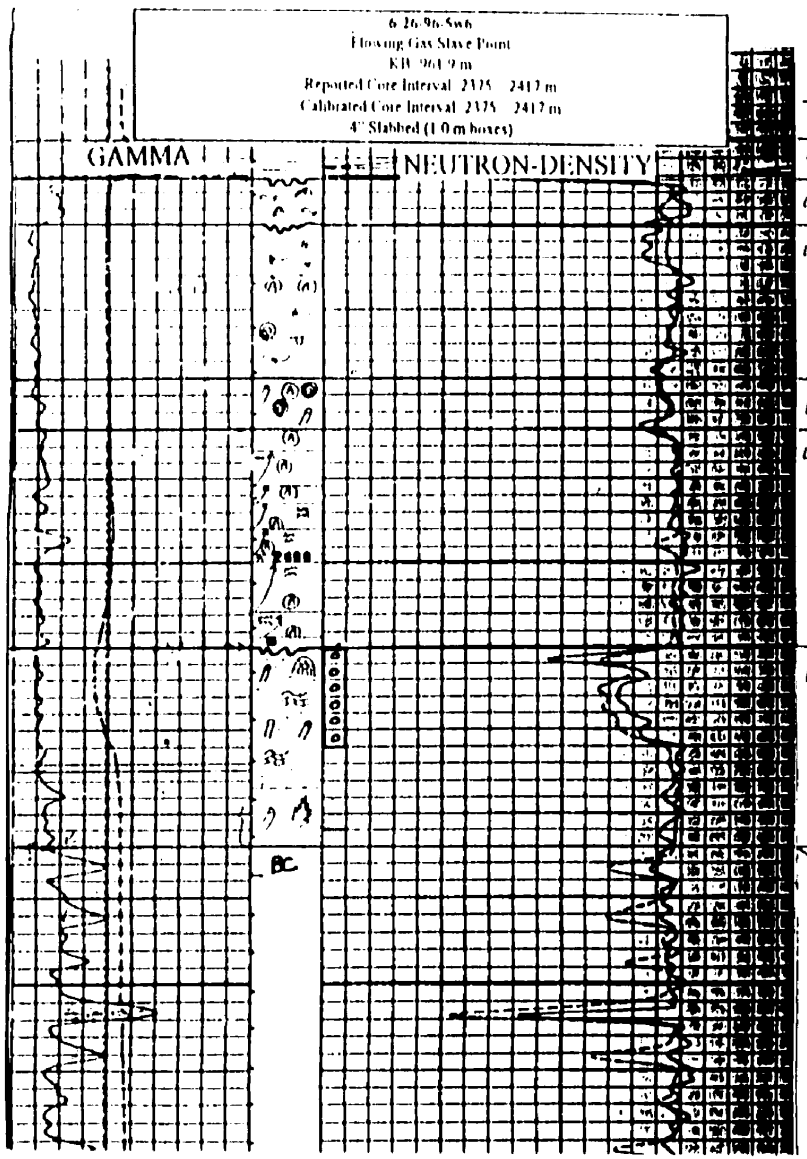

LITHOLOGY	NAME	MATRIX	OTHER FAUNA	SEDIMENTARY FEATURES	DIAGENETIC FEATURES	ϕ	OIL STAIN	DEPOS ENVIRON	REMARKS
SH	CALC. SH								
LS	Nodular Brachiopod WS	dk Br. MS WS	Bp Gp		OPV Dol(w)/F	-	-	Basin Fill	Sharp upper & Lower Contacts
LS	Bioturbated MS	Br. WS PS	B.D.		Dol(w)/F (CH)	FR IPV	-	Inferior Shoal	
LS	Stachyodes-Bulkbug Strom FS-RS	Br WS PS			Dol(w) /F	IPV	-	Lagoon	open marine
LS	Amphipora FS RS / Algal BiS	dk Br MS-WS	Bprc		/F Dol(w)	MP	-	Lagoon to Tidal Flat	S.U.S
LS	Stachyodes-Thamnopora FS / Tabular-Hemispherical Strom BiS-BnS	dk Br. WS PS / Br. GS	Bprc P P P		/F Dol(w)	IPV IP FR	✓	Lower foreshore to Upper foreshore	S.U.S Good ϕ in matrix

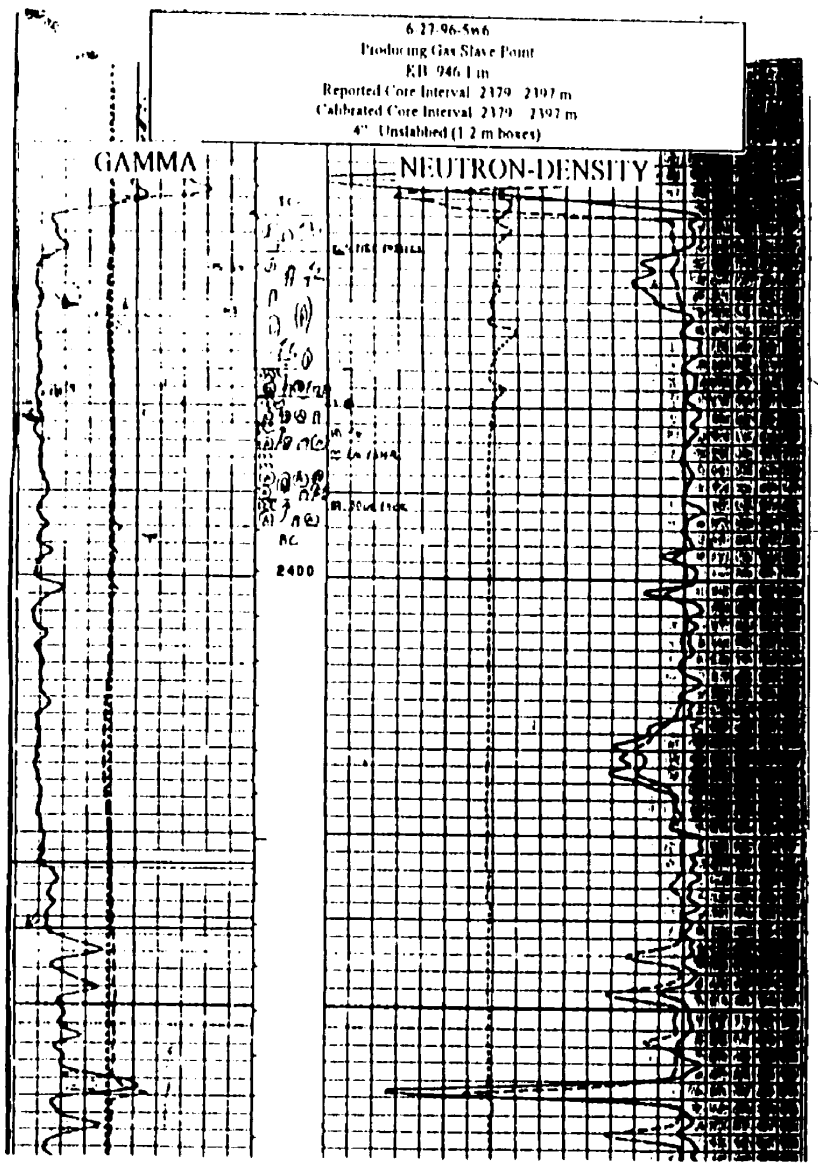

LITHOLOGY	NAME	MATRIX	OTHER FAUNA	SEDIMENTARY FEATURES	DIAGENETIC FEATURES	φ	OIL STAIN	DEPOS ENVIRON	REMARKS
LS	STYLOLAMINATED PEBBLY-[illegible] WS							OR	
LS						PPV frac		BR/LA	
LS								BR	

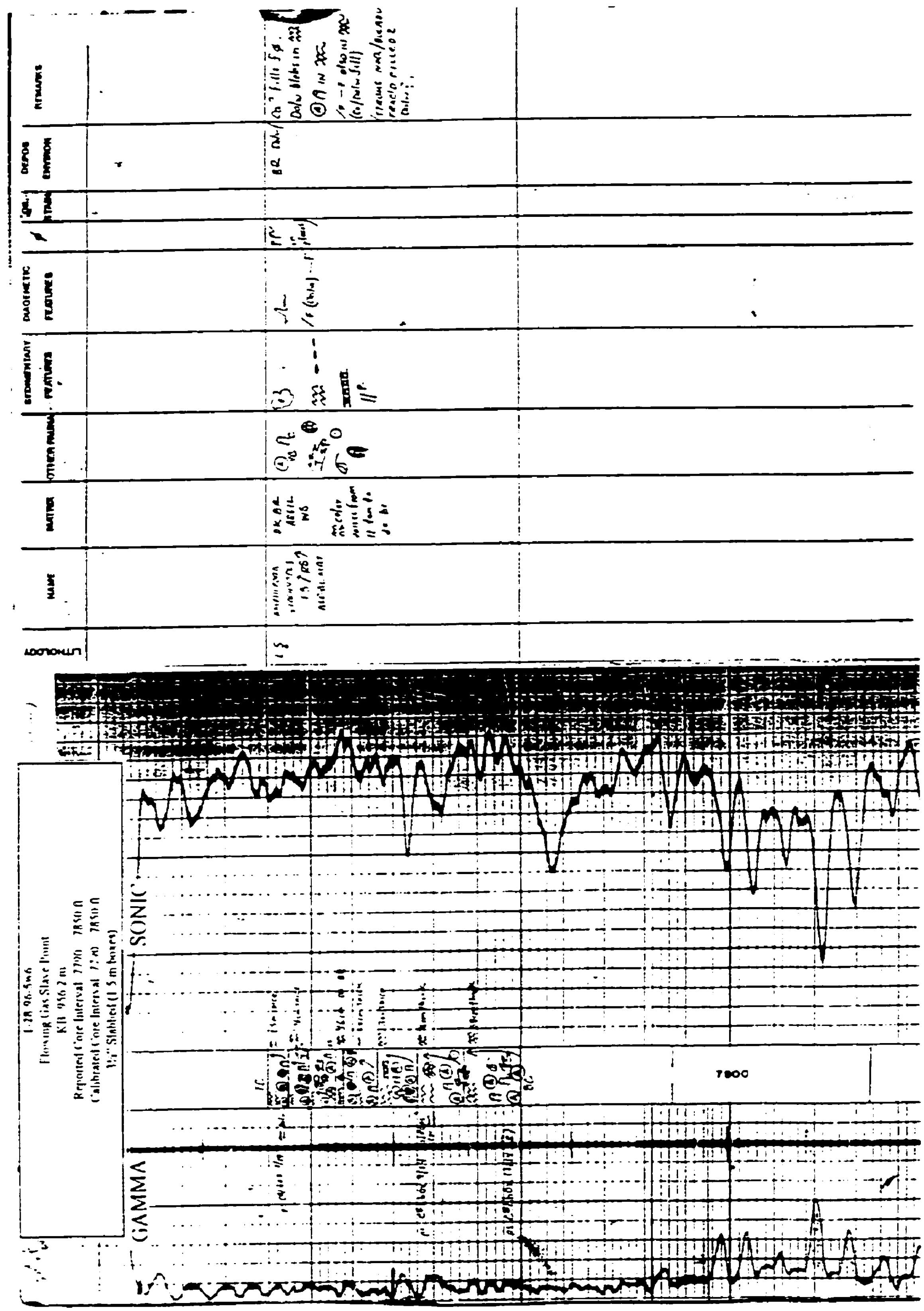
REMARKS
DEPOS ENVIRON
DIAGENETIC FEATURES
SEDIMENTARY FEATURES
OTHER FAUNA
MATRIX
NAME
LITHOLOGY
SONIC
GAMMA
7800

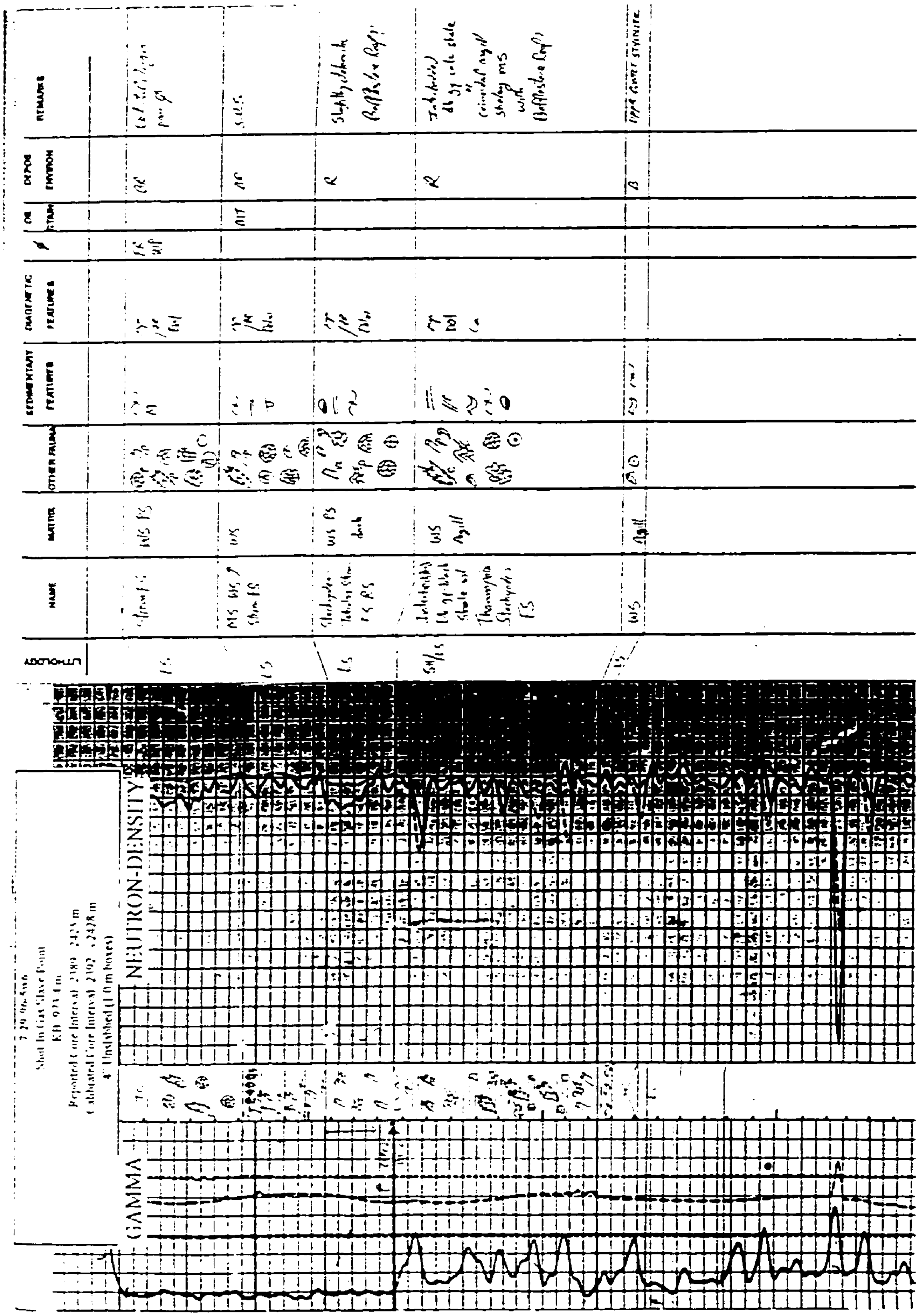
7-29-96-5w6
Shut In Gas Slave Point
KB 923.4 m
Reported Core Interval 2389 - 2425 m
Calibrated Core Interval 2392 - 2428 m
4" Unslabbed (1.0 m boxes)
GAMMA
NEUTRON-DENSITY
LITHOLOGY
NAME
MATRIX
OTHER FAUNA
SEDIMENTARY FEATURES
DIAGENETIC FEATURES
ø
OIL STAIN
DEPOS ENVIRON
REMARKS

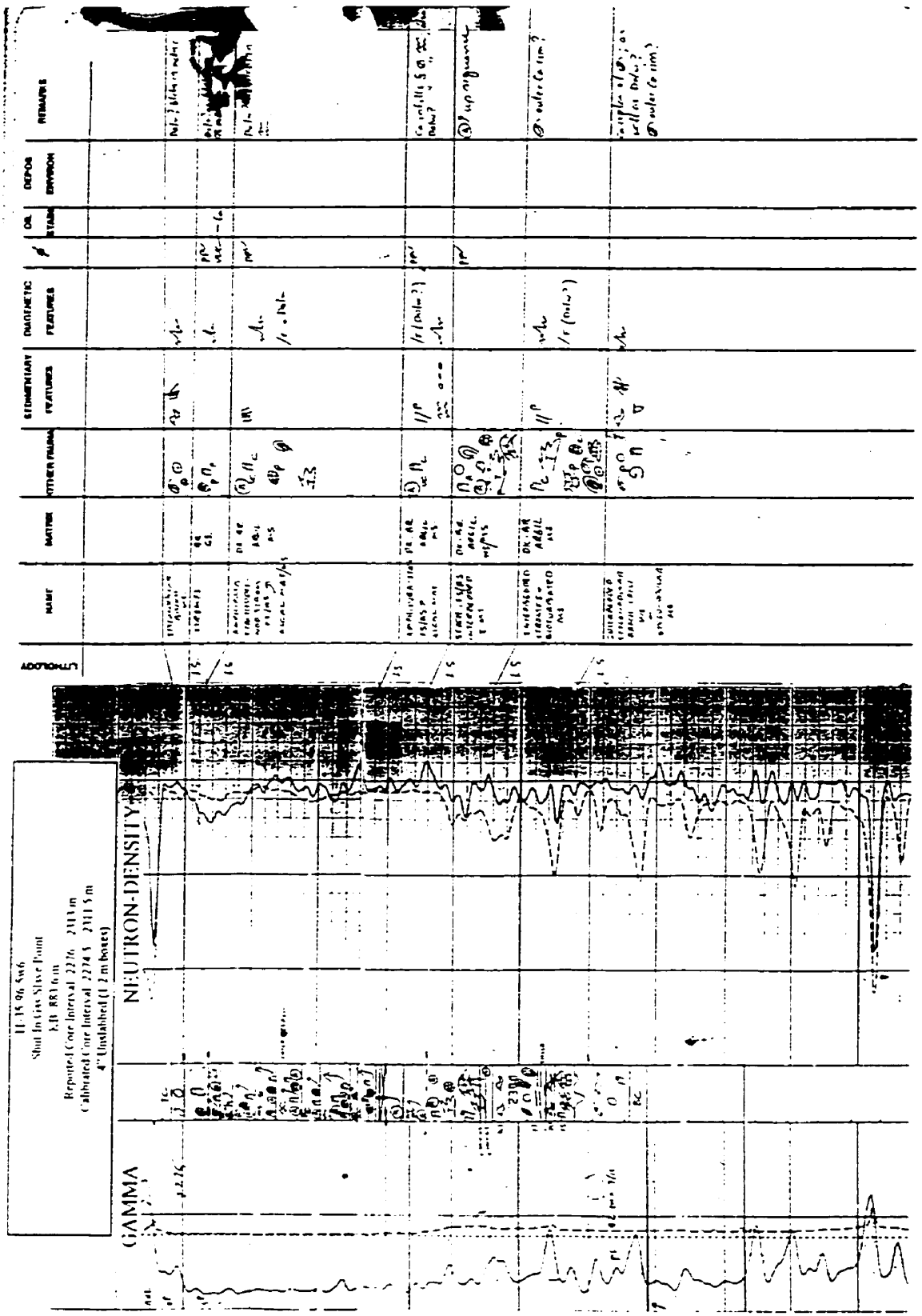
NEUTRON-DENSITY
GAMMA
LITHOLOGY
NAME
MATRIX
OTHER FAUNA
SEDIMENTARY FEATURES
DIAGENETIC FEATURES
OIL STAIN
DEPOS ENVIRON
REMARKS

LITHOLOGY
NAME
MATRIX
OTHER FRAMA
SEDIMENTARY FEATURES
DIAGENETIC FEATURES
OIL STAIN
DEPOS ENVIRON
REMARKS
SONIC
GAMMA
6800

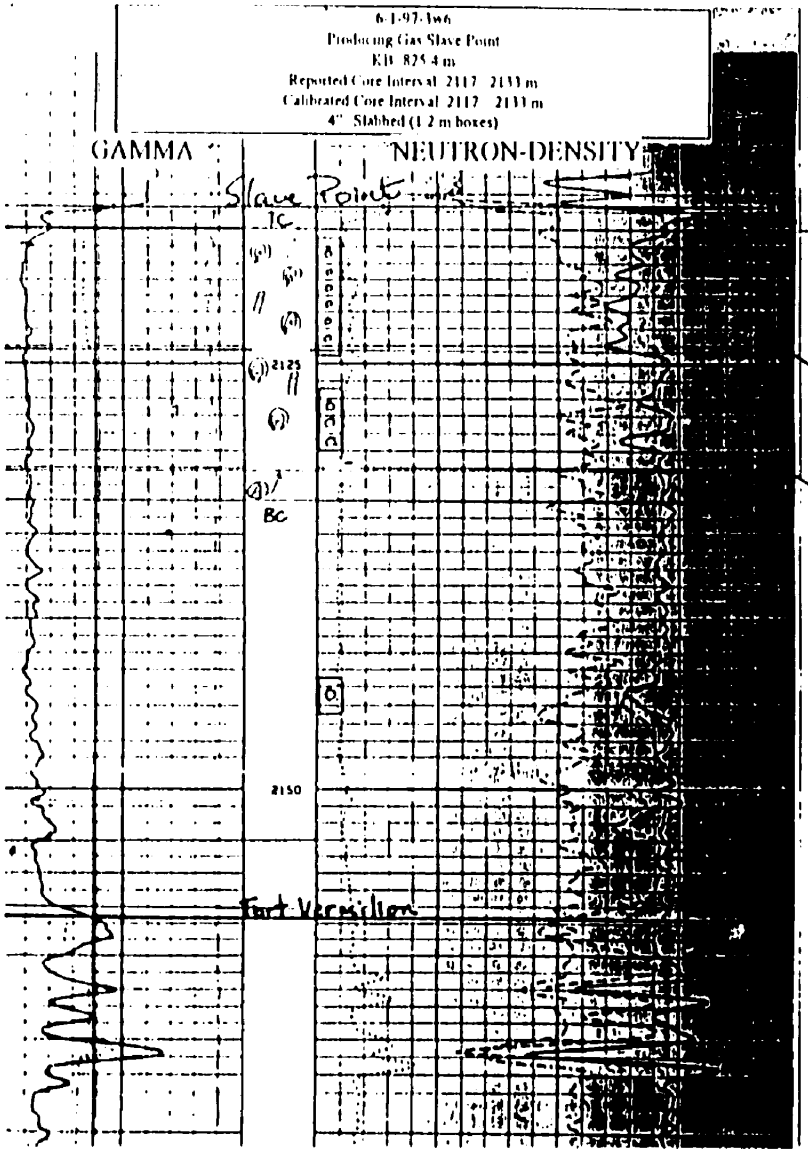

LITHOLOGY	%	NAME	MATRIX	OTHER FAUNA	SEDIMENTARY FEATURES	DIAGENETIC FEATURES	Φ	OIL STAIN	DEPOS ENVIRON	REMARKS
LS		Bulbous Strom FS	light GS	$\textcircled{Q}_{1c}$ Π_c		/f vNm Dol(w)	IPV IP		Shoal	Calcite cements in GS matrix Dolm blebs in GS matrix?
LS		Bulbous Strom FS	Br PS GS	$\textcircled{Q}_c$ Π_p Ⓐ	//	/f Dol(w)	PPV		Shoal	Calcite cements Dolm blebs Fracture cements
LS I		Amphipora FS ↗ Algal BiS	Br MS-PS	Ⓐc Π	//	vNm	—	—	Lagoon to tidal flat	Loss of fm Φ by Ca (Dolm + Blebs)

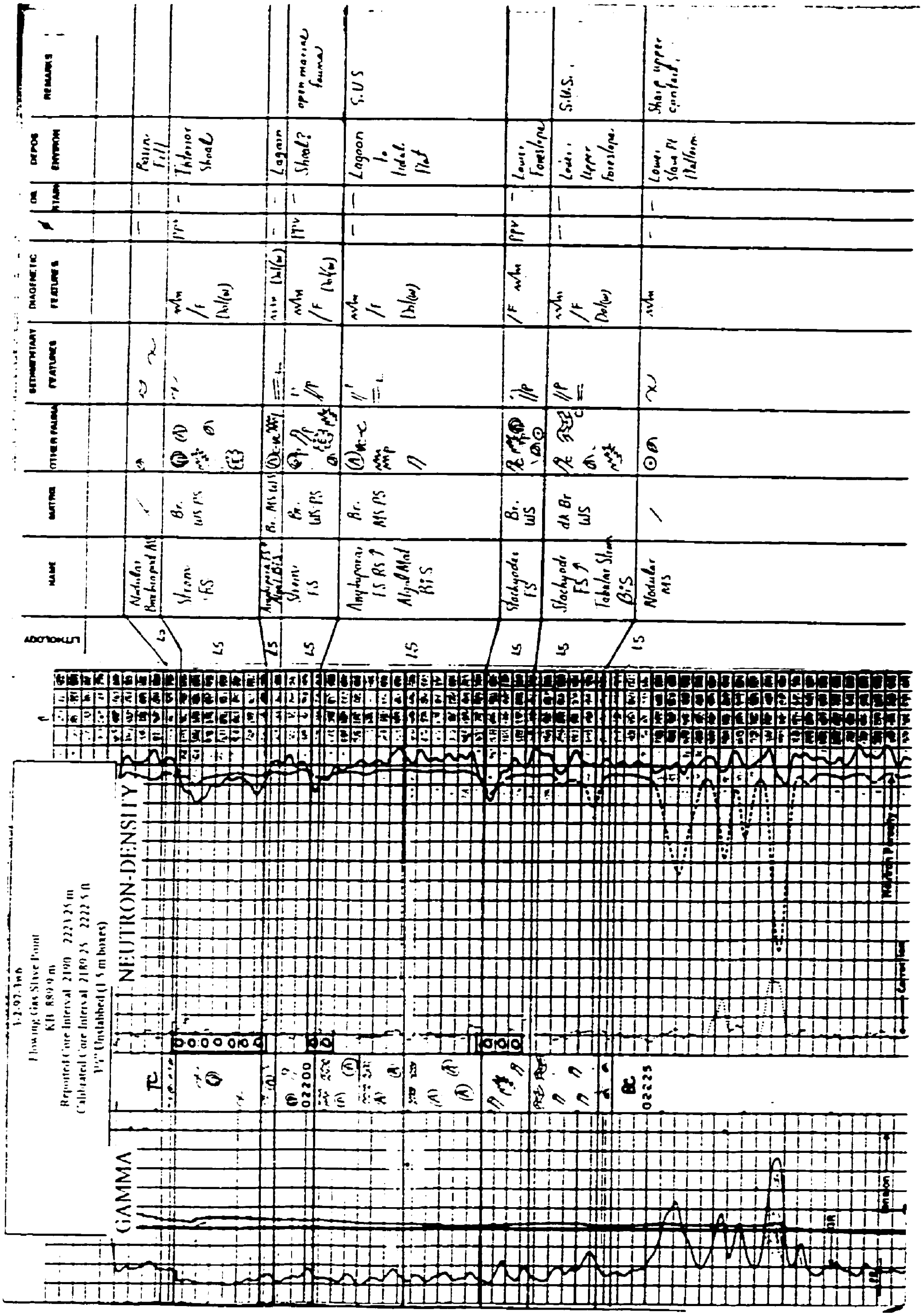
GAMMA
NEUTRON-DENSITY
LITHOLOGY
NAME
REMARKS
S.U.S.
Lagoon
Shoal?
open marine fauna
Sharp upper contact.

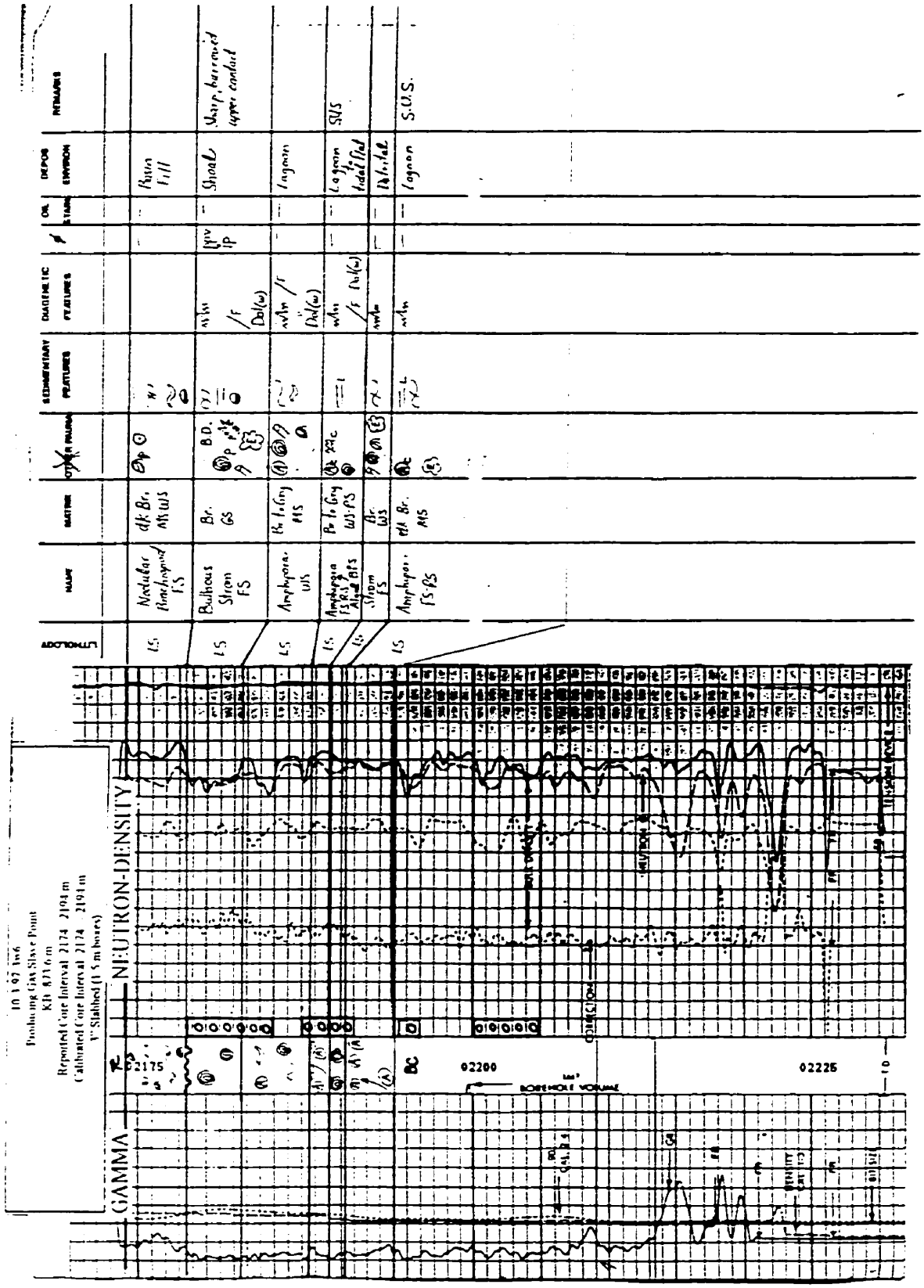
GAMMA
NEUTRON-DENSITY
CORRECTION
BOREHOLE VOLUME
02175
02200
02225
LITHOLOGY
NAME
MATRIX
OTHER FAUNA
SEDIMENTARY FEATURES
DIAGENETIC FEATURES
OIL STAIN
DEPOS ENVIRON
REMARKS
Nodular Packstone FS
Bulbous Stom FS
Amphipora WS
Amphipora Algal FS
Stom FS
Amphipor. FS-PS
Basin Fill
Shoal
Lagoon
Lagoon to tidal flat
Lagoon
Sharp, burrowed upper contact
SUS
S.U.S.

LITHOLOGY
NAME
MATRIX
OTHER FAUNA
SEDIMENTARY FEATURES
DIAGENETIC FEATURES
OIL STAIN
DEPOS ENVIRON
REMARKS
SONIC
GAMMA
7400

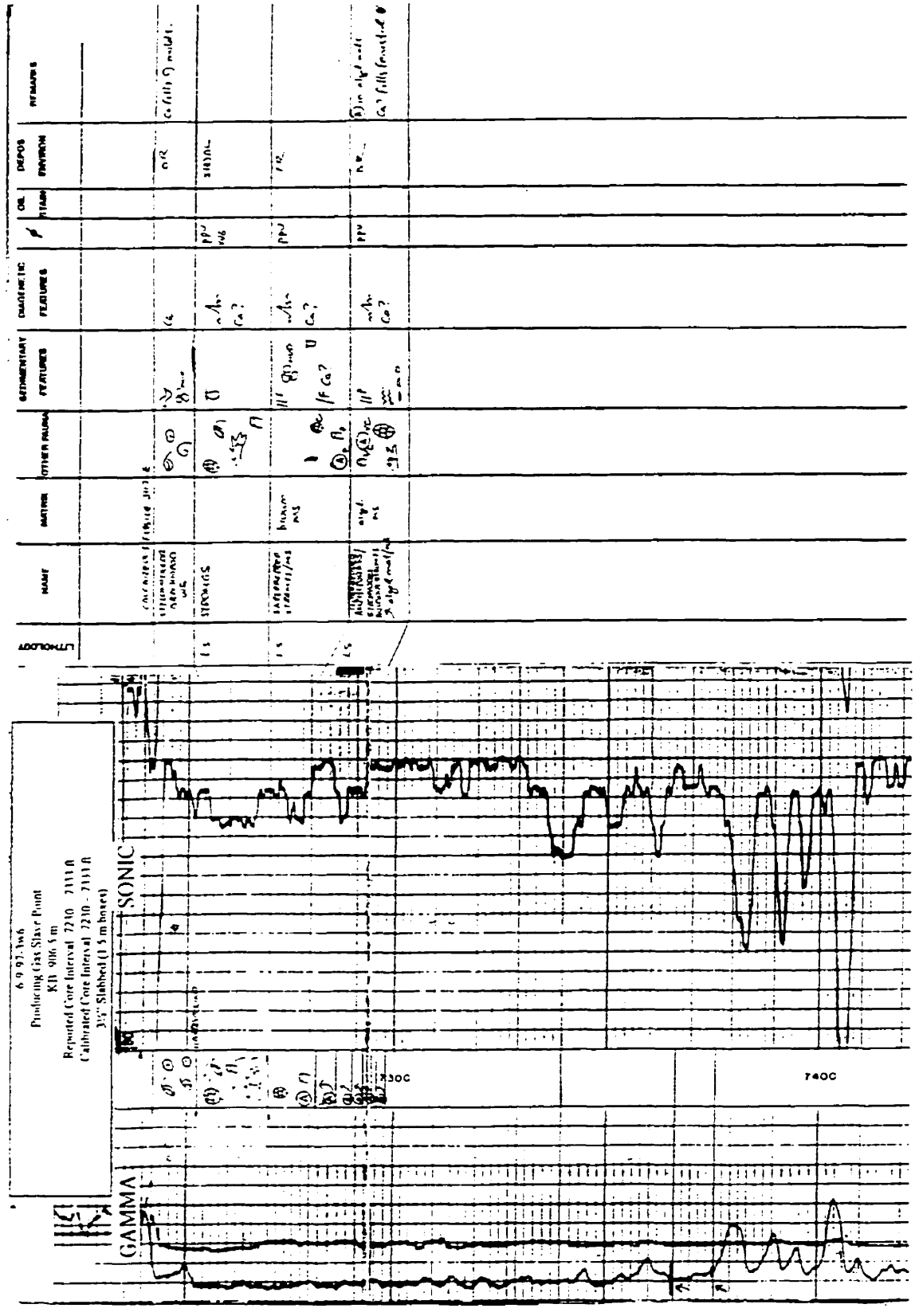
SONIC
GAMMA
7300
7400

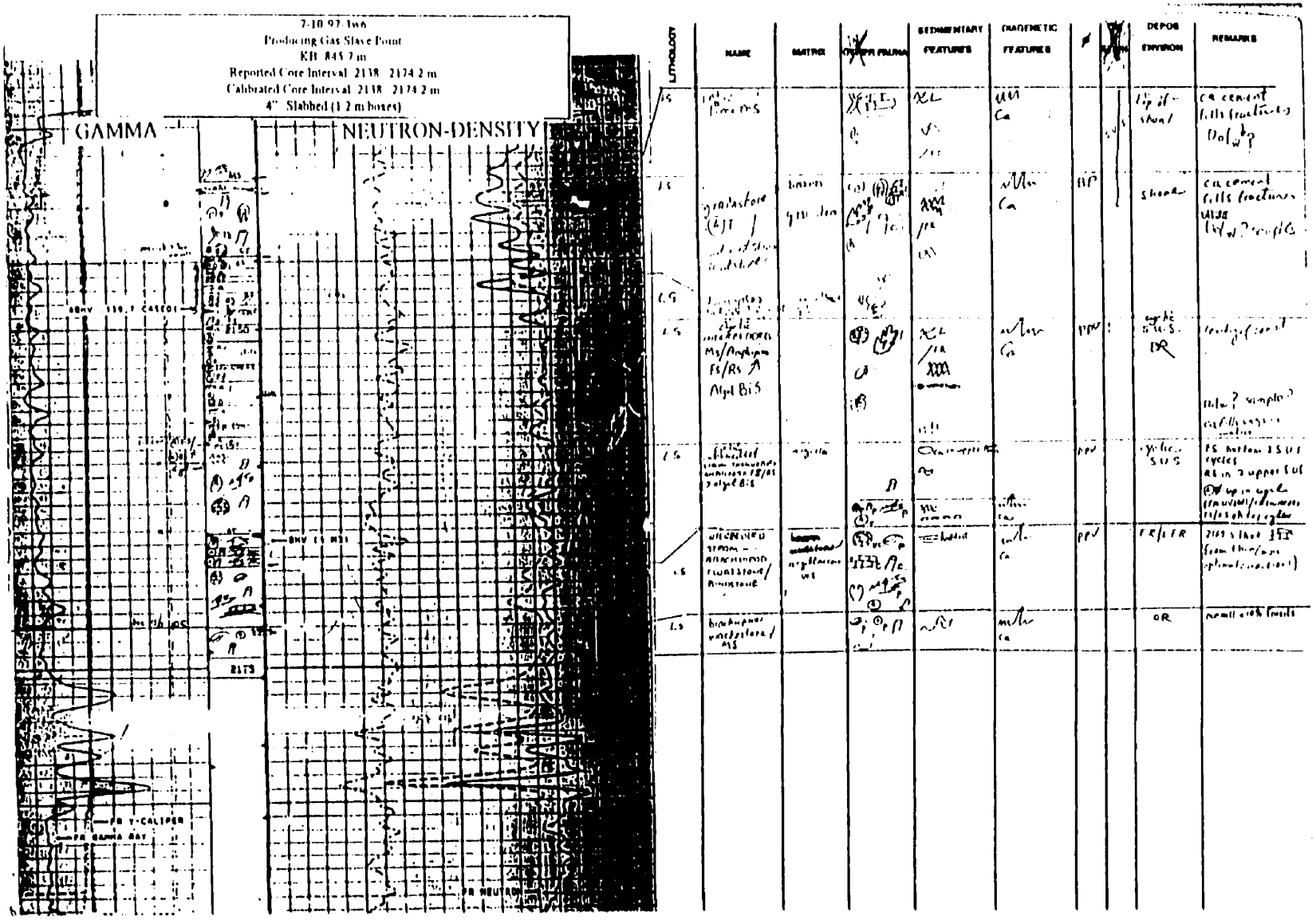
7-10 97-1w6
Producing Gas Slave Point
KB 845.7 m
Reported Core Interval 2138 - 2174.2 m
Calibrated Core Interval 2138 - 2174.2 m
4" Slabbed (1.2 m boxes)
GAMMA
NEUTRON-DENSITY
LITHOLOGY
NAME
MATRIX
OTHER FAUNA
SEDIMENTARY FEATURES
DIAGENETIC FEATURES
DEPOS ENVIRON
REMARKS

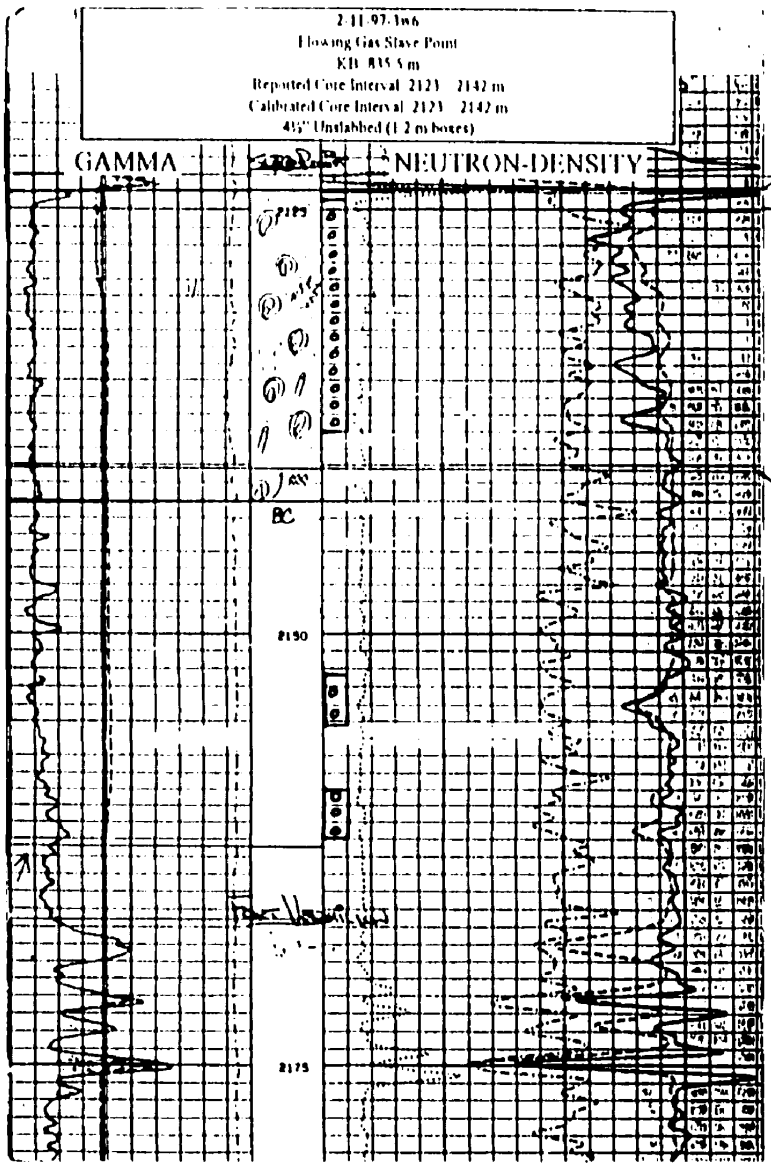

LITHOLOGY	NAME	MATRIX	OTHER FEATURES	SEDIMENTARY FEATURES	DIAGENETIC FEATURES	φ	OIL STAIN	DEPOS ENVIRON	REMARKS
Sh	Calc Shale	Black							
LS	Nodular WS	dk Br MS	$\mathcal{O}_p$ $\mathcal{O}_p$	~ ~		—	—	Basin fill	
LS	Bulbous Stromb FS	Br GS	$\mathcal{O}_c$ $\mathcal{O}_p$ $\mathcal{O}_p$ Ⓐ	///	/ Mic	ppv ip	—	Shoal	Ca as blebs Gamma ray up core shows fract'd - filled w Ca ? pyrite ? up core
LS	Amphipora FS ? Algal BFS	Br MS-PS	Ⓐ$_c$ / ∩ ≈	///		ppv	—	Lagoon to tidal flat	Ca cement fills fractures as well as vugs abnormal cool ∩ trough

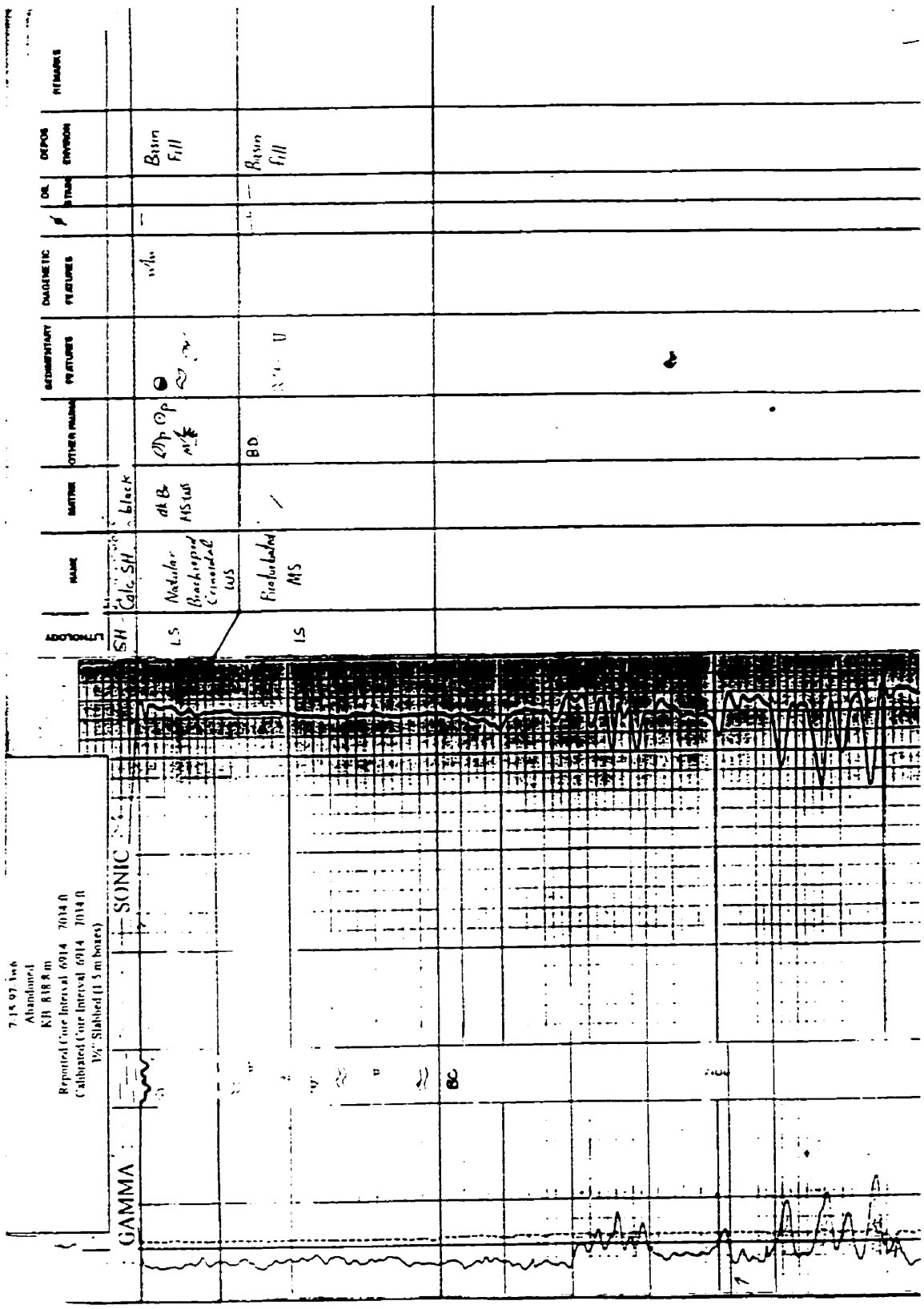
7.15 97 inch
Abandoned
KB 818.8 m
Reported Core Interval 6914 7014 ft
Calibrated Core Interval 6914 7014 ft
1½" Slabbed (1.5 m boxes)
SONIC
GAMMA
LITHOLOGY
SH
LS
NAME
Calc SH
Nodular Bioclastic Crinoidal WS
Fissile Laminated MS
BIOTURB
dk B
MS WS
black
OTHER FAUNA
Op
BD
SEDIMENTARY FEATURES
DIAGENETIC FEATURES
DEL STRUC
DEPOS ENVIRON
Basin Fill
Basin Fill
REMARKS

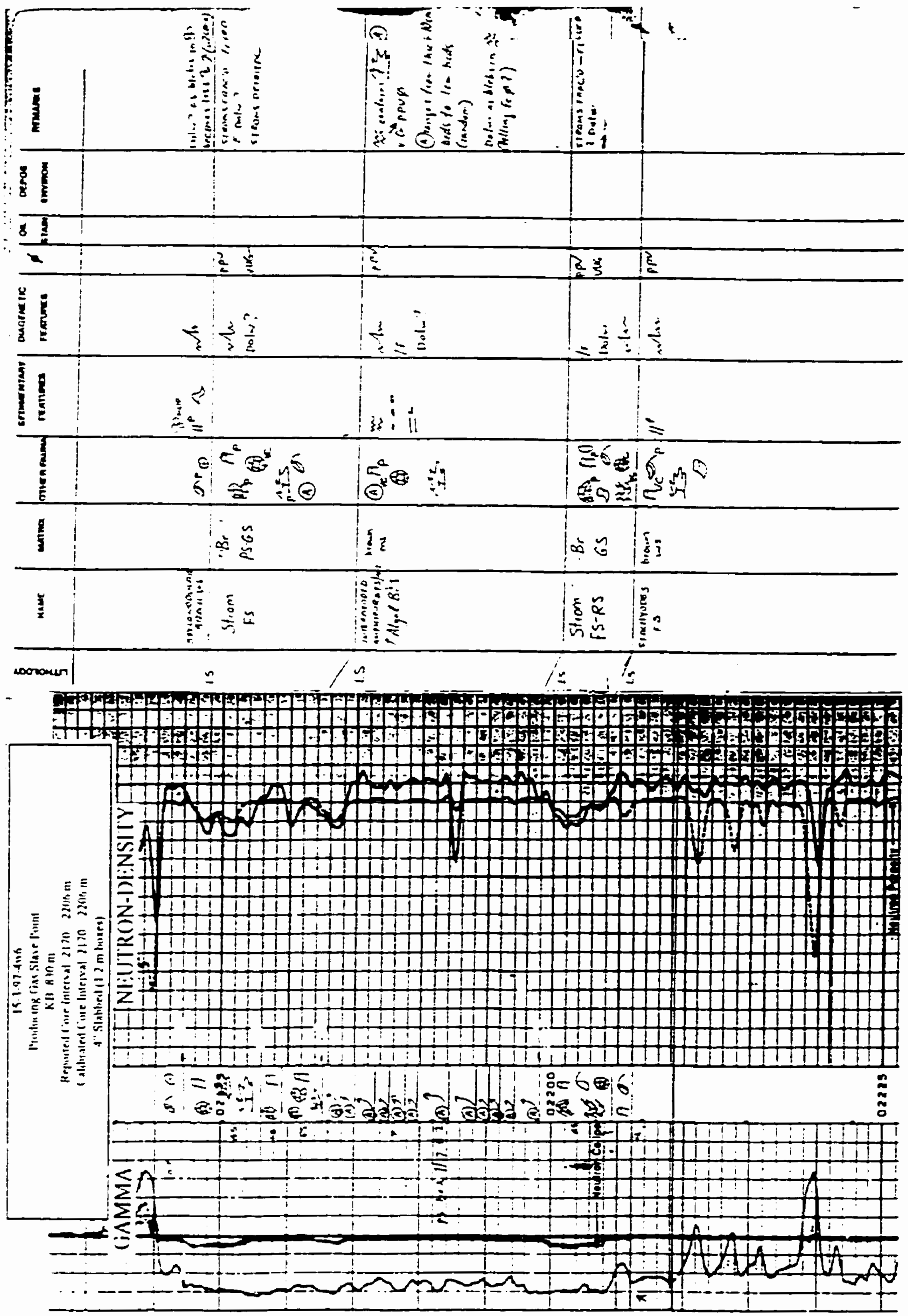
15-1-97-4w6
Producing Gas Slave Point
KB 810 m
Reported Core Interval 2170 - 2206 m
Calibrated Core Interval 2170 - 2206 m
4" Slabbed (1.2 m boxes)
NEUTRON-DENSITY
GAMMA
LITHOLOGY
NAME
MATRIX
OTHER FAUNA
SEDIMENTARY FEATURES
DIAGENETIC FEATURES
OIL STAIN
DEPOSITIONAL ENVIRONMENT
REMARKS
02200
02225

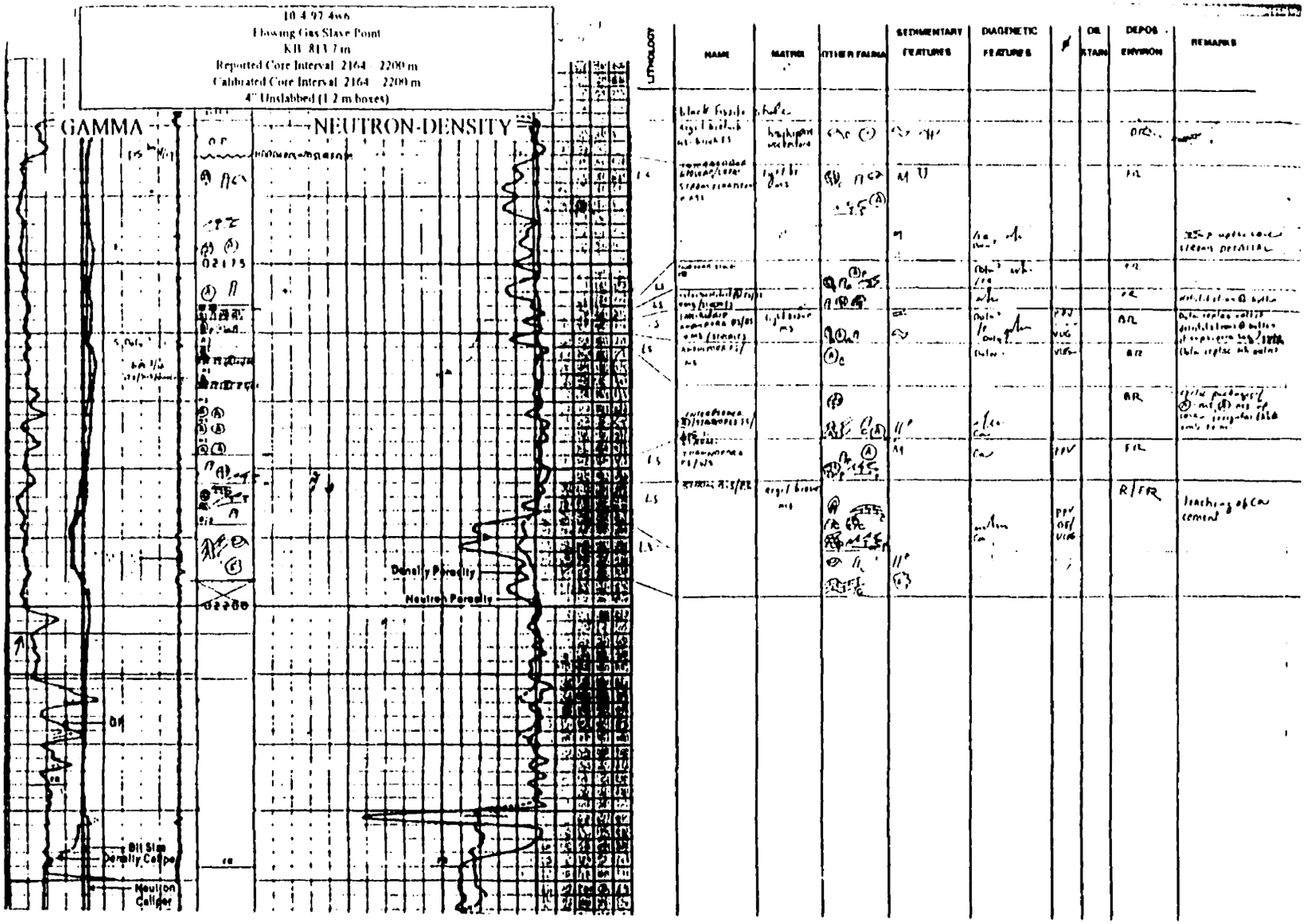
10 4 97 4ws
Flowing Gas Slave Point
KB 813.7 m
Reported Core Interval 2164 - 2200 m
Calibrated Core Interval 2164 - 2200 m
4" Unslabbed (1.2 m boxes)
GAMMA
NEUTRON-DENSITY
Density Porosity
Neutron Porosity
Bit Size
Density Caliper
Neutron Caliper
LITHOLOGY
NAME
MATRIX
OTHER FAUNA
SEDIMENTARY FEATURES
DIAGENETIC FEATURES
OIL STAIN
DEPOS ENVIRON
REMARKS

GAMMA
NEUTRON-DENSITY
7-5-97 4m6
Flowing Gas Show Point
KB 812.7 m
Reported Core Interval 2181 2227 m
Calibrated Core Interval 2181 2227 m
4" Uncalibrated (110 m bored)
02175
02225
ADDITIONALS
NAME
MATRIX
OTHER FAUNA
SEDIMENTARY FEATURES
DIAGENETIC FEATURES
OIL STAIN
DEPOS ENVIRON
REMARKS
LS
Bulbous Stromb FS
Br. GS
Shall
Lagoon
Amphipora FS RS
Algal BFS
dk Br MS WS
S.U.S.
Lagoon
Tabular Stom FS RS BFS
Br. GS
S.U.S.
Upper foreslope
Gold ϕ!
Thamnopora Stachyodes FS
dk Br WS PS
Lower foreslope
Baffle stone. Reef?
Nodular WS
dk Br. MS WS
Lower Shell Platform
Sharp burrowed upper contact

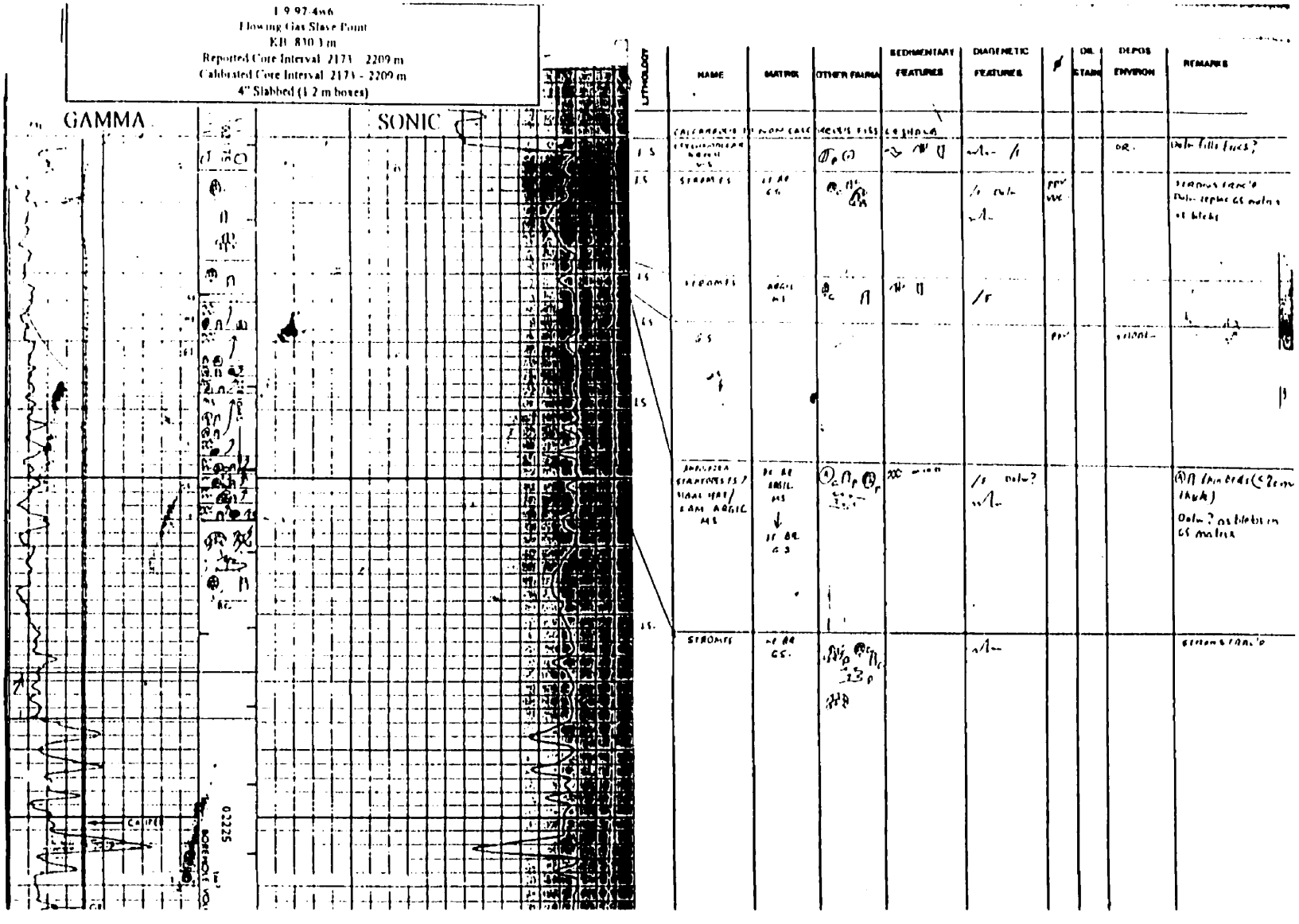
1 9 97-4w6
Flowing Gas Shaw Point
KB 830.3 m
Reported Core Interval 2173 - 2209 m
Calibrated Core Interval 2173 - 2209 m
4" Slabbed (1.2 m boxes)
GAMMA
SONIC
LITHOLOGY
NAME
MATRIX
OTHER FAUNA
SEDIMENTARY FEATURES
DIAGENETIC FEATURES
OIL STAIN
DEPOS ENVIRON
REMARKS
STROMATOPOROID BOUNDSTONE

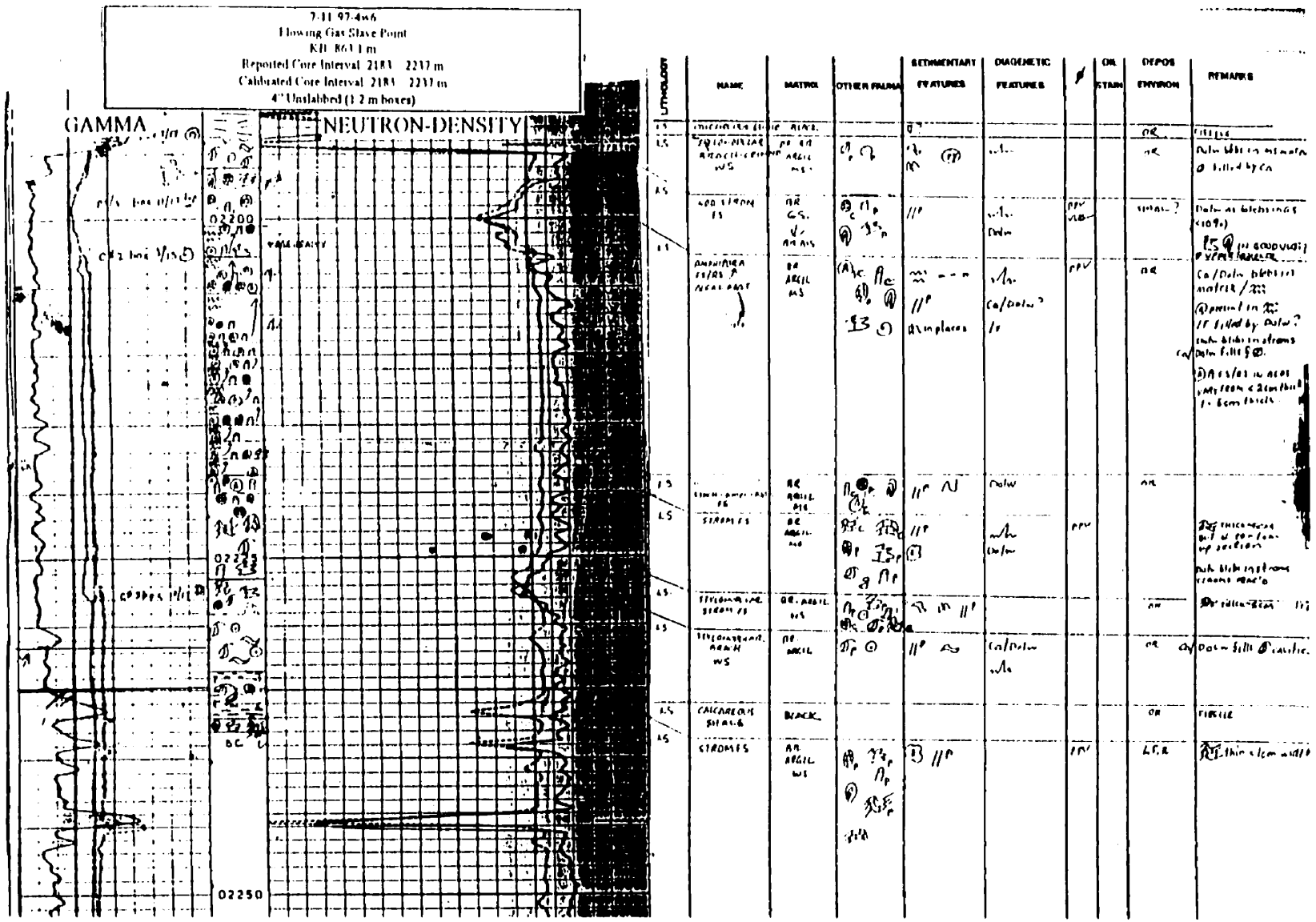
7-11-97-4w6
Flowing Gas Slave Point
KB 863.1 m
Reported Core Interval 2183 - 2237 m
Calculated Core Interval 2183 - 2237 m
4" Unslabbed (1.2 m boxes)
GAMMA
NEUTRON-DENSITY
02200
02250
LITHOLOGY
NAME
MATRIX
OTHER FAUNA
SEDIMENTARY FEATURES
DIAGENETIC FEATURES
OIL STAIN
DEPOS ENVIRON
REMARKS

6-12-97-4w6
Flowing Gas Slave Point
KB 881.5 m
Reported Core Interval 2215 - 2251 m
Calibrated Core Interval 2215 - 2251 m
4" Uninhibited (1.2 m boxes)
SONIC
GAMMA
LITHOLOGY
NAME
MATRIX
OTHER FAUNA
SEDIMENTARY FEATURES
DIAGENETIC FEATURES
OIL STAIN
DEPOS ENVIRON
REMARKS
2250

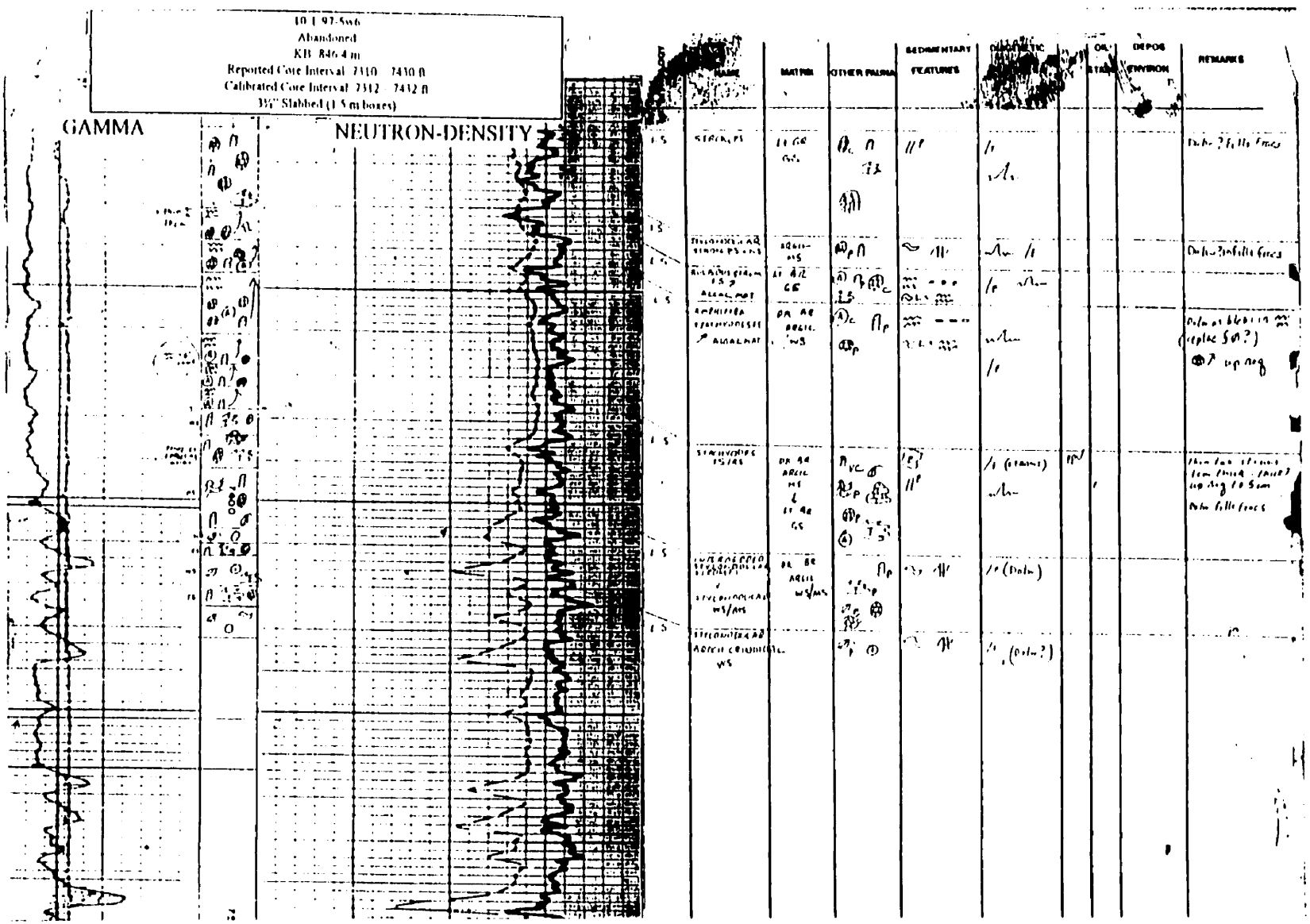
10 [97-Swb
Abandoned
KB 846.4 m
Reported Core Interval 7410 - 7430 ft
Calibrated Core Interval 7312 - 7432 ft
3½" Slabbed (1.5 m boxes)
GAMMA
NEUTRON-DENSITY
SEDIMENTARY FEATURES
REMARKS

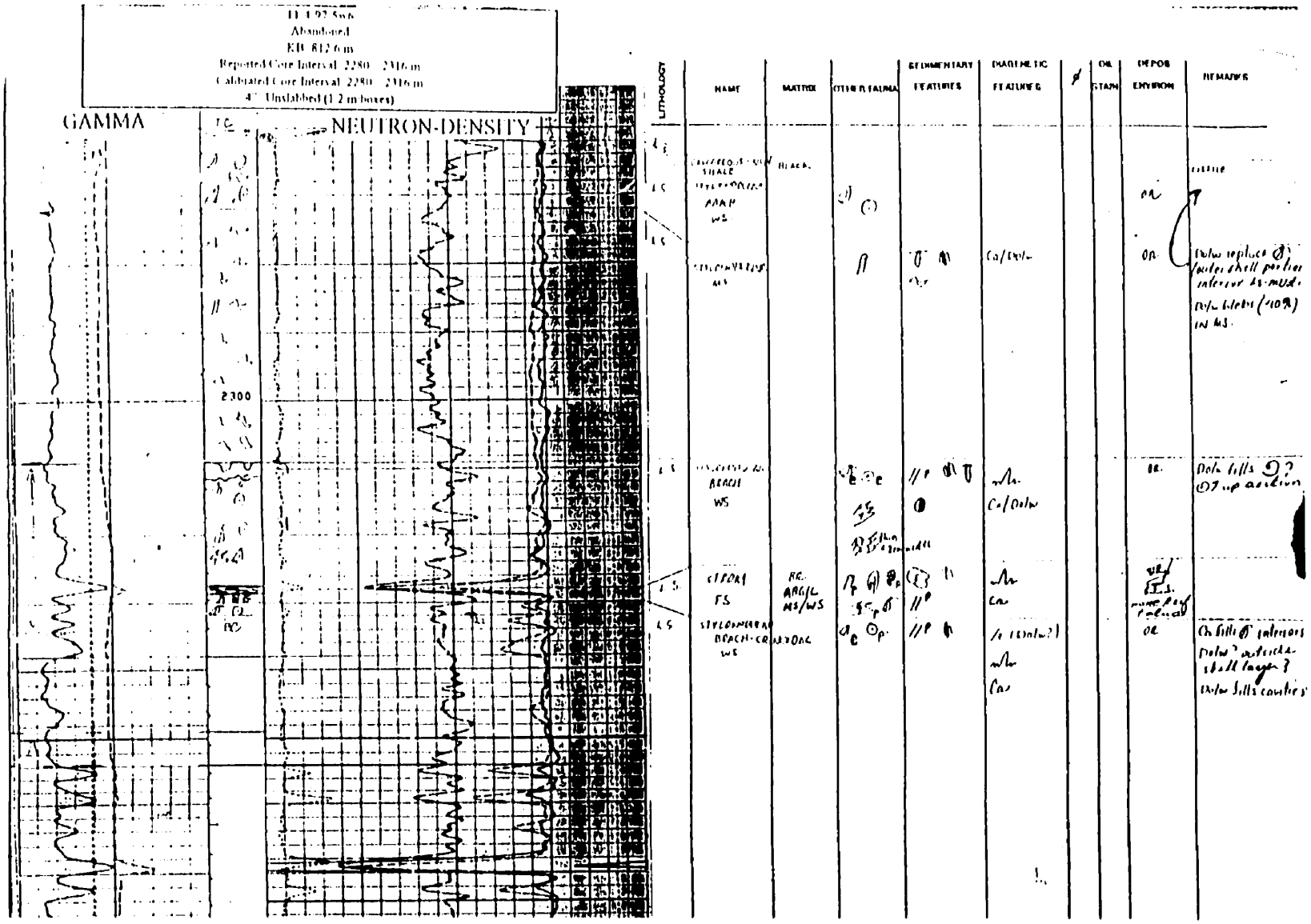
Abandoned
KB 812.6 m
Reported Core Interval 2280 – 2316 m
Calibrated Core Interval 2280 – 2316 m
4" Unslabbed (1.2 m boxes)
GAMMA
NEUTRON-DENSITY
2300
LITHOLOGY
NAME
MATRIX
OTHER FAUNA
SEDIMENTARY FEATURES
DIAGENETIC FEATURES
OIL STAIN
DEPOS ENVIRON
REMARKS
BLACK
BEACH
WS
CLIFFORD
FS
RG.
ARG/L
MS/WS
BEACH-CR
SS/OAC
Ca/Dolo
Dolo
Ca

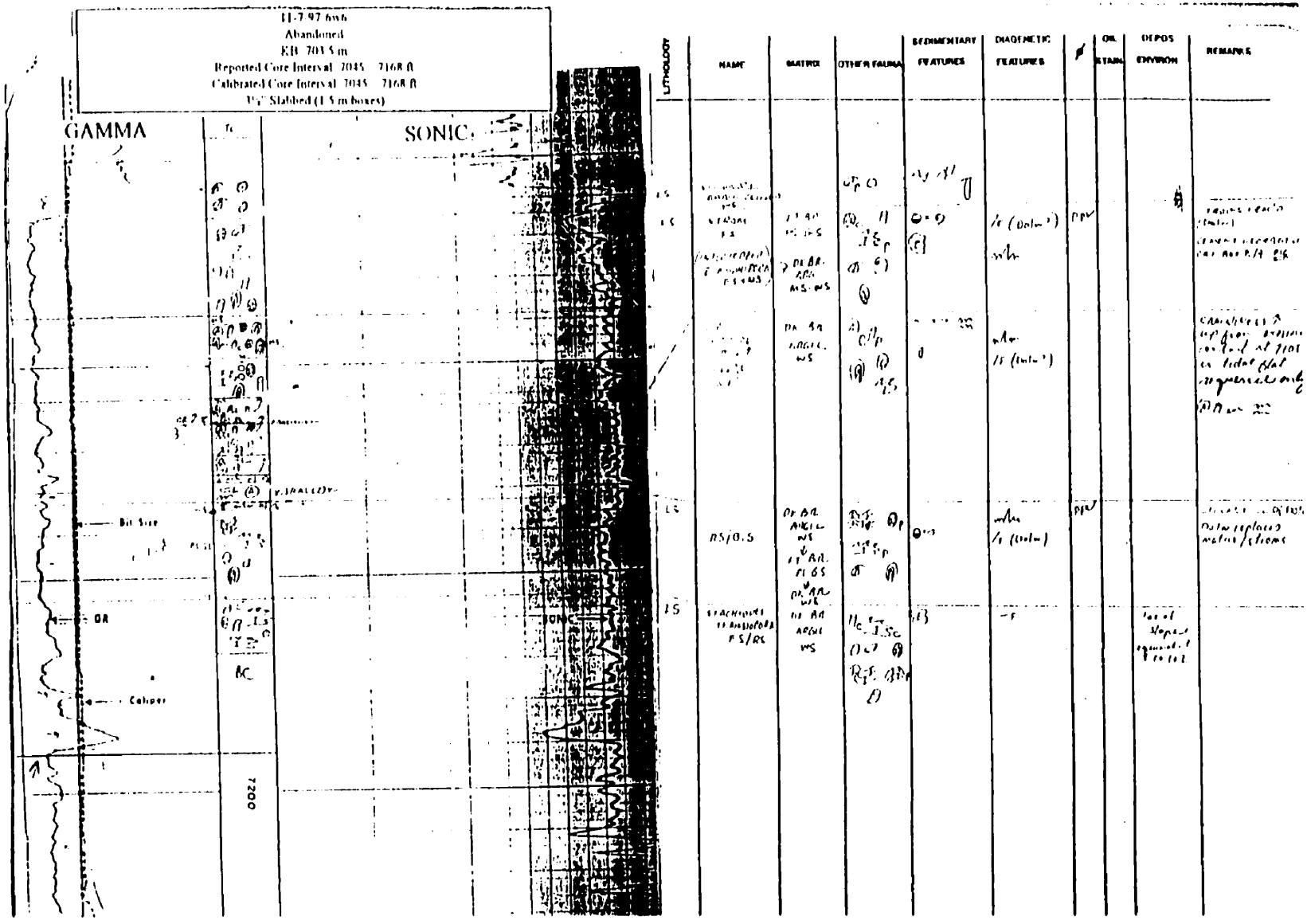
11-7-97 6w6
Abandoned
KB 703.5 m
Reported Core Interval 7045 - 7168 ft
Calibrated Core Interval 7045 - 7168 ft
3½" Slabbed (1.5 m boxes)
GAMMA
SONIC
LITHOLOGY
NAME
MATRIX
OTHER FAUNA
SEDIMENTARY FEATURES
DIAGENETIC FEATURES
OIL STAIN
DEPOS ENVIRON
REMARKS
Bit Size
GR
Caliper
BC
SONIC
7200

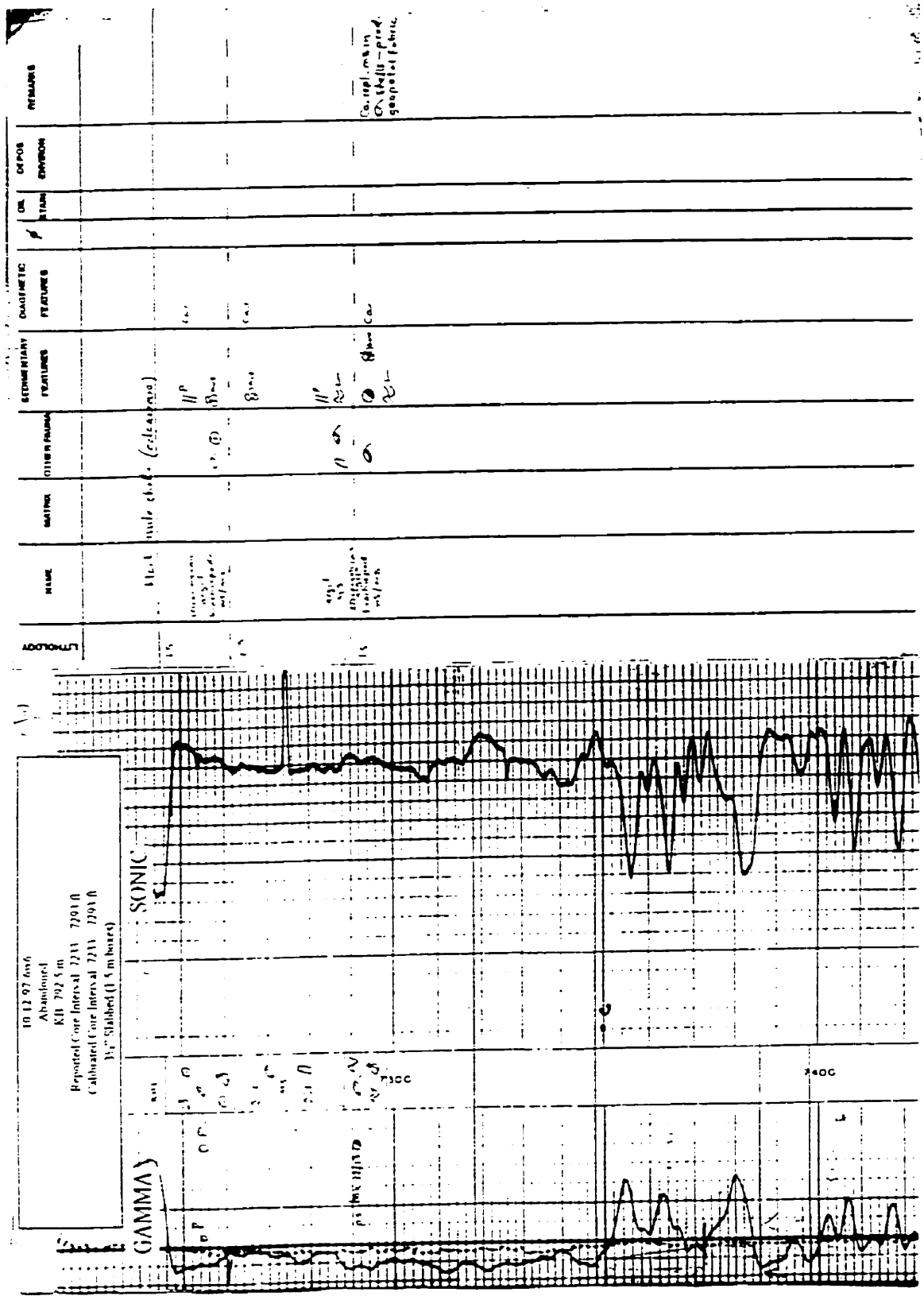
SONIC
GAMMA
7300
7400